

# BULLETIN OF RUSSIAN STATE MEDICAL UNIVERSITY

## BIOMEDICAL JOURNAL OF PIROGOV RUSSIAN NATIONAL RESEARCH MEDICAL UNIVERSITY

**EDITOR-IN-CHIEF** Denis Rebrikov, DSc, professor

**DEPUTY EDITOR-IN-CHIEF** Alexander Oettinger, DSc, professor

**EDITORS** Valentina Geidebrekht, Nadezda Tikhomirova

**TECHNICAL EDITOR** Nina Tyurina

**TRANSLATORS** Ekaterina Tretiyakova, Vyacheslav Vityuk

**DESIGN AND LAYOUT** Marina Doronina

### EDITORIAL BOARD

Averin VI, DSc, professor (Minsk, Belarus)  
Alipov NN, DSc, professor (Moscow, Russia)  
Belousov VV, DSc, professor (Moscow, Russia)  
Bogomilskiy MR, corr. member of RAS, DSc, professor (Moscow, Russia)  
Bozhenko VK, DSc, CSc, professor (Moscow, Russia)  
Bylova NA, CSc, docent (Moscow, Russia)  
Gainetdinov RR, CSc (Saint-Petersburg, Russia)  
Gendlin GYe, DSc, professor (Moscow, Russia)  
Ginter EK, member of RAS, DSc (Moscow, Russia)  
Gorbacheva LR, DSc, professor (Moscow, Russia)  
Gordeev IG, DSc, professor (Moscow, Russia)  
Gudkov AV, PhD, DSc (Buffalo, USA)  
Gulyaeva NV, DSc, professor (Moscow, Russia)  
Gusev EI, member of RAS, DSc, professor (Moscow, Russia)  
Danilenko VN, DSc, professor (Moscow, Russia)  
Zarubina TV, DSc, professor (Moscow, Russia)  
Zatevakhin II, member of RAS, DSc, professor (Moscow, Russia)  
Kagan VE, professor (Pittsburgh, USA)  
Kzyshkowska YuG, DSc, professor (Heidelberg, Germany)  
Kobrinikii BA, DSc, professor (Moscow, Russia)  
Kozlov AV, MD PhD, (Vienna, Austria)  
Kotelevtsev YuV, CSc (Moscow, Russia)  
Lebedev MA, PhD (Darem, USA)  
Manturova NE, DSc (Moscow, Russia)  
Milushkina OYu, DSc, professor (Moscow, Russia)  
Mitupov ZB, DSc, professor (Moscow, Russia)  
Moshkovskii SA, DSc, professor (Moscow, Russia)  
Munblit DB, MSc, PhD (London, Great Britain)

Negrebetsky VV, DSc, professor (Moscow, Russia)  
Novikov AA, DSc (Moscow, Russia)  
Pivovarov YuP, member of RAS, DSc, professor (Moscow, Russia)  
Platonova AG, DSc (Kiev, Ukraine)  
Polunina NV, corr. member of RAS, DSc, professor (Moscow, Russia)  
Poryadin GV, corr. member of RAS, DSc, professor (Moscow, Russia)  
Razumovskii AYU, corr. member of RAS, DSc, professor (Moscow, Russia)  
Rebrova OYu, DSc (Moscow, Russia)  
Rudoy AS, DSc, professor (Minsk, Belarus)  
Rylova AK, DSc, professor (Moscow, Russia)  
Savelieva GM, member of RAS, DSc, professor (Moscow, Russia)  
Semiglazov VF, corr. member of RAS, DSc, professor (Saint-Petersburg, Russia)  
Skobolina NA, DSc, professor (Moscow, Russia)  
Slavyanskaya TA, DSc, professor (Moscow, Russia)  
Smirnov VM, DSc, professor (Moscow, Russia)  
Spallone A, DSc, professor (Rome, Italy)  
Starodubov VI, member of RAS, DSc, professor (Moscow, Russia)  
Stepanov VA, corr. member of RAS, DSc, professor (Tomsk, Russia)  
Suchkov SV, DSc, professor (Moscow, Russia)  
Takhchidi KhP, corr. member of RAS, DSc (medicine), professor (Moscow, Russia)  
Trufanov GE, DSc, professor (Saint-Petersburg, Russia)  
Favorova OO, DSc, professor (Moscow, Russia)  
Filipenko ML, CSc, leading researcher (Novosibirsk, Russia)  
Khazipov RN, DSc (Marsel, France)  
Chundukova MA, DSc, professor (Moscow, Russia)  
Shimanovskii NL, corr. member of RAS, DSc, professor (Moscow, Russia)  
Shishkina LN, DSc, senior researcher (Novosibirsk, Russia)  
Yakubovskaya RI, DSc, professor (Moscow, Russia)

**SUBMISSION** <http://vestnikrgmu.ru/login?lang=en>

**CORRESPONDENCE** [editor@vestnikrgmu.ru](mailto:editor@vestnikrgmu.ru)

**COLLABORATION** [manager@vestnikrgmu.ru](mailto:manager@vestnikrgmu.ru)

**ADDRESS** ul. Ostrovityanova, d. 1, Moscow, Russia, 117997

Indexed in Scopus. CiteScore 2018: 0.16

**Scopus®**

Indexed in RSCI. IF 2018: 0,321

**НАУЧНАЯ ЭЛЕКТРОННАЯ  
БИБЛИОТЕКА  
LIBRARY.RU**

Indexed in WoS. JCR 2018: 0.13

**WEB OF SCIENCE™**

Listed in HAC 31.01.2020 (№ 507)



**ВЫСШАЯ  
АТТЕСТАЦИОННАЯ  
КОМИССИЯ (ВАК)**

Five-year h-index is 4

**Google  
scholar**

Open access to archive

**CYBERLENINKA**

Issue DOI: 10.24075/brsmu.2020-01

The mass media registration certificate no. 012769 issued on July 29, 1994

Founder and publisher is Pirogov Russian National Research Medical University (Moscow, Russia)

The journal is distributed under the terms of Creative Commons Attribution 4.0 International License [www.creativecommons.org](http://www.creativecommons.org)



Approved for print 29.02.2020  
Circulation: 100 copies. Printed by Print.Formula  
[www.print-formula.ru](http://www.print-formula.ru)

# ВЕСТНИК РОССИЙСКОГО ГОСУДАРСТВЕННОГО МЕДИЦИНСКОГО УНИВЕРСИТЕТА

НАУЧНЫЙ МЕДИЦИНСКИЙ ЖУРНАЛ РНИМУ ИМ. Н. И. ПИРОГОВА

**ГЛАВНЫЙ РЕДАКТОР** Денис Ребриков, д. б. н., профессор

**ЗАМЕСТИТЕЛЬ ГЛАВНОГО РЕДАКТОРА** Александр Эттингер, д. м. н., профессор

**РЕДАКТОРЫ** Валентина Гейдебрект, Надежда Тихомирова

**ТЕХНИЧЕСКИЙ РЕДАКТОР** Нина Тюрина

**ПЕРЕВОДЧИКИ** Екатерина Третьякова, Вячеслав Витюк

**ДИЗАЙН И ВЕРСТКА** Марина Доронина

## РЕДАКЦИОННАЯ КОЛЛЕГИЯ

В. И. Аверин, д. м. н., профессор (Минск, Белоруссия)  
Н. Н. Алипов, д. м. н., профессор (Москва, Россия)  
В. В. Белоусов, д. б. н., профессор (Москва, Россия)  
М. Р. Богомилский, член-корр. РАН, д. м. н., профессор (Москва, Россия)  
В. К. Боженко, д. м. н., к. б. н., профессор (Москва, Россия)  
Н. А. Былова, к. м. н., доцент (Москва, Россия)  
Р. Р. Гайнетдинов, к. м. н. (Санкт-Петербург, Россия)  
Г. Е. Гендлин, д. м. н., профессор (Москва, Россия)  
Е. К. Гинтер, академик РАН, д. б. н. (Москва, Россия)  
Л. Р. Горбачева, д. б. н., профессор (Москва, Россия)  
И. Г. Гордеев, д. м. н., профессор (Москва, Россия)  
А. В. Гудков, PhD, DSc (Буффало, США)  
Н. В. Гуляева, д. б. н., профессор (Москва, Россия)  
Е. И. Гусев, академик РАН, д. м. н., профессор (Москва, Россия)  
В. Н. Даниленко, д. б. н., профессор (Москва, Россия)  
Т. В. Зарубина, д. м. н., профессор (Москва, Россия)  
И. И. Затевахин, академик РАН, д. м. н., профессор (Москва, Россия)  
В. Е. Каган, профессор (Питтсбург, США)  
Ю. Г. Кжышковска, д. б. н., профессор (Гейдельберг, Германия)  
Б. А. Кобринский, д. м. н., профессор (Москва, Россия)  
А. В. Козлов, MD PhD (Вена, Австрия)  
Ю. В. Котелевцев, к. х. н. (Москва, Россия)  
М. А. Лебедев, PhD (Дарем, США)  
Н. Е. Мантурова, д. м. н. (Москва, Россия)  
О. Ю. Милушкина, д. м. н., доцент (Москва, Россия)  
З. Б. Митупов, д. м. н., профессор (Москва, Россия)  
С. А. Мошковский, д. б. н., профессор (Москва, Россия)  
Д. Б. Мунблит, MSc, PhD (Лондон, Великобритания)

В. В. Негребский, д. х. н., профессор (Москва, Россия)  
А. А. Новиков, д. б. н. (Москва, Россия)  
Ю. П. Пивоваров, д. м. н., академик РАН, профессор (Москва, Россия)  
А. Г. Платонова, д. м. н. (Киев, Украина)  
Н. В. Полунина, член-корр. РАН, д. м. н., профессор (Москва, Россия)  
Г. В. Порядин, член-корр. РАН, д. м. н., профессор (Москва, Россия)  
А. Ю. Разумовский, член-корр., профессор (Москва, Россия)  
О. Ю. Реброва, д. м. н. (Москва, Россия)  
А. С. Рудой, д. м. н., профессор (Минск, Белоруссия)  
А. К. Рылова, д. м. н., профессор (Москва, Россия)  
Г. М. Савельева, академик РАН, д. м. н., профессор (Москва, Россия)  
В. Ф. Семиглазов, член-корр. РАН, д. м. н., профессор (Санкт-Петербург, Россия)  
Н. А. Скоблина, д. м. н., профессор (Москва, Россия)  
Т. А. Славянская, д. м. н., профессор (Москва, Россия)  
В. М. Смирнов, д. б. н., профессор (Москва, Россия)  
А. Спаллоне, д. м. н., профессор (Рим, Италия)  
В. И. Стародубов, академик РАН, д. м. н., профессор (Москва, Россия)  
В. А. Степанов, член-корр. РАН, д. б. н., профессор (Томск, Россия)  
С. В. Сучков, д. м. н., профессор (Москва, Россия)  
Х. П. Тахчиди, член-корр. РАН, д. м. н., профессор (Москва, Россия)  
Г. Е. Труфанов, д. м. н., профессор (Санкт-Петербург, Россия)  
О. О. Фаворова, д. б. н., профессор (Москва, Россия)  
М. Л. Филиппенко, к. б. н. (Новосибирск, Россия)  
Р. Н. Хазипов, д. м. н. (Марсель, Франция)  
М. А. Чундокова, д. м. н., профессор (Москва, Россия)  
Н. Л. Шимановский, член-корр. РАН, д. м. н., профессор (Москва, Россия)  
Л. Н. Шишкина, д. б. н. (Новосибирск, Россия)  
Р. И. Якубовская, д. б. н., профессор (Москва, Россия)

**ПОДАЧА РУКОПИСЕЙ** <http://vestnikrgmu.ru/login>

**ПЕРЕПИСКА С РЕДАКЦИЕЙ** [editor@vestnikrgmu.ru](mailto:editor@vestnikrgmu.ru)

**СОТРУДНИЧЕСТВО** [manager@vestnikrgmu.ru](mailto:manager@vestnikrgmu.ru)

**АДРЕС РЕДАКЦИИ** ул. Островитянова, д. 1, г. Москва, 117997

Журнал включен в Scopus. CiteScore 2018: 0,16

Журнал включен в WoS. JCR 2018: 0,13

Индекс Хирша (h<sup>2</sup>) журнала по оценке Google Scholar: 4

Scopus®

WEB OF SCIENCE™

Google  
scholar

Журнал включен в РИНЦ. IF 2018: 0,321

Журнал включен в Перечень 31.01.2020 (№ 507)

Здесь находится открытый архив журнала

НАУЧНАЯ ЭЛЕКТРОННАЯ  
БИБЛИОТЕКА  
LIBRARY.RU



ВЫСШАЯ  
АТТЕСТАЦИОННАЯ  
КОМИССИЯ (ВАК)

CYBERLENINKA

DOI выпуска: 10.24075/vrgmu.2020-01

Свидетельство о регистрации средства массовой информации № 012769 от 29 июля 1994 г.

Учредитель и издатель — Российский национальный исследовательский медицинский университет имени Н. И. Пирогова (Москва, Россия)

Журнал распространяется по лицензии Creative Commons Attribution 4.0 International [www.creativecommons.org](http://www.creativecommons.org)



Подписано в печать 29.02.2020

Тираж 100 экз. Отпечатано в типографии Print.Formula  
[www.print-formula.ru](http://www.print-formula.ru)

## ORIGINAL RESEARCH

5

**Comparative phylogenetic analysis of *Neisseria gonorrhoeae* clinical isolates in Russia, European Union, and Japan**

Shaskolskiy BL, Kandinov ID, Chestkov AV, Solomka VS, Kubanov AA, Deryabin DG, Gryadunov DA, Dementieva EI

**Сравнительный филогенетический анализ клинических изолятов *Neisseria gonorrhoeae* России, стран Евросоюза и Японии**

Б. Л. Шаскольский, И. Д. Кандинов, А. В. Честков, В. С. Соломка, А. А. Кубанов, Д. Г. Дерябин, Д. А. Грядун, Е. И. Дементьева

## ORIGINAL RESEARCH

14

**The Use of Real-Time PCR for Evaluation of Endometrial Microbiota**

Voroshilina ES, Zornikov D, Kuposova OV, Islamidi DK, Ignatova KY, Abakumova EI, Kurbatova NV, Plotko EE

**Возможности оценки микробиоты полости матки с использованием ПЦР в реальном времени**

Е. С. Ворошилина, Д. Л. Зорников, О. В. Копосова, Д. К. Исламиди, К. Ю. Игнатова, Е. И. Абакумова, Н. В. Курбатова, Е. Э. Плотко

## ORIGINAL RESEARCH

21

**Isoniazid-resistant *Mycobacterium tuberculosis*: prevalence, resistance spectrum and genetic determinants of resistance**

Andreevskaya SN, Smirnova TG, Larionova EE, Andrievskaya IYu, Chernousova LN, Ergeshov A

**Изониазид-резистентные *Mycobacterium tuberculosis*: частота выявления, спектры резистентности и генетические детерминанты устойчивости**

С. Н. Андреевская, Т. Г. Смирнова, Е. Е. Ларионова, И. Ю. Андриевская, Л. Н. Черноусова, А. Эргешов

## ORIGINAL RESEARCH

27

**Hereditary risk factors for uterine leiomyoma: a search for marker SNPs**

Svirepova KA, Kuznetsova MV, Sogoyan NS, Zelensky DV, Lolomadze EA, Mikhailovskaya GV, Mishina ND, Donnikov AE, Trofimov DYU

**Наследственные факторы риска развития миомы матки: поиск маркерных однонуклеотидных полиморфизмов**

К. А. Свирипова, М. В. Кузнецова, Н. С. Согоян, Д. В. Зеленский, Е. А. Лоломадзе, Г. В. Михайловская, Н. Д. Мишина, А. Е. Донников, Д. Ю. Трофимов

## ORIGINAL RESEARCH

34

**The role of some xenobiotic biotransformation genes snp in the development of acute pancreatitis**

Samgina TA, Nazarenko PM, Polonikov AV, Lazarenko VA

**Значение однонуклеотидного полиморфизма некоторых генов системы биотрансформации ксенобиотиков в развитии острого панкреатита**

Т. А. Самгина, П. М. Назаренко, А. В. Полоников, В. А. Лазаренко

## ORIGINAL RESEARCH

40

**Cerebral cortex activation during the Sternberg verbal working memory task**

Bakulin IS, Zabirowa AH, Kopnin PN, Sinitsyn DO, Poydasheva AG, Fedorov MV, Gnedovskaya EV, Suponeva NA, Piradov MA

**Активация коры головного мозга при выполнении задачи Стернберга на вербальную рабочую память**

И. С. Бакулин, А. Х. Забиров, П. Н. Копнин, Д. О. Синицын, А. Г. Пойдашева, М. В. Федоров, Е. В. Гнедовская, Н. А. Супонева, М. А. Пирадов

## ORIGINAL RESEARCH

49

**Study of the new 4-phenylpyrrolidinone-2 derivative pharmacokinetics and neuroprotective effect in the ischemic stroke animal model**

Borozdenko DA, Lyakhmun DN, Golubev YaV, Tarasenko DV, Kiseleva NM, Negrebetzky VadV

**Изучение фармакокинетики и нейропротекторной активности нового производного 4-фенилпирролидинона-2 в модели ишемического инсульта на животных**

Д. А. Борозденко, Д. Н. Ляхман, Я. В. Голубев, Д. В. Тарасенко, Н. М. Киселева, Вад. В. Негребетский

## CLINICAL CASE

57

### Case report: morphological aspects of Buerger's disease

Tsimbalist NS, Suftin BA, Kriuchkova AV, Chupyatova EA, Babichenko II

### Морфологическая характеристика клинического случая болезни Бюргера

Н. С. Цимбалист, Б. А. Суфтин, А. В. Крючкова, Е. А. Чупятова, И. И. Бабиченко

## ORIGINAL RESEARCH

61

### The effect of acute somatic pain on the killing activity of neutrophils in newborn rats

Alekseev VV, Kade AKh

### Влияние острой соматической боли на киллинговую активность нейтрофилов новорожденных крыс

В. В. Алексеев, А. Х. Каде

## ORIGINAL RESEARCH

67

### Prognosis criteria of the severe postembolization syndrome in patients with uterine myoma

Nurmukhametova ET, Shlyapnikov ME

### Прогностические критерии развития тяжелого постэмболизационного синдрома у пациенток с миомой матки

Э. Т. Нурмухаметова, М. Е. Шляпников

## ORIGINAL RESEARCH

75

### Synthesis of a novel amide derivative of valproic acid and 1,3,4-thiadiazole with antiepileptic activity

Malygin AS, Demidova MA, Skachilova SYa, Shilova EV

### Синтез нового амидного производного вальпроевой кислоты и 1,3,4-тиадиазола с противоэпилептической активностью

А. С. Малыгин, М. А. Демидова, С. Я. Скачилова, Е. В. Шилова

## ORIGINAL RESEARCH

81

### Efficiency of the gynecologic malignancies identification measures at the level of primary health care

Bochkova AG, Domozhirova AS, Aksenova IA

### Оценка эффективности путей выявления опухолей женских половых органов на уровне первичного звена здравоохранения

А. Г. Бочкова, А. С. Доможирова, И. А. Аксенова

## CLINICAL CASE

89

### Intolerance of preservative-containing eye drops in a glaucoma patient: diagnostic and therapeutic challenges

Frolov MA, Kazakova KA, Dushina GN, Frolov AM, Gonchar PA

### Непереносимость консервантосодержащих глазных капель при глаукоме: трудности диагностики, сложности лечения

М. А. Фролов, К. А. Казакова, Г. Н. Душина, А. М. Фролов, П. А. Гончар

COMPARATIVE PHYLOGENETIC ANALYSIS OF *NEISSERIA GONORRHOEAE* CLINICAL ISOLATES IN RUSSIA, EUROPEAN UNION, AND JAPANShaskolskiy BL<sup>1</sup>✉, Kandinov ID<sup>1</sup>, Chestkov AV<sup>2</sup>, Solomka VS<sup>2</sup>, Kubanov AA<sup>2</sup>, Deryabin DG<sup>2</sup>, Gryadunov DA<sup>1</sup>, Dementieva EI<sup>1</sup><sup>1</sup> Center for Precision Genome Editing and Genetic Technologies for Biomedicine, Engelhardt Institute of Molecular Biology, Russian Academy of Sciences, Moscow, Russia<sup>2</sup> State Research Center of Dermatovenereology and Cosmetology, Russian Ministry of Health, Moscow, Russia

Surveillance of multidrug-resistant infections is a priority task for contemporary epidemiology. The aim of this study was to genotype modern clinical isolates of *N. gonorrhoeae* using the NG-MAST technique (*Neisseria gonorrhoeae* multi-antigen sequence typing) and to compare the phylogeny of the gonococcal pathogens coming from Russia, European Union and Japan. We studied a total of 822 isolates collected in Russia from 2013 through 2018. We also used NG-MAST data from the following databases: PathogenWatch (European Union, 1,071 isolates) and PubMLST (Japan, 206 isolates). Russian isolates represented 301 different NG-MAST types. The most common were types 807, 228, 1993, 5714, and 9476 (8.3%, 3.3%, 3.2%, 3.2%, and 2.7%, respectively). There were only 3 isolates (0.4%) from Russia that represented the epidemiologically significant sequence type 1407 prevailing in many countries and characterized by multiple determinants of antimicrobial resistance. A phylogenetic tree for the NG-MAST types found in Russia and European countries was constructed. The cluster analysis of the proportion of isolates belonging to unique sequence types and the country population size allowed us to identify 2 clusters (significance level — 0.01): the first cluster included Russia and Japan, the second, European countries. A distribution pattern was identified for unique sequence types: the greater is the population size, the higher is their proportion. The phylogenetic analysis demonstrated a genetic distance between the most common Russian, European and Japanese sequence types, suggesting that the Russian population of *N. gonorrhoeae* has been evolving relatively locally.

**Keywords:** *Neisseria gonorrhoeae*, NG-MAST, phylogenetic analysis

**Funding:** the study was supported by the Russian Science Foundation (Project 17-75-20039 on the assessment of genetic diversity of sequence types) and the Ministry of Science and Higher Education of the Russian Federation (Agreement № 075-15-2019-1660 on the collection and verification of clinical isolates and the establishment of the association between the unique sequence types and the population size). The isolates were sequenced at the facilities of the *Genome* center for collective use (Engelhardt Institute of Molecular Biology; [http://www.eimb.ru/ru1/ckp/ccu\\_genome\\_c.php](http://www.eimb.ru/ru1/ckp/ccu_genome_c.php)).

**Author contribution:** Shaskolskiy BL, Dementieva EI, Kandinov ID carried out the study, analyzed the data and wrote the manuscript; Gryadunov DA supervised the study and wrote the manuscript; Chestkov AV, Solomka VS, Kubanov AA, Deryabin DG collected and verified clinical isolates, analyzed the obtained data.

**Compliance with ethical standards:** the study was approved by the Ethics Committee of the State Research Centre of Dermatovenereology and Cosmetology (Protocol № 11, dated November 29, 2019). Specimens were collected in compliance with the Declaration of Helsinki (2000) and the European Convention on Human Rights and Biomedicine (1999).

✉ **Correspondence should be addressed:** Boris L. Shaskolskiy  
Vavilova, 32, Moscow, 119991; b.shaskolskiy@biochip.ru**Received:** 09.01.2020 **Accepted:** 08.02.2020 **Published online:** 21.02.2020**DOI:** 10.24075/brsmu.2020.009СРАВНИТЕЛЬНЫЙ ФИЛОГЕНЕТИЧЕСКИЙ АНАЛИЗ КЛИНИЧЕСКИХ ИЗОЛЯТОВ *NEISSERIA GONORRHOEAE* РОССИИ, СТРАН ЕВРОСОЮЗА И ЯПОНИИБ. Л. Шаскольский<sup>1</sup>✉, И. Д. Кандинов<sup>1</sup>, А. В. Честков<sup>2</sup>, В. С. Соломка<sup>2</sup>, А. А. Кубанов<sup>2</sup>, Д. Г. Дерябин<sup>2</sup>, Д. А. Грядун<sup>1</sup>, Е. И. Деметиева<sup>1</sup><sup>1</sup> Центр высокоточного редактирования и генетических технологий для биомедицины, Институт молекулярной биологии имени В. А. Энгельгардта Российской академии наук, Москва, Россия<sup>2</sup> Государственный научный центр дерматовенерологии и косметологии Минздрава России, Москва, Россия

Мониторинг возбудителей инфекционных заболеваний, развивающих множественную устойчивость к антимикробным препаратам, является важной и актуальной задачей. Целью работы являлось генотипирование современных российских клинических изолятов *N. gonorrhoeae* по протоколу NG-MAST (*Neisseria gonorrhoeae* multi-antigen sequence types) и сравнительный филогенетический анализ возбудителя гонококковой инфекции в России, странах ЕС и Японии. Всего исследовано 822 изолята, собранных в РФ в период с 2013 по 2018 гг. Использовали также данные NG-MAST-типирования из баз данных «PathogenWatch» (страны ЕС, 1071 образец) и «PubMLST» (Япония, 206 образцов). Изоляты РФ принадлежали к 301 различному NG-MAST типу, наиболее распространенными являлись 807, 228, 1993, 5714, 9476 (8,3%; 3,3%; 3,2%; 3,2%; 2,7% соответственно). В РФ обнаружено только 3 изолята (0,4%) пандемически значимого NG-MAST 1407, характеризующегося множественными детерминантами резистентности к антимикробным препаратам и доминирующего во многих странах мира. Построено филогенетическое древо NG-MAST типов, найденных в России и в европейских странах. Кластерный анализ данных по доле изолятов с уникальными сиквенс-типами и численности населения показал существование двух кластеров (уровень значимости 0,01): первый составили Россия и Япония, второй — европейские страны. Показана тенденция в распределении уникальных сиквенс-типов — их доля тем выше, чем больше численность населения страны. Филогенетический анализ показал генетическую отдаленность наиболее распространенных российских, европейских и японских сиквенс-типов, что указывает на локальный характер формирования и эволюции российской популяции *N. gonorrhoeae*.

**Ключевые слова:** филогения *Neisseria gonorrhoeae*, NG-MAST

**Финансирование:** работа выполнена при поддержке гранта РНФ 17-75-20039 (оценка генетического разнообразия сиквенс-типов) и Соглашения с Министерством науки и высшего образования РФ № 075-15-2019-1660 (сбор и верификация клинических изолятов, определение соответствия уникальных сиквенс-типов и численности населения). Секвенирование изолятов выполнено в ЦКП «Геном» ИМБ РАН ([http://www.eimb.ru/ru1/ckp/ccu\\_genome\\_c.php](http://www.eimb.ru/ru1/ckp/ccu_genome_c.php)).

**Вклад авторов:** Б. Л. Шаскольский, Е. И. Деметиева, И. Д. Кандинов — проведение исследования, анализ данных, написание статьи; Д. А. Грядун — организация исследования, работа над рукописью; А. В. Честков, В. С. Соломка, А. А. Кубанов, Д. Г. Дерябин — сбор и верификация клинических изолятов, анализ данных.

**Соблюдение этических стандартов:** исследование одобрено этическим комитетом Государственного научного центра дерматовенерологии и косметологии (протокол № 11 от 29 ноября 2019 г.). Отбор биологического материала для исследования был произведен с учетом положений Хельсинской декларации ВМА (2000) и протокола Конвенции Совета Европы о правах человека и биомедицине (1999).

✉ **Для корреспонденции:** Борис Леонидович Шаскольский  
ул. Вавилова, д. 32, г. Москва, 119991; b.shaskolskiy@biochip.ru**Статья получена:** 09.01.2020 **Статья принята к печати:** 08.02.2020 **Опубликована онлайн:** 21.02.2020**DOI:** 10.24075/vrgmu.2020.009

Molecular genetic typing techniques revealing intraspecies variability in pathogenic bacteria have been vigorously used in epidemiological research since the early 21st century [1]. Genotyping is especially important for the surveillance of multidrug-resistant infections, such as those caused by *Neisseria gonorrhoeae*. The World Health Organization (WHO) has included *N. gonorrhoeae* in the list of 12 pathogens that pose a global threat and require urgent development of novel antimicrobial drugs [2].

Surveillance of epidemiologically significant clones of *N. gonorrhoeae*, including multidrug-resistant isolates, and control of their global and regional spread rely on the use of *Neisseria gonorrhoeae* multi-antigen sequence typing (NG-MAST), Multilocus sequence typing (MLST) [3, 4] and whole-genome sequencing (WGS) [5]. WGS provides the most comprehensive information on the phylogeny of clinical isolates, but high costs and strict requirements for the quality of DNA samples still limit its application in routine practice. MLST was originally developed to type *N. meningitidis* and this method analyzes genes that are more conserved than *porB* and *tbpB* targeted by NG-MAST. Thus, NG-MAST currently remains the main and the most widely used technique to study the evolution of the pathogen and identify its transmission routes [4, 6]. Moreover, NG-MAST has demonstrated high resolution in the analysis of clinical isolates [7, 8].

NG-MAST consists in sequencing variable regions of two genes encoding the transmembrane porin protein (*porB*) and the transferrin-binding protein (*tbpB*). Based on sequencing data, each unique sequence is assigned a reference allele number, and the combination of allele numbers is assigned a sequence type (ST). The list of the identified alleles is constantly expanding. In January 2020, the database at [www.ng-mast.net](http://www.ng-mast.net) contained over 11,000 *porB* alleles and over 2,900 *tbpB* alleles that formed over 19,500 NG-MAST types.

The aim of this study was the NG-MAST typing of modern *N. gonorrhoeae* clinical isolates collected in Russia and the comparative phylogenetic analysis of bacteria causing gonococcal infection in Russia, European countries and Japan.

## METHODS

Clinical isolates of *N. gonorrhoeae* (822 specimens) collected in 17 Russian regions under the Russian Gonococcal Antimicrobial Surveillance Programme (RU-GASP) were shipped to the State Research Center for Dermatovenereology and Cosmetology (Moscow). The isolates had been collected in 2013–2018 in 7 of 8 federal districts, except the Far Eastern district, specifically from Arkhangelsk, Astrakhan, Bryansk, Irkutsk, Kaluga, Novosibirsk, Omsk, Penza, Pskov, Ryazan, Tomsk, Chelyabinsk and Stavropol regions, the city of Moscow, the Republics of Tatarstan, Tyva and Chuvash. The specimens came from specialized healthcare facilities for dermatology and venerology (1 specimen per patient). The number of the obtained clinical isolates varied across the regions between 1 and 10% of the total reported cases of gonococcal infection in a given region (5 to 35 strains a year), depending on the population density and the incidence of the infection. Sample collection, shipment, culture, verification and storage conditions are described in detail in [9–11]. The number of clinical isolates analyzed during each year of our study are provided in Table 1.

Molecular typing of *N. gonorrhoeae* consisted in sequencing the variable regions of the *porB* (490 bp) and *tbpB* (390 bp) genes according to the NG-MAST protocol [12]. After the first round of PCR amplification and purification of PCR products, the resulting DNA fragments were Sanger-sequenced using a 3730xl Genetic Analyzer (Applied Biosystems; USA). The obtained allele sequences were compared to the reference sequences from the NG-MAST database at [www.ng-mast.net](http://www.ng-mast.net) in order to identify a sequence type of each clinical isolate. Previously uncharacterized allele sequences detected in *porB* and *tbpB* or their combinations were submitted to the aforementioned NG-MAST database and assigned an NG-MAST sequence type.

Data on *N. gonorrhoeae* circulating in the European Union were retrieved from EUROGASP database at <https://pathogen.watch/collection/eurogasp2013>. We analyzed a total of 1,071 isolates from 21 EU countries, including Austria, Belgium, UK,

**Table 1.** The most common NG-MAST types found in the Russian population (2013–2018)

Year	Number of analyzed clinical isolates (number of identified sequence types)	The most common sequence types	Proportion of samples with a specified sequence type, %
2013	160 (81)	807	13.1
		1152*	5.6
		5941*	3.7
2015	123 (57)	9476*	11.4
		807	8.1
		1544*. 571	4.9
2016	261 (128)	807	6.5
		5714*	6.1
		1993	4.6
2017	127 (63)	807	10.2
		1751*	6.3
		13058*	5.5
2018	151 (67)	228*	14.6
		14942*	5.3
		807. 1993. 14020*	4.6

**Note:** \* — NG-MAST types unique to Russia.



Hungary, Germany, Greece, Denmark, Ireland, Iceland, Spain, Italy, Cyprus, Latvia, Malta, Netherlands, Norway, Portugal, Slovakia, Slovenia, France, and Sweden. NG-MAST data on 206 isolates of *N. gonorrhoeae* circulating in Japan (2015) were retrieved from the database at <https://pubmlst.org/> (we selected samples of *N. gonorrhoeae* with known variants of *porB* and *tbpB*). Isolates with a mixed or unknown NG-MAST type were excluded from the analysis. A total of 29 isolates were excluded, which amounts to 1.4% of the initial sample size (EU + Japan).

Phylogenetic analysis was performed on the concatenated sequences of *porB* and *tbpB*. Model selection was done using Bayesian and Akaike information criteria. The best substitution model for our dataset was GTR with the calculation of the proportion of invariant sites and the G model of rate heterogeneity. Based on the obtained sequences and the chosen model, a maximum likelihood phylogenetic tree was constructed in RAxML ver. 7.4.8 [13]. The phylogenetic tree was created using the software at <http://galaxy-dev.cnsi.ucsb.edu/osiris/>. The number of iterations applied was 999. The tree was constructed from the data on Russian and European clinical isolates of *N. gonorrhoeae* collected in 2013. For phylogenetic tree clades, bootstrap values of 90% or above were considered statistically significant.

The data on the population size and the proportion of isolates representing unique sequence types in each country were analyzed using Ward's agglomerative hierarchical clustering procedure in the «cluster» package for R. The optimal number of clusters was computed in the «Nbclust» package for R [14]. Information on the population size in different countries and the net migration rate (number of migrants per 1,000 population) were taken from The World Factbook: <https://www.cia.gov/library/publications/the-world-factbook/>.

## RESULTS

Based on the results of molecular typing, 822 clinical isolates of *N. gonorrhoeae* collected in Russia between 2013 and 2018 were attributed to 301 different NG-MAST types. The most prevalent sequence types were 807, 228, 1993, 5714, and 9476 (8.3%, 3.3%, 3.2%, 3.2%, and 2.7% of the total sample size, respectively). In 2013, isolates of NG-MAST type 807 made up over 13% of the Russian *N. gonorrhoeae* population; in the next few years, this number gradually declined, reaching 4.6% in 2018 (Table 1). Representatives of sequence types 807 and 1993 were also detected among European specimens, but occurred there sporadically: type 807 was found in the Spanish and Slovakian populations, whereas type 1993, in Denmark. In 2018, sequence type 228, which is unique to Russia, was the most common type in Russia, amounting to 14.6% of the gonococcal population. The proportion of Russian isolates classified as unique Russian sequence types (marked by an asterisk in Table 1) remained constant relative to the total number of isolates analyzed between 2013 and 2018 (80% on average).

Notably, the proportion of sequence types represented by only one specimen was high and stable over the entire studied period, amounting to 25–31% of the total number of isolates. In the European population of *N. gonorrhoeae*, it was as high as 24% in 2013 [6].

Results of *N. gonorrhoeae* molecular typing in European countries [5, 6] and the most common sequence types are shown in Table 2. In 2013, 389 sequence types were circulating in the EU, the most prevalent being sequence type 1407, which occurred in 13 countries and constituted 7.3% of the total analyzed clinical isolates.

The Japanese population of *N. gonorrhoeae* (Table 2) was very different from both Russian and European populations. Japanese isolates represented 65 molecular types, of which only 2 sequence types were present in Russia and European countries: NG-MAST 1407 (found in EU and Russia) and NG-MAST 4186 (one specimen from Sweden). The rest 63 molecular types were unique to Japan.

In order to establish a phylogenetic relationship between Russian and European clinical isolates of *N. gonorrhoeae*, a maximum likelihood phylogenetic tree was constructed. The phylogenetic tree colored according to the presence of NG-MAST type in each country is shown in Fig. 1.

The analysis of sequence types distribution on the tree for the isolates from Russia and EU identified 16 clades with bootstrap values higher than 90% (Fig. 1). Some clades fully or partially corresponded to the European genogroups established for *N. gonorrhoeae* samples collected in Europe in 2013 in the report of the European center for disease prevention and control [6].

Clade  $\alpha$  (bootstrap value = 100) comprises 40 NG-MAST-types (82 isolates) from 17 European countries and Russia; of them 6 sequence types are represented by 7 Russian isolates (8.5%). The clade also includes sequence type 5624 (represented by 15 specimens from 7 countries) and corresponds to the previously described European genogroup G5624 [6].

Clade  $\beta$  (bootstrap value = 94) is formed by 33 sequence types (91 isolates), including type 225 commonly found in Europe (24 specimens from 12 European countries) and type 292 (15 specimens from 6 countries; of those specimens, one comes from Russia). Russian contribution to this clade is represented by 19 isolates (21.3%) belonging to 12 different sequence types. Clade  $\beta$  corresponds to the European genogroup G225 [6].

Clade  $\gamma$  (bootstrap value = 96) is constituted by 14 sequence types (98 isolates) collected in 17 European countries (1 isolate comes from Russia), of them 78 isolates represent sequence type 2992, which is the second most common NG-MAST type in Europe. Clade  $\gamma$  corresponds to the European genogroup G2992 [6].

Clade  $\delta$  (bootstrap value = 98) comprises 3 sequence types (Portugal, Norway, UK). Clade  $\epsilon$  (bootstrap value = 100) consists of 4 sequence types (4 isolates from Norway, Greece and UK). Clade  $\zeta$  (bootstrap value = 100) contains only sequence types unique to Russia (7 specimens representing 5 NG-MAST types).

Clades  $\eta$  and  $\theta$  (bootstrap values 98 and 90, respectively) contain only European sequence types not found in Russia. Clade  $\eta$  is formed by 9 NG-MAST types (16 samples), clade  $\theta$  consists of 11 sequence types (34 samples). NG-MAST-types of these 2 clades represent the European genogroup G5333 [6].

Clade  $\iota$  (bootstrap value = 98) consists of 4 sequence types (4 samples collected in Portugal, Italy and the Netherlands).

Clade K (bootstrap value = 94) comprises 4 European sequence types (36 samples), including sequence type 4995 (the fourth most common type in Europe found in 10 European countries) represented by 31 isolates. Clade K corresponds to the European genogroup G4995 [6].

Clade  $\lambda$  (bootstrap value = 95) includes 3 sequence types from European countries represented by 10 samples, of which 8 represent NG-MAST type 5441 detected in 5 countries.

Clade  $\mu$  (bootstrap value = 94) comprises 4 sequence types (10 samples from Greece, Denmark, Slovenia, and Portugal). Clade  $\nu$  (bootstrap value = 98) is formed by 3 sequence types (5 samples from 5 European countries).

Table 2. NG-MAST types most common to EU and Japan

Country (ID)	Year	Number of analyzed clinical isolates (number of identified sequence types)	The most common sequence types	Proportion of samples representing a specified sequence type, %
Austria (AT)	2013	50 (24)	3785* 11575* 387, 4994	18.0 12.0 8.0 each
Belgium (BE)	2013	55 (24)	1407 387, 2992 2400, 5624	16.4 14.5 7.3 each
Cyprus (CY)	2013	6 (4)	1407 4269, 6146*, 10803*	49 17.0 each
Germany (DE)	2013	45 (30)	4995 359, 5441, 9500*	8.9 6.7 each
Denmark (DK)	2013	54 (28)	1993 1407 2400	20.4 14.8 7.4
Spain (ES)	2013	110 (64)	1407 2400 21	10.0 9.1 7.3
France (FR)	2013	56 (40)	645 4995, 5624, 11352*	8.9 5.4 each
Greece (GR)	2013	48 (20)	3128 225, 4730, 11055*	18.8 10.4 each
Hungary (HU)	2013	46 (20)	1407 995 387, 11046*	21.7 13.0 6.5 each
Ireland (IE)	2013	44 (26)	2992 384 21, 225, 437, 649*, 2400, 10843*, 10846*	15.9 11.4 4.5 each
Iceland (IS)	2013	5 (5)	1034, 2400, 9541*, 10640*, 11080*	20.0 each
Italy (IT)	2013	24 (13)	2992 6360 5624, 8826*	33.3 12.5 8.3 each
Latvia (LV)	2013	38 (15)	5 10828* 21, 4269	36.8 13.2 7.9
Malta (MT)	2013	20 (10)	2992 1407, 484*, 9905*, 10788*	35.0 10.0 each
Netherlands (NL)	2013	66 (38)	2992 2400 4995, 5624, 8154, 8919	13.6 12.1 4.5 each
Norway (NO)	2013	55 (41)	1407 4275 2400	9.1 7.3 5.5
Portugal (PT)	2013	103 (54)	1407 7445 1034	16.5 11.7 4.9
Sweden (SE)	2013	49 (31)	5445 3128, 7164, 7445	10.2 6.1 each
Slovenia (SI)	2013	53 (26)	21 10800, 10801* 10798*, 10799*	13.2 11.3 each 7.5 each
Slovakia (SK)	2013	38 (19)	1407, 10800, 11042* 359, 2992	13.2 each 10.5 each
UK (UK)	2013	106 (52)	2992 51 4995	11.3 10.4 6.6
Poland (PL)**	2012	–	1407 8391* 1861, 2992	47.0 7.0 5.0 each
Japan (JP)	2015	206 (65)	5687* 1407 6778*	7.8 6.3 4.4

Note: \* — NG-MAST types unique to the specified country; \*\* — NG-MAST types common to Poland and described in [17].



Clade  $\xi$  (bootstrap value = 100) consists of 3 sequence types (4 samples from Ireland and Denmark). Clade  $\alpha$  (bootstrap value = 98) is formed by 5 NG-MAST types (17 samples), including types 1993 and 5714 that are frequently found in Russia.

Clade  $\pi$  (bootstrap value = 97) includes 7 sequence types (12 isolates) found both in Russia and European countries. Those include sequence types 5792, 9485, 9490, and 9491, all of which are unique to Russia.

In each analyzed country there were isolates representing unique sequence types not found in any other country. For European countries, the proportion of isolates representing unique sequence types (relative to the total number of isolates in a given country) varied between 25 and 56%. The lowest proportion was observed in the UK and Belgium, the highest, in Austria, Slovenia and Sweden (> 50%). In Russia and Japan, the proportion of unique sequence type isolates exceeded 80% (Table 3).

To identify groups with similar distribution patterns for unique sequence types and their relationship with the population size in a country of interest, cluster analysis was carried out. Twenty-one countries were included in the

analysis (Table 3). Cyprus and Iceland were excluded due to the small number of isolates available (6 and 5, respectively). After applying Ward's agglomerative hierarchical clustering procedure, the optimal number of clusters was determined in NbClust for R using the majority rule. Nine out of 30 methods (Silhouette, Duda, PseudoT2, Beale, Ratkowsky, PtBiserial, McClain, Dunn, SDindex) showed that the optimal number of clusters was 2 (bootstrap value = 0.01); 6 methods (Hartigan, Scott, Marriot, TrCovW, TraceW, Ball) showed that the optimal number of clusters was 3. Following the majority rule, it was decided that two clusters were the optimal choice; at the same time there was a statistically based rationale for breaking down cluster 2 into 2 sub-clusters (Fig. 2A).

Cluster 1 included Russia and Japan (countries with a population size of over 125 million people). Cluster 2 comprised all European countries with a population size from 0.4 to 81 million. Cluster 2 was divided into 2 subclusters: 2a and 2b. Subcluster 2a was composed of the UK, Germany, Spain, Italy, and France (countries with a population size of 47–81 million); subcluster 2b included European countries with populations below 17 million (Ireland, Norway, Denmark, Slovakia, Malta,

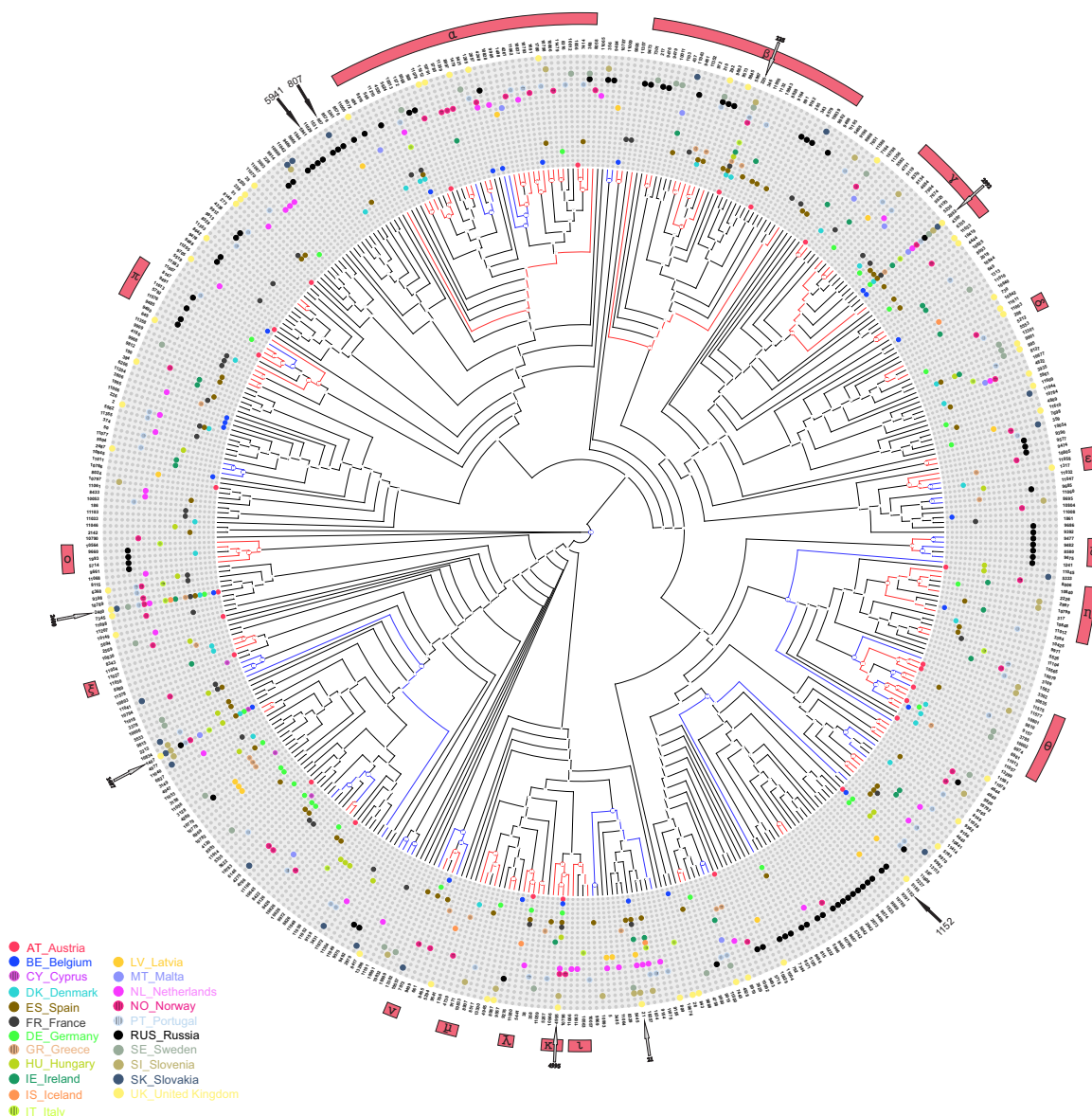


**Fig. 1.** A phylogenetic tree of *N. gonorrhoeae* NG-MAST types detected in Russia and EU. Branches with bootstrap values of 80-89 are shown in blue; red indicates bootstrap value of 90-100. Phylogenetic clades (bootstrap values  $\geq$  90%) are designated by Greek letters  $\alpha$ – $\pi$ . Black arrows indicate NG-MAST types that are most common in Russia. Gray dashed arrows indicate NG-MAST types that are most common in European countries

Latvia, Slovenia, Netherlands, Belgium, Portugal, Greece, Austria, Hungary, Sweden).

In general, the greater was the population size, the more isolates of unique sequence types were present in the country, as demonstrated by the countries with a population size over 47 million included in cluster 1 and subcluster 2a (Fig. 2B). This pattern was not observed for the countries with smaller population sizes constituting cluster 2b. Transition from cluster 2 to cluster 1 occurred for the countries with the population size over 125 million (Russia, Japan).

It was also interesting to analyze the contribution of migration to the distribution of unique sequence types across different countries. If only net migration rates and proportion of isolates of unique sequence types were analyzed, we were unable to find statistically significant clusters. When 3 parameters were included in the analysis (migration, population size and the proportion of unique sequence types), the agglomerative coefficient was 0.83, which is lower than 0.93, the value yielded by the analysis of 2 parameters (population size and the proportion of unique sequence types).

## DISCUSSION

The comparative analysis of *N. gonorrhoeae* molecular typing data revealed significant differences between Russian, European and Japanese gonococcal populations. The majority of Russian isolates belonged to the sequence types that were not detected in European countries or Japan in the analyzed period. In Russia, only 3 (0.4%) isolates represented the epidemiologically significant sequence type 1407, which prevailed in Belgium, Hungary, Denmark, Spain, Norway, Portugal, Slovakia, and Japan. It is worth mentioning that in 2010 this sequence type amounted to over 10% of all isolates in many European countries, including Austria, Belgium, UK, Netherlands, Spain, Italy, Portugal, Romania, Slovenia,

and Poland [15–17], as well as Japan and USA [18, 19]. This sequence type poses a great threat because it carries multiple determinants of antimicrobial resistance, including the mosaic penicillin-binding protein PBP2 and a mutation of the Ala501 residue in PBP2, both of which cause resistance to cephalosporins [16, 20, 21].

In the Russian dataset, there were only 3 (0.4%) *N. gonorrhoeae* isolates representing sequence type 2992 and 7 (0.9%) isolates representing type 2400. Those sequence types were second and third most common types in Europe in 2013 (7.0 and 4.7%, respectively). By contrast, types 228, 5714, and 1751 were not detected in the European population, although they were highly prevalent in the Russian population.

For Poland, NG-MAST data were retrieved from [17], as they were missing in the EUROGASP database. The distribution of NG-MAST types in Poland was closer to that in European Union than in Russia; the Polish gonococcal population was dominated by sequence type 1407 (Table 2).

The analysis of the phylogenetic tree constructed for NG-MAST types of clinical isolates collected in Europe and Russia reveals that *N. gonorrhoeae* populations are heterogeneous both in Russia and Europe. There are sequence types that are present in many countries; at the same time, isolates coming from one and the same country can belong to phylogenetically distant clades. The most common European sequence types (NG-MAST 1407, 2992, 2400, 4995, 21, 225) that amount to the total of 25.9% of all European strains are phylogenetically distant from each other and distributed throughout the entire tree. Notably, there is no close relationship between the most common European sequence types and Russian sequence types, including NG-MAST 807, 1152 and 5941. Sixteen clades of the tree are characterized by high bootstrap values and partially or fully correspond to the European genogroups [6].

Further phylogenetic analysis of NG-MAST types drove us to the conclusion that geographically distant populations

**Table 3.** Distribution of isolates of unique NG-MAST types (2013)

Country	Number of unique sequence types	Number of isolates of unique sequence types	Proportion of isolates of unique sequence types relative to the total number of isolates, %	Population, thousand	Net migration rate
Russia	73	129	80.6	142 500	1.69
Japan	63	192	93.2	126 920	0
Germany	15	18	40.0	81 147	0.89
France	24	27	48.2	65 952	1.10
UK	24	27	25.5	63 396	2.57
Italy	6	7	29.2	61 482	4.47
Spain	31	36	32.7	47 370	6.14
Netherlands	18	19	28.8	16 805	1.99
Portugal	32	40	38.8	10 799	2.82
Greece	10	21	43.8	10 773	2.32
Belgium	13	14	25.5	10 444	1.22
Hungary	10	14	30.4	9 939	1.36
Sweden	19	25	51.0	9 119	1.64
Austria	13	28	56.0	8 222	1.78
Denmark	14	17	31.5	5 556	2.30
Slovakia	9	13	34.2	5 488	0.28
Ireland	12	15	34.1	4 776	2.51
Norway	20	21	38.2	4 723	1.68
Latvia	11	16	42.1	2 178	– 2.36
Slovenia	14	27	50.9	1 993	0.38
Malta	5	8	40.0	411	1.99

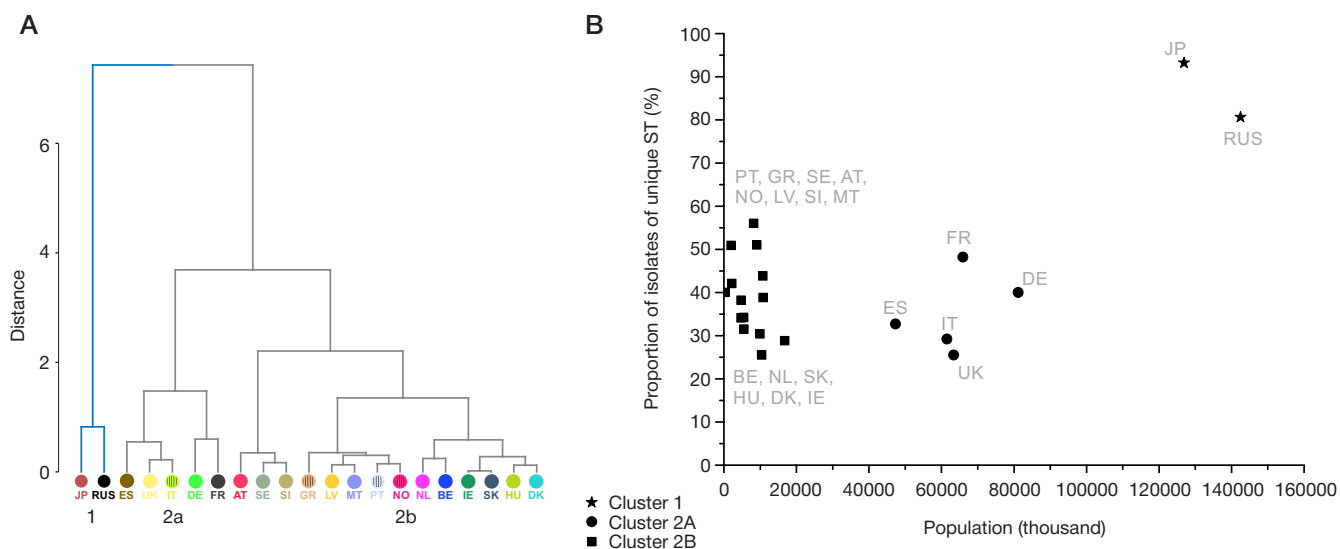


**Fig. 2.** Associations between the proportion of *N. gonorrhoeae* isolates of unique sequence types and the country population size. Country codes are given in Table 1. **A.** A dendrogram. The clusters are indicated by numbers. **B.** The relationship between the proportion of *N. gonorrhoeae* clinical isolates representing unique sequence types and the population size

of *N. gonorrhoeae* evolve more or less locally. This could be one of the reasons underlying the difference in the incidence of gonococcal infection in Russian and EU [22]: in Russia, the incidence of the infection is declining [9, 23] and there are no isolates resistant to ceftriaxone (the primary drug for gonorrhea treatment) [9, 10].

We have analyzed the associations between the proportion of isolates of unique sequence types and the population size of the country of interest. In Russia and Japan, the majority of isolates (> 80%) belonged to NG-MAST types unique to this country. The cluster analysis of the population size and the proportion of isolates belonging to unique sequence types detected in a country allowed us to identify two clusters: the first cluster included Russia and Japan (population over 125 million people), the second cluster included European countries with population between 0.4 and 81 million people. On the whole, there was a certain distribution pattern for unique sequence types: the greater the country's population, the higher the proportion of samples with unique sequence types.

## CONCLUSIONS

NG-MAST typing of *N. gonorrhoeae* clinical isolates collected in Russia has demonstrated their significant difference from the gonococcal populations circulating in the EU and Japan. The Russian *N. gonorrhoeae* population was dominated by sequence types 807, 1152 and 5941, which occurred only sporadically in other countries; sequence types 228, 5714 and 1751 were not detected in Russia at all. Between 2013 and 2018, in Russia there were only 3 isolates of epidemically significant sequence type 1407 (0.4% of the total samples

under study). This type poses a serious threat because it carries multiple determinants of antimicrobial resistance and prevails in many European countries and Japan. The phylogenetic analysis of NG-MAST types for Russian and European isolates has demonstrated their high heterogeneity and genetic distance between common European and common Russian NG-MAST types, suggesting that the Russian population of *N. gonorrhoeae* has been forming and evolving locally.

The majority (> 80%) of Russian and Japanese isolates are unique to the two countries. This number is higher than the proportion of isolates with unique sequence types in European countries. The cluster analysis of the proportion of isolates representing unique sequence types and the population size allowed us to identify two clusters: one cluster for Russia and Japan and another cluster for European countries. The following trend was observed for the countries with a total population size over 47 million (Spain, UK, Germany, Italy, France, Russia, Japan): the greater the population size, the higher the proportion of isolates representing unique sequence types. We were unable to establish an association between the proportion of isolates representing unique sequence types and the net migration rate.

Thus, the phylogenetic analysis has revealed a relative isolation of the currently existing Russian population of *N. gonorrhoeae*, which follows its own evolutionary patterns. Nevertheless, there is a need for continuous surveillance of the spread of gonococcal infection and antimicrobial resistance of *N. gonorrhoeae* in Russia. The objective of this surveillance is timely detection and effective elimination of globally spreading sequence types with multiple determinants of antimicrobial resistance.

## References

1. Foxman B, Riley L. Molecular epidemiology: focus on infection. Am J Epidemiol. 2001; 153 (12): 1135–41. DOI: 10.1093/aje/153.12.1135.
2. Tacconelli E, Carrara E, Savoldi A, Harbarth S, Mendelson M, Monnet DL, et al. Discovery, research, and development of new antibiotics: the WHO priority list of antibiotic-resistant bacteria and tuberculosis. Lancet Infect Dis. 2018; 18 (3): 318–27. DOI: 10.1016/S1473-3099(17)30753-3.
3. Unemo M, Dillon JA. Review and international recommendation of methods for typing *Neisseria gonorrhoeae* isolates and their implications for improved knowledge of gonococcal epidemiology, treatment, and biology. Clin Microbiol Rev. 2011; (24): 447–58. DOI: 10.1128/CMR.00040-10.
4. Town K, Bolt H, Croxford S, Cole M, Harris S, Field N, et al. *Neisseria gonorrhoeae* molecular typing for understanding

- sexual networks and antimicrobial resistance transmission: A systematic review. *J Infect.* 2018; (76): 507–14. DOI: 10.1016/j.jinf.2018.02.011.
5. Harris SR, Cole MJ, Spiteri G, Sánchez-Busó L, Golparian D, Jacobsson S, et al. Public health surveillance of multidrug-resistant clones of *Neisseria gonorrhoeae* in Europe: a genomic survey. *Lancet Infect Dis.* 2018; 18 (7): 758–68. DOI: 10.1016/S1473-3099(18)30225-1.
  6. European Centre for Disease Prevention and Control. Technical Report. Molecular typing of *Neisseria gonorrhoeae* — a study of 2013 isolates. Stockholm: ECDC; 2018. Available from: <https://www.ecdc.europa.eu/sites/portal/files/documents/Molecular-typing-N-gonorrhoeae-web.pdf>.
  7. Ilna EN, Oparina NY, Shitikov EA, Borovskaya AD, Govorun VM. Molecular surveillance of clinical *Neisseria gonorrhoeae* isolates in Russia. *J Clin Microbiol.* 2010; 48 (10): 3681–89. DOI: 10.1128/JCM.00565-10.
  8. Shpilevaya MV, Obraztsova OA, Chestkov AV. The use of current genotyping assay methods for *Neisseria gonorrhoeae*. *Vestnik Dermatologii i Venerologii.* 2015; (6): 33–40. DOI: 10.25208/0042-4609-2015-0-6-33-40. Russian.
  9. Kubanov A, Solomka V, Plakhova X, Chestkov A, Petrova N, Shaskolskiy B, et al. Summary and trends of the Russian Gonococcal Antimicrobial Surveillance Programme, 2005–2016. *J Clin Microbiol.* 2019; 5 (6): e02024–18. DOI: 10.1128/JCM.02024-18.
  10. Shaskolskiy B, Dementieva E, Kandinov I, Filippova M, Petrova N, Plakhova X, et al. Resistance of *Neisseria gonorrhoeae* isolates to beta-lactam antibiotics (benzylpenicillin and ceftriaxone) in Russia, 2015–2017. *PLoS One.* 2019; 14 (7): e0220339. DOI: 10.1371/journal.pone.0220339.
  11. Vorobiev DV, Solomka VS, Plakhova KI, Deryabin DG, Kubanov AA. NG-MAST genotyping of *Neisseria gonorrhoeae* strains isolated in Russian Federation in 2012–2015. *Journal of microbiology, epidemiology, immunobiology.* 2016; (4): 42–51. Russian.
  12. Martin IMC, Ison CA, Aanensen DM, Fenton KA, Sprat BG. Rapid sequence-based identification of gonococcal transmission clusters in a large metropolitan area. *J Infect Dis.* 2004; (189): 1497–505. DOI: 10.1086/383047.
  13. Stamatakis A. Using RAxML to infer phylogenies. *Curr Protoc Bioinformatics.* 2015; 51 (1): 6.14.1–14.14. DOI: 10.1002/0471250953.bi0614s51.
  14. Charrad M, Ghazzali N, Boiteau V, Niknafs A. NbClust: an R package for determining the relevant number of clusters in a data set. *Journal of Statistical Software.* 2014; 61 (6): 1–36. DOI: 10.18637/jss.v061.i06.
  15. European Centre for Disease Prevention and Control. Technical Report. Molecular typing of *Neisseria gonorrhoeae* — results from a pilot study 2010–2011. Stockholm: ECDC; 2012. Available from: <https://www.ecdc.europa.eu/sites/portal/files/media/en/publications/Publications/201211109-Molecular-typing-gonorrhea.pdf>.
  16. Chisholm SA, Unemo M, Quaye N, Johansson E, Cole MJ, Ison CA, et al. Molecular epidemiological typing within the European Gonococcal Antimicrobial Resistance Surveillance Programme reveals predominance of a multidrug-resistant clone. *Euro Surveill.* 2013; 18 (3): pii 20358. DOI: 10.2807/ese.18.03.20358-en.
  17. Mlynarczyk-Bonikowska B, Malejczyk M, Majewski S, Unemo M. Antibiotic resistance and NG-MAST sequence types of *Neisseria gonorrhoeae* isolates in Poland compared to the world. *Postepy Dermatol Alergol.* 2018; 5 (6): 346–51. DOI: 10.5114/ada.2018.79780.
  18. Shimuta K, Watanabe Y, Nakayama S, Morita-Ishihara T, Kuroki T, Unemo M, et al. Emergence and evolution of internationally disseminated cephalosporin-resistant *Neisseria gonorrhoeae* clones from 1995 to 2005 in Japan. *BMC Infect Dis.* 2015; (15): 378. DOI: 10.1186/s12879-015-1110-x.
  19. Pandori M, Barry PM, Wu A, Ren A, Whittington WL, Liska S, et al. Mosaic penicillin-binding protein 2 in *Neisseria gonorrhoeae* isolates collected in 2008 in San Francisco, California. *Antimicrob Agents Chemother.* 2009; (53): 4032–34. DOI: 10.1128/AAC.00406-09.
  20. Unemo M, Shafer WM. Antimicrobial resistance in *Neisseria gonorrhoeae* in the 21st century: past, evolution, and future. *Clin Microbiol Rev.* 2014; 27 (3): 587–613. DOI: 10.1128/CMR.00010-14.
  21. Unemo M. Current and future antimicrobial treatment of gonorrhoea — the rapidly evolving *Neisseria gonorrhoeae* continues to challenge. *BMC Infect Dis.* 2015; (15): 364. DOI: 10.1186/s12879-015-1029-2.
  22. European Centre for Disease Prevention and Control. Gonorrhoea. Annual epidemiological report for 2017. Stockholm: ECDC; 2019. Available from: <https://www.ecdc.europa.eu/sites/default/files/documents/gonorrhoea-annual-epidemiological-report-2017.pdf>.
  23. Kubanova AA, Kubanov AA, Melekhina LE, Bogdanova EV. Results of work of dermatovenereologic healthcare organizations in 2016. *Vestnik Dermatologii i Venerologii.* 2017; (4): 12–27. DOI: 10.25208/0042-4609-2017-0-4-20-21. Russian.

## Литература

1. Foxman B, Riley L. Molecular epidemiology: focus on infection. *Am J Epidemiol.* 2001; 153 (12): 1135–41. DOI: 10.1093/aje/153.12.1135.
2. Tacconelli E, Carrara E, Savoldi A, Harbarth S, Mendelson M, Monnet DL, et al. Discovery, research, and development of new antibiotics: the WHO priority list of antibiotic-resistant bacteria and tuberculosis. *Lancet Infect Dis.* 2018; 18 (3): 318–27. DOI: 10.1016/S1473-3099(17)30753-3.
3. Unemo M, Dillon JA. Review and international recommendation of methods for typing *Neisseria gonorrhoeae* isolates and their implications for improved knowledge of gonococcal epidemiology, treatment, and biology. *Clin Microbiol Rev.* 2011; (24): 447–58. DOI: 10.1128/CMR.00040-10.
4. Town K, Bolt H, Croxford S, Cole M, Harris S, Field N, et al. *Neisseria gonorrhoeae* molecular typing for understanding sexual networks and antimicrobial resistance transmission: A systematic review. *J Infect.* 2018; (76): 507–14. DOI: 10.1016/j.jinf.2018.02.011.
5. Harris SR, Cole MJ, Spiteri G, Sánchez-Busó L, Golparian D, Jacobsson S, et al. Public health surveillance of multidrug-resistant clones of *Neisseria gonorrhoeae* in Europe: a genomic survey. *Lancet Infect Dis.* 2018; 18 (7): 758–68. DOI: 10.1016/S1473-3099(18)30225-1.
6. European Centre for Disease Prevention and Control. Technical Report. Molecular typing of *Neisseria gonorrhoeae* — a study of 2013 isolates. Stockholm: ECDC; 2018. Available from: <https://www.ecdc.europa.eu/sites/portal/files/documents/Molecular-typing-N-gonorrhoeae-web.pdf>.
7. Ilna EN, Oparina NY, Shitikov EA, Borovskaya AD, Govorun VM. Molecular surveillance of clinical *Neisseria gonorrhoeae* isolates in Russia. *J Clin Microbiol.* 2010; 48 (10): 3681–89. DOI: 10.1128/JCM.00565-10.
8. Шpileвaya M. B., Obraztsova O. A., Chestkov A. B. Использование методов генотипирования *Neisseria gonorrhoeae*. *Вестник дерматологии и венерологии.* 2015; (6): 33–40. DOI: 10.25208/0042-4609-2015-0-6-33-40.
9. Kubanov A, Solomka V, Plakhova X, Chestkov A, Petrova N, Shaskolskiy B, et al. Summary and trends of the Russian Gonococcal Antimicrobial Surveillance Programme, 2005–2016. *J Clin Microbiol.* 2019; 5 (6): e02024–18. DOI: 10.1128/JCM.02024-18.
10. Shaskolskiy B, Dementieva E, Kandinov I, Filippova M, Petrova N, Plakhova X, et al. Resistance of *Neisseria gonorrhoeae* isolates to beta-lactam antibiotics (benzylpenicillin and ceftriaxone) in Russia, 2015–2017. *PLoS One.* 2019; 14 (7): e0220339. DOI: 10.1371/journal.pone.0220339.
11. Воробьев Д. В., Соломка В. С., Плахова К. И., Дерябин Д. Г., Кубанов А. А. NG-MAST генотипирование штаммов *Neisseria gonorrhoeae*, выделенных на территории Российской Федерации в 2012–2015 годах. *Журнал Микробиологии, эпидемиологии и иммунобиологии.* 2016; (4): 42–51.



12. Martin IMC, Ison CA, Aanensen DM, Fenton KA, Sprat BG. Rapid sequence-based identification of gonococcal transmission clusters in a large metropolitan area. *J Infect Dis.* 2004; (189): 1497–505. DOI: 10.1086/383047.
13. Stamatakis A. Using RAxML to infer phylogenies. *Curr Protoc Bioinformatics.* 2015; 51 (1): 6.14.1–14.14. DOI: 10.1002/0471250953.bi0614s51.
14. Charrad M, Ghazzali N, Boiteau V, Niknafs A. NbClust: an R package for determining the relevant number of clusters in a data set. *Journal of Statistical Software.* 2014; 61 (6): 1–36, DOI: 10.18637/jss.v061.i06.
15. European Centre for Disease Prevention and Control. Technical Report. Molecular typing of *Neisseria gonorrhoeae* — results from a pilot study 2010–2011. Stockholm: ECDC; 2012. Available from: <https://www.ecdc.europa.eu/sites/portal/files/media/en/publications/Publications/201211109-Molecular-typing-gonorrhea.pdf>.
16. Chisholm SA, Unemo M, Quaye N, Johansson E, Cole MJ, Ison CA, et al. Molecular epidemiological typing within the European Gonococcal Antimicrobial Resistance Surveillance Programme reveals predominance of a multidrug-resistant clone. *Euro Surveill.* 2013; 18 (3): pii 20358. DOI: 10.2807/es.e18.03.20358-en.
17. Mlynarczyk-Bonikowska B, Malejczyk M, Majewski S, Unemo M. Antibiotic resistance and NG-MAST sequence types of *Neisseria gonorrhoeae* isolates in Poland compared to the world. *Postepy Dermatol Alergol.* 2018; 5 (6): 346–51. DOI: 10.5114/ada.2018.79780.
18. Shimuta K, Watanabe Y, Nakayama S, Morita-Ishihara T, Kuroki T, Unemo M, et al. Emergence and evolution of internationally disseminated cephalosporin-resistant *Neisseria gonorrhoeae* clones from 1995 to 2005 in Japan. *BMC Infect Dis.* 2015; (15): 378. DOI: 10.1186/s12879-015-1110-x.
19. Pandori M, Barry PM, Wu A, Ren A, Whittington WL, Liska S, et al. Mosaic penicillin-binding protein 2 in *Neisseria gonorrhoeae* isolates collected in 2008 in San Francisco, California. *Antimicrob Agents Chemother.* 2009; (53): 4032–34. DOI: 10.1128/AAC.00406-09.
20. Unemo M, Shafer WM. Antimicrobial resistance in *Neisseria gonorrhoeae* in the 21st century: past, evolution, and future. *Clin Microbiol Rev.* 2014; 27 (3): 587–613. DOI: 10.1128/CMR.00010-14.
21. Unemo M. Current and future antimicrobial treatment of gonorrhoea — the rapidly evolving *Neisseria gonorrhoeae* continues to challenge. *BMC Infect Dis.* 2015; (15): 364. DOI: 10.1186/s12879-015-1029-2.
22. European Centre for Disease Prevention and Control. Gonorrhoea. Annual epidemiological report for 2017. Stockholm: ECDC; 2019. Available from: <https://www.ecdc.europa.eu/sites/default/files/documents/gonorrhoea-annual-epidemiological-report-2017.pdf>.
23. Кубанова А. А., Кубанов А. А., Мелехина Л. Е., Богданова Е. В. Результаты деятельности медицинских организаций дерматовенерологического профиля, достигнутые в 2016 г. *Вестник дерматологии и венерологии.* 2017; (4): 12–27. DOI: 10.25208/0042-4609-2017-0-4-20-21.

## THE USE OF REAL-TIME PCR FOR EVALUATION OF ENDOMETRIAL MICROBIOTA

Voroshilina ES<sup>1,2</sup>✉, Zornikov DL<sup>2</sup>, Koposova OV<sup>2</sup>, Islamidi DK<sup>1,2</sup>, Ignatova KY<sup>1</sup>, Abakumova EI<sup>1</sup>, Kurbatova NV<sup>1</sup>, Plotko EE<sup>1</sup><sup>1</sup> "Garmonia" Medical Center, Yekaterinburg, Russia<sup>2</sup> Ural State Medical University, Yekaterinburg, Russia

Chronic endometritis (CE) in women of the reproductive age is associated with infertility and recurrent pregnancy loss. The aim of this study was to evaluate the endometrial microbiota by means of real-time PCR in reproductive-age women depending on the morphological pattern of the endometrium. Using the Androflor real-time PCR kit, we analyzed endometrial aspirate collected from 23 patients with chronic endometritis, 30 patients with endometrial hyperplasia, and 19 healthy women. DNA of up to 9 groups of microorganisms was detected in all the analyzed samples in the amounts exceeding negative control. The total bacterial load (TBL) of the detected microorganisms was  $10^3$ – $10^{6.4}$  (median  $10^{3.8}$ ) GE/ml. *Lactobacillus spp.* were detected the most often (86.1% of all samples). Opportunistic microorganisms (OM) were identified in 36.1% of all samples, including 22.2% of samples with lactobacilli and 13.9% — without lactobacilli. The variant of microbiota composition with *Lactobacillus*-dominance (more than 90% in the TBL) was detected significantly less often in women with chronic endometritis compared to healthy women. Real-time PCR could be used for assessment of endometrial microbiota and allows us to determine its characteristics depending on the morphological pattern.

**Keywords:** endometrial microbiota, real-time PCR, chronic endometritis, *Lactobacillus spp.*

**Acknowledgement:** the authors thank Khayutin V, director of "Garmonia" Medical Center (Yekaterinburg), for letting them use its facilities for this research study. We thank to the Center for Precision Genome Editing and Genetic Technologies for Biomedicine (Moscow) for the genetic research methods.

**Author contribution:** Voroshilina ES organized the study, reviewed the literature, performed real-time PCR and statistical analysis, contributed to manuscript preparation; Zornikov DL reviewed the literature, conducted statistical analysis, contributed to manuscript preparation; Koposova OV reviewed the literature, performed molecular genetic assays; Islamidi DK analyzed medical histories, recruited patients, performed endometrial aspiration and pipelle biopsies, contributed to manuscript preparation; Ignatova KY conducted histological examinations; Abakumova EI reviewed medical histories, recruited patients, performed endometrial aspiration and pipelle biopsies; Kurbatova NV reviewed medical histories, recruited patients, performed endometrial aspiration and pipelle biopsies; Plotko EE organized the study, reviewed the literature, contributed to manuscript preparation.

**Compliance with ethical standards:** the study was approved by the Ethics Committee of Ural State Medical University (Protocol № 7 dated September 20, 2019). Informed consent was obtained from all study participants.

✉ **Correspondence should be addressed:** Ekaterina C. Voroshilina  
Furmanova, 30, Yekaterinburg, 620142; voroshilina@gmail.com

**Received:** 03.02.2020 **Accepted:** 17.02.2020 **Published online:** 29.02.2020

**DOI:** 10.24075/brsmu.2020.012

## ВОЗМОЖНОСТИ ОЦЕНКИ МИКРОБИОТЫ ПОЛОСТИ МАТКИ С ИСПОЛЬЗОВАНИЕМ ПЦР В РЕАЛЬНОМ ВРЕМЕНИ

Е. С. Ворошилина<sup>1,2</sup>✉, Д. Л. Зорников<sup>2</sup>, О. В. Копосова<sup>2</sup>, Д. К. Исламиди<sup>1,2</sup>, К. Ю. Игнатова<sup>1</sup>, Е. И. Абакумова<sup>1</sup>, Н. В. Курбатова<sup>1</sup>, Е. Э. Плотко<sup>1</sup><sup>1</sup> Медицинский центр «Гармония», Екатеринбург, Россия<sup>2</sup> Уральский государственный медицинский университет, Екатеринбург, Россия

Наличие хронического эндометрита (ХЭ) у женщин репродуктивного возраста ассоциируют с бесплодием и невынашиванием беременности. Целью работы было оценить состояние микробиоты полости матки методом полимеразной цепной реакции в режиме реального времени (ПЦР-РВ) у женщин репродуктивного возраста в зависимости от морфологической картины эндометрия. С помощью теста «Андрофлор» исследовали микробиоту аспириата эндометрия, полученного от 23 пациенток с ХЭ, 30 пациенток с гиперплазией эндометрия и 19 здоровых женщин. Во всех исследуемых образцах обнаружили ДНК от 1–9 групп микроорганизмов в количествах, превышающих показатели, полученные для отрицательных контрольных образцов. Общая бактериальная масса выявляемых микроорганизмов (ОБМ) составила  $10^3$ – $10^{6.4}$  (медиана  $10^{3.8}$ ) ГЭ/мл. В 86,1% случаев выявили *Lactobacillus spp.* Условно-патогенные микроорганизмы идентифицировали в 36,1% образцов, в том числе в 22,2% — в сочетании с лактобациллами и в 13,9% — без лактобацилл. У пациенток с ХЭ достоверно реже в сравнении с группой здоровых женщин выявляли вариант микробиоты, характеризующийся наличием *Lactobacillus spp.* с удельным весом в ОБМ не менее 90%. Таким образом, метод ПЦР-РВ может быть использован для оценки микробиоты полости матки и позволяет определить ее особенности при различной морфологической картине эндометрия.

**Ключевые слова:** микробиота эндометрия, ПЦР-РВ, хронический эндометрит, *Lactobacillus spp.*

**Благодарности:** авторы благодарят В. Хаютина, директора медицинского центра «Гармония» (г. Екатеринбург), за возможность выполнения исследования на базе центра. Авторы признательны Центру высокоточного редактирования и генетических технологий для биомедицины (Москва) за помощь в методах исследования.

**Вклад авторов:** Е. С. Ворошилина — организация исследования, молекулярно-генетические исследования, анализ данных, статистический анализ, написание статьи; Д. Л. Зорников — анализ данных, статистический анализ, написание статьи; О. В. Копосова — анализ данных, молекулярно-генетические исследования; Д. К. Исламиди — клинический анализ, отбор пациентов, взятие образцов, написание статьи; К. Ю. Игнатова — патоморфологические исследования; Е. И. Абакумова — клинический анализ, отбор пациентов, взятие образцов; Н. В. Курбатова — клинический анализ, отбор пациентов, взятие образцов; Е. Э. Плотко — организация исследования, анализ данных, написание статьи.

**Соблюдение этических стандартов:** исследование одобрено этическим комитетом Уральского государственного медицинского университета (протокол № 7 от 20 сентября 2019 г.). Все участники исследования подписали добровольное информированное согласие на проведение исследования.

✉ **Для корреспонденции:** Екатерина Сергеевна Ворошилина  
ул. Фурманова, д. 30, г. Екатеринбург, 620142; voroshilina@gmail.com

**Статья получена:** 03.02.2020 **Статья принята к печати:** 17.02.2020 **Опубликована онлайн:** 29.02.2020

**DOI:** 10.24075/vrgmu.2020.012



For a long time, uterine cavity was thought to be sterile [1]. Recently, the implementation of molecular-based assays has made it possible to identify difficult to culture or unculturable microorganisms collected from the endometrial surface of reproductive-age women [2–7]. There is no consensus on the contribution of opportunistic microorganisms (OM) to the development of endometrial inflammation [8, 9], and this raises doubts about the necessity of antimicrobial therapy in patients with chronic endometritis (CE). Importantly, CE is diagnosed in about 10% of women of reproductive age [10] and is associated with infertility and recurrent pregnancy loss [1, 8, 11–14].

For weak positive results of molecular assays, interpretation is always difficult due to the possibility of contamination of the analyzed sample. On the one hand, vaginal or cervical microbiota could be the source of such contamination because the transcervical method for endometrial sampling is common in clinical practice [5, 6]. On the other hand, small concentrations of bacterial DNA could be present in DNA extraction kits (this is known as kitome) due to a number of reasons, and it is almost impossible to fully exclude the presence of contaminating DNA [15]. The latter does not present a problem when analyzing biotopes with high bacterial concentrations, such as feces or vaginal discharge, because in this case the concentrations of the analyzed DNA by far exceed those of the kitome. However, even minor amounts of such contaminants can endanger endometrial testing: in the endometrium, microbial concentrations rarely exceed  $10^4$  cells per sample [16].

Currently, most endometrial microbiota testing relies on the use of next-generation sequencing (NGS) [3–6], which is an expensive and labor-intensive approach more suitable for scientific research rather than routine analysis and not universally available in practical healthcare. By contrast, quantitative real-time polymerase chain reaction (real-time PCR) is a molecular technique most suitable for routine usage: robust, simple, affordable and easily standardized. However, there have been only few reports on the use of real-time PCR for endometrial microbiota analysis [7, 17].

The aim of this study is to evaluate a potential correlation of the state of endometrial microbiota and the morphological pattern of the endometrium in women of reproductive age by means of real-time PCR.

## METHODS

### Participants

Seventy-two reproductive-age women (age range 21–45 years, mean age  $33 \pm 5.2$  years) who sought preconception care or medical advice about their reproductive health at the “Garmonia” Medical Center (Yekaterinburg) between September and December 2019 were recruited for the study.

The following inclusion criteria were applied: age of 18–45 years; no current pregnancy; a regular menstrual cycle; bad obstetric and gynecological history including infertility, induced or spontaneous abortion, missed abortion, chronic endometritis.

Exclusion criteria: intake of hormonal contraceptives or an intrauterine device at the time of examination or within 6 months before it; cancer; HIV; pelvic or lower genital tract inflammation at the time of examination; antibacterial treatment within 4 weeks before the study.

### Endometrial sampling

Endometrial aspirates were collected on day 7–10 of the menstrual cycle using Endobrush Standard for Endometrial

Cytology (Laboratoire C.C.D.; France). Endobrush is protected from endocervical contamination by a sheath. It opens only after being introduced into the endometrial cavity and retracts into the sheath before withdrawal. For sampling, the cervix was brought into full view using a speculum. The cervix was swabbed with 0.05% chlorhexidine solution applied on a cotton ball, and the brush was inserted into the endometrial cavity so that it did not come in contact with the vaginal wall. After the brush was withdrawn from the endometrial cavity, the sheath surface was cleaned with a sterile swab soaked in 95% ethanol in order to remove cervical discharge and prevent contamination of the specimen with cervical microbiota. Then the brush was released from the sheath and the specimen was immersed in PreservCyt Solution (Hologic, Inc.; USA) intended for the preservation of cell samples for *in vitro* diagnostic tests.

After endometrial aspiration, Pipelle biopsy was performed on all the participants in order to collect endometrial samples for a histopathological examination. Biopsy samples were placed into test tubes containing 10% buffered formalin.

### DNA extraction

DNA extraction was done using PREP-NA-PLUS kit (DNA-Technology, Russia). Before DNA extraction, endometrial specimens were deproteinized. Briefly, test tubes containing endometrial aspirates were centrifuged in a MiniSpin centrifuge (Eppendorf; Germany) at 13,000 rpm for 10 min; the supernatant was removed, and the pellet was resuspended in 100  $\mu$ l of the lysing solution from the PREP-NA-PLUS kit. The homogenized sample (50  $\mu$ l) was transferred into a clean tube containing a mixture of 25  $\mu$ l of the lysing solution (from the PREP-NA-PLUS kit), 5  $\mu$ l of proteinase K (20 mg/ml) (VWR Life Science; USA) and 120  $\mu$ l of sterile normal 0.9% saline. After the components were mixed, the samples were incubated at 60 °C for 30 min and then at 95 °C for 10 min. Upon incubation, the tubes were centrifuged at 13,000 rpm for 60 s. The supernatant (100  $\mu$ l) was then used for DNA extraction following the manufacturer's protocol.

### Evaluation of endometrial microbiota

Detection of DNA of sexually transmitted obligate pathogens and of opportunistic microorganisms (OM) in the endometrial samples by means of real-time PCR was performed using the Androflor real-time PCR kit and DTPPrime 4M1 real-time PCR instrument (DNA-Technology, Russia). The kit allows detection of a wide range of bacteria, which could play a role in endometrial inflammation. Androflor allows quantification of 24 groups of bacteria, including *Lactobacillus* spp., *Staphylococcus* spp., *Streptococcus* spp., *Corynebacterium* spp., *Gardnerella vaginalis* (*G. vaginalis*), *Megasphaera* spp., *Veillonella* spp., *Dialister* spp., *Sneathia* spp., *Leptotrichia* spp., *Fusobacterium* spp., *Ureaplasma urealyticum* (*U. urealyticum*), *Ureaplasma parvum* (*U. parvum*), *Mycoplasma hominis* (*M. hominis*), *Atopobium* cluster, *Bacteroides* spp., *Porphyromonas* spp., *Prevotella* spp., *Anaerococcus* spp., *Peptostreptococcus* spp., *Parvimonas* spp., *Eubacterium* spp., *Haemophilus* spp., *Pseudomonas aeruginosa*, *Ralstonia* spp., *Burkholderia* spp., *Enterobacteriaceae* spp./*Enterococcus* spp., *Trichomonas vaginalis* (*T. vaginalis*), *Neisseria gonorrhoeae* (*N. gonorrhoeae*), *Chlamydia trachomatis* (*C. trachomatis*), *Mycoplasma genitalium* (*M. genitalium*), and *Candida* spp.

The quantity of each bacterium/group of bacteria was automatically estimated from threshold cycle values, and the proportion of the microorganism in relation to the total bacterial

load (TBL) was calculated. Sterile deionized water was used as a negative control (NC). For some groups of bacteria, NC produced positive signals at the cycle of quantification (Cq) with value more than 35 (which corresponded to the bacterial DNA concentration of  $< 10^3$  genome equivalents per sample, GE/sample). With that in mind, we assumed the DNA concentration of at least  $10^3$  GE/sample to be significant (Cq values less than 35). Lower values were interpreted as negative, considering the high sensitivity of the method and the inability to differentiate between potential DNA-contaminations and very weak positive signals in the samples.

*U. urealyticum*, *U. parvum* and *M. hominis* were an exception, as no positive signal was recorded in the NC. For these groups of microorganisms, a detectable signal during any amplification cycle was interpreted as positive.

### Histopathological examination

Pipelle biopsy samples were subjected to a histopathological examination. The specimens were fixed in 10% neutral buffered formalin and processed following the standard protocol. Paraffin sections of standard thickness (5.0  $\mu$ m) were stained with hematoxylin-eosin. Microscopy was carried out using a light binocular microscope Eclipse E200 (Nikon; Japan) (10 $\times$ , 40 $\times$  objective lens, 10 $\times$  eyepiece lens).

### Statistical analysis

The mean age of the patients was expressed as an average and a standard deviation. Average TBL and microbial concentrations were expressed as medians. Dispersion within the groups was described using 5<sup>th</sup> and 95<sup>th</sup> percentiles. These parameters were calculated in Microsoft Office Excel 2007 (Microsoft Corp.; USA).

The significance of differences between mean TBL and microbial concentrations was measured using the Kruskal-Wallis test (for the comparison of 3 groups) and the Mann-

Whitney U test (for the comparison of 2 groups). The data were processed in IBM SPSS Statistics 20 (IBM Corp.; USA). To compare frequencies between the groups, two-tailed Fisher's exact test was applied (WinPepi; JH Abramson; Israel). In all cases the differences were considered significant at  $p < 0.05$ .

## RESULTS

### Histopathological examination results

Depending on the morphological appearance of the endometrium, the participants were divided into 3 groups [18].

Group 1 (chronic endometritis, CE) included 23 patients with CE. The diagnosis was based on the signs of productive inflammation, formation of lymphoid follicles, endometrial stromal fibrosis, and sclerotic changes to the walls of spiral arteries.

Group 2 (endometrial hyperplasia, EHP) consisted of 30 patients with simple endometrial hyperplasia without atypia. The diagnosis was based on histology findings showing signs of cell proliferation in endometrial crypts and cytogenous stroma, spiral arteries with/without cell and nuclear polymorphism.

Group 3 (healthy women) included 19 patients without any structural changes in the endometrium; its morphology matched the day of the menstrual cycle.

### Molecular screening results

Bacterial DNA was detected in all of 72 endometrial samples: TBL ranged from  $10^3$  to  $10^{6.4}$  (median:  $10^{3.8}$ ) GE/sample. No significant differences in TBL were detected between the group of patients with endometrial pathology and healthy women. Endometrial TBL measured by real-time PCR varied 100–10,000-fold from vaginal TBL typically observed in reproductive-age women [19].

*Lactobacillus spp.* were detected the most often (in 86.1% of cases;  $n = 62$ ). *G.vaginalis* were detected in 19

**Table 1.** Detection rate of bacterial groups determined by real-time PCR in morphologically different endometrial samples

Groups of bacteria	Detection rate in the studied patient groups (n / %)			
	Group 1 — CE N = 23	Group 2 — EHP N = 30	Group 3 — healthy women N = 19	Total N = 72
<i>Lactobacillus spp.</i>	19/82.6	25/83.3	18/94.7	62/86.1
<i>Staphylococcus spp.</i>	0	0	0	0
<i>Streptococcus spp.</i>	1 / 4.3	0	0	1/1.4
<i>Corynebacterium spp.</i>	0	3/10.0	0	3/4.2
<i>Gardnerella vaginalis</i>	7/30.4	9/30.0	3/15.8	19/26.4
<i>Megasphaera spp. / Veillonella spp. / Dialister spp.</i>	1/4.3	2/6.7	0	3/4.2
<i>Sneathia spp. / Leptotrichia spp. / Fusobacterium spp.</i>	1/4.3	0	0	1/1.4
<i>Atopobium cluster</i>	1/4.3	3/10.0	0	4/5.6
<i>Bacteroides spp. / Porphyromonas spp. / Prevotella spp.</i>	2/8.7	3/10.0	2/10.5	7/9.7
<i>Anaerococcus spp.</i>	0	1/3.3	0	1/1.4
<i>Peptostreptococcus spp. / Parvimonas spp.</i>	2/8.7	0	2/10.5	4/5.6
<i>Eubacterium spp.</i>	2/8.7	3/10.0	1/5.3	6/8.3
<i>Haemophilus spp.</i>	1/4.3	0	0	1/1.4
<i>Pseudomonas aeruginosa / Ralstonia spp. / Burkholderia spp.</i>	0	1/3.3	0	1/1.4
<i>Enterobacteriaceae spp. / Enterococcus spp.</i>	4/17.4	3/10.0	1/5.6	8/11.3
<i>Ureaplasma urealyticum</i>	0	1/3.3	0	1/1.4
<i>Ureaplasma parvum</i>	4/17.4	4/13.3	1/5.3	9/12.5
<i>Mycoplasma hominis</i>	3/13.0%	2/6.7	0	5/6.9

(26.8%) samples, *U. parvum*, in 9 (12.7%) samples, and *Enterobacteriaceae* spp. / *Enterococcus* spp., in 8 (11.3%) samples. Other groups of microorganisms were detected in single samples (Table 1).

The detection rate of certain groups of bacteria varied in women with different histological pattern. Although the variance was insignificant, which might be explained by the small sample size, we noticed a few interesting trends. Only a few groups of OM included in the kit were detected in the samples with normal histological pattern. By contrast, OM detected in the samples collected from patients with CE and EHP represented the entire range of the target microorganisms, except for *Staphylococcus* spp.

Some OM were detected more frequently in women with CE and EHP. For example, DNA of *G. vaginalis* was found in 30% of patients with endometrial pathology, whereas only 16.7% of healthy women had this pathogen. *U. parvum* and *M. hominis* were detected in 17.4 and 13.0% of the samples that met the criteria for CE, respectively, whereas only one woman from the group of healthy women had *U. parvum*.

No obligate sexually transmitted pathogens were detected in the endometrial tissue of our patients.

We detected from 1 up to 9 microbial groups in every sample (Fig. 1.) The endometrial microbiota of healthy women was represented by one group of bacteria in 78.9% of cases (15 of 19 samples), in their endometrium, whereas only 9 (39.1%) of 23 patients with CE had one group of bacteria detected in their specimens ( $p = 0.013$ ). Most often, the microbiota of patients with CE was represented by two microbial groups (11 or 47.8% of 23 samples). In patients with EHP, one group of bacteria was detected in 16 (53.3%) of 30 samples; for the remaining 14 patients, the microbiota was represented by two or more bacterial groups. On the whole, the microbiota of patients whose histology was suggestive of EHP or CE tended to be more diverse in its composition than in healthy women.

Quantitative parameters for every group of bacteria are shown in Table 2. No statistical differences were observed between 3 groups of patients (CE, EHP, healthy women).

Given the large number of microbial groups identified by the kit, we decided to calculate the quantity of OM per sample for further analysis. Then, we calculated the proportion of lactobacilli and the proportion of OM relative to TBL per sample. Based on these calculations, 3 types of endometrial microbiota were distinguished:

Type 1) *Lactobacilli-dominated type of microbiota*. The proportion of Lactobacilli constituted no less than 90% of the TBL; the rest groups of bacteria were either undetected or found in very small quantities (less than 10% of the TBL).

Type 2) *Mixed type microbiota*. The proportion of Lactobacilli was no more than 90% (but at least 10%) of the TBL, OM made up at least 10% of the TBL. Depending on the prevalent microorganisms, there can be subtypes of this microbiota type.

Type 3) *Opportunistic microorganisms (OM)-dominated type microbiota (in the total absence of Lactobacillus spp.)*. Depending on the OM group detected, this type of microbiota can be also divided into a few subtypes.

Forty-six (63.9%) of 72 samples met the criteria for type 1 microbiota; 16 (22.2%), for type 2, and 10 (13.9%), for type 3. Thus, in the majority of the participants, the endometrial microbiota was represented by either lactobacilli or a combination of lactobacilli and the OM. In the next step, we analyzed the detection rate of the identified microbiota types in the studied groups of patients.

The endometrial microbiota of 16 (84.2%) out of 19 healthy women fitted the criteria for type 1 (Lactobacilli-dominated) (Fig. 2). Two (10.5%) of 19 samples met the criteria for type 2. Type 3 (OM-dominated) was identified in one (5.3%) sample. Interestingly, OM were represented by *G. vaginalis* in all the 3 samples.

In patients with EHP, microbiota types 2 and 3 were detected more frequently than in healthy women, but the differences were statistically insignificant. Five (16.7%) of 30 samples were classified as type 2; in all those samples, OM were represented by *G. vaginalis*. Type 3 was observed in 5 (16.7%) samples; in 4 of them, OM were represented by *G. vaginalis*; in one case, by *Enterobacteriaceae* spp. / *Enterococcus* spp.

The greatest diversity was observed for the microbiota of women with CE. Type 1 (dominated by lactobacilli) was identified in 10 (43.5%) of 23 women ( $p = 0.012$ , comparison with healthy women). Type 2 microbiota was observed in 9 (39.1%) samples; in 5 of them, OM were represented by obligate anaerobes (*G. vaginalis* and *Bacteroides* spp. / *Porphyromonas* spp. / *Prevotella* spp.) and in other 4 samples, OM were represented by facultative gram-positive and gram-negative anaerobes. Type 3 microbiota was identified in 4 (17.4%) of 23 samples. In this subset, OM were represented by *G. vaginalis* in 2 cases and by *Enterobacteriaceae* spp. / *Enterococcus* spp. in one case; the association of *Peptostreptococcus* spp. /

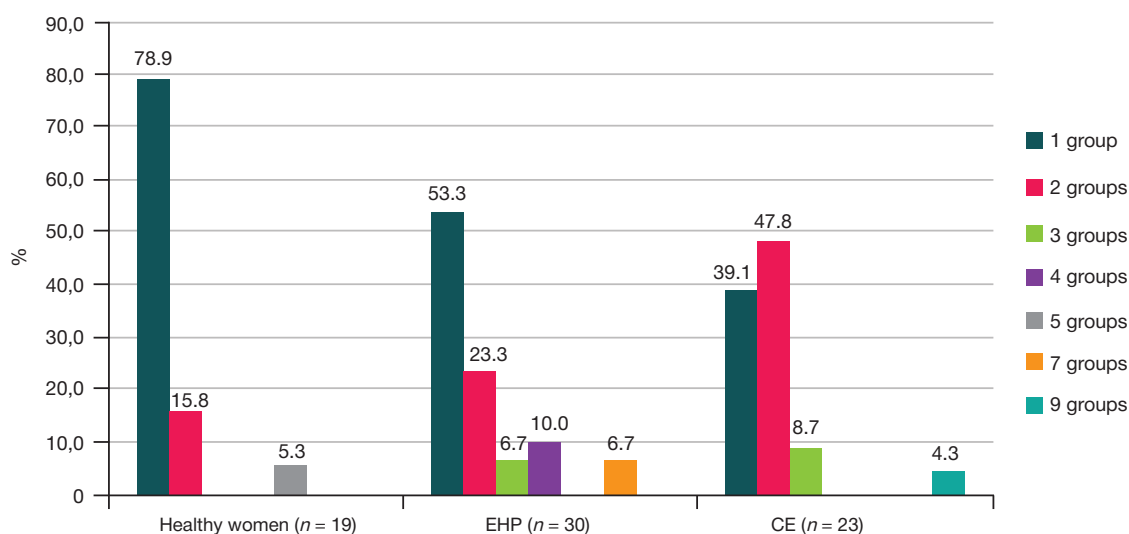


Fig. 1. The number of microbial groups detected per sample in patients with different morphological appearance of the endometrium (\* $p = 0.013$ )

**Table 2.** Qualitative and quantitative endometrial microbiota composition assessed by real-time PCR in the study participants ( $N = 72$ )

Groups of bacteria	Median (5 <sup>th</sup> –95 <sup>th</sup> percentile)			
	Group 1 CE, $N = 23$	Group 2 EHP, $N = 30$	Group 3 Healthy women, $N = 19$	Total $N = 72$
TBL	$10^{3.8}$ ( $10^{3.2}$ – $10^{4.7}$ )	$10^{3.8}$ ( $10^{3.3}$ – $10^{5.1}$ )	$10^{3.9}$ ( $10^{3.3}$ – $10^{5.1}$ )	$10^{3.8}$ ( $10^{3.3}$ – $10^{5.1}$ )
<i>Lactobacillus</i> spp.	$10^{3.8}$ ( $0$ – $10^{4.6}$ )	$10^{3.7}$ ( $0$ – $10^{5.1}$ )	$10^{3.8}$ ( $10^{2.6}$ – $10^{5.1}$ )	$10^{3.8}$ ( $0$ – $10^{4.9}$ )
<i>Staphylococcus</i> spp.	0 0	0 0	0 0	0 0
<i>Streptococcus</i> spp.	0 0	0 0	0 0	0 0
<i>Corynebacterium</i> spp.	0 0	0 ( $0$ – $10^{3.1}$ )	0 0	0 0
<i>Gardnerella vaginalis</i>	0 ( $0$ – $10^{3.8}$ )	0 ( $0$ – $10^{3.7}$ )	0 ( $0$ – $10^{3.2}$ )	0 ( $0$ – $10^{3.8}$ )
<i>Megasphaera</i> spp. / <i>Veillonella</i> spp. / <i>Dialister</i> spp.	0 0	0 0	0 0	0 0
<i>Sneathia</i> spp. / <i>Leptotrichia</i> spp. / <i>Fusobacterium</i> spp.	0 0	0 0	0 0	0 0
<i>Atopobium</i> cluster	0 0	0 ( $0$ – $10^{3.2}$ )	0 0	0 ( $0$ – $10^{1.5}$ )
<i>Bacteroides</i> spp. / <i>Porphyromonas</i> spp. / <i>Prevotella</i> spp.	0 0	0 ( $0$ – $10^{3.2}$ )	0 ( $0$ – $10^{3.3}$ )	0 ( $0$ – $10^{3.2}$ )
<i>Anaerococcus</i> spp.	0 0	0 0	0 0	0 0
<i>Peptostreptococcus</i> spp. / <i>Parvimonas</i> spp.	0 ( $0$ – $10^{2.8}$ )	0 0	0 ( $0$ – $10^{3.0}$ )	0 ( $0$ – $10^{1.5}$ )
<i>Eubacterium</i> spp.	0 ( $0$ – $10^{2.7}$ )	0 ( $0$ – $10^{3.0}$ )	0 ( $0$ – $10^{0.5}$ )	0 ( $0$ – $10^{3.0}$ )
<i>Haemophilus</i> spp.	0 0	0 0	0 0	0 0
<i>Pseudomonas aeruginosa</i> / <i>Ralstonia</i> spp. / <i>Burkholderia</i> spp.	0 0	0 0	0 0	0 0
<i>Enterobacteriaceae</i> spp. / <i>Enterococcus</i> spp.	0 ( $0$ – $10^{3.3}$ )	0 ( $0$ – $10^{3.1}$ )	0 ( $0$ – $10^{0.5}$ )	0 ( $0$ – $10^{3.2}$ )
<i>Ureaplasma urealyticum</i>	0 0	0 0	0 0	0 0
<i>Ureaplasma parvum</i>	0 ( $0$ – $10^{1.9}$ )	0 ( $0$ – $10^{1.9}$ )	0 ( $0$ – $10^{0.1}$ )	0 ( $0$ – $10^{1.8}$ )
<i>Mycoplasma hominis</i>	0 ( $0$ – $10^{2.4}$ )	0 ( $0$ – $10^{1.1}$ )	0 0	0 ( $0$ – $10^{2.2}$ )

*Parvimonas* spp. and *Enterobacteriaceae* spp. / *Enterococcus* spp. was observed in one sample.

Thus, OM-dominated endometrial microbiota was more commonly observed in patients with CE.

## DISCUSSION

In this study, endometrial microbiota was evaluated by real-time PCR, an inexpensive and technologically advanced technique. Our findings were consistent with the reports of other researchers who used costly techniques like NGS [2–6].

Bacterial DNA was detected in all endometrial samples in quantities ranging from  $10^3$  to  $10^5$  GE/sample; DNA content differed between the samples 10–100-fold. Similar results are reported by other authors who collected samples transcervically [2, 5, 6]. This sampling approach carries a risk of contamination [5, 6]. This could explain the presence of bacterial DNA in all samples analyzed in our study. For the sake of the experiment, the researchers analyzed endometrial samples collected

from the middle section of the endometrial cavity after transabdominal hysterectomy in females of late reproductive age with uterine/endometrial pathology [20]. Bacterial DNA (in quantities exceeding NC counts) was detected in 60% of the samples. However, such approach is unacceptable in clinical practice. The sampling technique and the device we used for transcervical collection of endometrial samples minimized the risk of contamination, but could not eliminate it completely.

Lactobacilli DNA was detected in the majority of the analyzed samples, which is also consistent with the literature [7]. Lactobacilli-dominated endometrial microbiota is considered to be a positive prognostic factor for successful embryo implantation via assisted reproductive technology and for good pregnancy outcome [2]. In our study, lactobacilli were detected in the majority of the samples, but their concentrations and proportion in relation to TBL varied.

Obligate and facultative anaerobes were detected in every third sample, both in the presence or absence of lactobacilli.

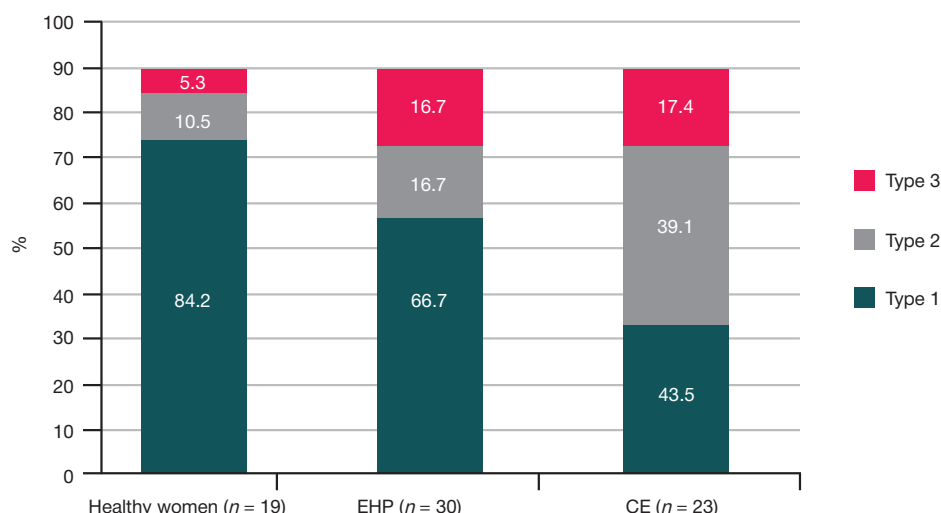


Fig. 2. Detection rate of different endometrial microbiota types in women with different morphological appearance of the endometrium (\* $p = 0.011$ )

OM were detected significantly less often in healthy women than in patients with CE.

Based on the proportion of lactobacilli and OM, we identified 3 types of endometrial microbiota; their detection rates varied in patients with CE or EHP and healthy women. In most cases, the endometrial microbiota of healthy women was represented by one group of microorganisms; as a rule, it was *Lactobacillus spp.* The presence of this microbiota type in women with CE does not seem to require antibacterial treatment and is consistent with contemporary views on the leading role of autoimmune mechanisms in the pathogenesis of CE. OM detected in the endometrial cavity of women with histology results suggestive of endometritis could be an additional marker indicating the significance of these bacteria for promoting inflammation. Further research is needed to explore a possible association between the presence of OM and EHP.

Our findings confirm that endometrial cavity is not a sterile environment. In some aspects, endometrial microbiota is similar to vaginal microbiota: in our study, lactobacilli were detected in the uterine cavity in 86.1% of all samples and were prevalent in the endometrial microbiota in 63.9% of all cases. At the same time, the quantity of bacteria present in the uterine cavity is much lower (100 to 10,000-fold) than that in the vagina. Compositional similarities between the microbiotas of upper and lower female genital tracts and the role of lactobacilli found in the endometrial cavity are yet to be elucidated. Also, it is not clear whether the bacteria detected in the endometrium should be considered resident or transient microorganisms.

## CONCLUSIONS

1. The use of real-time PCR allowed us to detect bacterial DNA in quantities exceeding those for the negative control in all endometrial aspirates.
2. In each sample of endometrial aspirate, 1–9 groups of microorganisms were detected. *Lactobacillus spp.* were the most common microorganism. They were detected in 86.1% of the specimens, of which 22.2% were characterized by a combination of Lactobacilli and OM. The endometrial microbiota of 13.9% patients was represented by OM only (mostly, obligate anaerobes).
3. Comprehensive evaluation of the endometrial microbiota profile, based on the proportion of *Lactobacillus spp.* and OM in relation to the TBL allowed us to distinguish three microbiota types: Lactobacilli-dominated type, OM-dominated type, and mixed type.
4. In most women with histologically confirmed CE, OM were detected in the endometrial microbiota, while in histologically normal endometrium *Lactobacillus spp.* were prevalent in the microbiota (the proportion in the TBL is not less than 90%).
5. Currently, there is no unified approach to the diagnosis and treatment of chronic endometritis. Thus, the use of modern molecular-based techniques seems promising for evaluating endometrial microbiota and its role in the onset of the inflammatory process. A study of the microbiota of the endometrium by means of real-time PCR will allow us to verify the diagnosis and prescribe pathogenetically based therapy, which will improve the outcomes of subsequent pregnancies.

## References

1. Cicinelli E, Matteo M, Tinelli R, Pinto V, Marinaccio M, Indraccolo U, et al. Chronic endometritis due to common bacteria is prevalent in women with recurrent miscarriage as confirmed by improved pregnancy outcome after antibiotic treatment. *Reprod Sci.* 2014; (21): 640–7.
2. Moreno I, Codoñer FM, Vilella F, Valbuena D, Martínez-Blanch JF, Jiménez-Almazán J, et al. Evidence that the endometrial microbiota has an effect on implantation success or failure. *Am J Obstet Gynecol.* 2016 Dec; 215 (6): 684–703.
3. Moreno I, Franasiak JM. Endometrial microbiota-new player in town. *Fertil Steril.* 2017 Jul; 108 (1): 32–39.
4. Perez-Muñoz ME, Arrieta MC, Ramer-Tait AE, Walter J. A critical assessment of the "sterile womb" and "in utero colonization" hypotheses: implications for research on the pioneer infant microbiome. *Microbiome.* 2017 Apr 28; 5 (1): 48.
5. Baker JM, Chase DM, Herbst-Kralovetz MM. Uterine Microbiota: Residents, Tourists, or Invaders? *Front Immunol.* 2018 Mar 2; (9): 208.
6. Peric A, Weiss J, Vulliamoz N, Baud D, Stojanov M. Bacterial Colonization of the Female Upper Genital Tract. *Int J Mol Sci.* 2019 Jul 11; 20 (14) pii: E3405.
7. Tsyurdeeva ND, Shipitsyna EV, Savicheva AM, Gzgyan AM, Kogan IYu. Composition of endometrial microbiota and chronic endometritis severity in patients with in vitro fertilization failures. Is there any connection? *Journal of Obstetrics and Women's Diseases.* 2018; 67 (2): 5–15. Russian.
8. Cicinelli E, Resta L, Nicoletti R, Tartagni M, Marinaccio M, Bulletti C,




- et al. Detection of chronic endometritis at fluid hysteroscopy. *J Minim Invasive Gynecol.* 2005 Nov-Dec; 12 (6): 514–8.
9. Espinoza J, Erez O, Romero R, Preconceptional antibiotic treatment to prevent preterm birth in women with a previous preterm delivery. *Am J Obstet Gynecol.* 2006 Mar; 194 (3): 630–7.
  10. Gombolevskaia NA, Marchenko LA. Modern diagnostic criteria of chronic endometritis (a review). *Russian Journal of Human Reproduction.* 2012; 18 (1): 42–6. Russian.
  11. Kushnir VA, Solouki S, Sarig-Meth T, Vega MG, Albertini DF, Darmon SK et al. Systemic inflammation and autoimmunity in women with chronic endometritis. *Am J Reprod Immunol.* 2016; (75): 672–7.
  12. Yang R, Du X, Wang Y, Song X, Yang Y, Qiao J. The hysteroscopy and histological diagnosis and treatment value of chronic endometritis in recurrent implantation failure patients. *Arch Gynecol Obstet.* 2014; (289): 1363–9.
  13. Cicinelli E, Matteo M, Tinelli R, Lepera A, Alfonso R, Indraccolo U, et al. Prevalence of chronic endometritis in repeated unexplained implantation failure and the IVF success rate after antibiotic therapy. *Hum Reprod.* 2015; (30): 323–30.
  14. Johnston-MacAnanny EB, Hartnett J, Engmann LL, Nulsen JC, Sanders MM, Benadiva CA. Chronic endometritis is a frequent finding in women with recurrent implantation failure after in vitro fertilization. *Fertil Steril.* 2010; (93): 437–41.
  15. de Goffau MC, Lager S, Salter SJ, Wagner J1, Kronbichler A, Charnock-Jones DS, et al. Recognizing the reagent microbiome. *Nat Microbiol.* 2018 Aug; 3 (8): 851–3.
  16. Salter SJ, Cox MJ, Turek EM, Calus ST, Cookson WO, Moffatt MF, et al. Reagent and laboratory contamination can critically impact sequence-based microbiome analyses. *BMC Biol.* 2014 Nov 12; (12): 87.
  17. Mitchell CM, Haick A, Nkwopara E, Garcia R, Rendi M, Agnew K, et al. Colonization of the upper genital tract by vaginal bacterial species in nonpregnant women. *Am J Obstet Gynecol.* 2015 May; 212 (5): 611.e1–9.
  18. Palcev MA, Kakturskij LV, Zajrat'janc OV, editors. *Pathological anatomy: national guide.* M.: GJeOTAR-Media, 2014; 1264 p.
  19. Voroshilina ES, Tumbinskaya LV, Donnikov AE, Plotko EA, Khayutin LV. Vaginal biocenosis in the context of view of quantitative polymerase chain reaction: what is its norm? *Obstetrics and Gynecology.* 2011; (1): 57–65. Russian.
  20. Winters AD, Romero R, Gervasi MT, Gomez-Lopez N, Tran MR, Garcia-Flores V, et al. Does the endometrial cavity have a molecular microbial signature? *Sci Rep.* 2019 Jul 9; 9 (1): 9905.

## Литература

1. Cicinelli E, Matteo M, Tinelli R, Pinto V, Marinaccio M, Indraccolo U, et al. Chronic endometritis due to common bacteria is prevalent in women with recurrent miscarriage as confirmed by improved pregnancy outcome after antibiotic treatment. *Reprod Sci.* 2014; (21): 640–7.
2. Moreno I, Codoñer FM, Vilella F, Valbuena D, Martinez-Blanch JF, Jimenez-Almazán J, et al. Evidence that the endometrial microbiota has an effect on implantation success or failure. *Am J Obstet Gynecol.* 2016 Dec; 215 (6): 684–703.
3. Moreno I, Franasiak JM. Endometrial microbiota-new player in town. *Fertil Steril.* 2017 Jul; 108 (1): 32–39.
4. Perez-Muñoz ME, Arrieta MC, Ramer-Tait AE, Walter J. A critical assessment of the "sterile womb" and "in utero colonization" hypotheses: implications for research on the pioneer infant microbiome. *Microbiome.* 2017 Apr 28; 5 (1): 48.
5. Baker JM, Chase DM, Herbst-Kralovetz MM. Uterine Microbiota: Residents, Tourists, or Invaders? *Front Immunol.* 2018 Mar 2; (9): 208.
6. Peric A, Weiss J, Vulliemoz N, Baud D, Stojanov M. Bacterial Colonization of the Female Upper Genital Tract. *Int J Mol Sci.* 2019 Jul 11; 20 (14) pii: E3405.
7. Цыпурдеева Н. Д., Шипицына Е. В., Савичева А. М., Гэгззян А. М., Коган И. Ю. Состав микробиоты эндометрия и степень выраженности хронического эндометрита у пациенток с неэффективными протоколами экстракорпорального оплодотворения. Есть ли связь? *Журнал акушерства и женских болезней.* 2018; 67 (2): 5–15.
8. Cicinelli E, Resta L, Nicoletti R, Tartagni M, Marinaccio M, Bulletti C, et al. Detection of chronic endometritis at fluid hysteroscopy. *J Minim Invasive Gynecol.* 2005 Nov-Dec; 12 (6): 514–8.
9. Espinoza J, Erez O, Romero R, Preconceptional antibiotic treatment to prevent preterm birth in women with a previous preterm delivery. *Am J Obstet Gynecol.* 2006 Mar; 194 (3): 630–7.
10. Гомболевская Н. А., Марченко Л. А. Современные критерии диагностики хронического эндометрита (обзор литературы). *Проблемы репродукции.* 2012; 18 (1): 42–46.
11. Kushnir VA, Solouki S, Sarig-Meth T, Vega MG, Albertini DF, Darmon SK et al. Systemic inflammation and autoimmunity in women with chronic endometritis. *Am J Reprod Immunol.* 2016; (75): 672–7.
12. Yang R, Du X, Wang Y, Song X, Yang Y, Qiao J. The hysteroscopy and histological diagnosis and treatment value of chronic endometritis in recurrent implantation failure patients. *Arch Gynecol Obstet.* 2014; (289): 1363–9.
13. Cicinelli E, Matteo M, Tinelli R, Lepera A, Alfonso R, Indraccolo U, et al. Prevalence of chronic endometritis in repeated unexplained implantation failure and the IVF success rate after antibiotic therapy. *Hum Reprod.* 2015; (30): 323–30.
14. Johnston-MacAnanny EB, Hartnett J, Engmann LL, Nulsen JC, Sanders MM, Benadiva CA. Chronic endometritis is a frequent finding in women with recurrent implantation failure after in vitro fertilization. *Fertil Steril.* 2010; (93): 437–41.
15. de Goffau MC, Lager S, Salter SJ, Wagner J1, Kronbichler A, Charnock-Jones DS, et al. Recognizing the reagent microbiome. *Nat Microbiol.* 2018 Aug; 3 (8): 851–3.
16. Salter SJ, Cox MJ, Turek EM, Calus ST, Cookson WO, Moffatt MF, et al. Reagent and laboratory contamination can critically impact sequence-based microbiome analyses. *BMC Biol.* 2014 Nov 12; (12): 87.
17. Mitchell CM, Haick A, Nkwopara E, Garcia R, Rendi M, Agnew K, et al. Colonization of the upper genital tract by vaginal bacterial species in nonpregnant women. *Am J Obstet Gynecol.* 2015 May; 212 (5): 611.e1–9.
18. Пальцев М. А., Кактурский Л. В., Зайратьянц О. В., редакторы. *Патологическая анатомия: национальное руководство.* М.: ГЭОТАР-Медиа, 2014; 1264 с.
19. Ворошилина Е. С., Тумбинская Л. В., Донников А. Е., Плотно Е. Э., Хаютин Л. В. Биоценоз влагалища с точки зрения количественной полимеразной цепной реакции: что есть норма? *Акушерство и гинекология.* 2011; (1): 57–65.
20. Winters AD, Romero R, Gervasi MT, Gomez-Lopez N, Tran MR, Garcia-Flores V, et al. Does the endometrial cavity have a molecular microbial signature? *Sci Rep.* 2019 Jul 9; 9 (1): 9905.



## ISONIAZID-RESISTANT *MYCOBACTERIUM TUBERCULOSIS*: PREVALENCE, RESISTANCE SPECTRUM AND GENETIC DETERMINANTS OF RESISTANCE

Andreevskaya SN , Smirnova TG, Larionova EE, Andrievskaya IYu, Chernousova LN, Ergeshov A

Central Tuberculosis Research Institute, Moscow, Russia

The lack of simple, rapid diagnostic tests for isoniazid-resistant rifampicin-susceptible tuberculosis infection (Hr-TB) can result in low treatment efficacy and further amplification of drug resistance. Based on the clinical data, this study sought to estimate the prevalence of Hr-TB in the general population and characterize the phenotypic susceptibility and genetic determinants of isoniazid resistance in *M. tuberculosis* strains. Molecular-genetic and culture-based drug susceptibility tests were performed on *M. tuberculosis* isolates and *M. tuberculosis* DNA obtained from the patients with pulmonary TB undergoing treatment at the Central Tuberculosis Research Institute between 2011 and 2018. The tests revealed that Hr-TB accounted for 12% of all TB cases in the studied sample. Hr-TB strains were either resistant to isoniazid only (45%) or had multiple resistance to 2–6 anti-TB agents. Resistance to isoniazid was caused by mutations in the *katG* gene. Based on the literature analysis and our own observations, we emphasize the importance of developing simple molecular drug susceptibility tests capable of detecting simultaneous resistance to rifampicin and isoniazid and the necessity of their translation into clinical practice.

**Keywords:** *M. tuberculosis*, isoniazid resistance, drug susceptibility, molecular diagnostics, single nucleotide polymorphism, tuberculosis

**Funding:** this study was supported by the Ministry of Science and Higher Education of the Russian Federation and carried out under the Federal Targeted Program for Research and Development in Priority Areas of Development of the Russian Scientific and Technological Complex for 2014–2020, Project № 05.586.21.0065 (Project ID RFMEFI58619X0065).

**Author contribution:** Ergeshov A, Chernousova LN — study design; Larionova EE, Andrievskaya IYu — data acquisition; Smirnova TG — data analysis; Andreevskaya SN — manuscript preparation, literature analysis. All authors have equally contributed to the discussion of the obtained results.

**Compliance with ethical standards:** we retrospectively analyzed the results of routine laboratory tests performed on the patients undergoing treatment for tuberculosis at the Central Tuberculosis Research Institute. All patients gave informed consent.

✉ **Correspondence should be addressed:** Sofya N. Andreevskaya  
Yauzskaya alley, 2, Moscow, 107564; andsofia@mail.ru

**Received:** 11.12.2019 **Accepted:** 07.01.2020 **Published online:** 12.01.2020

**DOI:** 10.24075/brsmu.2020.001

## ИЗОНАЗИД-РЕЗИСТЕНТНЫЕ *MYCOBACTERIUM TUBERCULOSIS*: ЧАСТОТА ВЫЯВЛЕНИЯ, СПЕКТРЫ РЕЗИСТЕНТНОСТИ И ГЕНЕТИЧЕСКИЕ ДЕТЕРМИНАНТЫ УСТОЙЧИВОСТИ

С. Н. Андреевская , Т. Г. Смирнова, Е. Е. Ларионова, И. Ю. Андриевская, Л. Н. Черноусова, А. Эргешов

Центральный научно-исследовательский институт туберкулеза, Москва, Россия

Отсутствие ускоренной диагностики туберкулеза с устойчивостью возбудителя к изониазиду с сохраненной чувствительностью к рифампицину (ИР-ТБ) может быть причиной низкой эффективности терапии и приводить к амплификации лекарственной резистентности, в том числе к формированию множественной лекарственной устойчивости. Целью работы было определить частоту встречаемости ИР-ТБ в современной популяции, охарактеризовать фенотипическую чувствительность и генетические детерминанты устойчивости к изониазиду представителей этой группы *M. tuberculosis* на репрезентативном материале. Анализировали результаты определения лекарственной чувствительности, полученные при исследовании молекулярно-генетическими и/или культуральными методами изолятов *M. tuberculosis* / ДНК *M. tuberculosis*, выделенных от больных туберкулезом легких из клинических отделений Центрального научно-исследовательского института туберкулеза за период 2011–2018 гг. Частота ИР-ТБ составила 12% от всех выявленных случаев туберкулеза. *M. tuberculosis* с ИР были как монорезистентными к изониазиду (45%), так и полирезистентными (устойчивыми к 2–6 противотуберкулезным препаратам), а устойчивость к изониазиду была обусловлена мутациями в гене *katG*, приводящими к высокому уровню резистентности. На основании анализа литературных данных и собственных наблюдений подчеркивается важность разработки и внедрения новых простых молекулярных тестов для определения устойчивости одновременно к рифампицину и изониазиду.

**Ключевые слова:** *M. tuberculosis*, изониазид-резистентность, лекарственная чувствительность, молекулярная диагностика, однонуклеотидный полиморфизм, туберкулез

**Финансирование:** работа выполнена при финансовой поддержке Министерства науки и высшего образования Российской Федерации в рамках Федеральной целевой программы «Исследования и разработки по приоритетным направлениям развития научно-технологического комплекса России на 2014–2020 годы», соглашение № 05.586.21.0065 (уникальный идентификатор соглашения RFMEFI58619X0065).

**Вклад авторов:** А. Эргешов, Л. Н. Черноусова — разработка дизайна исследования; Е. Е. Ларионова, И. Ю. Андриевская — получение данных для анализа; Т. Г. Смирнова — анализ полученных данных; С. Н. Андреевская — написание текста рукописи, обзор публикаций по теме статьи; все авторы участвовали в обсуждении результатов.

**Соблюдение этических стандартов:** был проведен ретроспективный анализ результатов, полученных при выполнении рутинных лабораторных исследований для пациентов, проходящих лечение в Центральном НИИ туберкулеза; все пациенты подписали добровольное информированное согласие на проведение исследования.

✉ **Для корреспонденции:** Софья Николаевна Андреевская  
Яузская аллея, д. 2, г. Москва, 107564; andsofia@mail.ru

**Статья получена:** 11.12.2019 **Статья принята к печати:** 07.01.2020 **Опубликована онлайн:** 12.01.2020

**DOI:** 10.24075/vrgmu.2020.001

Drug-resistant tuberculosis (TB) is a serious public health concern. At present, the major focus is on fighting multidrug-resistant TB (MDR-TB), i.e. caused by strains resistant to at least 2 most effective anti-TB drugs: isoniazid and rifampicin

[1]. Russia has the third-highest burden of MDR-TB [2]. In 2018, the incidence and prevalence of MDR-TB in Russia stabilized at 5.6 and 23.6 cases per 100, 000 population, respectively. However, the share of patients with MDR-TB among individuals

with active TB disease increased both in terms of incident cases (from 27.4% in 2017 to 29.3% in 2018) and the total respiratory TB burden (from 54.0% in 2017 to 55.3% in 2018) [3].

By contrast, other forms of drug-resistant TB are receiving less attention, including isoniazid-resistant TB (Hr-TB) assigned to a separate category by WHO. Its causative agent is resistant to isoniazid but sensitive to rifampicin [4]. Isoniazid is a first-line drug that exerts a bactericidal effect on *M. tuberculosis* and is highly effective in treating active TB forms. Phenotypic resistance to isoniazid is associated with mutations in *katG*, *inhA*, *ahpC* and some other genes that encode proteins involved in the pharmacokinetics and pharmacodynamics of isoniazid in the bacterial cell [5, 6].

Inadequate therapy for Hr-TB promotes a high risk of acquiring resistance to other anti-TB drugs, including rifampicin, and results in MDR [7]. According to WHO, Hr-TB prevalence varies from 5 to 11% across WHO regions [8]. The data on Hr-TB prevalence in Russia is scarce.

This study aimed to estimate the prevalence of isoniazid-resistant *M. tuberculosis* in patients presenting with pulmonary TB at the clinical departments of Central Tuberculosis Research Institute between 2011 and 2018, as well as to provide an extensive phenotypic drug sensitivity profile and describe genetic determinants of resistance to isoniazid in this group of *M. tuberculosis* isolates.

## METHODS

### Object of research

In this study, we looked at *M. tuberculosis* isolates and/or DNA isolated from the clinical specimens collected from the patients with pulmonary TB who had presented at the counselling and clinical departments of Central Tuberculosis Research Institute in 2011–2018. All microbiological tests were performed on the same sample.

### Culture tests

The cultures were grown and analyzed for the presence of *M. tuberculosis* in a Middlebrook 7H9 broth base in a BACTEC MGIT 960 system (BD; USA) following the manufacturer's protocol [9]. For drug susceptibility testing, we used BACTEC MGIT 960 instrumentation (BD; USA) and a modified proportion method. The isolates were tested for sensitivity to 8 drugs taken at critical concentrations, including isoniazid (H, 0.1 µg/ml), rifampicin (R, 1.0 µg/ml), ethambutol (E, 5.0 µg/ml), pyrazinamide (Z, 100.0 µg/ml), ethionamide (Eto, 5.0 µg/ml), amikacin (Am, 1.0 µg/ml), capreomycin (Cm 2.5 µg/ml), and levofloxacin (Lfx, 1.0 µg/ml). Standard protocols were applied [9, 10].

### DNA isolation

DNA was isolated from the clinical specimens using an AmpliTub-RV reagent kit 1 for the isolation, detection and quantification of mycobacterial DNA by real-time PCR (Syntol; Russia) following the manufacturer's protocol.

Detection of *M. tuberculosis* DNA was performed using an AmpliTub-RV reagent kit 2 for the isolation, detection and quantification of mycobacterial DNA by real-time PCR (Syntol; Russia) following the manufacturer's protocol. DNA fragments were amplified in a thermocycler equipped with a CFX96 optical reaction module (Bio-Rad; USA).

Genotypic resistance to rifampicin, isoniazid and fluoroquinolones was tested using either TB-Biochip-1 and

TB-Biochip-2 kits that utilize a microarray technology (Biochip-IMB; Russia) or AmpliTub-MDR-RV and AmpliTub-FQ-RV kits (Syntol; Russia). All procedures were carried out in compliance with the manufacturers' guidelines.

### Statistical analysis

Descriptive statistics were used to analyze the results of the study, including the number of observations, frequencies, percentages, and 95% CI. The analysis was conducted in MS Excel (Microsoft; USA).

## RESULTS

Clinical specimens collected from 4056 patients with pulmonary TB were subjected to culture-based and molecular testing. In 71 cases, neither *M. tuberculosis* DNA nor tubercle bacilli themselves were detected; so those cases were excluded from the analysis. Phenotypic/genotypic drug susceptibility was determined for *M. tuberculosis* DNA/cultures isolated from the remaining 3985 samples. If the results of culture tests contradicted those of molecular tests, priority was given to culture-based data (Table 1). For example, 38 strains that demonstrated resistance to both isoniazid and rifampicin in culture tests but had no mutations in the *rpoB* gene implicated in rifampicin resistance were put into the MDR category because molecular rifampicin susceptibility tests used in our study could only detect a limited number of mutations, meaning that genetic determinants of rifampicin resistance might have been overlooked in the analysis. And, vice versa, 29 strains that tested positive for mutations in the *rpoB* gene and did not have the rifampicin-resistant phenotype were categorized as isoniazid-resistant.

The total sample of drug-resistant *M. tuberculosis* strains was dominated by MDR isolates (Table 1). However, isoniazid-resistant strains that were susceptible to rifampicin were also well represented in the sample (502/3985; 12.60%).

The analysis of clinical data over the period from 2011 to 2018 revealed that Hr-TB amounted to about 14% of all TB cases per year reported in 2011–2012 and 2017–2018. In 2013–2016, the rate of detection for this TB form was lower (10–11%). We were unable to describe this linear trend with a sufficient degree of reliability (Table 2).

Because culture-based tests are less sensitive than molecular methods, the growth of *M. tuberculosis* in culture media was not detected for some specimens. Therefore, phenotypic sensitivity to anti-TB drugs was only determined for 260 isoniazid-resistant isolates of *M. tuberculosis* (Table 3). The following definitions were applied to identify the type of drug resistance of *M. tuberculosis* isolates [1]: monoresistance, i.e. resistance of the mycobacterium to only one anti-TB drug, and polyresistance, i.e. resistance of the mycobacterium to 2 or more anti-TB drugs but not to the combination of isoniazid and rifampicin.

Mono-resistant isolates amounted to 117/260 (45%) cases. The rest 143 (55%) isolates were polyresistant (to 2–6 drugs). Polyresistant isolates were equally represented by *M. tuberculosis* strains resistant to both isoniazid and first-line drugs (42/143; 29.37%) and by the strains resistant to both isoniazid and second-line drugs (38/143; 26.57%); resistance to second-line drugs almost always included resistance to ethionamide (31/38; 81.58%). Co-resistance to first- and second-line drugs was the most common among the polyresistant isolates (63/143; 44.06%). Of them, co-resistance to isoniazid, ethambutol and ethionamide (HEEto), including

their combinations with other second-line medications, was detected in 20/63 (31.75%) cases; polyresistance to isoniazid, pyrazinamide and ethionamide (HZEto), including their combinations with other second-line drugs, was not so common (9/63 cases or 14.29%). Polyresistance to HEZEto was observed in 15/63 (23.81%) isolates. In 19/63 (30.16%) isolates, resistance spectra included other combinations of drugs (a total of 12 resistance spectra with 3 to 5 drugs).

Data on mutations in the genes associated with resistance to isoniazid were acquired for 451 *M. tuberculosis* isolates resistant to isoniazid (Table 4). In most cases (386/451 isolates or 85.59%), single nucleotide polymorphisms (SNPs) were detected in one of the genes associated with resistance to isoniazid. The presence of SNPs in 2 genes associated with isoniazid resistance was not so common (65/451 cases or 14.41%). The most prevalent were mutations at codon 315 of the *katG* gene (413/451 cases or 91.57%). In 348/413 (84.26%) cases, mutations were detected only in *katG*; in 62/413 (15.01%) isolates, mutations in *katG* co-occurred with SNPs in the *inhA* gene. In single cases, *katG* mutations co-occurred with SNPs in the *ahpC* gene.

The *inhA15\_C*->T substitution was quite common (94/451; 20.84%); in 33/94 (35.11%) cases it was the only mutation detected. In other samples, this mutation co-occurred with an SNP at codon 315 of the *katG* gene.

For 209 isolates of *M. tuberculosis* with phenotypically confirmed resistance to isoniazid, the following distribution of mutant variants was observed: 152/209 (72.73%) carried a mutation in the *katG* gene only (315\_Ser->Thr(1)); 32/209 (15.31%) carried a combination of *katG*315\_Ser->Thr(1) and *inhA15\_C*->T; 17/209 (8.13%) only *inhA15\_C*->T was detected. The remaining 8 (3.83%) isolates with phenotypically confirmed resistance to isoniazid had mutations in other regions of the genes associated with isoniazid resistance (*ahpC*10\_C->T in

the absence of other mutations, *katG*315\_Ser->Asn; co-occurring *katG*315\_Ser->Gly + *inhA15\_C*->T, *katG*315\_Ser->Thr(1) + *inhA8\_T*->G, *katG*315\_Ser->Thr(1) + *ahpC*10\_C->T).

Thus, our sample of isoniazid-resistant *M. tuberculosis* was dominated by the *katG*315\_Ser->Thr(1) mutation corresponding to the substitution AGC->ACC (333/451; 73.84%), followed by the co-occurring *katG*315\_Ser->Thr(1) + *inhA15\_C*->T (60/451; 13.30%), and single *inhA15\_C*->T (33/451; 7.32%). On the whole, these 3 mutant variants amounted to 426/451 (94.46%) isoniazid-resistant *M. tuberculosis* isolates.

## DISCUSSION

We attempted to estimate the prevalence of isoniazid-resistant, rifampicin-susceptible *M. tuberculosis* strains isolated from the patients with pulmonary TB, who had presented at clinical departments of Central Tuberculosis Research Institute in 2011–2018.

The prevalence of this TB form and the rate of its spread vary across the world's regions. For example, the analysis of data on drug susceptibility collected by WHO from 131 specialized healthcare institutions in 1994–2009 reveals that Eastern Europe had the highest burden of Hr-TB (15%), followed by Western and Central Europe (11%); in other WHO regions, Hr-TB prevalence did not exceed 8% [11]. In some regions, the prevalence of Hr-TB tended to decrease, whereas in others, it was increasing. No clear linear dynamics were established for the majority of WHO regions. In our study, the prevalence of isoniazid-resistant *M. tuberculosis* (12%) was similar to that in Eastern Europe and its dynamics were non-linear, just like in the majority of the world's regions.

The systematic review of the link between primary resistance to isoniazid and the acquisition of secondary resistance to other anti-TB drugs [12] concludes that monoresistant strains acquire

**Table 1.** *M. tuberculosis* isolates and drug susceptibility tests

Types of sensitivity to antituberculous drugs	Number of isolates for which data on drug sensitivity was obtained (abs.)			The total number of <i>M. tuberculosis</i> isolates assigned to each sensitivity type based on culture and molecular testing	
	Molecular and culture tests	Culture tests only	Molecular tests only	abs.	% (95% CI)
Sensitive	478	207	673 <sup>1)</sup>	1358	34.08 (32.62–35.56)
MDR	1179 <sup>2)</sup>	256	613	2048	51.39 (49.84–52.94)
Hr	209 <sup>3)</sup>	51	242	502	12.60 (11.60–13.66)
Other <sup>4)</sup>	42	23	12	77	1.93 (1.55–2.41)
Total	1908	537	1540	3985	100

**Note:** <sup>1</sup> — including cases for which no mutations were detected in the genes associated with resistance to isoniazid, rifampicin and fluoroquinolones; <sup>2</sup> — including 38 *M. tuberculosis* isolates for which no mutations in the *rpoB* gene (see the article) were detected; <sup>3</sup> — including 29 *M. tuberculosis* isolates carrying mutant *rpoB* but having no resistance phenotype; <sup>4</sup> — mono- or polyresistance to antituberculous drugs, excluding isoniazid.

**Table 2.** The frequency of detection of isoniazid-resistant *M. tuberculosis* in 2011–2018

Year	Number of <i>M. tuberculosis</i> isolates		
	Total isolates studied (abs.)	Hr isolates	
		abs.	% (95% CI)
2011	458	67	14.63 (11.69–18.16)
2012	355	52	14.65 (11.35–18.70)
2013	530	54	10.19 (7.89–13.06)
2014	554	65	11.73 (9.31–14.68)
2015	569	65	11.42 (9.06–14.30)
2016	502	56	11.16 (8.69–14.21)
2017	557	76	13.64 (11.04–16.75)
2018	460	67	14.57 (11.64–18.08)

additional resistance (no necessarily MDR) to other anti-TB drugs 5.1 times more often than drug-susceptible strains. High occurrence rates of polyresistant strains demonstrated in our study (55% of all Hr-TB isolates) insensitive to 1–5 drugs apart from isoniazid corroborate the possibility of drug resistance amplification in isoniazid-resistant *M. tuberculosis*.

Because first-line antituberculous drugs ethambutol and pyrazinamide are included in the standard chemotherapy regimen often prescribed empirically to newly diagnosed patients, it would be reasonable to expect high prevalence rates of Hr *M. tuberculosis* strains additionally resistant to these 2 drugs. Indeed, resistance to ethambutol was detected in almost half of all polyresistant *M. tuberculosis* isolates analyzed in our study (70/143, 48.95%; 95% CI: 40.89–57.06%); pyrazinamide-resistant isolates were slightly rarer (57/143, 39.86%; 95% CI: 32.20–48.05%).

Polyresistant *M. tuberculosis* strains resistant to ethionamide (the second-line medication) were much more prevalent (80/143, 55.94%; 95% CI: 47.76–63.82%). This can be explained by the fact that ethionamide is a structural analogue of isoniazid; it inhibits synthesis of mycolic acids, thereby disrupting the structure of the bacterial cell wall. Therefore, these two drugs may have common targets and genetic determinants of resistance [5, 13].

In general, the use of first-line drugs in the therapy of Hr-TB leads to poor outcomes, including the lack of therapeutic effect, relapses, acquired MDR. Besides, standard empiric treatment of Hr-TB can promote MDR-TB epidemics, especially in the regions where such TB forms are not rare [7]. At the same time, timely adjustments to the regimen based on results of isoniazid susceptibility testing and the use of modified regimens reinforce therapeutic success and reduce the risk of relapses [14–16].

In this light, 2 clinical studies should be mentioned that aimed to establish an association between mutations in *M. tuberculosis* and the efficacy of treatment of Hr-TB with high doses of isoniazid [17, 18]. It is known that mutations in the *katG* gene, which dominated our sample, result in a high level of resistance to isoniazid whereas mutations in *inhA*, in a low level of resistance [5]. The studies revealed that therapy with isoniazid was effective when mycobacteria carried mutations in the *inhA* gene; *katG* mutations were associated with poor treatment outcomes [17, 18].

This emphasizes the need for effective regimens for the therapy of Hr-TB [8, 19]. Rapid drug susceptibility testing is critical. Molecular diagnostic methods are highly sensitive and rapid (1–2 days in comparison with weeks required for culture); they also provide valuable information about mutations carried by the strain and the level of isoniazid resistance [1]. Therefore, the demand for molecular methods in the diagnosis of TB and drug susceptibility testing is high. However, although tests based on allele specific PCR, bioarray technologies or DNA strips used in large TB healthcare centers expedite diagnosis, they impose strict requirements on staff qualifications and laboratory infrastructure.

Today, the only molecular test that can be deployed in any laboratory is Xpert MTB/RIF that utilizes the GeneXpert platform [20]. Unfortunately, this test can detect only genotypic resistance to rifampicin because these days all diagnostic procedures are largely focused on detecting MDR strains, which are resistant to rifampicin. Therefore, Xpert MTB/RIF cannot detect resistance to isoniazid in the strains that are sensitive to rifampicin (12% of our isolates). In the absence of additional diagnostic tools, isoniazid resistance of such strains will never be revealed, leading to inadequate chemotherapy regimens and amplification of MDR. This indicates the need for

a simple molecular test that is as convenient as Xpert MTB/RIF and can be used in any laboratory.

## CONCLUSIONS

Isoniazid-resistant tuberculosis can be regarded as a potential predecessor of MDR disease. It is important to control the spread of primary resistance to isoniazid and prevent acquisition of further resistance. Our analysis revealed high prevalence

**Table 3.** Resistance spectra of isoniazid-resistant strains of *M. tuberculosis*

Resistance spectra	Number of <i>M. tuberculosis</i> strains	
	abs.	% (95% CI)
<b>Monoresistance (H)</b>	<b>117</b>	<b>45.00 (39.07–51.08)</b>
Polyresistance (H + other anti-TB drugs except R):	143	55.00 (48.95–61.05)
<b>To 2 anti-TB drugs:</b>	<b>71</b>	<b>27.31 (22.25–33.02)</b>
HE	17	
HZ	16	
H Eto	31	
H Am	3	
H Cp	1	
H Lfx	3	
<b>To 3 anti-TB drugs:</b>	<b>36</b>	<b>13.85 (10.17–18.57)</b>
HEZ	9	
HE Eto	13	
HE Lfx	1	
HZ Cp	1	
HZ Eto	7	
H AmCp	2	
H EtoAm	3	
<b>To 4 anti-TB drugs:</b>	<b>21</b>	<b>8.08 (5.34–12.03)</b>
HEZ Eto	6	
HEZ Am	1	
HEZ Lfx	3	
HE AmCp	2	
HE EtoAm	4	
HE EtoLfx	2	
HZ EtoCp	1	
H EtoAmCp	1	
H AmCpLfx	1	
<b>To 5 anti-TB drugs:</b>	<b>12</b>	<b>4.62 (2.66–7.89)</b>
HEZ EtoAm	2	
HEZ EtoLfx	4	
HEZ AmCp	2	
HE EtoAmLfx	1	
HZ AmCpLfx	1	
HZ EtoAmLfx	1	
H EtoAmCpLfx	1	
<b>To 6 anti-TB drugs:</b>	<b>3</b>	<b>1.15 (0.39–3.34)</b>
HEZ EtoAmCp	2	
HEZ EtoAmLfx	1	
<b>Total</b>	<b>260</b>	<b>100</b>

**Note:** in the lists of resistance spectra, first-line drugs are separated from second-line medications by a space character.



**Table 4.** Isoniazid-resistant *M. tuberculosis* isolates with different combinations of mutations in the genes associated with isoniazid resistance

Mutations in <i>katG</i> Mutations in <i>ahpC</i> and <i>inhA</i>			Not detected	At codon 351, substitution of Ser to					Total
				Arg	Asn	Gly	Thr(1)*	Thr(2)*	
No detected mutations in <i>ahpC</i> or <i>inhA</i>			–	4 (0.89; 0.35–2.26)	7 (1.55; 0.75–3.17)	3 (0.67; 0.23–1.94)	333 (73.84; 69.59–77.68)	1 (0.22; 0.04–	348 (77.16; 73.07–80.80)
SNP in <i>ahpC</i> at position	6	G→A	–	–	–	–	1 (0.22; 0.04–1.25)	–	1 (0.22; 0.04–1.25)
	10	C→A	1 (0.22; 0.04–1.25)	–	–	–	–	–	1 (0.22; 0.04–1.25)
		C→T	1 (0.22; 0.04–1.25)	–	–	–	1 (0.22; 0.04–1.25)	–	2 (0.44; 0.12–1.60)
	12	C→T	–	–	–	–	1 (0.22; 0.04–1.25)	–	1 (0.22; 0.04–1.25)
SNP in <i>inhA</i> at position	8	T→A	2 (0.44; 0.12–1.60)	–	–	–	–	–	2 (0.44; 0.12–1.60)
		T→G	–	–	–	–	1 (0.22; 0.04–1.25)	–	1 (0.22; 0.04–1.25)
	15	C→G	1 (0.22; 0.04–1.25)	–	–	–	–	–	1 (0.22; 0.04–1.25)
		C→T	33 (7.32; 5.26–10.10)	–	–	1 (0.22; 0.04–1.25)	60 (13.30; 10.48–16.75)	–	94 (20.84; 17.35–24.83)
Total			38 (8.43; 6.20–11.35)	4 (0.89; 0.35–2.26)	7 (1.55; 0.75–3.17)	4 (0.89; 0.35–2.26)	397 (88.03; 84.70–90.71)	1 (0.22; 0.04–1.25)	451 (100)

**Note:** SNPs occurring in only one gene associated with isoniazid resistance are highlighted in gray; other cells show combinations of >1 mutation. \* Thr(1) represents the AGC→ACC substitution, Ser→Thr(2) represents the AGC→ACA substitution.

of Hr-TB (over 12% of all analyzed cases) among isoniazid-resistant rifampicin-susceptible *M. tuberculosis* strains isolated from patients with pulmonary TB. The majority of such isolates carried mutations causing strong resistance to isoniazid. Our

findings indicate the importance of rapid testing for sensitivity to both rifampicin and isoniazid based on molecular-genetic methods. There is a need for simple point-of-care tests that do not impose high requirements on laboratory infrastructure.

## References

- Order of the Ministry of Health of the Russian Federation of 9 December 2014 «Ob utverzhenii metodicheskikh rekomendatsiy po sovershenstvovaniyu diagnostiki i lecheniya tuberkuleza organov dykhaniya». Russian.
- World Health Organization. Global tuberculosis report 2018. Geneva: World Health Organization; 2018. (WHO/CDS/TB/2018.20).
- Nechaeva OB. TB situation Russian. Tuberculosis and Lung Diseases. 2018; 96 (8): 15–24. Russian.
- World Health Organization. WHO consolidated guidelines on drug-resistant tuberculosis treatment. Geneva: World Health Organization; 2019 (WHO/CDS/TB/2019.33).
- Zhang Y, Yew WW. Mechanisms of drug resistance in Mycobacterium tuberculosis. Int J Tuberc Lung Dis. 2009; (13): 1320–30.
- Sandgren A, Strong M, Muthukrishnan P, Weiner BK, Church GM, Murray MB. Tuberculosis drug resistance mutation database. PLoS Med. 2009; 6 (2): e2.
- Gegia M, Winters N, Benedetti A, van Soolingen D, Menzies D. Treatment of isoniazid-resistant tuberculosis with first-line drugs: a systematic review and meta-analysis. Lancet Infect Dis. 2017; 17 (2): 223–34.
- World Health Organization. WHO treatment guidelines for isoniazid-resistant tuberculosis: Supplement to the WHO treatment guidelines for drug-resistant tuberculosis. Geneva: World Health Organization; 2018 (WHO/CDS/TB/2018.7).
- Siddiqi SH, Rusch-Gerdes S. MGIT procedure manual for BACTEC MGIT 960 TB System. 2006.
- Chernousova LN, Smirnova TG, Larionova EE, i dr. Standartnyye operatsionnyye protsedury. Opredelelye chuvstvitel'nosti mikobakteriy tuberkuleza k protivotuberkuleznym preparatam vtorogo ryada s ispol'zovaniyem sistemy BACTEC MGIT 960/320. Moscow, 2015. Russian.
- Jenkins HE, Zignol M, Cohen T. Quantifying the Burden and Trends of Isoniazid Resistant Tuberculosis, 1994–2009. PLoS ONE. 2011; 6 (7): e22927.
- Menzies D, Benedetti A, Paydar A, Martin I, Royce S, Pai M, et al. Effect of duration and intermittency of rifampin on tuberculosis treatment outcomes: a systematic review and meta-analysis. PLoS Med. 2009; 6 (9): e1000146.
- Jeon CY, Hwang SH, Min JH, Prevots DR, Goldfeder LC, Lee H, et al. Extensively drug-resistant tuberculosis in South Korea: risk factors and treatment outcomes among patients at a tertiary referral hospital. Clin Infect Dis. 2008; (46): 42–9.
- Bang D, Andersen PH, Andersen AB, Thomsen VØ. Isoniazid-resistant tuberculosis in Denmark: mutations, transmission and treatment outcome. J Infect. 2010; 60 (6): 452–7.
- Salindri AD, Sales RF, DiMiceli L, Schechter MC, Kempker RR, Magee MJ. Isoniazid monoresistance and rate of culture conversion among patients in the state of Georgia with confirmed tuberculosis, 2009–2014. Ann Am Thorac Soc. 2018; 15 (3): 331–40.
- Cattamanchi A, Dantes RB, Metcalfe JZ, Jarlsberg LG, Grinsdale J, Kawamura LM, et al. Clinical characteristics and treatment outcomes of patients with isoniazid-monoresistant tuberculosis. Clin Infect Dis. 2009; 48 (2): 179–85.
- Tolani MP, D'souza DT, Mistry NF. Drug resistance mutations and heteroresistance detected using the GenoType MTBDRplus assay and their implication for treatment outcomes in patients from Mumbai, India. BMC Infect Dis. 2012; (12): 9.
- Huyen MN, Cobelens FG, Buu TN, Lan NT, Dung NH, Kremer K, et al. Epidemiology of isoniazid resistance mutations and their effect on tuberculosis treatment outcomes. Antimicrob Agents Chemother. 2013; 57 (8): 3620–7.
- Stagg HR, Harris RJ, Hatherell HA, Obach D, Zhao H, Tsuchiya N, et

- al. What are the most efficacious treatment regimens for isoniazid-resistant tuberculosis? A systematic review and network meta-analysis. *Thorax*. 2016; 71 (10): 940–9.
20. World Health Organization. WHO meeting report of a technical

expert consultation: non-inferiority analysis of Xpert MTB/RIF Ultra compared to Xpert MTB/RIF. Geneva: World Health Organization; 2017. WHO/HTM/TB/2017.04. Available from: <https://www.who.int/tb/publications/2017/XpertUltra/en/>. Accessed: 18 May 2019.

## Литература

1. Приказ Министерства здравоохранения Российской Федерации от 29 декабря 2014 № 951 «Об утверждении методических рекомендаций по совершенствованию диагностики и лечения туберкулеза органов дыхания».
2. World Health Organization. Global tuberculosis report 2018. Geneva: World Health Organization; 2018. (WHO/CDS/TB/2018.20).
3. Нецаева О. Б. Эпидемическая ситуация по туберкулезу в России. *Туберкулез и болезни легких*. 2018; 96 (8): 15–24.
4. World Health Organization. WHO consolidated guidelines on drug-resistant tuberculosis treatment. Geneva: World Health Organization; 2019 (WHO/CDS/TB/2019.33).
5. Zhang Y, Yew WW. Mechanisms of drug resistance in *Mycobacterium tuberculosis*. *Int J Tuberc Lung Dis*. 2009; (13): 1320–30.
6. Sandgren A, Strong M, Muthukrishnan P, Weiner BK, Church GM, Murray MB. Tuberculosis drug resistance mutation database. *PLoS Med*. 2009; 6 (2): e2.
7. Gegia M, Winters N, Benedetti A, van Soolingen D, Menzies D. Treatment of isoniazid-resistant tuberculosis with first-line drugs: a systematic review and meta-analysis. *Lancet Infect Dis*. 2017; 17 (2): 223–34.
8. World Health Organization. WHO treatment guidelines for isoniazid-resistant tuberculosis: Supplement to the WHO treatment guidelines for drug-resistant tuberculosis. Geneva: World Health Organization; 2018 (WHO/CDS/TB/2018.7).
9. Siddiqi SH, Rusch-Gerdes S. MGIT procedure manual for BACTEC MGIT 960 TB System. 2006.
10. Черноусова Л. Н., Смирнова Т. Г., Ларионова Е. Е., и др. Стандартные операционные процедуры. Определение чувствительности микобактерий туберкулеза к противотуберкулезным препаратам второго ряда с использованием системы BACTEC MGIT 960/320. Москва, 2015.
11. Jenkins HE, Zignol M, Cohen T. Quantifying the Burden and Trends of Isoniazid Resistant Tuberculosis, 1994–2009. *PLoS ONE*. 2011; 6 (7): e22927.
12. Menzies D, Benedetti A, Paydar A, Martin I, Royce S, Pai M, et al. Effect of duration and intermittency of rifampin on tuberculosis treatment outcomes: a systematic review and meta-analysis. *PLoS Med*. 2009; 6 (9): e1000146.
13. Jeon CY, Hwang SH, Min JH, Prevots DR, Goldfeder LC, Lee H, et al. Extensively drug-resistant tuberculosis in South Korea: risk factors and treatment outcomes among patients at a tertiary referral hospital. *Clin Infect Dis*. 2008; (46): 42–9.
14. Bang D, Andersen PH, Andersen AB, Thomsen VØ. Isoniazid-resistant tuberculosis in Denmark: mutations, transmission and treatment outcome. *J Infect*. 2010; 60 (6): 452–7.
15. Salindri AD, Sales RF, DiMiceli L, Schechter MC, Kempker RR, Magee MJ. Isoniazid monoresistance and rate of culture conversion among patients in the state of Georgia with confirmed tuberculosis, 2009–2014. *Ann Am Thorac Soc*. 2018; 15 (3): 331–40.
16. Cattamanchi A, Dantes RB, Metcalfe JZ, Jarlsberg LG, Grinsdale J, Kawamura LM, et al. Clinical characteristics and treatment outcomes of patients with isoniazid-monoresistant tuberculosis. *Clin Infect Dis*. 2009; 48 (2): 179–85.
17. Tolani MP, D'souza DT, Mistry NF. Drug resistance mutations and heteroresistance detected using the GenoType MTBDRplus assay and their implication for treatment outcomes in patients from Mumbai, India. *BMC Infect Dis*. 2012; (12): 9.
18. Huyen MN, Cobelens FG, Buu TN, Lan NT, Dung NH, Kremer K, et al. Epidemiology of isoniazid resistance mutations and their effect on tuberculosis treatment outcomes. *Antimicrob Agents Chemother*. 2013; 57 (8): 3620–7.
19. Stagg HR, Harris RJ, Hatherell HA, Obach D, Zhao H, Tsuchiya N, et al. What are the most efficacious treatment regimens for isoniazid-resistant tuberculosis? A systematic review and network meta-analysis. *Thorax*. 2016; 71 (10): 940–9.
20. World Health Organization. WHO meeting report of a technical expert consultation: non-inferiority analysis of Xpert MTB/RIF Ultra compared to Xpert MTB/RIF. Geneva: World Health Organization; 2017. WHO/HTM/TB/2017.04. Available from: <https://www.who.int/tb/publications/2017/XpertUltra/en/>. Accessed: 18 May 2019.



## HEREDITARY RISK FACTORS FOR UTERINE LEIOMYOMA: A SEARCH FOR MARKER SNPS

Svirepova KA<sup>1</sup>✉, Kuznetsova MV<sup>1</sup>, Sogoyan NS<sup>1</sup>, Zelensky DV<sup>2</sup>, Lolomadze EA<sup>1</sup>, Mikhailovskaya GV<sup>1</sup>, Mishina ND<sup>1</sup>, Donnikov AE<sup>1</sup>, Trofimov DY<sup>1</sup><sup>1</sup> Kulakov National Medical Research Center for Obstetrics, Gynecology and Perinatology, Moscow, Russia<sup>2</sup> Valuyki Central Hospital, Valuyki, Russia

Uterine leiomyomas are a worrying reproductive health issue that has serious social implications. The aim of this study was to conduct a search for marker single nucleotide polymorphisms (SNPs) associated with uterine leiomyoma. To test the hypothesis about the contribution of genetic predisposition to the pathogenesis of myomas, the initial group of 100 patients with a verified diagnosis of uterine leiomyoma was divided into 2 subgroups: subgroup 1a (women with a family history of the disease) and subgroup 1b (women with no family history of the disease). The control group consisted of 30 postmenopausal patients who did not have a medical history of uterine fibroids and denied uterine fibroids in their close female relatives. DNA sequences were read using Sanger sequencing. Statistically significant differences ( $p < 0.05$ ) were discovered between the analyzed groups in terms of genotype frequencies for rs12637801 and rs12457644. Also, previously unknown protective SNPs were identified whose rare alleles could predict the reduced risk of uterine leiomyomas.

**Keywords:** leiomyoma, somatic mutation, single nucleotide polymorphism**Funding:** this study was part of the State Assignment (2019) on the Improved management of patients with benign reproductive system neoplasms with hi-tech diagnostic imaging techniques and molecular panels for predicting the progression and relapse of the disease.**Author contribution:** Svirepova KA analyzed the literature, carried out the research and wrote the manuscript with input from all authors; Kuznetsova MV carried out the research and wrote the manuscript with input from all authors; Sogoyan NS collected tissue samples and documented them in the biobank's register; Zelensky DV collected tissue samples for research; Lolomadze EA, Mikhailovskaya GV helped with the laboratory part of the research; Mishina ND performed statistical analysis; Donnikov AE, Trofimov DY supervised the study and revised the manuscript.**Compliance with ethical standards:** the study was approved by the Ethics Committee of Kulakov National Medical Research Center for Obstetrics, Gynecology and Perinatology. Informed consent was obtained from all participants.✉ **Correspondence should be addressed:** Ksenia A. Svirepova  
Akademika Oparina, 4, Moscow, 117997; kseswi@yandex.ru**Received:** 05.02.2020 **Accepted:** 19.02.2020 **Published online:** 28.02.2020**DOI:** 10.24075/brsmu.2020.011НАСЛЕДСТВЕННЫЕ ФАКТОРЫ РИСКА РАЗВИТИЯ МИОМЫ МАТКИ:  
ПОИСК МАРКЕРНЫХ ОДНОНУКЛЕОТИДНЫХ ПОЛИМОРФИЗМОВК. А. Свирепова<sup>1</sup>✉, М. В. Кузнецова<sup>1</sup>, Н. С. Согоян<sup>1</sup>, Д. В. Зеленский<sup>2</sup>, Е. А. Лоломадзе<sup>1</sup>, Г. В. Михайловская<sup>1</sup>, Н. Д. Мишина<sup>1</sup>, А. Е. Донников<sup>1</sup>, Д. Ю. Трофимов<sup>1</sup><sup>1</sup> Национальный медицинский исследовательский центр акушерства, гинекологии и перинатологии имени В. И. Кулакова, Москва, Россия<sup>2</sup> Валуysкая центральная районная больница, Валуysки, Россия

Миома матки является одной из важнейших социально значимых проблем женского репродуктивного здоровья. Целью исследования было найти маркерные однонуклеотидные полиморфизмы (SNP), ассоциированные с развитием миомы матки. Для проверки гипотезы о том, что наследственность играет важную роль в патогенезе миом, группу из 100 пациенток с подтвержденным диагнозом миомы матки разделили на две подгруппы: подгруппу 1а с отягощенным семейным анамнезом, подгруппу 1б с неотягощенным семейным анамнезом по миоме матки. Группа сравнения была сформирована из 30 пациенток (женщины в постменопаузе, не имевшие в анамнезе миому матки, отрицавшие наличие миом у ближайших родственников). Первичную нуклеотидную последовательность определяли с помощью секвенирования по методу Сэнгера. Были выявлены статистически значимые ( $p < 0,05$ ) различия между исследованными группами по частотам генотипов по rs12637801 и rs12457644. Впервые обнаружены «протективные» SNP, редкие аллели которых могут служить маркерами пониженного риска развития лейомиомы матки.

**Ключевые слова:** миома матки, соматические мутации, однонуклеотидные полиморфизмы**Финансирование:** работа выполнена в рамках госзадания 2019 г. «Совершенствование тактики ведения больных доброкачественными заболеваниями органов репродуктивной системы с использованием высокотехнологичных методов функциональной визуальной диагностики и панели молекулярно-биологических маркеров прогрессирования и рецидива заболеваний».**Вклад авторов:** К. А. Свирепова — анализ литературы, проведение исследования, написание текста статьи; М. В. Кузнецова — проведение исследования, написание текста статьи; Н. С. Согоян — сбор материала и ведение коллекции в биобанке; Д. В. Зеленский — сбор и предоставление материала для исследования; Е. А. Лоломадзе, Г. В. Михайловская — помощь в проведении лабораторной части исследования; Н. Д. Мишина — статистическая обработка результатов; А. Е. Донников, Д. Ю. Трофимов — общее руководство и редактирование статьи.**Соблюдение этических стандартов:** исследование одобрено этическим комитетом Национального медицинского исследовательского центра акушерства, гинекологии и перинатологии имени В. И. Кулакова. Все пациентки подписали добровольное информированное согласие на участие в исследовании.✉ **Для корреспонденции:** Ксения Александровна Свирепова  
ул. Академика Опарина, д. 4, г. Москва, 117997; kseswi@yandex.ru**Статья получена:** 05.02.2020 **Статья принята к печати:** 19.02.2020 **Опубликована онлайн:** 28.02.2020**DOI:** 10.24075/vrgmu.2020.011

Uterine leiomyomas (fibroids, leiomyomas) are some of the most common benign neoplasms of the female reproductive system [1]. Its prevalence among women of reproductive age is as high as 40–50%; in one-third of patients, uterine leiomyomas manifest themselves in serious symptoms [1–4].

That said, uterine leiomyomas are often asymptomatic, especially at the onset of the disease or in women with small or not too many nodules. However, some symptoms can have a huge negative impact on the patient's quality of life. Patients often complain of pain accompanying fibroid

growth; fatigue, weakness and absent-mindedness resulting from menometrorrhagia and chronic anemia; dyspareunia, psychological stress related to the symptoms, fear of possible medical interventions or reproductive dysfunction [5–8].

This gynecologic pathology is one of the causes underlying female infertility. Uterine leiomyomas are diagnosed in 23.5% of women seeking medical advice about primary or secondary infertility [9]. Worldwide, leiomyoma is associated with 10% of infertility cases in women and is the only cause of infertility in 1–3% of female patients. The contribution of leiomyoma to infertility is determined by the location of nodular growths [10].

The social implications of this disease cannot be overestimated. The modern woman is socially active, and the symptoms associated with leiomyoma can significantly reduce her quality of life, impair the ability to work, increase the number of hospital stays and therefore become a great financial burden for the state.

There is an extensive body of literature on the search of factors that cause uterine leiomyomas, including genetic, hormonal and some others. But so far, no clear association between these factors and the pathogenesis of the disease has been established. According to the population studies focusing on the prevalence of uterine leiomyomas, genetic predisposition plays the key role in their development: in about 5 to 10% of women, the disease is familial [1]. There are some publications pointing out that women of Afro-American descent are at increased risk for uterine leiomyomas, suggesting genetic differences between races in terms of risk for this pathology. Today, it is reported that about 70–80% of women aged 50 have at least one uterine fibroid nodule and 15–30% of patients with myomas develop serious complications [11–14].

The search for leiomyoma-specific genetic markers has been going on for over 20 years now. Uterine myomas are monoclonal neoplasms arising from a single progenitor cell, and the advent of next-generation sequencing stimulated vigorous research into the somatic mutations found in myomas. Mutations in the *MED12* gene have been shown to be the most common somatic mutations in uterine leiomyomas; the majority of them are single nucleotide polymorphisms in codons 43 and 44 of exon 2 [15] and are found in 70% of uterine nodules. So far, this is the most important discovery about the pathogenesis of uterine leiomyomas as no other somatic mutations have been detected in the tumors carrying the mutant *MED12* gene. Besides, uterine leiomyomas with mutant *MED12* are characterized by elevated RAD51B expression, which can stimulate cell proliferation and promote tumor growth [16–17]. The *MED12* gene is located on the X chromosome and encodes a 250 kDa subunit of a big mediator protein complex participating in the regulation of RNA polymerase II transcription.

Subsequent research revealed that the most common somatic mutation in the *MED12* gene is 131G>A. In total, 6 SNPs were identified at 3 different positions in exon 2 of *MED12*: 130G>A, 130G>C, 130G>T, 131G>T, 130G>T, 131G>C (listed in the ascending frequency of occurrence) [18].

Although *MED12* mutations are frequently found in human leiomyomas, their causes and mechanisms of action are still unknown. In a study by our research team published in 2006, somatic mutations in exon 2 of the *MED12* gene occurred in 50% of uterine fibroid tissue samples collected from a population of Russian females [19–20]. Further search for genetic markers associated with the risk of uterine leiomyoma seems very promising. This approach is now used to study some types of cancer. A few SNPs have already been identified whose pathogenic alleles increase the risk of endometriosis [21].

Today, the search for uterine leiomyoma-specific genetic markers is being conducted globally. A meta-analysis study carried out in 2020 [22] showed a direct link between 9 SNPs and the risk for uterine leiomyoma at the genomic level of significance ( $p < 6.6 \cdot 10^{-9}$ ): rs3820282 (1p36.12), rs124793436 (2p25.1), rs2251795 (3q26.2), rs2242652 (5p15.33), rs75228775 (10q24.33), rs2280543 (11p15.5), rs17033114 (12q23.2), rs7989971 (13q14.11) and rs12484776 (22q13.1) in a population of Japanese women. Some SNPs, including rs2251795, rs2242652, rs75228775, rs2280543, and rs7989971, had statistically significant effects in patients with multiple myomatous nodules in comparison with patients who had single nodules. Two SNPs (rs2251795 and rs75228775) were associated with the submucosal leiomyoma of the uterus, while rs2280543 on 11p15.5 was linked to the intramural uterine leiomyoma. These associations emphasize the importance of further research in the field aimed at identifying the effects of different alleles on the pathogenesis of this widespread and yet understudied disease.

The objective of the study was to find genetic markers, i.e. SNPs, specific to uterine leiomyoma.

## METHODS

Patients were recruited at the Department of Gynecologic Surgery (Kulakov Research Center for Obstetrics, Gynecology and Perinatology) and at the Gynecologic Department of Valuyki Central Hospital in 2018–2019. The study included 100 patients with uterine leiomyoma who met the following criteria: reproductive age; uterine leiomyoma confirmed by clinical examination and functional diagnostic tests (the main group); indications for surgery. Patients with acute infections, grade III/IV adenomyosis, pelvic cancers and contraindications for surgery were excluded from the study. To test the hypothesis about genetic predisposition to uterine leiomyomas, we divided the main group consisting of 100 patients with confirmed uterine leiomyomas into 2 subgroups: subgroup 1a comprised 53 patients aged 20–46 years with single or multiple fibroids and a family history of the disease (leiomyomas diagnosed in close maternal relatives, including the mother, grandmothers, sisters, or aunts); subgroup 1b included patients aged 19 to 42 years with single or multiple fibroids and no family history of leiomyomas. The subgroups were formed upon history taking. The control group included 30 postmenopausal women who had no personal or family history of uterine leiomyomas.

## Sampling

Fibroid tissue samples were collected during myomectomy or hysterectomy (the extent of surgery was determined by the number and size of the fibroids). The samples were placed in normal saline, shipped to the biobank and frozen at  $-70^{\circ}\text{C}$  for further storage. Each specimen was subjected to a histopathological examination to confirm that the excised mass was exclusively a myomatous nodule and did not contain a pseudocapsule or myometrial tissue.

## DNA extraction

DNA was extracted using a QIAamp DNA Blood Mini Kit (Qiagen; USA) following the manufacturer's protocol.

## PCR

PCR was performed in a S1000™ thermocycler (BioRad; USA). The following protocol was applied: initial denaturation at

94 °C for 2 min followed by 35 cycles of 94 °C for 60 s, primer annealing at 64 °C for 60 s and extension at 72 °C for 1.5 min; then, final extension at 72 °C min for 10 s (Table 1). Amplification efficacy was assessed by electrophoresis on 2% agarose gel stained with ethidium bromide. Imaging and documentation of electrophoresis results were done using a ChemiDoc XRS+ Gel Photo Documentation System (Bio-Rad; USA).

## Sequencing

DNA sequences were read using Sanger sequencing with a Big Dye® -terminator v. 1.1 kit (Applied Biosystems; USA). The obtained amplicons were analyzed in an ABI PRISM 3130 Genetic Analyzer (Applied Biosystems; USA). Amplicon sequences were compared to the reference sequences for each rs. BioEdit (Tom Hall; USA) was used for sequence alignment.

## DNA precipitation in mild conditions

Purified PCR products were obtained by direct DNA precipitation in mild conditions suitable for removing primers and other components of PCR from the mixture. Instead of commercial kits, we used a  $\text{NH}_4\text{Ac}$  + EtOH mix (the final concentrations of ammonium acetate and ethanol were 0.125 M and 70%, respectively). Ammonium acetate combined with ethanol (50  $\mu\text{l}$ ) was added to each test tube containing a PCR amplicon, vortexed or stirred by turning the test tube upside down. Precipitation was carried out at room temperature for 20 min; then the mixture was centrifuged at 13, 000 rpm for 15 min, the supernatant was removed, the sediment was washed with 100  $\mu\text{l}$  of 70% ethanol taken at room temperature and centrifuged again at 13, 000 rpm for 15 min. After that, the supernatant was removed and the resulting product was dried in a thermocycler or a vacuum centrifuge. Then, 20  $\mu\text{l}$  of formamide were added to each test tube.

## Data processing in BioEdit

Based on the obtained sequence chromatograms, genotypes of 5 analyzed polymorphisms were identified using BioEdit sequence aligning software (Tom Hall; USA).

## Statistical analysis

The following software was used for statistical analysis: Microsoft Excel 2013 (Microsoft; USA), SciPy libraries (SciPy

1.4.1, Python Software Foundation; USA), and Pandas for Python 2.7 (pandas 1.0.1., Wes McKinney; USA). Distribution of quantitative variables was assessed with the Shapiro-Wilk W test. In the majority of cases, the distribution was non-normal, so nonparametric statistics were used for further analysis. The median (Me) was chosen to measure central trends for quantitative variables; the spread of data was assessed with upper (H) and lower (L) quartiles. Below, the results are presented as Me (L–H). To assess the significance of intergroup differences, the Mann-Whitney U test for independent groups was applied. Differences between the sets of categorical variables were tested using Pearson's chi-squared test ( $\chi^2$ ) with the likelihood ratio. Conformance of genotype frequencies to the Hardy-Weinberg equilibrium was tested using the  $\chi^2$  test. Differences were considered statistically significant at  $p < 0.05$  (the 95% significance level). In this article, odds ratios (OR) are provided with a 95%CI. 95%CI were calculated based on  $\chi^2$  distribution as described in *Statistical Methods for Rates and Proportions* [23]. To explore possible associations between the allele of interest and a phenotypic trait (the presence of uterine leiomyoma and a family history of the disease), genotype frequencies of the analyzed allele were compared in the groups of patients with and without this trait. If differences in the distribution of allele frequencies were significant, distribution of genotype frequencies was compared in the groups. We also tested the hypotheses about the autosomal dominant and autosomal recessive inheritance patterns for the analyzed trait by constructing 4x4 contingency tables. Two-sided Fisher's test ( $F$ ) was performed for each table if the number of observations for one cell was less than 5; alternatively,  $\chi^2$  was calculated. We also calculated the probability (OR) for the trait to appear in the corresponding genotype (homozygous genotypes with the autosomal recessive inheritance pattern and hetero/homozygous genotypes with the autosomal dominant inheritance pattern). The most probable inheritance type was inferred from the results of model comparisons: the model with the highest statistical significance of differences in genotype distribution was considered the best.

## RESULTS

The following loci were genotyped: *KCNMB2* — rs12637801, *CELF4* — rs2861221, *ESR1* — rs3020434, *FBN2* — rs11742635, *CELF4* — rs12457644. These specific SNPs were chosen based on the results of the pilot study assisted by SNP array 6.0 technology (ThermoFisher; USA) and conducted

**Table 1.** Oligonucleotide primers for sequencing genome regions containing the analyzed polymorphisms

ID	Gene	Nucleotide sequence 5'→3'
rs12637801	<i>KCNMB2</i>	s3: p-5'-CCA Tgg gCT ACA gTT TAC CA-3'
		a4: p-5'-gTC CCT gTA AgA ATg CTT ggA C-3'
rs2861221	<i>CELF4</i>	s1: 5'-GCC CTC TgT gCT Cgg gAA -3'
		a2: 5'-Tgg CCC AgC AgT gAT AAA gT -3'
rs3020434	<i>ESR1</i>	s1: 5'-TTg CgC TTT gCT gTT AAT gAA g -3'
		a2: 5'-TgA CCC TAA TAC ACC TAg gAA AgT g -3'
rs11742635	<i>FBN2</i>	s1: 5'-ATC CAA ATA gTg AAA ACT Cag Tag gTA C -3'
		a2: 5'-gTg gAg CAT CAg TTA TAg gAA ggC -3'
rs12457644	<i>CELF4</i>	s3: p-5'-TAC ggg CAg ACA ACg ggT-3'
		a4: p-5'-AAg CCC TTg gTA TTC TAg CCT TAC-3'

in 20 patients with a family history of uterine leiomyomas and somatic mutations in the *MED12* gene plus another 14 patients constituting the control group (postmenopausal women without a history of uterine leiomyomas). The frequencies of 906, 600 SNPs were compared between the groups, and 6 candidate SNPs differing in the frequencies of allele and genotype distribution were selected for further genotyping of a larger sample made up of 100 patients with leiomyomas (Table 2).

We analyzed the associations between the presence of the disease/family history of the disease and the allele frequency distribution for a polymorphism of interest. The distribution of genotype frequencies conformed to the Hardy-Weinberg equilibrium for all studied polymorphisms. To explore the association of a given genotype with uterine leiomyoma, genotype distributions of the studied polymorphisms were compared between 3 groups of patients (Table 3, 4).

Comparison of the control group, which was smaller than the main group, and with group Ia (patients with a family history of uterine leiomyoma) revealed a statistically significant difference in the frequency of protective polymorphisms and alleles associated with the risk of uterine leiomyoma, suggesting that these polymorphisms can be used to predict uterine leiomyoma. Increased frequencies of minor alleles in the control group, as compared to the group of women with uterine leiomyomas, were detected with higher significance in the group of patients with a family history of the disease, which indicates the contribution of genetic component to the development of familial leiomyomas.

Statistical analysis of the data provided in Table 4 shows that the frequency of the common allele G of SNP rs11742635 is significantly higher in the subgroup of women with no family history of the disease, which makes it a risk factor for uterine leiomyoma but does not establish an association between this allele and genetic predisposition to the disease. Perhaps, this allele is more associated with other factors contributing to the pathology.

## DISCUSSION

There is an ongoing search for genetic markers of gynecologic pathologies that have serious social implications; the search is aimed at creating panels for genetic diagnostic tests that can help to predict relapses, optimize treatment strategies and develop new drugs for this disease.

Factors causing uterine leiomyoma have not been yet identified, although there is a plethora of literature on the

epidemiology, genetics, hormonal aspects, and molecular biology of this nodular growth. This determines the importance of research into the pathogenesis of uterine leiomyomas.

Familial uterine leiomyomas and the associations between the prevalence/severity of the disease and the ethnicity of the patient were first shown in a study by American geneticists [24–25]. The researchers were able to discover genomic associations with the development of uterine leiomyoma after genotyping 261 female Caucasian members of the same family (first-degree relatives). Immunohistochemistry and genetic screening of this group of patients identified the risk allele predisposing them to uterine leiomyoma in the *FASN* gene coding for fatty acid synthase located on 17q25.3 [24–25].

In another whole-genome study, 457, 044 SNPs were analyzed in 1,607 women diagnosed with uterine leiomyoma and 1,428 controls [26]. SNPs with a significant association ( $p < 5 \cdot 10^{-5}$ ) were additionally genotyped in 3,466 female patients with uterine leiomyomas and 3,245 women without a medical history of uterine leiomyomas. Throughout the genome, significant associations with uterine leiomyoma were detected in 3 chromosomal loci: 10q24.33, 22q13.1 and 11p15.5. Combination analysis revealed that the most significant SNP in each of these loci were rs7913069 ( $p = 8.65 \cdot 10^{-14}$ , OR = 1.47), rs12484776 ( $p = 2.79 \cdot 10^{-12}$ , OR = 1.23) and rs2280543 ( $p = 3.82 \cdot 10^{-12}$ , OR = 1.39), so further research into these SNPs could help to elucidate the causes of uterine leiomyoma.

In a pilot study conducted in 2017–2018 and aimed at finding the genetic markers for leiomyomas, 906, 600 SNPs were genotyped. The study was conducted in patients with uterine leiomyomas and a family history of uterine leiomyomas in their maternal first-degree relatives; the control group included women without a history of uterine leiomyoma [27]. Genotyping identified 6 polymorphisms (rs3020434, rs11742635, rs124577644, rs12637801, rs2861221, rs17677069) in genes *ESR1*, *FBN2*, *CELF4*, *KCWMB2* occurring with frequencies that were statistically different from other SNPs in both analyzed groups; the differences were more significant in the group of women with a family history of the disease, as compared to the controls. Subsequent research focused on the 6 identified polymorphisms that might be associated with uterine leiomyoma. No rare alleles of rs3020434, rs11742635, rs2861221, and rs17677069 were detected in patients with a family history of the disease [27].

Summing up, we have genotyped 5 SNPs (rs12637801, rs2861221, rs3020434, rs11742635, rs12457644) in the

**Table 2.** The list of candidate polymorphisms and genes in which they are located

ID	Gene	Mutations/SNPs	Sequence	Genomic coordinates (g.) according to HGVS
rs12637801	<i>KCNMB2</i>	C>A	GRCh37.p13 chr 3 GRCh38.p12 chr 3	NC_000003.11:g.178379500C>A NC_000003.12:g.178661712C>A
rs2861221	<i>CELF4</i>	C>G	GRCh37.p13 chr 18 GRCh38.p12 chr 18	NC_000018.9:g.34940179 C>G NC_000018.10:g.37360216 C>G
rs3020434	<i>ESR1</i>	C>T	GRCh37.p13 chr 6 GRCh38.p12 chr 6	NC_000006.11:g.152358940C>T NC_000006.12:g.152037805C>T
rs11742635	<i>FBN2</i>	G>T	GRCh37.p13 chr 5 GRCh38.p12 chr 5	NC_000005.9:g.127788794G>T NC_000005.10:g.128453101G>T
rs12457644	<i>CELF4</i>	G>A	RCh37.p13 chr 18 GRCh38.p12 chr 18	NC_000018.9:g.34944976 G>A NC_000018.10:g.37365013G>A



samples of patients with a family history of uterine leiomyoma (close maternal relatives, including the mother, grandmothers, sisters and aunts), who constituted subgroup Ia, patients without a history of uterine leiomyomas, who formed subgroup Ib, and patients from the control group without a history of uterine leiomyoma. The obtained results demonstrate that genotype frequency of allele C of *KCNMB2* (rs12637801) is significantly higher in the group of patients with the familial disease in comparison with the controls (87% vs 77%;  $p = 0.04$ ; OR = 2.63) and the genotype frequency of allele G of *CELF4* (rs12457644) is also significantly higher in the subgroup of patients with the familial disease in comparison with the controls (85% vs 0.70%,  $p = 0.04$ , OR = 2.63). These

alleles might be associated with increased risk of uterine leiomyoma and be a result of genetic predisposition to this pathologic condition.

## CONCLUSIONS

We have established an association between SNPs rs12637801, rs2861221, rs3020434, rs11742635, rs12457644 and the presence of uterine leiomyomas in the medical history of the patient's family. We have also assessed the relationship between the risk of this disease and the genotype of the analyzed polymorphisms. Perhaps, our strategy of studying gene polymorphisms could help to explain the causes

**Table 3.** Allele frequency distribution for the studied polymorphisms in the control group, subgroup Ia (women with a family history of the disease) and the main group (women with uterine leiomyomas)

ID	Allele variant	Frequency, %			Fisher's F		OR	
		Controls, $n = 30$	Subgroup Ia (women with a history of the disease) $n = 53$	Main group (women with uterine leiomyomas) $n = 100$	Subgroup Ia (women with a history of the disease)	Main group (women with leiomyomas)	Subgroup Ia (women with a history of the disease)	Main group (women with uterine leiomyomas)
<i>KCNMB2</i> rs12637801	AA	0.00	0.02	0.02	<b>0.04</b>	0.09	2.63	2.01
	AC	0.47	0.23	0.28				
	CC	0.53	0.75	0.70				
<i>CELF4</i> rs2861221	CC	0.60	0.71	0.66	0.30	0.32	1.64	0.48
	CG	0.30	0.23	0.29				
	GG	0.10	0.06	0.05				
<i>ESR1</i> rs3020434	CC	0.43	0.61	0.58	0.11	0.17	2.09	1.77
	CT	0.50	0.33	0.35				
	TT	0.07	0.06	0.07				
<i>FBN2</i> rs11742635	GG	0.57	0.67	0.73	0.27	0.09	0.27	2.04
	GT	0.37	0.31	0.25				
	TT	0.06	0.02	0.02				
<i>CELF4</i> rs12457644	AA	0.13	0.06	0.05	<b>0.04</b>	0.09	2.63	2.01
	AG	0.33	0.19	0.25				
	GG	0.53	0.75	0.70				

**Table 4.** Allele frequency distribution for the studied polymorphisms in the control group, subgroup Ib (women with no family history of the disease) and the main group of patients with uterine leiomyomas

ID	Allele variant	Frequency, %			Fisher's F		OR	
		Control group, $n = 30$	Subgroup Ib (women with no family history of the disease), $n = 47$	Main group (women with uterine leiomyomas), $n = 100$	Subgroup Ib (women with no family history of the disease)	Main group (women with uterine leiomyomas)	Subgroup Ib (women with no family history of the disease)	Main group (women with uterine leiomyomas)
<i>KCNMB2</i> rs12637801	AA	0.00	0.02	0.02	0.35	0.09	1.54	2.01
	AC	0.47	0.34	0.28				
	CC	0.53	0.64	0.70				
<i>CELF4</i> rs2861221	CC	0.60	0.60	0.66	0.30	0.32	1.64	0.48
	CG	0.30	0.36	0.29				
	GG	0.10	0.04	0.05				
<i>ESR1</i> rs3020434	CC	0.43	0.53	0.58	0.40	0.17	2.83	1.77
	CT	0.50	0.38	0.35				
	TT	0.07	0.09	0.07				
<i>FBN2</i> rs11742635	GG	0.57	0.79	0.73	<b>0.04</b>	0.09	2.83	2.04
	GT	0.37	0.19	0.25				
	TT	0.06	0.02	0.02				
<i>CELF4</i> rs12457644	AA	0.13	0.79	0.05	0.15	0.09	0.29	2.01
	AG	0.33	0.19	0.25				
	GG	0.53	0.02	0.70				

underlying familial uterine leiomyomas, as well as to create a genetic diagnostic panel for predicting the risk of this condition. Further research will be focused on the genotyping of patients

with a family history of uterine leiomyomas in order to confirm the associations between the disease and the identified genetic markers.

## References

1. Adamyan LV, Andreeva EN, Artymuk NV, Belocerkovceva LD, Bezhenar VF, Gevorkyan MA, i dr. Mioma matki: diagnostika, lechenie i reabilitacija. 2015; 101. Russian.
2. Adamyan LV, Spicyn VA, Andreeva EN. Geneticheskie aspekty ginekologicheskikh zabolevanij. M., GJeOTAR-Media, 2008; 215. Russian.
3. Sogoyan NS, Kuznetsova MV, Asaturova AV, Adamyan LV, Trofimov DYU. Somaticheskie mutacii v jekzone 2 gena MED12 u zhenshin s odinochnoj i mnozhestvennoj miomoy matki. Akusherstvo i ginekologija. 2018; (12): 63–70. Russian.
4. Sogoyan NS, Adamyan LV. Geneticheskie mehanizmy razvitiya miomy matki. Problemy reprodukcii. 2016; 22 (1): 28–34. Russian.
5. Kudrina EA, Baburin DV. Mioma matki: sovremennye aspekty patogeneza i lechenija (klinicheskaja lekcija). Arhiv akusherstva i ginekologii im. VF Snegireva. 2016; 3 (1): 4–10. Russian.
6. Kuznetsova MV, Trofimov DYU, Tihonchuk EYu, Sogoyan NS, Adamyan LV, Suhij GT. Molekuljarnye mehanizmy patogeneza miomy matki: analiz mutacij gena MED12 v Rossijskoj populjacii. Akusherstvo i ginekologija. 2016; (10): 85–90. Russian.
7. Sidorova IS. Mioma matki: vozmozhnosti lechenija i profilaktiki. Russkij medicinskij zhurnal. (Spec. nomer: Mat' i ditja.) 2002; 10 (7): 336–9. Russian.
8. Barjon K, Mikhail LN. Uterine Leiomyomata (Fibroids). StatPearls Publishing, Treasure Island (FL) StatPearls. 2019; 15.
9. Baird DD, Dunson DB, Hill MC, Cousins D, Schectman, JM. High cumulative incidence of uterine leiomyoma in black and white women: ultrasound evidence. American journal of obstetrics and gynecology. 2003; 188 (1): 100–107.
10. Gracia M, Carmona F. Uterine myomas: clinical impact and pathophysiological bases. European Journal of Obstetrics and Gynecology and Reproductive Biology. 2020; (1): 1–5.
11. Tihomirov AL. Patogeneticheskoe obosnovanie rannej diagnostiki, lechenija i profilaktiki miomy matki [dissertacija]. M., 1998. Russian.
12. Tihomirov AL. Mioma, patogeneticheskoe obosnovanie organosohranjajushhego lechenija. M.: Medicina, 2013; 319. Russian.
13. Brouwer MW, Tebbe-Gholami M, Starink MV. Hereditary leiomyomatosis: a woman with red-brown nodules. Nederlands tijdschrift voor geneeskunde. 2015; (159): A8867–A8867.
14. Bulun SE. Uterine fibroids. New England Journal of Medicine. 2013; 369 (14): 1344–55.
15. Mäkinen N, Mehine M, Tolvanen J, Kaasinen E, Li Y, Lehtonen HJ, et al. MED12, the mediator complex subunit 12 gene, is mutated at high frequency in uterine leiomyomas. Science. 2011; 334 (6053): 252–5.
16. Mittal P, Shin YH, Yatsenko SA, Castro CA, Surti U, Rajkovic A. MED12 gain-of-function mutation causes leiomyomas and genomic instability. The Journal of clinical investigation. 2015; 125 (8): 3280–4.
17. Akbari M, Do AA, Yassaee F, Mirfakhraie R. MED12 Exon 1 Mutational Screening in Iranian Patients with Uterine Leiomyoma. Reports of biochemistry & molecular biology. 2019; 8 (1): 1–21.
18. Markowski DN, Bartnitzke S, Löning T, Drieschner N, Helmke BM, Bullerdiek J. MED12 mutations in uterine fibroids — their relationship to cytogenetic subgroups. International journal of cancer. 2012; 131 (7): 1528–36.
19. Savickij GA, Savickij AG. Mioma matki (problemy patogeneza i patogeneticheskoy terapii). Novoe v akusherstve i ginekologii. Sankt-Peterburg: JeLBI, 2000; 236. Russian.
20. Samojlova TE. Vozmozhnosti i perspektivy medikamentoznogo lechenija miomy matki. Medicinskij sovet. 2013; (3): 106–9. Russian.
21. Pshenichnjuk EYu, Kuznetsova MV, Burmenskaja OV, Kochetkova TO, Nepsha OS, Trofimov DYU, i dr. Associacija mezhdru chastotami vstrechaemosti odnonukleotidnyh polimorfizmov v genah ZNF366 i VEZT i riskom razvitiya naruzhnogo genital'nogo jendometrioz: dannye po rossijskoj populjacii. Akusherstvo i ginekologija. 2017; (6): 64–73. Russian.
22. Sakai K, Tanikawa C, Hirasawa A, Chiyoda T, Yamagami W, Kataoka F. Identification of a novel uterine leiomyoma GWAS locus in a Japanese population. Scientific Reports. 2020; 10 (1): 1–8.
23. LaFleur B. Book Review: Statistical methods for rates and proportions. Clinical Trials. 2004; 1 (6): 567–8.
24. Gallagher CS, Makinen N, Harris HR, Uimari O, Cook JP, Shiges N, et al. Genome-wide association analysis identifies 27 novel loci associated with uterine leiomyomata revealing common genetic origins with endometriosis. Biorxiv. 2018; 1–26.
25. Gallagher CS, Mäkinen N, Harris HR, Rahmioglu N, Uimari O, Cook JP, et al. Genome-wide association and epidemiological analyses reveal common genetic origins between uterine leiomyomata and endometriosis. Nature communications. 2019; 10 (1): 1–11.
26. Cha PC, Takahashi A, Hosono N, Low SK, Kamatani N, Kubo M, et al. A genome-wide association study identifies three loci associated with susceptibility to uterine fibroids. Nature genetics. 2011; 43 (5): 447.
27. Sogoyan NS, Kuznetsova MV, Lolomadze EA, Mikhailovskaya GV, Mishina ND, Trofimov DYU, et al. A study of polymorphisms rs3020434, rs 1742635, rs124577644, rs12637801, rs2861221, and rs 17677069 in women with uterine leiomyomas and a family history of the disease. Obstetrics and Gynecology. 2019; (10): 115–28.

## Литература

1. Адамян Л. В., Андреева Е. Н., Артымук Н. В., Белоцерковцева Л. Д., Беженарь В. Ф., Геворкян М. А. и др. Миома матки: диагностика, лечение и реабилитация. 2015; 101.
2. Адамян Л. В., Спичин В. А., Андреева Е. Н. Генетические аспекты гинекологических заболеваний. М.: ГЭОТАР-Медиа, 2008; 215.
3. Согоян Н. С., Кузнецова М. В., Асатурова А. В., Адамян Л. В., Трофимов Д. Ю. Соматические мутации в экзоне 2 гена MED12 у женщин с одиночной и множественной миомой матки. Акушерство и гинекология. 2018; (12): 63–70.
4. Согоян Н. С., Адамян Л. В. Генетические механизмы развития миомы матки. Проблемы репродукции. 2016; 22 (1): 28–34.
5. Кудрина Е. А., Бабуринов Д. В. Миома матки: современные аспекты патогенеза и лечения (клиническая лекция). Архив акушерства и гинекологии им. В. Ф. Снегирева. 2016; 3 (1): 4–10.
6. Кузнецова М. В., Трофимов Д. Ю., Тихончук Е. Ю., Согоян Н. С., Адамян Л. В., Сухих Г. Т. Молекулярные механизмы патогенеза миомы матки: анализ мутаций гена MED12 в Российской популяции. Акушерство и гинекология. 2016; (10): 85–90.
7. Сидорова И. С. Миома матки: возможности лечения и профилактики. Русский медицинский журнал. (Спец. номер: Мать и дитя.) 2002; 10 (7): 336–9.
8. Barjon K, Mikhail LN. Uterine Leiomyomata (Fibroids). StatPearls Publishing, Treasure Island (FL) StatPearls. 2019; 15.
9. Baird DD, Dunson DB, Hill MC, Cousins D, Schectman, JM. High cumulative incidence of uterine leiomyoma in black and white women: ultrasound evidence. American journal of obstetrics and gynecology. 2003; 188 (1): 100–107.
10. Gracia M, Carmona F. Uterine myomas: clinical impact and pathophysiological bases. European Journal of Obstetrics and



- Gynecology and Reproductive Biology. 2020; (1): 1–5.
11. Тихомиров А. Л. Патогенетическое обоснование ранней диагностики, лечения и профилактики миомы матки [диссертация]. М., 1998.
  12. Тихомиров А. Л. Миома, патогенетическое обоснование органосохраняющего лечения. М.: Медицина, 2013; 319.
  13. Brouwer MW, Tebbe-Gholami M, Starink MV. Hereditary leiomyomatosis: a woman with red-brown nodules. *Nederlands tijdschrift voor geneeskunde*. 2015; (159): A8867–A8867.
  14. Bulun SE. Uterine fibroids. *New England Journal of Medicine*. 2013; 369 (14): 1344–55.
  15. Mäkinen N, Mehine M, Tolvanen J, Kaasinen E, Li Y, Lehtonen HJ, et al. MED12, the mediator complex subunit 12 gene, is mutated at high frequency in uterine leiomyomas. *Science*. 2011; 334 (6053): 252–5.
  16. Mittal P, Shin YH, Yatsenko SA, Castro CA, Surti U, Rajkovic A. MED12 gain-of-function mutation causes leiomyomas and genomic instability. *The Journal of clinical investigation*. 2015; 125 (8): 3280–4.
  17. Akbari M, Do AA, Yassaee F, Mirfakhraie R. MED12 Exon 1 Mutational Screening in Iranian Patients with Uterine Leiomyoma. *Reports of biochemistry & molecular biology*. 2019; 8 (1): 1–21.
  18. Markowski DN, Bartnitzke S, Löning T, Drieschner N, Helmke BM, Bullerdiek J. MED12 mutations in uterine fibroids—their relationship to cytogenetic subgroups. *International journal of cancer*. 2012; 131 (7): 1528–36.
  19. Савицкий Г. А., Савицкий А. Г. Миома матки (проблемы патогенеза и патогенетической терапии). Новое в акушерстве и гинекологии. Санкт-Петербург: ЭЛБИ, 2000; 236.
  20. Самойлова Т. Е. Возможности и перспективы медикаментозного лечения миомы матки. *Медицинский совет*. 2013; (3): 106–9.
  21. Пшеничнюк Е. Ю., Кузнецова М. В., Бурменская О. В., Кочеткова Т. О., Непша О. С., Трофимов Д. Ю. и др. Ассоциация между частотами встречаемости однонуклеотидных полиморфизмов в генах ZNF366 и VEZT и риском развития наружного генитального эндометриоза: данные по российской популяции. *Акушерство и гинекология*. 2017; (6): 64–73.
  22. Sakai K, Tanikawa C, Hirasawa A, Chiyoda T, Yamagami W, Kataoka F. Identification of a novel uterine leiomyoma GWAS locus in a Japanese population. *Scientific Reports*. 2020; 10 (1): 1–8.
  23. LaFleur B. Book Review: Statistical methods for rates and proportions. *Clinical Trials*. 2004; 1 ( 6): 567–8.
  24. Gallagher CS, Mäkinen N, Harris HR, Uimari O, Cook JP, Shigesu N, et al. Genome-wide association analysis identifies 27 novel loci associated with uterine leiomyomata revealing common genetic origins with endometriosis. *Biorxiv*. 2018; 1–26.
  25. Gallagher CS, Mäkinen N, Harris HR, Rahmioglu N, Uimari O, Cook JP, et al. Genome-wide association and epidemiological analyses reveal common genetic origins between uterine leiomyomata and endometriosis. *Nature communications*. 2019; 10 (1): 1–11.
  26. Cha PC, Takahashi A, Hosono N, Low SK, Kamatani N, Kubo M, et al. A genome-wide association study identifies three loci associated with susceptibility to uterine fibroids. *Nature genetics*. 2011; 43 (5): 447.
  27. Согоян Н. С., Кузнецова М. В., Лоломадзе Е. А., Михайловская Г. В., Мишина Н. Д., Трофимов Д. Ю., и др. Исследование полиморфизмов rs3020434, rs11742635, rs124577644, rs12637801, rs2861221, rs17677069 у женщин с миомой матки и отягощенным анамнезом. *Акушерство и гинекология*. 2019; (10): 115–28.

## THE ROLE OF SOME XENOBIOTIC BIOTRANSFORMATION GENES SNP IN THE DEVELOPMENT OF ACUTE PANCREATITIS

Samgina TA ✉, Nazarenko PM, Polonikov AV, Lazarenko VA

Kursk State Medical University, Kursk, Russia

Genetically determined features of the xenobiotic biotransformation system play an important role in the development of acute pancreatitis (AP) and its complications. The aim of this study was to assess the contribution of 3 SNPs (*CYP1A1* -462 T>C rs1048943, *CYP2E1* -1293 G>C rs3813867 and *ABCB1* -3435 G>A rs1045642) to the development of AP and its complications. DNA samples were collected from 547 unrelated patients with AP (154 women and 393 men; mean age  $48.9 \pm 13.1$  years) undergoing therapy at surgery departments of Kursk and 573 unrelated individuals without gastrointestinal diseases (161 women and 412 men; mean age  $47.8 \pm 12.1$  years). The polymorphisms were genotyped by PCR using TaqMan probes for allele discrimination. Infected pancreatic necrosis (IPN) was observed in 97 patients; 101 patients developed a pseudocyst (PC); 111 patients had a peripancreatic necrosis (PN). AP was the most common in the carriers of the A allele in *ABCB1* G>A (rs1045642) ( $p = 0.0008$ ). The carriers of the G/G genotype rarely developed both AP ( $p = 5 \cdot 10^{-4}$ ) and its complications: IPN ( $p = 0.03^{\circ}$ ), PN ( $p = 0.036^{\circ}$ ), PC ( $p = 0.04^{\circ}$ ). The carriers of the G/C–C/C *CYP2E1* G>C (rs3813867) genotypes who had no long-term history of alcohol abuse rarely developed AP ( $p = 0.03$ ). The carriers of the G/C *CYP2E1* (rs3813867) genotype tended to develop pseudocysts ( $p = 0.050^{\circ}$ ). AP was more frequently complicated by IPN ( $p = 0.009^{\circ}$ ), PN ( $p = 0.003^{\circ}$ ) and PC ( $p = 0.003^{\circ}$ ) in the carriers of the C/C *CYP1A1* T>C (rs1048943) genotype. A milder course of AP was typical for the carriers of the G/G *ABCB1* G>A (rs1045642) genotype; a more severe course was characteristic of the carriers of the C/C *CYP1A1* T>C (rs1048943) genotype.

**Keywords:** acute pancreatitis, xenobiotic biotransformation enzyme genes, genetic polymorphism, rs1045642, rs1048943, rs3813867

**Author contribution:** Samgina TA conceived and designed the study, conducted clinical and molecular-genetic tests, analyzed and interpreted the obtained data, and wrote the manuscript; Nazarenko PM supervised surgical treatment and postoperative care at Kursk City Clinical Hospital № 4 and recruited patients for the study; Polonikov AV supervised genetic testing; Lazarenko VA supervised the study.

**Compliance with ethical standards:** the study was approved by the Ethics Committee of Kursk State Medical University (Protocol № 3 dated March 11, 2013). The patients gave informed consent to participate.

✉ **Correspondence should be addressed:** Tatiana A. Samgina  
K. Marksa, 3, 305000; Kursk, tass@list.ru

**Received:** 05.01.2020 **Accepted:** 08.02.2020 **Published online:** 15.02.2020

**DOI:** 10.24075/brsmu.2020.008

## ЗНАЧЕНИЕ ОДНОНУКЛЕОТИДНОГО ПОЛИМОРФИЗМА НЕКОТОРЫХ ГЕНОВ СИСТЕМЫ БИОТРАНСФОРМАЦИИ КСЕНОБИОТИКОВ В РАЗВИТИИ ОСТРОГО ПАНКРЕАТИТА

Т. А. Самгина ✉, П. М. Назаренко, А. В. Полоников, В. А. Лазаренко

Курский государственный медицинский университет, Курск, Россия

Генетически детерминированные особенности функционирования системы биотрансформации ксенобиотиков играют важную роль в развитии острого панкреатита (ОП) и его осложнений. Целью работы было определить вклад однонуклеотидных полиморфизмов генов *CYP1A1* -462 T>C rs1048943, *CYP2E1* -1293 G>C rs3813867 и *ABCB1* -3435 G>A rs1045642 в развитие ОП и его осложнений. Образцы ДНК получали от 547 неродственных больных ОП (154 женщины и 393 мужчины; средний возраст составил  $48,9 \pm 13,1$ ), находившихся на стационарном лечении в хирургических отделениях города Курска и 573 неродственных индивидов без заболеваний ЖКТ (161 женщина и 412 мужчин; средний возраст —  $47,8 \pm 12,1$ ). Генотипирование полиморфизма изучаемых генов выполняли методом ПЦР путем дискриминации аллелей с помощью TaqMan-зондов. У 97 пациентов развился инфицированный панкреонекроз (ИП), у 101 — псевдокиста (ПК), у 111 — гнойно-некротический перипанкреатит (ГНП). Установлено, что у носителей аллеля А гена *ABCB1* G>A (rs1045642) чаще развивался ОП ( $p = 0,0008$ ), у носителей генотипа G/G редко развивался как ОП ( $p = 5 \cdot 10^{-4}$ ), так и его осложнения: ИП ( $p = 0,03^{\circ}$ ), ГНП ( $p = 0,036^{\circ}$ ), ПК ( $p = 0,04^{\circ}$ ). Отсутствие длительного злоупотребления алкогольными напитками у носителей генотипов G/C–C/C *CYP2E1* G>C (rs3813867) редко приводило к развитию ОП ( $p = 0,03$ ), у носителей генотипа G/C *CYP2E1* (rs3813867) ( $p = 0,050^{\circ}$ ) чаще возникала псевдокиста. У носителей генотипа C/C *CYP1A1* T>C (rs1048943) ОП чаще осложнялся ИП ( $p = 0,009^{\circ}$ ), ГНП ( $p = 0,003^{\circ}$ ), ПК ( $p = 0,003^{\circ}$ ). В целом, для носителей генотипов G/G *ABCB1* G>A (rs1045642) было характерно более легкое течение ОП, тяжелое течение было характерно для носителей C/C *CYP1A1* T>C (rs1048943).

**Ключевые слова:** острый панкреатит, гены ферментов биотрансформации ксенобиотиков, генетический полиморфизм, rs1045642, rs1048943, rs3813867

**Информация о вкладе авторов:** Т. А. Самгина — написание статьи, разработка концепции и дизайна, анализ и интерпретация данных, реализация клинических и молекулярно-генетических методов исследования, статистическая обработка данных; П. М. Назаренко — руководство хирургической частью исследования, лечение и подбор больных в ОБУЗ КГКБ № 4; А. В. Полоников — руководство генетической частью исследования; В. А. Лазаренко — руководство исследованием.

**Соблюдение этических стандартов:** исследование одобрено этическим комитетом Курского государственного университета (протокол № 3 от 11 марта 2013 г.). Все участники исследования подписали добровольное информированное согласие.

✉ **Для корреспонденции:** Татьяна Александровна Самгина  
ул. К. Маркса, д. 3, 305000; г. Курск; tass@list.ru

**Статья получена:** 05.01.2020 **Статья принята к печати:** 08.02.2020 **Опубликована онлайн:** 15.02.2020

**DOI:** 10.24075/vrgmu.2020.008

In recent years, there has been a lot of research into the contribution of environmental chemicals and disrupted prooxidant-antioxidant balance to the development of acute pancreatitis (AP). For example, acute nonbiliary pancreatitis

has been associated with smoking [1]; smokers and alcohol abusers with AP have been shown to be at increased risk for necrotizing pancreatitis [2]. Despite numerous research efforts, though, genetic mechanisms underlying predisposition

to AP and its complications remain understudied. Still, it is obvious that an important role here is played by the genetically determined features of xenobiotic biotransformation and antioxidant defense systems.

The transmembrane protein ABCB1 is a member of the subfamily of broad-specificity ATP-dependent drug/xenobiotic transporters. This protein inhibits accumulation of narcotic drugs in multidrug resistant cells and often mediates resistance to antitumor medications. ABC genes constitute 7 different subfamilies. The ABCB1 protein is a member of the MDR/TAP subfamily; the gene encoding this protein is located on the chromosomal region 7q21.12. *ABCB1* is primarily expressed in the testicles, muscles, stomach and pancreas. There have been studies of its role in the development of colorectal cancer [3, 4] but no statistically significant associations have been reported. The role of this gene in AP has never been investigated.

So far, the cytochrome P450 oxidase system remains the most well-studied. It comprises CYP1, CYP2 and CYP3 enzyme families responsible for the metabolism of foreign compounds in mammals.

It is reported that polymorphisms of the *P450*, *CYP1A1* and *CYP2E1* genes are associated with increased activity of enzymes in patients with pancreatitis [5]. The researchers conclude that *CYP1A1* is the most implicated in pancreatitis; it triggers the proteinase cascade, promoting DNA replication and tissue proliferation, generates oxygen radicals, forms reactive intermediates during xenobiotic metabolism, and can activate various carcinogens.

It is known that *CYP1A1* (aromatic ligand-dependent aryl hydrocarbon hydroxylase) converts polycyclic aromatic hydrocarbons into highly active mutagenic metabolites in the first phase of xenobiotic biotransformation. The gene encoding the key enzyme involved in this process is located on the chromosomal region 15q24.1. Today, 19 gene polymorphisms are known that play a role in the development of cancer and occupational diseases [6].

*CYP2E1* (cytochrome P450 2E1) encodes cytochrome P450 proteins (monooxygenases) that catalyze many reactions related to the metabolism of medicinal drugs and the production of cholesterol, steroids and other lipids. This protein is found in the endoplasmic reticulum and can be activated by ethanol, diabetes and fasting. The enzyme participates in the metabolism of ethanol, acetone, ethylene glycol, and tobacco smoke premutagens [7]. The gene itself is located on 10q26.3 and expressed primarily in adipose tissue, esophageal mucosa and peripheral blood.

Comparison of allelic and genotype frequencies of *ADH2*, *ADH3*, *ALDH2*, *CYP2E1*, *IL1*, *IL6*, *IL8*, and *TNF* has revealed that *CYP2E1* and *ALDH2* are significantly less frequent in patients with chronic pancreatitis than in healthy controls [8]. At the same time, no association has been detected between the *CYP2E1* polymorphism and alcohol-induced pancreatitis in a studied Asian population [9, 10]. It is reported that carriers of the m2/m2 *CYP1A1* genotype might be more predisposed to alcoholic cirrhosis and alcohol-related pancreatitis [11]. An association has been established between the polymorphism *P450 CYP1A1* Ile105Val and the increased risk of chronic pancreatitis [12]. The A→G transition results in a leucine-to-valine substitution in codon 462 of the cytochrome molecule (Ile462Val); consequently, the activity of the produced enzyme increases twofold in comparison with the "original" protein, which can increase the concentrations of underoxidized toxic intermediates and lead to the accumulation of free radicals [13–15].

Thus, polymorphic variants of genes coding for the enzymes of xenobiotic biotransformation may be implicated

in AP. The aim of this study was to investigate a possible association between AP/its complications and the following SNPs: *CYP1A1*-462 T>C rs1048943, *CYP2E1*-1293 G>C rs3813867 and *ABCB1* -3435 G>A rs1045642.

## METHODS

DNA samples were collected from 547 unrelated inpatients with AP (154 women and 393 men) undergoing therapy at surgery departments of Kursk in 2012–2015 and 573 unrelated individuals without gastrointestinal diseases (161 women and 412 men). The mean age of the patients was  $48.9 \pm 13.1$  years, the mean age of the healthy controls,  $47.8 \pm 12.1$  years. The following inclusion criteria were applied: 1) the established diagnosis of AP; 2) age of 18–80 years; 3) the absence of biliary pathology, such as gallstones, *pancreas divisum* and pancreatic injury, including injuries due to surgery/endoscopic manipulations; 4) no previous history of pancreotoxic drugs (hypothiazid, NSAIDs, steroid anti-inflammatory drugs), the absence of autoimmune disorders, infections, allergies (to paints and varnishes), pregnancy/menopause-related endocrine pathology, diseases of neighboring gastrointestinal organs; 5) no family history of AP. Patients who did not meet the inclusion criteria were excluded from the study.

AP was diagnosed using the AP classification developed by the Russian Society of Surgeons in 2014, which is based on the Atlanta-92 classification and its modifications proposed by the International Association of Pancreatology in collaboration with the International Acute Pancreatitis Classification Working Group in Cochlin in 2011 [16,17]; the patients underwent a standard examination, as well as laboratory (complete blood count and biochemistry) and instrumental (US and MRI of the pancreas, EGD) tests.

The patients were also asked about their lifestyle, including addictions such as smoking and alcohol abuse regarded as the major risk factors for AP [18,19].

The participants were distributed into two groups depending on the amount of weekly consumed alcohol: 1) consumption below 200 g ethanol a week; 2) consumption above 200 g ethanol a week. This threshold is the median value (grams of pure ethanol) of the maximum weekly alcohol intake considered safe in many countries [20]. Another two groups were formed based on the frequency of alcohol consumption: 1) 1 or 2 days a month or less often; 2) 1 day a week or more often. Also, the participants were divided into two groups based on the total duration of alcohol consumption: 1) less than 10 years; 2) 10 years or more.

Samples of the patients' whole venous blood (5–10 ml) were collected into plastic EDTA-containing (0.5M) test tubes. Then, the samples were frozen and stored at  $-20^{\circ}\text{C}$  until further DNA isolation. DNA was isolated using a standard two-step phenol-chloroform extraction and precipitation in ethanol. First, white blood cells were lysed. Briefly, the white blood cell pellet obtained by centrifuging the sample twice with a sodium phosphate buffer (pH = 7.8) was lysed in the solution containing a TE-buffer, proteinase K and 0.4% sodium dodecyl sulfate (SDS) for 12 h at  $42^{\circ}\text{C}$ . Then, genomic DNA was isolated from the obtained cell lysate. The first step was extraction in phenol and 10 mM Tris-HCl (pH = 8.0), the second, in phenol and chloroform (1:1); in the final step, extraction was performed in chloroform only. Genomic DNA was precipitated in ice-cold 96% ethanol, air-dried and dissolved in the TE-buffer. Then, the DNA concentration was measured. The obtained DNA was frozen at  $-20^{\circ}\text{C}$  until genotyping.

Genotyping of *CYP1A1* -462 T>C rs1048943, *CYP2E1* -1293 G>C rs3813867 and *ABCB1* -3435 G>A rs1045642

was performed using real-time PCR. Alleles were discriminated using TaqMan probes, a CFX96 PCR detection system (Bio-Rad Laboratories; USA) and commercial TaqMan SNP Genotyping Assays (Applied Biosystems; USA). Repeated genotyping of randomly (blindly) selected samples (10% of the total sample size) demonstrated 100% repeatability of the results. Categorical variables were compared using Pearson's  $\chi^2$ . Normally distributed quantitative variables were compared using Student's T-test; Mann-Whitney U test was applied to compare the variables with non-normal distribution. Conformity genotype frequencies to Hardy-Weinberg expectations was tested using Pearson's  $\chi^2$ . Associations of alleles and genotypes with the risk of pancreatitis were measured using the odds ratio (OR). Statistical analysis was carried out in Statistica 6.0 (StatSoft; USA).

## RESULTS

No associations were established between the risk of AP and the two following polymorphisms: *CYP1A1* T>C and *CYP2E1* G>C (Table 1).

The carriers of the A allele in *ABCB1* G>A (rs1045642) were at increased risk for AP, unlike the carriers of the G/G genotype, who were at low risk for this condition.

AP was rarely observed in the carriers of the G/C–C/C *CYP2E1* G>C (rs3813867) genotypes who did not have a long history of alcohol abuse (Table 2).

Infected pancreatic necrosis occurred more frequently in the carriers of the C/C *CYP1A1* T>C (rs1048943) genotype than in the carriers of the G/G *ABCB1* G>A (rs1045642) genotype (Table 3).

Pancreatic pseudocysts were observed in the carriers of the C/C *CYP1A1* T>C (rs1048943) and G/C *CYP2E1* (rs3813867) genotypes more often than in the carriers of the G/G *ABCB1* G>A rs1045642 genotype (Table 4).

Peripancreatic necrosis was the most common complication of AP in the carriers of the C/C *CYP1A1* T>C (rs1048943) genotype; it rarely occurred in the carriers of the G/G *ABCB1* G>A (rs1045642) genotype (Table 5).

## DISCUSSION

Biotransformation is the enzyme-driven metabolic conversion of foreign compounds (xenobiotics) that can be broken down into 3 stages: activation, detoxication and clearance [21,22]. A lot of enzymes participate in this process. The role of genes involved in xenobiotic biotransformation (*CYP2E1* and *CYP1A1*) in promoting alcohol-induced pancreatitis and liver cirrhosis has been studied in Brazilian alcohol abusers; no association has been detected between these genes and pancreatitis [11].

It is known that cytochromes P450 are involved in the bioactivation of polycyclic aromatic hydrocarbons. *CYP1A1* is not found in healthy tissue; its expression is only induced by xenobiotics. The association between the C/C *CYP1A1* T>C (rs1048943) genotype and the increased risk of AP established in this study suggests a change in the activity of the encoded enzyme and a rise in the concentration of underoxidized toxic metabolites that exert an aggressive effect on pancreatic tissue.

The role of *CYP2E1* polymorphisms in the development of acute pancreatitis has not been studied before, but there are reports suggesting that the minor allele of this gene might be protective against methanol poisoning [23]. In our study, AP was more often observed in the carriers of the G/C *CYP2E1* (rs3813867) genotype, but if the total duration of alcohol abuse was less than 10 years, the carriers of the G/C–C/C *CYP2E1* G>C (rs3813867) genotypes were more resistant to the harmful effects of alcohol and rarely developed AP.

The *ABCB1* gene codes for P-glycoprotein; it is an efflux transporter that participates in the clearance of xenobiotics, preventing their accumulation in a person's organs and tissues

**Table 1.** The analysis of the associations between the risk of AP and the alleles/genotypes of the polymorphic genes encoding the enzymes involved in xenobiotic biotransformation and antioxidant defense (the codominant model)

Gene (SNP ID)	Genotype, allele	n (%)		p	OR (95%CI) <sub>cor</sub>
		Healthy individuals (n = 573)	Patients (n = 547)		
<i>CYP1A1</i> -462 T>C (rs1048943)	T/T	507 (91.0)	489 (90.2)	0.07	1.00
	T/C	49 (8.8)	46 (8.5)		0.97 (0.64–1.48)
	C/C	1 (0.2)	7 (1.3)		7.26 (0.89–59.21)
	C	0.05	0.06	0.3	1.22 (0.83–1.79)
<i>CYP2E1</i> -1293 G>C (rs3813867)	G/G	532 (95.0)	513 (94.0)	0.46	1.00
	G/C	22 (3.9)	29 (5.3)		1.37 (0.78–2.41)
	C/C	6 (1.1)	4 (0.7)		0.69 (0.19–2.46)
	C	0.03	0.034	0.64	1.12 (0.70–1.80)
<i>ABCB1</i> -3435 G>A (rs1045642)	A/A	158 (28.3)	183 (33.5)	5·10 <sup>-4</sup>	1.00
	G/A	269 (48.2)	284 (52.0)		0.91 (0.70–1.19)
	G/G	131 (23.5)	79 (14.5)		0.52 (0.37–0.74)
	A	0.52	0.6	0.0008	1.33 (1.13–1.58)

**Table 2.** The impact of alcohol abuse on the development of AP in the presence of alcohol-induced pancreatitis in the carriers of the studied polymorphisms

Genotype	No risk factor (F)			Risk factor (F+) <sup>3</sup>		
	Healthy individuals	Patients	OR (95%CI) <sub>inter</sub> P 1	Healthy individuals	Patients	OR (95%CI) <sub>inter</sub> P 1
<b><i>CYP2E1</i> (rs3813867)</b>						
G/G	119 (90.8)	173 (96.6)	0.34 (0.13–0.94) 0.03	98 (96.1)	116 (95.1)	1.27 (0.35–4.62) 0.72 <sup>D</sup>
G/C–C/C	12 (9.2)	6 (3.4)		4 (3.9)	6 (4.9)	

**Note:** <sub>inter</sub>P — significance threshold in the analysis of interactions between SNPs and the risk factor; the risk factor (F+)<sup>3</sup> is long-term alcohol abuse (over 10 years).

**Table 3.** The analysis of the associations between the risk of infected pancreatic necrosis and the genotypes of the studied polymorphisms (the most significant models)

Gene (SNP ID)	Genotype, allele	n (%)		$p^1$	$_{cor}OR$ (95%CI) <sup>2</sup>
		Control (n = 573)	Patients with IPN (n = 97)		
<i>CYP1A1</i> -462 T>C rs1048943	T/T–T/C	556 (99.8%)	93 (96.9%)	0.0095 <sup>R</sup>	1.00
	C/C	1 (0.2%)	3 (3.1%)		15.65 (1.61–152.54)
<i>ABCB1</i> -3435 G>A rs1045642	A/A–G/A	427 (76.5%)	82 (85.4%)	0.036 <sup>R</sup>	1.00
	G/G	131 (23.5%)	14 (14.6%)		0.54 (0.30–0.99)

**Table 4.** The analysis of the associations between the risk of pancreatic pseudocysts in patients with AP and the genotypes of the studied polymorphisms (the most significant model)

Gene (SNP ID)	Genotype, allele	n (%)		$p^1$	$_{cor}OR$ (95%CI)
		Control (n = 573)	Patients with PC (n = 101)		
<i>CYP1A1</i> -462 T>C rs1048943	T/T–T/C	556 (99.8%)	97 (96%)	0.003 <sup>D</sup>	1.00
	C/C	1 (0.2%)	4 (4%)		18.36 (2.03–166.52)
<i>CYP2E1</i> -1293 G>C rs3813867	G/G–C/C	538 (96.1%)	92 (91.1%)	0.05 <sup>OD</sup>	1.00
	G/C	22 (3.9%)	9 (8.9%)		2.43 (1.07–5.56)
<i>ABCB1</i> -3435 G>A rs1045642	A/A–G/A	427 (76.5%)	86 (85.2%)	0.04 <sup>R</sup>	1.00
	G/G	131 (23.5%)	15 (14.8%)		0.55 (0.30–0.99)

**Table 5.** The analysis of the associations between the risk of peripancreatic necrosis and the genotypes of the studied polymorphisms (the most significant model)

Gene (SNP ID)	Genotype, allele	n (%)		$p^1$	$_{cor}OR$ (95%CI)
		Control (n = 573)	Patients with PN (n = 111)		
<i>CYP1A1</i> -462 T>C rs1048943	T/T–T/C	556 (99.8%)	106 (96.4%)	0.003 <sup>R</sup>	1.00
	C/C	1 (0.2%)	4 (3.6%)		18.00 (1.99–163.22)
<i>ABCB1</i> -3435 G>A (rs1045642)	A/A–G/A	427 (76.5%)	94 (85.5%)	0.03 <sup>R</sup>	1.00
	G/G	131 (23.5%)	16 (14.6%)		0.56 (0.31–0.98)

[24]. Research into the contribution of the *ABCB1* rs1045642 polymorphism to the development of arterial hypertension and the evaluation of amlodipine-based therapy outcomes in different populations [25–27] have demonstrated a high antihypertensive effect in TT carriers; the researchers explained this effect by a decline in *ABCB1* expression. The same research team reported a link between the TT genotype and the high risk of hemorrhagic complications in patients undergoing dabigatran therapy after knee replacement surgery. Our findings demonstrate that reduced *ABCB1* expression negatively affects the ability of the body to detoxify alcohol and increases the risk of AP in the carriers of the A allele.

On the whole, a milder course of AP was typical for the carriers of the G/G *ABCB1* G>A (rs1045642) genotype; a more severe course was characteristic of the carriers of the C/C *CYP1A1* T>C (rs1048943) genotype.

## CONCLUSIONS

This study aimed at assessing the contribution of SNPs of some xenobiotic biotransformation genes to the development of AP in the residents of Kursk region has detected a few associations between the studied genotypes and the risk for AP /its complications, as well as established the trigger effect of the risk factors on the disease in the carriers of certain genotypes. Based on the analysis of genetic factors, including polymorphic variants of the genes coding for xenobiotic biotransformation enzymes, one can predict the risk of AP and the severity of its clinical course. This opens new opportunities for early diagnosis and timely prevention of the disease. Research into genetic polymorphisms might help to predict the outcomes of the disease and develop personalized approaches to its treatment and prevention.

## References

- Setiawan VW, Pandol SJ, Porcel J, Wilkens LR, Le Marchand L, Pike MC, et al. Prospective Study of Alcohol Drinking, Smoking, and Pancreatitis: The Multiethnic Cohort. *Pancreas*. 2016; 45 (6): 819–25.
- Ali UA, Issa Y, Hagenaars JC, Bakker OJ, van Goor H, Nieuwenhuijs VB, Schaapherder AF. Risk of recurrent pancreatitis and progression to chronic pancreatitis after a first episode of acute pancreatitis. *Clinical gastroenterology and hepatology*. 2016; 14 (5): 738–46.
- Mrozikiewicz-Rakowska B, Malinowski M, Nehring P, Bartkowiak-Wieczorek J, Bogacz A, Żurawińska-Grzelka E, et al. The MDR1/*ABCB1* gene rs 1045642 polymorphism in colorectal cancer. *Archives of Medical Science*. 2017; 13 (1).
- Zhao L, Li K, Li W, Yang Z. Association between the C3435T polymorphism of *ABCB1*/MDR1 gene (rs1045642) and colorectal cancer susceptibility. *Tumor Biology*. 2013; 34 (3): 1949–57.
- Vinnik YuS, Cherdancev DV, Markova EV, Konovalenko AN, Pervova OV, Miller MS. Geneticheskie aspekty pankreatita. *Sibirskij medicinskij zhurnal (Irkutsk)*. 2004; 43 (2). Russian.
- Hosagrahara VP, Rettie AE, Hassett C, Omiecinski CJ. Functional analysis of human microsomal epoxide hydrolase genetic variants. *Chem Biol Interact*. 2004; (150): 149–59.



7. Wang X, Cheung CM, Lee WY, Or PM, Yeung JH. Major tanshinones of Danshen (*Salvia miltiorrhiza*) exhibit different modes of inhibition on human CYP1A2, CYP2C9, CYP2E1 and CYP3A4 activities in vitro. *Phytomedicine*. 2010; 17 (11): 868–75.
8. Kim MS, Lee DH, Kang HS, Park HS, Jung S, Lee JW, et al. Genetic polymorphisms of alcohol-metabolizing enzymes and cytokines in patients with alcohol induced pancreatitis and alcoholic liver cirrhosis. *Korean J Gastroenterol*. 2004; (43): 355–63.
9. Frenzer A, Butler WJ, Norton ID, Wilson JS, Apte MV, Pirola RC, et al. Polymorphism in alcohol-metabolizing enzymes, glutathione S-transferases and apolipoprotein E and susceptibility to alcohol-induced cirrhosis and chronic pancreatitis. *J Gastroenterol Hepatol*. 2002; (17): 177–82.
10. Yang B, O'Reilly DA, Demaine AG, Kingsnorth AN. Study of polymorphisms in the CYP2E1 gene in patients with alcoholic pancreatitis. *Alcohol*. 2001; (23): 91–7.
11. Burim RV, Canalle R, Martinelli Ade L, Takahashi C. Polymorphisms in glutathione S-transferases GSTM1, GSTT1 and GSTP1 and cytochromes P450 CYP2E1 and CYP1A1 and susceptibility to cirrhosis or pancreatitis in alcoholics. *Mutagenesis*. 2004; (19): 291–8.
12. Natal'skij AA, Bogomolov AY, Andrianova KV. Polimorfizm genov u bol'nyh hronicheskim pankreatitom. V sbornike: Teorija i praktika sovremennoj hirurgii: Materialy X Vserossijskoj konferencii obshhih hirurgov; Rjazan', 2018; s. 219–220. Russian.
13. Smithies AM, Sargen K, Demaine AG, Kingsnorth AN. Investigations of the interleukin 1 gene cluster and its association with acute pancreatitis. *Pancreas*. 2000; 20 (3): 234–40.
14. Teich N, Bauer N, Mössner J, Keim V. Mutational screening of patients with nonalcoholic chronic pancreatitis: identification of further trypsinogen variants. *The American journal of gastroenterology*. 2002; 97 (2): 341–6.
15. Ulrich AB, Standop J, Schmied BM, Schneider MB, Lawson TA, Pour PM. Species differences in the distribution of drug-metabolizing enzymes in the pancreas. *Toxicologic pathology*. 2002; 30 (2): 247–53.
16. Dellinger EP, Forsmark CE, Laver P, Levy P, Maravi-Poma E, Petrov MS, et al. Determinant-based classification of acute pancreatitis severity: an international multidisciplinary consultation. *Ann Surg*. 2012; 256 (6): 875–80.
17. Banks PA, Bollen TL, Dervenis C, Gooszen HG, Johnson CD, Sarr MG, et al. Acute Pancreatitis Classification Working Group. Classification of acute pancreatitis 2012: revision of the Atlanta classification and definitions by international consensus. *Gut*. 2013; 62 (1): 102–11.
18. Klyaritskaya IL, Rabotyagova YuS. Novye faktory riska razvitiya hronicheskogo pankreatita. *Krymskij terapevicheskij zhurnal*. 2012; (2): 63–69. Russian.
19. Lazarenko VA, Antonov AE. Sovremennoe sostojanie problemy vrednyh privyчек kak faktora riska razvitiya pankreatita. *Social'nye aspekty zdorov'ja naselenija*. 2017; 55 (3). Russian.
20. Furtwängler NA, de Visser RO. Lack of international consensus in low-risk drinking guidelines. *Drug and alcohol review*. 2013; 32 (1): 11–18.
21. Baranov VS, Baranova EV, Ivashchenko TYe, Aseev MV. Genom cheloveka i geny «predraspolozhennosti»: vvedenie v prediktivnuju medicinu. SPb.: Intermedika, 2000; 271 s. Russian.
22. Spicyn VA, Makarov SV, Paj GV, Bychkovskaja LS. Polimorfizm v genah cheloveka, associirujushhihsja s biotransformaciej ksenobiotikov. *Vestnik VOGiS*. 2006; 10 (1): 97–105. Russian.
23. Hubacek JA, Zakharov S. Response to 'CYP2E1 Polymorphism and Better Outcome After Methanol Poisoning'. *Basic and clinical pharmacology and toxicology*. 2015; 117 (1): 3–4.
24. Marzolini C, Paus E, Buclin T, Kim RB. Polymorphisms in human MDR1 (P-glycoprotein): recent advances and clinical relevance. *Clinical Pharmacology and Therapeutics*. 2004; 75 (1): 13–33.
25. Guo HQ, Zhang GN, Wang YJ, Zhang YK, Sodani K, Talele T, Chen ZS.  $\beta$ -Elemene, a compound derived from *Rhizoma zedoariae*, reverses multidrug resistance mediated by the ABCB1 transporter. *Oncology reports*. 2014; 31 (2): 858–66.
26. Sychev DA, Levanov AN, Shelekhova TV, Bochkov PO, Denisenko NP, Ryzhikova KA, Kozlov AV. The impact of ABCB1 (rs1045642 and rs4148738) and CES1 (rs2244613) gene polymorphisms on dabigatran equilibrium peak concentration in patients after total knee arthroplasty. *Pharmacogenomics and Personalized Medicine*. 2018; (11): 127.
27. Sychev D, Shikh N, Morozova T, Grishina E, Ryzhikova K, Malova E. Effects of ABCB1 rs1045642 polymorphisms on the efficacy and safety of amlodipine therapy in Caucasian patients with stage I-II hypertension. *Pharmacogenomics and personalized medicine*. 2018; (11): 157.

## Литература

1. Setiawan VW, Pandol SJ, Porcel J, Wilkens LR, Le Marchand L, Pike MC, et al. Prospective Study of Alcohol Drinking, Smoking, and Pancreatitis: The Multiethnic Cohort. *Pancreas*. 2016; 45 (6): 819–25.
2. Ali UA, Issa Y, Hagenaars JC, Bakker OJ, van Goor H, Nieuwenhuijs VB, Schaapherder AF. Risk of recurrent pancreatitis and progression to chronic pancreatitis after a first episode of acute pancreatitis. *Clinical gastroenterology and hepatology*. 2016; 14 (5): 738–46.
3. Mrozikiewicz-Rakowska B, Malinowski M, Nehring P, Bartkowiak-Wieczorek J, Bogacz A, Żurawińska-Grzelka E, et al. The MDR1/ABCB1 gene rs 1045642 polymorphism in colorectal cancer. *Archives of Medical Science*. 2017; 13 (1).
4. Zhao L, Li K, Li W, Yang Z. Association between the C3435T polymorphism of ABCB1/MDR1 gene (rs1045642) and colorectal cancer susceptibility. *Tumor Biology*. 2013; 34 (3): 1949–57.
5. Винник Ю. С., Черданцев Д. В., Маркова Е. В., Коноваленко А. Н., Первова О. В., Миллер М. С. Генетические аспекты панкреатита. *Сибирский медицинский журнал (Иркутск)*. 2004; 43 (2).
6. Hosagrahara VP, Rettie AE, Hassett C, Omiecinski CJ. Functional analysis of human microsomal epoxide hydrolase genetic variants. *Chem Biol Interact*. 2004; (150): 149–59.
7. Wang X, Cheung CM, Lee WY, Or PM, Yeung JH. Major tanshinones of Danshen (*Salvia miltiorrhiza*) exhibit different modes of inhibition on human CYP1A2, CYP2C9, CYP2E1 and CYP3A4 activities in vitro. *Phytomedicine*. 2010; 17 (11): 868–75.
8. Kim MS, Lee DH, Kang HS, Park HS, Jung S, Lee JW, et al. Genetic polymorphisms of alcohol-metabolizing enzymes and cytokines in patients with alcohol induced pancreatitis and alcoholic liver cirrhosis. *Korean J Gastroenterol*. 2004; (43): 355–63.
9. Frenzer A, Butler WJ, Norton ID, Wilson JS, Apte MV, Pirola RC, et al. Polymorphism in alcohol-metabolizing enzymes, glutathione S-transferases and apolipoprotein E and susceptibility to alcohol-induced cirrhosis and chronic pancreatitis. *J Gastroenterol Hepatol*. 2002; (17): 177–82.
10. Yang B, O'Reilly DA, Demaine AG, Kingsnorth AN. Study of polymorphisms in the CYP2E1 gene in patients with alcoholic pancreatitis. *Alcohol*. 2001; (23): 91–7.
11. Burim RV, Canalle R, Martinelli Ade L, Takahashi C. Polymorphisms in glutathione S-transferases GSTM1, GSTT1 and GSTP1 and cytochromes P450 CYP2E1 and CYP1A1 and susceptibility to cirrhosis or pancreatitis in alcoholics. *Mutagenesis*. 2004; (19): 291–8.
12. Натальский А. А., Богомолов А. Ю., Андрианова К. В. Полиморфизм генов у больных хроническим панкреатитом. В сборнике: Теория и практика современной хирургии: Материалы X Всероссийской конференции общих хирургов; Рязань, 2018; с. 219–220.
13. Smithies AM, Sargen K, Demaine AG, Kingsnorth AN. Investigations of the interleukin 1 gene cluster and its association with acute pancreatitis. *Pancreas*. 2000; 20 (3): 234–40.
14. Teich N, Bauer N, Mössner J, Keim V. Mutational screening of patients with nonalcoholic chronic pancreatitis: identification of further trypsinogen variants. *The American journal of gastroenterology*. 2002; 97 (2): 341–6.
15. Ulrich AB, Standop J, Schmied BM, Schneider MB, Lawson TA, Pour PM. Species differences in the distribution of drug-metabolizing enzymes in the pancreas. *Toxicologic pathology*. 2002; 30 (2): 247–53.

- 2002; 30 (2): 247–53.
16. Dellinger EP, Forsmark CE, Luyer P, Levy P, Maravi-Poma E, Petrov MS, et al. Determinant-based classification of acute pancreatitis severity: an international multidisciplinary consultation. *Ann Surg*. 2012; 256 (6): 875–80.
  17. Banks PA, Bollen TL, Dervenis C, Gooszen HG, Johnson CD, Sarr MG, et al. Acute Pancreatitis Classification Working Group. Classification of acute pancreatitis 2012: revision of the Atlanta classification and definitions by international consensus. *Gut*. 2013; 62 (1): 102–11.
  18. Кляритская И. Л., Работягова Ю. С. Новые факторы риска развития хронического панкреатита. *Крымский терапевтический журнал*. 2012; (2): 63–69.
  19. Лазаренко В. А., Антонов А. Е. Современное состояние проблемы вредных привычек как фактора риска развития панкреатита. *Социальные аспекты здоровья населения*. 2017; 55 (3).
  20. Furtwängler NA, de Visser RO. Lack of international consensus in low-risk drinking guidelines. *Drug and alcohol review*. 2013; 32 (1): 11–18.
  21. Баранов В. С., Баранова Е. В., Иващенко Т. Э., Асеев М. В. Геном человека и гены «предрасположенности»: введение в предиктивную медицину. СПб.: Интермедика, 2000; 271 с.
  22. Спицын В. А., Макаров С. В., Пай Г. В., Бычкова Л. С. Полиморфизм в генах человека, ассоциирующихся с биотрансформацией ксенобиотиков. *Вестник ВОГиС*. 2006; 10 (1): 97–105.
  23. Hubacek JA, Zakharov S. Response to 'CYP2E1 Polymorphism and Better Outcome After Methanol Poisoning'. *Basic and clinical pharmacology and toxicology*. 2015; 117 (1): 3–4.
  24. Marzolini C, Paus E, Buclin T, Kim RB. Polymorphisms in human MDR1 (P-glycoprotein): recent advances and clinical relevance. *Clinical Pharmacology and Therapeutics*. 2004; 75 (1): 13–33.
  25. Guo HQ, Zhang GN, Wang YJ, Zhang YK, Sodani K, Talele T, Chen ZS.  $\beta$ -Elemene, a compound derived from *Rhizoma zedoariae*, reverses multidrug resistance mediated by the ABCB1 transporter. *Oncology reports*. 2014; 31 (2): 858–66.
  26. Sychev DA, Levanov AN, Shelekhova TV, Bochkov PO, Denisenko NP, Ryzhikova KA, Kozlov AV. The impact of ABCB1 (rs1045642 and rs4148738) and CES1 (rs2244613) gene polymorphisms on dabigatran equilibrium peak concentration in patients after total knee arthroplasty. *Pharmacogenomics and Personalized Medicine*. 2018; (11): 127.
  27. Sychev D, Shikh N, Morozova T, Grishina E, Ryzhikova K, Malova E. Effects of ABCB1 rs1045642 polymorphisms on the efficacy and safety of amlodipine therapy in Caucasian patients with stage I–II hypertension. *Pharmacogenomics and personalized medicine*. 2018; (11): 157.

## CEREBRAL CORTEX ACTIVATION DURING THE STERNBERG VERBAL WORKING MEMORY TASK

Bakulin IS<sup>1</sup>✉, Zabirowa AH<sup>1</sup>, Kopnin PN<sup>1</sup>, Sinitsyn DO<sup>1</sup>, Poydasheva AG<sup>1</sup>, Fedorov MV<sup>2</sup>, Gnedovskaya EV<sup>1,2</sup>, Suponeva NA<sup>1</sup>, Piradov MA<sup>1</sup><sup>1</sup> Research Center of Neurology, Moscow, Russia<sup>2</sup> Skolkovo Institute of Science and Technology, Moscow, Russia

Despite intensive study, the data regarding functional role of specific brain regions in the working memory processes still remain controversial. The study was aimed to determine the activation of cerebral cortex regions at different stages of the working memory task (information encoding, maintenance and retrieval). Functional magnetic resonance imaging (fMRI) with the modified Sternberg task was applied to 19 healthy volunteers. The objective of the task was to memorize and retain in memory the sequence of 7 letters with the subsequent comparison of one letter with the sequence. Activation was analyzed during three periods of the task compared to the rest period, as well as temporal dynamics of changes in BOLD signal intensity in three regions: left dorsolateral prefrontal, left posterior parietal and left occipital cortex. According to the results, significant activation of the regions in prefrontal and posterior parietal cortex was observed during all periods of the task ( $p < 0.05$ ), but there were changes in its localization and lateralization. The activation pattern during the maintenance period corresponded to the fronto-parietal control network components. According to the analysis of temporal dynamics of changes in BOLD signal intensity, the most prominent activation of the dorsolateral prefrontal cortex and parietal cortex was observed in the end of the encoding period, during the maintenance period and in the beginning of the retrieval period, which confirmed the role of those areas in the working memory processes. The maximum of occipital cortex activation was observed during encoding period. The study confirmed the functional role of the dorsolateral prefrontal cortex and posterior parietal cortex in the working memory mechanisms during all stages of the Sternberg task.

**Keywords:** working memory, functional magnetic resonance imaging, the Sternberg task, delayed-response task, prefrontal cortex, fronto-parietal control network

**Author contribution:** Bakulin IS, Fedorov MV, Gnedovskaya EV, Suponeva NA, Piradov MA — study planning and design; Bakulin IS, Zabirowa AH — literature analysis; Bakulin IS, Poydasheva AG — data acquisition; Zabirowa AH, Kopnin PN, Sinitsyn DO — data analysis; Bakulin IS, Zabirowa AH, Sinitsyn DO, Fedorov MV, Gnedovskaya EV, Suponeva NA, Piradov MA — data interpretation; Bakulin IS, Zabirowa AH — manuscript draft preparation; Kopnin PN, Sinitsyn DO, Poydasheva AG, Fedorov MV, Gnedovskaya EV, Suponeva NA, Piradov MA — manuscript draft editing; all the authors — final version of the article preparation.

**Compliance with ethical standards:** the study was approved by the Ethics Committee of Research Center of Neurology (protocol № 9-3/17 dated August 30, 2017). All volunteers submitted the informed consent to participation in the study.

✉ **Correspondence should be addressed:** Ilya S. Bakulin  
Volokolamskoye shosse, 80, Moscow, 125367; bakulin@neurology.ru

**Received:** 22.01.2020 **Accepted:** 22.02.2020 **Published online:** 29.02.2020

**DOI:** 10.24075/brsmu.2020.013

## АКТИВАЦИЯ КОРЫ ГОЛОВНОГО МОЗГА ПРИ ВЫПОЛНЕНИИ ЗАДАЧИ СТЕРНБЕРГА НА ВЕРБАЛЬНУЮ РАБОЧУЮ ПАМЯТЬ

И. С. Бакулин<sup>1</sup>✉, А. Х. Забиrowa<sup>1</sup>, П. Н. Копнин<sup>1</sup>, Д. О. Синицын<sup>1</sup>, А. Г. Пойдашева<sup>1</sup>, М. В. Федоров<sup>2</sup>, Е. В. Гнедовская<sup>1,2</sup>, Н. А. Супонева<sup>1</sup>, М. А. Пирадов<sup>1</sup><sup>1</sup> Научный центр неврологии, Москва, Россия<sup>2</sup> Сколковский институт науки и технологий, Москва, Россия

Несмотря на интенсивное изучение, данные о функциональном значении отдельных областей головного мозга для процессов рабочей памяти (РП) остаются противоречивыми. Целью данного исследования было определить активацию участков коры на разных этапах выполнения задачи на РП (запечатление, удержание и извлечение информации). На 19 здоровых добровольцах была использована функциональная магнитная резонансная томография (фМРТ) с модифицированной задачей Стернберга. Суть задачи — в запоминании и удержании в памяти последовательности из семи букв с последующим сравнением с ней одной буквы. Проанализирована активация в трех периодах задачи по сравнению с периодом покоя, а также динамика изменения интенсивности BOLD-сигнала в зависимости от времени в трех областях: левой дорсолатеральной префронтальной коре (ДЛПФК), левой задней теменной коре и левой затылочной коре. По результатам анализа, на протяжении всех периодов задачи наблюдали статистически значимую активацию участков ПФК и задней теменной коры ( $p < 0.05$ ), но с изменением их локализации и латерализации. При этом паттерн активации в периоде удержания соответствовал компонентам лобно-теменной сети контроля. По результатам анализа изменения интенсивности BOLD-сигнала наиболее выраженную активацию ДЛПФК и теменной коры наблюдали в конце периода запечатления, периоде удержания и начале периода извлечения, что подтверждает роль данных областей в процессах РП. Пик активации затылочной коры соответствовал периоду запечатления. Данное исследование подтверждает функциональное значение ДЛПФК и задней теменной коры для процессов РП на всех этапах выполнения задачи Стернберга.

**Ключевые слова:** рабочая память, функциональная магнитно-резонансная томография, задача Стернберга, задача с отсроченным воспроизведением, префронтальная кора, лобно-теменная сеть контроля

**Вклад авторов:** И. С. Бакулин, М. В. Федоров, Е. В. Гнедовская, Н. А. Супонева, М. А. Пирадов — планирование и дизайн исследования; И. С. Бакулин, А. Х. Забиrowa — анализ литературы; И. С. Бакулин, А. Г. Пойдашева — сбор данных; А. Х. Забиrowa, П. Н. Копнин, Д. О. Синицын — анализ данных; И. С. Бакулин, А. Х. Забиrowa, Д. О. Синицын, М. В. Федоров, Е. В. Гнедовская, Н. А. Супонева, М. А. Пирадов — интерпретация данных; И. С. Бакулин, А. Х. Забиrowa — подготовка черновика рукописи статьи; П. Н. Копнин, Д. О. Синицын, А. Г. Пойдашева, М. В. Федоров, Е. В. Гнедовская, Н. А. Супонева, М. А. Пирадов — внесение правок в черновик рукописи статьи; все авторы — подготовка финального варианта статьи.

**Соблюдение этических стандартов:** исследование одобрено этическим комитетом ФГБНУ «Научный центр неврологии» (протокол № 9-3/17 от 30 августа 2017 г.). Все участники исследования подписали добровольное информированное согласие на участие в исследовании.

✉ **Для корреспонденции:** Илья Сергеевич Бакулин  
Волоколамское шоссе, д. 80, г. Москва, 125367; bakulin@neurology.ru

**Статья получена:** 22.01.2020 **Статья принята к печати:** 22.02.2020 **Опубликована онлайн:** 29.02.2020

**DOI:** 10.24075/vrgmu.2020.013

Working memory is the ability to maintain and process a limited amount of information for a short time for its use in the ongoing cognitive activity. The working memory decline is associated with normal aging [1], it is also observed in patients with various neurological and psychiatric disorders [2], that confirms the importance of the working memory study.

Research data regarding working memory mechanisms remain controversial [3]. One of the brain areas, most investigated in context of working memory, is the dorsolateral prefrontal cortex. The persistent neural activity during the maintenance period of the working memory task was firstly observed in the prefrontal cortex of primates [4]. Later, the similar activity was detected in other regions. However, a number of studies confirmed the importance of the persistent neural activity in prefrontal cortex. For example, despite the simultaneous activation of prefrontal and temporal cortex during the task, inactivation of prefrontal cortex led to the inhibition of persistent neural activity in the temporal cortex of primates, while inactivation of the temporal cortex did not affect the prefrontal cortex [5]. The temporary inactivation of the prefrontal cortex led to a more pronounced working memory decline than inactivation of the posterior parietal cortex [6].

The role of the dorsolateral prefrontal cortex in the working memory in humans was confirmed by fMRI with different tasks (n-back, delayed match-to-sample task, Sternberg task, etc.) [7–9], as well as by transcranial magnetic stimulation (TMS) [10]. However, many cerebral cortex regions are activated during a working memory task: parietal lobe (areas around the intraparietal sulcus, superior parietal lobule), insula, anterior cingulate gyrus [7, 11, 12], visual cortex [13]. At the same time, the question of the link between activation and working memory mechanisms (information maintenance and manipulation) remains open, since activation can be caused by additional cognitive processes involved in the working memory task performance, for example, the perception of a stimulus [13]. The use of the delayed response tasks (the Sternberg task in particular) [14] allows to separate some working memory processes by analyzing different task stages: encoding, maintenance and retrieval.

The assessment of temporal dynamics of activation can be helpful in comparison of fMRI results with the studies using causal methods (for example, TMS) where the online effects at the different stages of the task execution were studied. Given the increasing interest in the use of non-invasive brain stimulation techniques for the improvement of cognitive functions [15, 16] the issue is also important for clinical neurology. fMRI results can help in determination of the TMS target which might increase the stimulation effectiveness [17]. The data of the cortical activity dynamics might also be used for combination of TMS protocols with cognitive load.

Despite the frequent use of the Sternberg task in neuroimaging studies of verbal working memory [11], the analysis of activation at different time was performed in a relatively small number of studies [9, 18–20]. Considering the limitations caused by the fMRI temporal resolution, the reproducibility of the results of such studies, which is necessary to confirm the possibility of using fMRI for the investigation of individual working memory mechanisms, still remains important.

The study was aimed to determine the activation of cerebral cortex regions at the different stages of the modified Sternberg task for verbal working memory, and to assess the dynamics of individual regions activation by the analysis of temporal dynamics of BOLD signal changes. The following cerebral cortex regions were chosen for assessment (according to their potential functional role in the Sternberg task performance,

including participation in the working memory processes): left dorsolateral prefrontal cortex [9, 10], left posterior parietal cortex [7, 11, 21] and left occipital cortex [13].

## METHODS

### Study participants

The study was performed in 2017–2019 at the Research Center of Neurology.

Inclusion criteria: age 18–55; dominant right hand (according to the Edinburgh Handedness Inventory [22]); normal (corrected to normal) vision. Exclusion criteria: contraindications for MRI [23]; neurological or psychiatric disorders; intake of drugs that affect the central nervous system at the time of the study; severe chronic somatic disorders.

In accordance with the inclusion criteria, 19 healthy volunteers (6 men) aged 22–31 were recruited, all of them right-handed. The study was performed as a part of the project “Effects of high-frequency repetitive transcranial magnetic stimulation over the left dorsolateral prefrontal cortex on working memory in healthy volunteers”.

### fMRI with the Sternberg task

fMRI with the modified Sternberg task for verbal working memory was used in the study [9, 14]. The participants received instructions about all stages of the investigation before performing the task in the MRI scanner. During the investigation, participants were wearing headphones to reduce the scanner noise. The participants could see the task screen located in the scanning room through a mirror, which was installed on the 8-channel head coil. Hand-held grips with buttons were given to each participant, which they pressed according to the instructions.

Task-fMRI used in our study had a block design and consisted of 24 task presentations (Fig. 1). Each presentation included the activation period (the Sternberg task) and the rest period. The activation period was divided into three blocks (periods): encoding, maintenance and retrieval. During the encoding period (1st–3rd seconds from the start of the task) the stimulus (7 latin consonants selected in random order using the algorithm created in the MATLAB R2017a (Mathworks, Natick, MA; USA)) was shown on the screen. Angular size of the letters was 1.5. During the maintenance period (4–12<sup>th</sup> second) the participant maintained the stimuli in memory, while the screen remained blank (without fixation point). During the retrieval period (13–15<sup>th</sup> second) a single latin letter appeared on the screen. The participant was instructed to press a button in the right hand-held grip if the letter presented during the retrieval period matched to the sequence, and a button in the left hand-held grip if the letter had not. Matching and non-matching stimuli were presented in random order, with 12 presentations of each stimulus type. The duration of activation period, as well as of the rest period without any stimulus (black screen), was 15 seconds. Participants were instructed to keep their eyes open during all periods. The experiment duration was 12 minutes.

### Image acquisition and preprocessing

The study was performed using a 3 T scanner Magnetom Verio (Siemens; Germany). Anatomical data were acquired using the 3D-T1-gradient echo (T1-MPR) MRI sequence and consisted of 176 sagittal slices with the following parameters:



TR 1900 ms, TE 2.47 ms, slice thickness 1.0 mm, distance factor 50%; voxel size  $1.0 \cdot 1.0 \cdot 1.0 \text{ mm}^3$ , field-of-view 250 mm. The functional data were acquired by investigation of the BOLD signal changes using T2\*-gradient echo MRI sequence with the following parameters: TR 3000 ms, TE 30 ms, slice thickness 3 mm, distance factor 25%, voxel size  $3.0 \cdot 3.0 \cdot 3.0 \text{ mm}^3$ , field-of-view 192 mm, 36 axial slices. To ensure dynamic magnetic equilibrium, first five images were excluded from the analysis. Preprocessing and statistical analysis were performed using the SPM12 software (Institute of Neurology, London; UK) based on the MATLAB R2017a (Mathworks, Natick, MA; USA).

Image preprocessing included following stages: 1) image realignment for correction of motion artifacts using the shifting and rotation transformations; 2) co-registration of anatomical and functional data; 3) segmentation of the obtained structural images and their spatial normalization to transform the individual images into the Montreal Neurological Institute (MNI) space; 4) spatial smoothing with a Gaussian kernel 8 mm FWHM to reduce the impact of anatomical variability.

The low-frequency drift was removed using the high-pass filter (time constant 128 s).

### Statistical analysis

Statistical parametric mapping was performed using general linear models, estimated separately for the signal of each voxel. During the 1<sup>st</sup> level analysis, individual activation data were obtained for the encoding, maintenance and retrieval periods. The last 9 seconds of the rest period (22–30<sup>th</sup> seconds) were used as the control state for the activation level calculation. Head motion parameters were included as nuisance regressors. The data of 19 participants were included in the group analysis (separately for each period). Activation was assessed both at peak and cluster levels. The threshold for the inclusion of an individual voxel in the clusters was set at  $p < 0.0001$ . The clusters in the gray matter of cerebral hemispheres and cerebellum were selected for the analysis with a significance level of  $p < 0.05$  (with the family-wise error, FWE correction for multiple comparisons).

For regions showing significant activation during the maintenance period, the additional comparison with activation of the frontoparietal control network (FPCN) was performed, according to the resting state fMRI data [24]. The results were visualized using xjView [25] through overlay of the FPCN from the atlas [24] with the activation map of the maintenance period.

The temporal dynamics of the changes in BOLD signal intensity was analyzed in three regions of interest: left

dorsolateral prefrontal cortex, left posterior parietal cortex and left occipital cortex. To determine the specific regions that were active during the task performance, the difference between the signal intensity in the maintenance period and the rest period was used as contrast within the selected regions of interest. Voxels with activation above the threshold were selected in the regions of interest ( $p < 0.0001$ ). Activation clusters containing selected voxel and restricted to spheres with the centers in a voxel with locally maximal activation were identified on group data. Radii were selected manually to obtain the region of intersection of the sphere and cluster with a sufficient number of voxels without spreading to adjacent anatomical regions (7 mm for dorsolateral prefrontal cortex, 8 mm for posterior parietal cortex, 10 mm for occipital cortex). At the individual level, BOLD signal was extracted from voxels in the determined cluster, as well as a signal adjusted for alignment effects and temporal non-sphericity in the framework of the autoregressive process AR(1). The extracted and simulated signals were averaged over the cluster voxels, and then over all participants. After that, the signal was averaged over the 24 task presentations and interpolated with periodic boundary conditions by the fast Fourier transformation method with a step of TR/10 (equal to 0.3 s). By the interpretation of the data, 5 s were subtracted from the onsets of BOLD events to account for the hemodynamic response delay.

### RESULTS

The activation of the cerebral cortex regions at different stages of the modified Sternberg task is shown in Fig. 2.

During the encoding period significant activation was detected in the clusters within the right and left parietal lobes (supramarginal and postcentral gyri, superior parietal lobule), and also in the cerebellar cortex and occipital lobe (cuneus) bilaterally. Activation was observed in the right middle frontal and superior frontal gyri, and in the lower part of the left middle frontal gyrus spreading to the inferior frontal gyrus. A cluster of activation was also detected in the left Rolandic operculum (Table 1, Fig. 2A).

During the maintenance period significant activation was found in the medial parts of the frontal lobes (bilaterally), prefrontal cortex (right middle frontal gyrus, left middle frontal and inferior frontal gyri), parietal lobe (supramarginal gyrus and superior parietal lobule bilaterally, right angular gyrus). In addition, activation was detected in the anterior parts of the insula (bilaterally) and in the left prefrontal cortex (middle frontal gyrus) (Table 2, Fig. 2B).

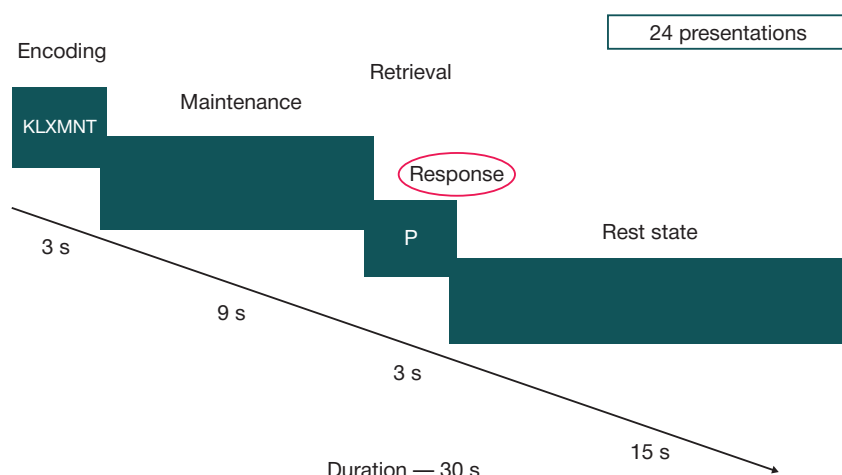
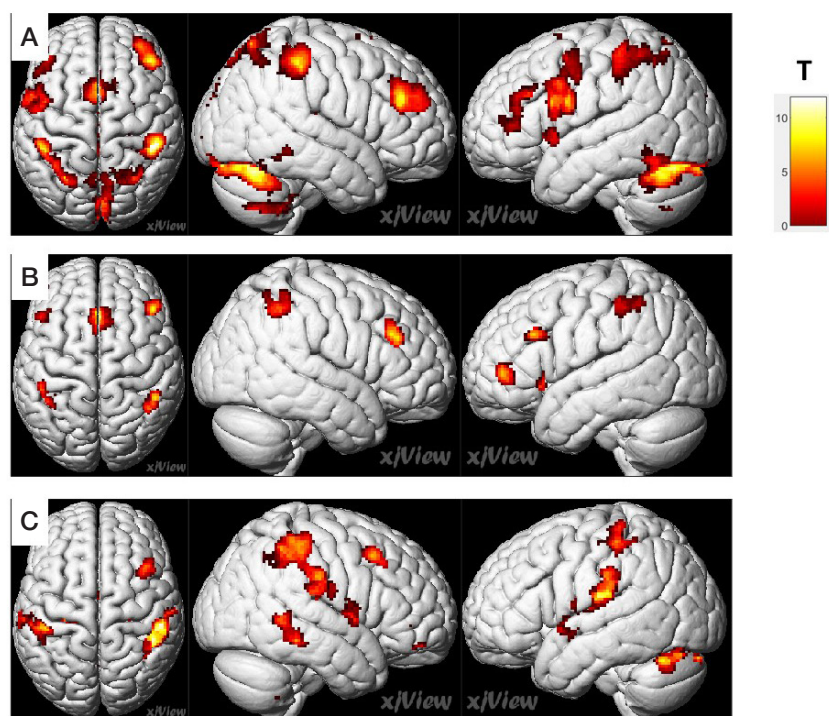


Fig. 1. fMRI with the modified Sternberg task for verbal memory (delayed item recognition task)





**Fig. 2.** Graphical depiction of significant activation regions on the cerebral cortex convexital surface during three periods of task compared with rest state (clusters containing more than 100 voxels are shown). **A** — encoding period; **B** — maintenance period; **C** — retrieval period. Left to right: top view, right view, left view. Color bars display the T-statistics level

Comparing the activation pattern in maintenance period with the FPCN, a partial overlap of the activation zones in the parietal and frontal lobes was noted, as well as in the medial parts of the frontal lobes and insular cortex (bilaterally) (Fig. 3).

During the retrieval period the regions of significant activation were detected in the right medial orbital and anterior orbital gyri, right middle temporal gyrus, in the cerebellar hemispheres bilaterally (spreading to the fusiform gyrus on the left). A cluster of activation was also detected in the right anterior insula and in the operculum. Within the parietal lobe clusters of activation were found in the right supramarginal gyrus, as well as in the left postcentral and supramarginal gyri. A cluster of activation was also identified in the right middle frontal gyrus. Activation was detected in the cerebellar vermis spreading to the lingual gyri bilaterally (Table 3, Fig. 2C).

A cluster of activation in the left middle frontal gyrus at the intersection with a sphere with a radius of 7 mm and center at the point of maximal activation  $[-36; 47; 5]$  (according to MNI space) containing 21 voxels was selected as the region of interest, in which temporal change of BOLD signal intensity was analyzed. According to the analysis results, an increase in signal intensity in the left middle frontal gyrus begins at the beginning of the task. The activation curve contains two peaks, 6 and 15 seconds from the beginning of the block. After the latter the signal intensity gradually decreases and reaches a plateau (Fig. 4).

The temporal change of BOLD signal intensity was analyzed for a cluster in the left inferior parietal lobule at the intersection with a sphere with a radius of 8 mm and the center at the point of maximum activation  $[-42; -49; 54]$  (according to MNI space)

**Table 1.** Regions of significant activation during the encoding period of the modified Sternberg task for verbal working memory

Region	Cluster level		Peak level		Peak coordinates, MNI [x; y; z]
	Volume, voxels	pFWE	T	pFWE	
Supramarginal gyrus, D	3587	<0.001	14.56	<0.001	[50; -32; 46]
Cerebellar hemisphere, D	8293	<0.001	12.55	0.001	[28; -58; -46]
Supramarginal gyrus, S	1502	<0.001	11.34	0.002	[-42; -34; 42]
Superior parietal lobule, S			11.28	0.002	[-28; -60; 46]
Postcentral gyrus, S			9.43	0.019	[-44; -36; 60]
Middle frontal gyrus, D	935	<0.001	10.49	0.005	[36; 34; 26]
Cuneus, bilateral	569	<0.001	9.99	0.009	[2; -84; 34]
Cerebellar hemisphere, S	75	0.008	7.55	0.131	[-36; -46; -46]
Middle frontal gyrus, S	362	<0.001	8.58	0.038	[2; -22; 16]
Inferior frontal gyrus (pars triangularis), S					
Rolandic operculum, S	128	0.001	7.45	0.046	[34; -32; 6]
Middle and superior frontal gyri, D	48	0.037	6.15	0.516	[28; 8; 54]
Cerebellar hemisphere, S	152	<0.001	5.97	0.597	[-30; -62; -46]

**Note:** MNI — Montreal Neurological Institute, FWE — family-wise error, T — T-statistics, D (dexter) — right, S (sinister) — left.

**Table 2.** Regions of significant activation during the maintenance period of the modified Sternberg task for verbal working memory

Region	Cluster level		Peak level		Peak coordinates, MNI [x; y; z]
	Volume, voxels	pFWE	T	pFWE	
Superior frontal gyrus medial parts, bilateral	420	<0.001	14.12	<0.001	[0; 26; 44]
Supplementary motor area, bilateral			10.37	0.006	[2; 20; 52]
Cerebellar hemisphere, D	78	0.009	8.87	0.030	[24; -64; -50]
Middle frontal gyrus, S Inferior frontal gyrus (pars triangularis), S	207	<0.001	8.26	0.057	[-40; 44; 2]
Middle frontal gyrus, D	261	<0.001	8.1	0.067	[42; 30; 32]
Supramarginal gyrus, D	276	<0.001	7.86	0.086	[48; -42; 50]
Angular gyrus, D			7.1	0.192	[46; -50; 46]
Superior parietal lobule, D			7	0.213	[40; -46; 42]
Superior parietal lobule, S	317	<0.001	6.96	0.223	[-36; -48; 46]
Supramarginal gyrus, S			6.19	0.47	[-46; -38; 48]
Anterior insula, S	126	0.001	6.93	0.229	[-32; 20; -4]
Anterior insula D	96	0.004	6.89	0.238	[34; 22; -2]
Middle frontal gyrus, S	149	<0.001	6.86	0.245	[-44; 24; 30]

**Note:** MNI — Montreal Neurological Institute, FWE — family-wise error, T — T-statistics, D (dexter) — right, S (sinister) — left.

containing 23 voxels. The temporal pattern of the BOLD signal intensity change in this region is similar to the curve obtained for the dorsolateral prefrontal cortex. It contains two peaks, 6 and 18 seconds from the beginning of the block. Between the peaks, a decrease in activation was observed with a local minimum at 13 seconds from the beginning of the block. Similar to the left dorsolateral prefrontal cortex, an increase in signal intensity begins with the beginning of the block, and the minimum is detected 24–29 seconds from the beginning of the module (Fig. 4).

In the left middle occipital gyrus a cluster of activation was selected at the intersection with a sphere with a radius of 10 mm and the center at [-24; -82; 1] (MNI space), containing 33 voxels. In this region of interest an increase in the BOLD signal intensity is observed from the beginning of the task. The maximum is observed 5–6 seconds after the beginning of the block, then the signal level decreases. The minimum is registered 11 seconds from the beginning followed by a slight increase in signal intensity with a subsequent decrease in activation (Fig. 4).

## DISCUSSION

In this study, the activation in regions of cerebral cortex at different stages of the modified Sternberg verbal working

memory task was assessed in 19 healthy volunteers using fMRI. Temporal pattern of changes in the left dorsolateral prefrontal, left posterior parietal and left occipital cortex activation was analyzed. During the encoding and retrieval periods activation in prefrontal cortex was observed (bilaterally and in the right hemisphere, respectively), as well as bilateral activation in parietal cortex, cerebellar hemispheres and occipital cortex. During the maintenance period the activation in FPCN components was found: symmetrical regions of the prefrontal and posterior parietal cortex, insular cortex, and medial parts of the superior frontal gyrus. The maximal activation of the left prefrontal and parietal cortex was observed during the encoding period and at the end of the maintenance period, between them it remained relatively constant, while for the occipital cortex, the peak of activation matched to the encoding period. Thus, according to the results of fMRI analysis, activation of prefrontal and posterior parietal cortex (components of FPCN) was detected during maintenance of verbal information in working memory.

Regions of activation in our study were generally consistent with the data of other researchers who used a similar modification of the Sternberg task for verbal working memory assessment [9]. Activation of the upper and lower parts of the left prefrontal cortex, parietal cortex bilaterally and the occipital cortex was observed during the encoding period. However, in our study, we detected additional activation in the right

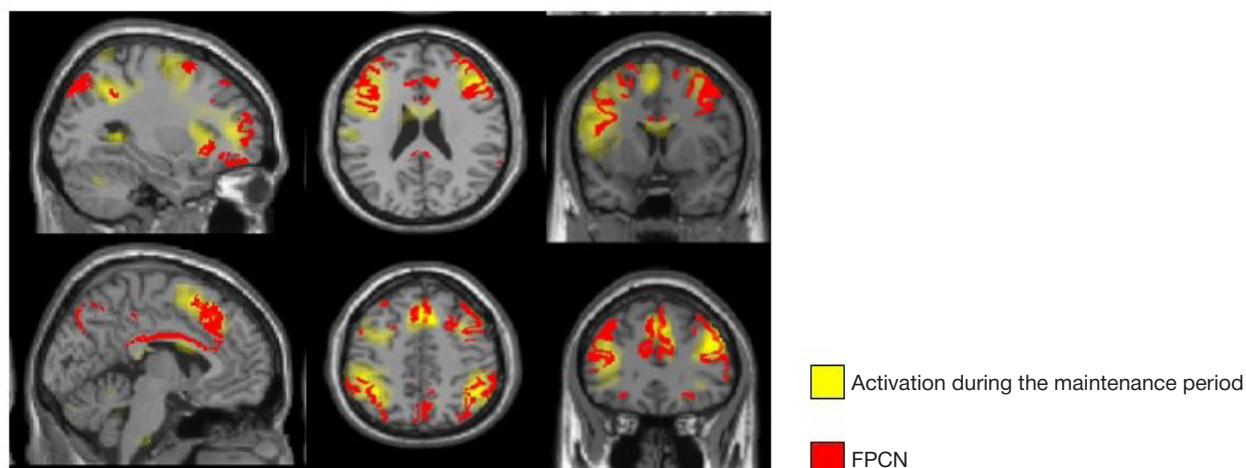


**Fig. 3.** Comparison of activation map during the maintenance period with FPCN. FPCN is the fronto-parietal control network (according to [24])

**Table 3.** Regions of significant activation during the retrieval period of the modified Sternberg task for verbal working memory

Region	Cluster level		Peak level		Peak coordinates, MNI [x; y; z]
	Volume, voxels	pFWE	T	pFWE	
Anterior and medial orbital gyrus, D	1074	<0.001	11.36	0.002	[26; 44; -18]
Middle temporal gyrus, D	309	<0.001	9.24	0.018	[50; -40; -8]
Cerebellar hemisphere, D	206	<0.001	9	0.023	[24; -52; -48]
Cerebellar hemisphere, S	294	<0.001	8.76	0.029	[-48; -70; -30]
Fusiform gyrus, S			6.87	0.212	[-36; -72; -22]
Frontal insular cortex, D			8.03	0.062	[42; 4; 6]
Operculum, D	171	<0.001	5.68	0.64	[46; -2; 18]
Supramarginal gyrus, D	1465	<0.001	8.02	0.063	[56; -32; 52]
Postcentral gyrus, S	263	<0.001	7.97	0.067	[-42; -34; 66]
Supramarginal gyrus, S			6.04	0.482	[-48; -40; 54]
Middle frontal gyrus, D	201	<0.001	7.95	0.068	[38; 18; 48]
Supramarginal gyrus, S	588	<0.001	7.56	0.103	[-48; -28; 28]
ПPostcentral gyrus, S					
Operculum, S					
Cerebellar vermis	259	<0.001	6.86	0.214	[8; -60; -8]
Lingual gyrus, bilateral					
Cerebellar hemisphere, S	97	0.006	6.60	0.282	[-2; -42; 0]

**Note:** MNI — Montreal Neurological Institute, FWE — family-wise error, T — T-statistics, D (dexter) — right, S (sinister) — left.

prefrontal cortex and the cerebellar hemispheres (bilaterally). In addition, activation of the parietal cortex was more prominent, and the activation region in the visual cortex was relatively small. During the maintenance period we detected activation regions in the parietal and prefrontal cortex bilaterally, while in the study described above the activation was observed mainly in the left hemisphere. At the retrieval period the regions of activation in the parietal cortex on the left and bilateral regions

of the operculum are consistent. Compared to [9], additional regions of activation were found in the right parietal cortex and the temporal lobe, but no activation of the left prefrontal cortex was observed. This difference could be due to the different task complexity (the researchers [9] used sequences of 4–6 letters, unlike 7 letters in our study) or due to the different duration of the encoding, maintenance and retrieval periods (2.16; 6.48 and 2.16 seconds respectively [9]). The differences could

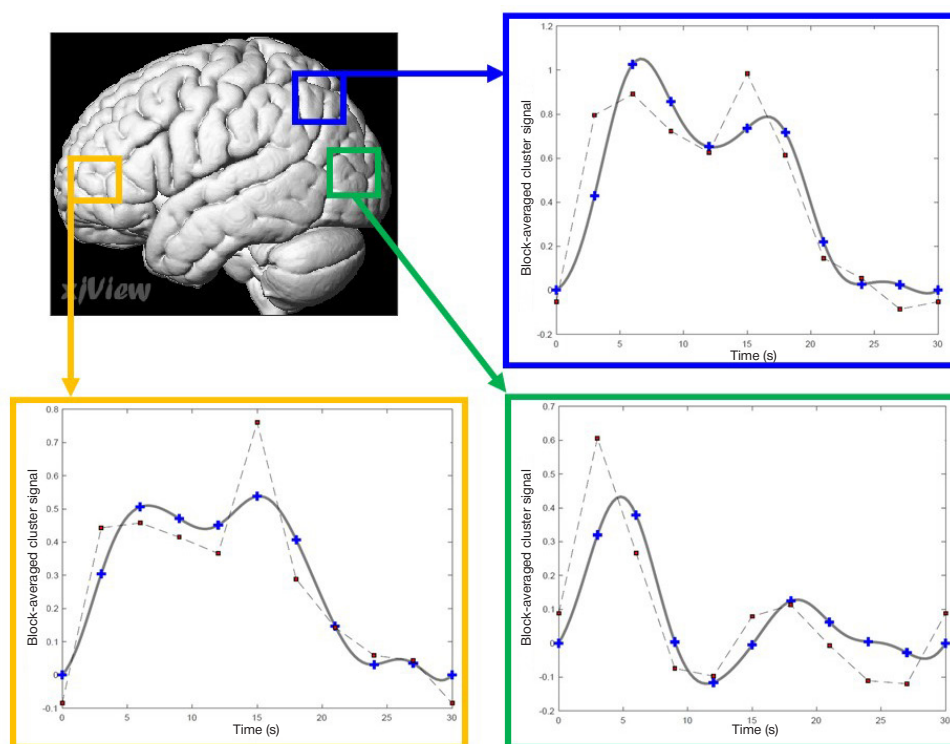


**Fig. 4.** Temporal dynamics of BOLD signal intensity change in the clusters of activation in the left middle frontal gyrus, left inferior parietal lobule and left middle occipital gyrus, averaged over all participants and task blocks. All regions are shown on the surface of the left hemisphere. *Solid line* — periodically interpolated simulated signal, *dashed line* — filtered measured signal corrected for non-sphericity and head motion. The BOLD signal intensity is measured in arbitrary units. The origin corresponds to the rest state at the beginning of the block. Interpretation of these data in terms of neuronal events involved the subtraction of 5 seconds from the onsets of BOLD events to account for the hemodynamic delay

also result from the different task performance strategies: the activation pattern in the maintenance period of our experiment was similar to the activation detected during the working memory task performance with articulatory suppression [26], which could indicate the use of non-articulatory maintenance mechanisms by participants.

Activation of clusters in the functionally different regions during the encoding and maintenance periods can be explained by the combination of several types of activity: visual information processing, subvocal speaking, choosing the strategy of maintenance, as well as attention and motor activity. Thus, during the encoding period, significant activation of the occipital cortex regions can be observed, associated with the visual information processing [9]. The activation of left inferior frontal gyrus region at encoding period might be associated with the verbal information retention [12]. Bilateral activation of parietal cortex at the same time with activation of the inferior frontal gyrus is consistent with the preferential activation of dorsal attention network (DAN) during the encoding period [27, 28]. Activation of a region in the cerebellar hemisphere has also been shown in a meta-analysis and is consistent with the hypothesis that the right cerebellar hemisphere is involved in the verbal working memory [11].

The activation of FPCN components was revealed during the maintenance period [24], which is consistent with the data of a meta-analysis demonstrating a gradual increase in FPCN activity and a decrease in DAN activity from the encoding period to the maintenance period in delayed response tasks [27]. At the same time, a decrease in the total number of activation regions during the maintenance period compared to encoding and retrieval may be associated with fewer types of activity involved (only maintenance of information).

During the retrieval period, activation was detected in the parietal lobes bilaterally with the predominance of the right one, which might be due to attention processes [13, 29]. Activation of the right middle temporal gyrus may be due to attention switching [29]. As in the encoding period, activation of the occipital cortex might be associated with visual perception. Observed activation in the right anterior insula is consistent with the evidence of their control function [28]. As opposed to the meta-analysis results [27], in our study, the activation of both FPCN and DAN components has been confirmed in the retrieval period. Activation of the right prefrontal cortex during the retrieval period with presentation of a verbal stimulus emphasizes the ambiguity of the idea about the lateralization of the regions with a functional role in working memory.

According to the results of the BOLD signal changes analysis with a correction for the hemodynamic response delay, activation of the left dorsolateral prefrontal cortex achieves its

maximum in the middle of the encoding period. Then, during the maintenance period it experiences a slight decrease remaining relatively high, after that it increases slightly at the end of the maintenance period and decreases during the retrieval period (neural events in the range of 12–15 seconds from the beginning of the task). This is mostly consistent with the data of other researchers [9, 18, 20] and the hypothesis of the importance of persistent neural activity in working memory [4]. Compared to dorsolateral prefrontal cortex, the parietal cortex activation decreases more strongly in the middle of the maintenance period. Then it experiences a slight increase with a maximum at the beginning of the retrieval period, which is consistent with the results of another study and is especially characteristic for the high-load Sternberg task (6–9 letters) [18]. On the contrary, the occipital cortex activation achieves its maximum during the encoding period and then decreases, which suggests its role in the processes of visual stimulus perception, but not the working memory itself [9, 13, 18].

When interpreting the results, it is necessary to take into account the limitations of the method used to determine the task stages, during which every brain region is active. Since the task periods follow each other in a fixed order, it is impossible to separate the effects of each state on the BOLD signal completely using a model based on the canonical hemodynamic response function, in the absence of detailed information about this function for each subject and brain region. A number of approaches has been proposed in the literature to reduce the impact of this problem, but has not completely solved it [20, 30]. Other limitations include different individual task performance strategies, which could affect the group analysis. The short duration of the encoding and retrieval periods compared with the rest period should also be noted.

## CONCLUSION

The study revealed the activation of prefrontal and posterior parietal cortex (parts of the frontoparietal control network, FPCN) in healthy volunteers during the verbal working memory delayed response task. The results are consistent with the ideas about the key role of prefrontal cortex in the working memory mechanisms of information maintenance, while during the encoding and retrieval periods predominant activation of the parietal cortex was found. Despite the limitations of the method, the study results are consistent with the results of other research using the Sternberg task for the investigation of visual and verbal working memory by fMRI, which speaks in favor of the reproducibility and possible use the results to study the distinct working memory mechanisms.

## References

1. Archer JA, Lee A, Qiu A, Chen SA. Working memory, age and education: A lifespan fMRI study. *PLoS One*. 2018; 13 (3): e0194878.
2. Chai WJ, Abd Hamid AI, Abdullah JM. Working Memory From the Psychological and Neurosciences Perspectives: A Review. *Front Psychol*. 2018; 9: 401.
3. D'Esposito M, Postle BR. The cognitive neuroscience of working memory. *Annu Rev Psychol*. 2015; 66: 115–42.
4. Fuster JM. Unit activity in prefrontal cortex during delayed-response performance: neuronal correlates of transient memory. *J Neurophysiol*. 1973; 36 (1): 61–78.
5. Fuster JM, Bauer RH, Jervey JP. Functional interactions between inferotemporal and prefrontal cortex in a cognitive task. *Brain Res*. 1985; 330 (2): 299–307.
6. Riley MR, Constantinidis C. Role of Prefrontal Persistent Activity in Working Memory. *Front Syst Neurosci*. 2016; 9: 181.
7. Egli T, Coyne D, Spalek K, Fastenrath M, Freytag V, Heck A et al. Identification of Two Distinct Working Memory-Related Brain Networks in Healthy Young Adults. *eNeuro*. 2018; 5 (1): pii: ENEURO.0222-17.2018.
8. Cohen JR, Sreenivasan KK, D'Esposito M. Correspondence between stimulus encoding- and maintenance-related neural processes underlies successful working memory. *Cereb Cortex*. 2014; 24 (3): 593–9.
9. Narayanan NS, Prabhakaran V, Bunge SA, Christoff K, Fine EM,



- Gabrieli JD. The role of the prefrontal cortex in the maintenance of verbal working memory: an event-related fMRI analysis. *Neuropsychology*. 2005; 19 (2): 223–32.
10. Beynel L, Davis SW, Crowell CA, Hilbig SA, Lim W, Nguyen D, et al. Online repetitive transcranial magnetic stimulation during working memory in younger and older adults: A randomized within-subject comparison. *PLoS One*. 2019; 14 (3): e0213707.
  11. Emch M, von Bastian CC, Koch K. Neural correlates of verbal working memory: An fMRI meta-analysis. *Front Hum Neurosci*. 2019; 13: 180.
  12. Rottschy C, Langner R, Dogan I, Reetz K, Laird AR, Schulz JB, et al. Modelling neural correlates of working memory: a coordinate-based meta-analysis. *Neuroimage*. 2012; 60 (1): 830–46.
  13. Xu Y. Reevaluating the Sensory Account of Visual Working Memory Storage. *Trends Cogn Sci*. 2017; 21 (10): 794–815.
  14. Sternberg, S. High-speed scanning in human memory. *Science*. 1966; 153 (3736): 652–4.
  15. Brunoni AR, Vanderhasselt MA. Working memory improvement with non-invasive brain stimulation of the dorsolateral prefrontal cortex: a systematic review and meta-analysis. *Brain Cogn*. 2014; 86: 1–9.
  16. Jiang Y, Guo Z, Xing G, He L, Peng H, Du F, et al. Effects of High-Frequency Transcranial Magnetic Stimulation for Cognitive Deficit in Schizophrenia: A Meta-Analysis. *Front Psychiatry*. 2019; 10: 135.
  17. Sack AT, Kadosh RC, Schuhmann T, Moerel M, Walsh V, Goebel R. Optimizing functional accuracy of TMS in cognitive studies: A comparison of methods. *J Cogn Neurosci*. 2009; 21 (2): 207–21.
  18. Wen X, Wang H, Liu Z, Liu C, Li K, Ding M, et al. Dynamic Top-down Configuration by the Core Control System During Working Memory. *Neuroscience*. 2018; 391: 13–24.
  19. Woodward TS, Feredoes E, Metzack PD, Takane Y, Manoach DS. Epoch-specific functional networks involved in working memory. *Neuroimage*. 2013; 65: 529–39.
  20. Motes MA, Rypma B. Working memory component processes: Isolating BOLD signal changes. *Neuroimage*. 2010; 49 (2): 1933–41.
  21. Hamidi M, Tononi G, Postle BR. Evaluating the role of prefrontal and parietal cortices in memory-guided response with repetitive transcranial magnetic stimulation. *Neuropsychologia*. 2009; 47 (2): 295–302.
  22. Oldfield RC. The assessment and analysis of handedness: The Edinburgh inventory. *Neuropsychologia*. 1971; 9 (1): 97–113.
  23. Kanal E, Barkovich AJ, Bell C, Borgstede JP, Bradley Jr. WG, Froelich JW, et al. ACR guidance document on MR safe practices: 2013. *J Magn Reson Imaging*. 2013; 37 (3): 501–30.
  24. Yeo BT, Krienen FM, Sepulcre J, Sabuncu MR, Lashkari D, Hollinshead M, et al. The organization of the human cerebral cortex estimated by intrinsic functional connectivity. *J Neurophysiol*. 2011; 106 (3): 1125–65. Available from: [http://www.freesurfer.net/fswiki/CorticalParcellation\\_Yeo2011](http://www.freesurfer.net/fswiki/CorticalParcellation_Yeo2011).
  25. xjView. Version 9.6 [software]. Available from: <http://www.alivelearn.net/xjview>.
  26. Trapp S, Mueller K, Lepsien J, Kraemer B, Gruber O. Different neural capacity limitations for articulatory and non-articulatory maintenance of verbal information. *Exp Brain Res*. 2014; 232 (2): 619–28.
  27. Kim H. Neural activity during working memory encoding, maintenance, and retrieval: A network-based model and meta-analysis. *Hum Brain Mapp*. 2019; 40 (17): 4912–33.
  28. Soreq E, Leech R, Hampshire A. Dynamic network coding of working-memory domains and working-memory processes. *Nat Commun*. 2019; 10 (1): 936.
  29. Nee DE, Brown JW, Askren MK, Berman MG, Demiralp E, Krawitz A, et al. A meta-analysis of executive components of working memory. *Cereb Cortex*. 2013; 23 (2): 264–82.
  30. Rozovskaya RI, Pechenkova EV, Mershina EA, Machinskaya RI. fMRI Study of Retention of Images with Different Emotional Valence in the Working Memory. *Psychology. Journal of the Higher School of Economics*. 2014; 11 (1): 27–48. Russian.

## Литература

1. Archer JA, Lee A, Qiu A, Chen SA. Working memory, age and education: A lifespan fMRI study. *PLoS One*. 2018; 13 (3): e0194878.
2. Chai WJ, Abd Hamid AI, Abdullah JM. Working Memory From the Psychological and Neurosciences Perspectives: A Review. *Front Psychol*. 2018; 9: 401.
3. D'Esposito M, Postle BR. The cognitive neuroscience of working memory. *Annu Rev Psychol*. 2015; 66: 115–42.
4. Fuster JM. Unit activity in prefrontal cortex during delayed-response performance: neuronal correlates of transient memory. *J Neurophysiol*. 1973; 36 (1): 61–78.
5. Fuster JM, Bauer RH, Jervey JP. Functional interactions between inferotemporal and prefrontal cortex in a cognitive task. *Brain Res*. 1985; 330 (2): 299–307.
6. Riley MR, Constantinidis C. Role of Prefrontal Persistent Activity in Working Memory. *Front Syst Neurosci*. 2016; 9: 181.
7. Egli T, Coynel D, Spalek K, Fastenrath M, Freytag V, Heck A et al. Identification of Two Distinct Working Memory-Related Brain Networks in Healthy Young Adults. *eNeuro*. 2018; 5 (1): pii: ENEURO.0222-17.2018.
8. Cohen JR, Sreenivasan KK, D'Esposito M. Correspondence between stimulus encoding- and maintenance-related neural processes underlies successful working memory. *Cereb Cortex*. 2014; 24 (3): 593–9.
9. Narayanan NS, Prabhakaran V, Bunge SA, Christoff K, Fine EM, Gabrieli JD. The role of the prefrontal cortex in the maintenance of verbal working memory: an event-related fMRI analysis. *Neuropsychology*. 2005; 19 (2): 223–32.
10. Beynel L, Davis SW, Crowell CA, Hilbig SA, Lim W, Nguyen D, et al. Online repetitive transcranial magnetic stimulation during working memory in younger and older adults: A randomized within-subject comparison. *PLoS One*. 2019; 14 (3): e0213707.
11. Emch M, von Bastian CC, Koch K. Neural correlates of verbal working memory: An fMRI meta-analysis. *Front Hum Neurosci*. 2019; 13: 180.
12. Rottschy C, Langner R, Dogan I, Reetz K, Laird AR, Schulz JB, et al. Modelling neural correlates of working memory: a coordinate-based meta-analysis. *Neuroimage*. 2012; 60 (1): 830–46.
13. Xu Y. Reevaluating the Sensory Account of Visual Working Memory Storage. *Trends Cogn Sci*. 2017; 21 (10): 794–815.
14. Sternberg, S. High-speed scanning in human memory. *Science*. 1966; 153 (3736): 652–4.
15. Brunoni AR, Vanderhasselt MA. Working memory improvement with non-invasive brain stimulation of the dorsolateral prefrontal cortex: a systematic review and meta-analysis. *Brain Cogn*. 2014; 86: 1–9.
16. Jiang Y, Guo Z, Xing G, He L, Peng H, Du F, et al. Effects of High-Frequency Transcranial Magnetic Stimulation for Cognitive Deficit in Schizophrenia: A Meta-Analysis. *Front Psychiatry*. 2019; 10: 135.
17. Sack AT, Kadosh RC, Schuhmann T, Moerel M, Walsh V, Goebel R. Optimizing functional accuracy of TMS in cognitive studies: A comparison of methods. *J Cogn Neurosci*. 2009; 21 (2): 207–21.
18. Wen X, Wang H, Liu Z, Liu C, Li K, Ding M, et al. Dynamic Top-down Configuration by the Core Control System During Working Memory. *Neuroscience*. 2018; 391: 13–24.
19. Woodward TS, Feredoes E, Metzack PD, Takane Y, Manoach DS. Epoch-specific functional networks involved in working memory. *Neuroimage*. 2013; 65: 529–39.
20. Motes MA, Rypma B. Working memory component processes: Isolating BOLD signal changes. *Neuroimage*. 2010; 49 (2): 1933–41.
21. Hamidi M, Tononi G, Postle BR. Evaluating the role of prefrontal and parietal cortices in memory-guided response with repetitive transcranial magnetic stimulation. *Neuropsychologia*. 2009; 47 (2): 295–302.
22. Oldfield RC. The assessment and analysis of handedness: The Edinburgh inventory. *Neuropsychologia*. 1971; 9 (1): 97–113.
23. Kanal E, Barkovich AJ, Bell C, Borgstede JP, Bradley Jr. WG, Froelich JW, et al. ACR guidance document on MR safe practices: 2013. *J Magn Reson Imaging*. 2013; 37 (3): 501–30.



24. Yeo BT, Krienen FM, Sepulcre J, Sabuncu MR, Lashkari D, Hollinshead M, et al. The organization of the human cerebral cortex estimated by intrinsic functional connectivity. *J Neurophysiol.* 2011; 106 (3): 1125–65. Available from: [http://www.freesurfer.net/fswiki/CorticalParcellation\\_Yeo2011](http://www.freesurfer.net/fswiki/CorticalParcellation_Yeo2011).
25. xjView. Version 9.6 [software]. Available from: <http://www.alivelearn.net/xjview>.
26. Trapp S, Mueller K, Lepsien J, Kraemer B, Gruber O. Different neural capacity limitations for articulatory and non-articulatory maintenance of verbal information. *Exp Brain Res.* 2014; 232 (2): 619–28.
27. Kim H. Neural activity during working memory encoding, maintenance, and retrieval: A network-based model and meta-analysis. *Hum Brain Mapp.* 2019; 40 (17): 4912–33.
28. Soreq E, Leech R, Hampshire A. Dynamic network coding of working-memory domains and working-memory processes. *Nat Commun.* 2019; 10 (1): 936.
29. Nee DE, Brown JW, Askren MK, Berman MG, Demiralp E, Krawitz A, et al. A meta-analysis of executive components of working memory. *Cereb Cortex.* 2013; 23 (2): 264–82.
30. Розовская Р. И., Печенкова Е. В, Мершина Е. А., Мачинская Р. И. фМРТ-исследование удержания в рабочей памяти изображений различной эмоциональной валентности. *Психология. Журнал высшей школы экономики.* 2014; 11 (1): 27–48.

## STUDY OF THE NEW 4-PHENYLPYRROLIDINONE-2 DERIVATIVE PHARMACOKINETICS AND NEUROPROTECTIVE EFFECT IN THE ISCHEMIC STROKE ANIMAL MODEL

Borozdenko DA , Lyakhmun DN, Golubev YaV, Tarasenko DV, Kiseleva NM, Negrebetsky VadV

Pirogov Russian National Research Medical University, Moscow, Russia

The development of methods of drug therapy and rehabilitation in different periods of ischemic cerebral lesion is currently an urgent problem. Our study was aimed to investigate the pharmacokinetics and anti-ischemic effect of the new 4-phenylpyrrolidone-2 derivative in rats. To study the drug pharmacokinetics, the *Wistar* rats were once administered with the substance at a dose of 250 mg/kg, then, the substance distribution in blood and cerebral cortex was evaluated. Elimination half-life value was determined, which was 83.2 min. The substance remained in the brain tissue for 24 hours. To assess the anti-ischemic effect, the stroke was modeled by endovascular middle brain artery transition occlusion, and the drug was administered intravenously for 5 days at two doses, 250 and 125 mg/kg. After that the lesion focus volume was evaluated by MRI, as well as the neurological deficit severity, locomotor and explorative behavior. The studied drug significantly decreased the neurological deficit in model animals compared to control group (1.72 vs 4.4,  $p < 0.05$ ). According to the MRI data, the effect on the ischemic focus was negligible, while the explorative behavior significantly increased under the influence of the 4-phenylpyrrolidone-2 derivative (hole board test, horizontal activity  $12.1 \pm 6.8$ ,  $22.5 \pm 10.5$ ,  $p < 0.05$ ). The data obtained allow us to conclude that the studied substance penetrates the blood-brain barrier (BBB), and accumulates in the brain tissue promoting the neurological deficit correction and increasing the explorative behavior in the ischemic stroke model animals.

**Keywords:** neuroprotective activity, pharmacokinetics, stroke, 4-phenylpyrrolidone-2, ischemic stroke models

**Funding:** the study was performed as a part of the 2018–2020 Pirogov Russian National Research Medical University public assignment, R&D registration № AAAA-A18-118051590108-1.

**Acknowledgments:** to Kamkin AG PhD, head of the department of Physiology of the Faculty of Biomedicine, head of the laboratory of Electrophysiology of the Institute of Translational Medicine of Pirogov Russian National Research Medical University for the opportunity to use the equipment of the Scientific and Educational Center for the study of molecular and cellular mechanisms of hypoxia and ischemia; to Abakumov MA PhD, associate professor of the department of Medical Nanobiotechnology of the Faculty of Biomedicine, for his assistance in modelling, MRI scanning and interpretation of the results.

**Author contribution:** Borozdenko DA — working with animals, primary data acquisition and analysis, manuscript writing; Lyakhmun DN — working with animals, functional testing; Golubev YaV — substance concentration analysis; Tarasenko DV — synthesis of substance; Kiseleva NM — study design, study management, manuscript preparation; Negrebetsky VadV — study design, study management.


**Compliance with ethical standards:** the study was approved by the Animal Care and Use Committee of Pirogov Russian National Research Medical University (protocol № 48/2018 dated June 13, 2018). The animals were treated in strict compliance with the Declaration of Helsinki, Directive 2010/63/EU of the European Parliament and the Council (September 22, 2010) on the protection of animals used for scientific purposes, and Good Laboratory Practice guidelines established by the Order 708n of the Ministry of Healthcare of the Russian Federation (August 23, 2010).

✉ **Correspondence should be addressed:** Denis A. Borozdenko  
Ostrovityanova, 1, Moscow, 117997; borozdenko@phystech.edu

**Received:** 28.01.2020 **Accepted:** 11.02.2020 **Published online:** 22.02.2020

**DOI:** 10.24075/brsmu.2020.010

## ИЗУЧЕНИЕ ФАРМАКОКИНЕТИКИ И НЕЙРОПРОТЕКТОРНОЙ АКТИВНОСТИ НОВОГО ПРОИЗВОДНОГО 4-ФЕНИЛПИРРОЛИДИНОНА-2 В МОДЕЛИ ИШЕМИЧЕСКОГО ИНСУЛЬТА НА ЖИВОТНЫХ

Д. А. Борозденко , Д. Н. Ляхман, Я. В. Голубев, Д. В. Тарасенко, Н. М. Киселева, Вад. В. Негребетский

Российский национальный исследовательский медицинский университет имени Н. И. Пирогова, Москва, Россия

Разработка методов медикаментозной терапии и реабилитации в разных периодах ишемического поражения головного мозга в настоящее время является актуальной проблемой. Целью исследования было изучить фармакокинетику и антиишемическое действие нового производного 4-фенилпирролидинона-2 на крысах. Для изучения фармакокинетики крысам линии *Wistar* однократно вводили вещество в дозе 250 мг/кг, затем оценивали его распределение в плазме и коре головного мозга. Установлен период полувыведения ( $T_{1/2}$ ), 83,2 мин. Время нахождения вещества в тканях головного мозга составило 24 ч. Для оценки антиишемического действия проводили моделирование инсульта методом эндоваскулярной транзиторной окклюзии средней мозговой артерии, препарат вводили внутривенно в течение 5 дней в двух дозах, 250 и 125 мг/кг. Затем определяли размер очага поражения (с помощью МРТ), степень неврологического дефицита, локомоторную и исследовательскую активность. Исследуемое вещество значительно снижало неврологический дефицит у модельных животных по сравнению с контрольной группой (1,72 vs 4,4;  $p < 0,05$ ). Влияние на очаг ишемии по МРТ было незначительным, а ориентировочно-исследовательское поведение под воздействием производного 4-фенилпирролидинона-2 значительно активизировалось («норковая камера», горизонтальная активность  $12,1 \pm 6,8$ ,  $22,5 \pm 10,5$ ;  $p < 0,05$ ). Полученные данные позволяют сделать вывод, что исследуемое вещество проходит через гематоэнцефалический барьер (ГЭБ), накапливается в коре головного мозга, способствуя коррекции неврологического дефицита и повышая исследовательскую активность у животных в модели ишемического инсульта.

**Ключевые слова:** нейропротекторная активность, фармакокинетика, инсульт, 4-фенилпирролидинон-2, модели ишемического инсульта

**Финансирование:** работа выполнена в рамках государственного задания ФГБОУ ВО РНИМУ имени Н. И. Пирогова на 2018–2020 гг., № гос. регистрации НИР AAAA-A18-118051590108-1.

**Благодарности:** А. Г. Камкину, д. м. н., заведующему кафедрой физиологии МБФ, заведующему научно-исследовательской лабораторией электрофизиологии НИИ трансляционной медицины РНИМУ им. Н. И. Пирогова, за возможность использовать оборудование Научно-образовательного центра по исследованию молекулярных и клеточных механизмов гипоксии и ишемии; М. А. Абакумову, к. х. н., доценту кафедры медицинских нанобиотехнологий МБФ за помощь в моделировании и проведении МРТ-сканирования, интерпретации результатов.

**Вклад авторов:** Д. А. Борозденко — работа с животными, сбор, обработка и анализ первичных данных, написание статьи; Д. Н. Ляхман — работа с животными, проведение функциональных тестов; Я. В. Голубев — анализ концентраций вещества; Д. В. Тарасенко — синтез вещества; Н. М. Киселева — дизайн исследования, научное руководство, работа со статьей; Вад. В. Негребетский — дизайн исследования, научное руководство.

**Соблюдение этических стандартов:** все процедуры с животными рассмотрены и утверждены комиссией по уходу и использованию животных РНИМУ имени Н. И. Пирогова (протокол № 48/2018 от 13.06.2018 г.). Условия содержания животных и работы с ними соответствовали принципам Хельсинкской декларации о гуманном отношении к животным, директиве Европейского парламента и Совета Европейского Союза 2010/63/ЕС от 22 сентября 2010 г. о защите животных, используемых для научных целей, «Правилам лабораторной практики в Российской Федерации», утвержденным приказом Министерства здравоохранения РФ № 708н от 23.08.2010 г.

✉ **Для корреспонденции:** Денис Андреевич Борозденко  
ул. Островитянова, д. 1, г. Москва, 117997; borozdenko@phystech.edu

**Статья получена:** 28.01.2020 **Статья принята к печати:** 11.02.2020 **Опубликована онлайн:** 22.02.2020

**DOI:** 10.24075/vrgmu.2020.010

Stroke is the second leading cause of death in Russia, by the number of cases it follows the myocardial infarction. According to the World Health Organization, 70–80% of stroke survivors become disabled [1–2]. Only thrombolytic therapy has proven pharmacological efficacy in the acute period of ischemic stroke, but it has a whole range of restrictions, the main of which is a narrow time interval. Only 5% of patients with acute ischemic stroke receive the thrombolytic therapy [1]. Rehabilitation therapy covers a much wider time interval, measured in weeks and months, so many researchers develop drugs in the context of rehabilitation medicine.

In recent years, both in Russia and abroad, a number of innovative solutions have appeared [3–5].

In the Department of Medical Chemistry and Toxicology of the Institute of Translational Medicine of Pirogov Russian National Research Medical University the new compound (laboratory number VRF\_11) has been synthesized, which contains 4-phenylpyrrolidone-2 derivative as a pharmacophore [6]. According to *in silico* studies [7], the substance has an anti-ischemic, nootropic and cytoprotective potential.

The safety profile of the substance was established. To confirm the anti-ischemic effect of the new substance it was necessary to define the dose regimen and to estimate the main pharmacokinetic parameters.

The study was aimed to investigate the VRF\_11 pharmacokinetics and to deduce the most effective dose regimen for the correction of neurological symptoms in the rat model of focal cerebral ischemia.

## METHODS

The experiments were carried out on 85 adult male *Wistar* rats weighing  $220 \pm 12$  g at the beginning of the study. The rats were received from the Stolbovaya nursery station. Animals were kept in the conventional vivarium of Pirogov Russian National Research Medical University with automatic change of day and night cycle (08:00–20:00, “day”, 20:00–08:00, “night”) and at least 12-fold change in the air volume of the room within an hour (temperature 20–24 °C, humidity 45–65%). Animals were fed with the “Chara” full-grain dry granular feed for laboratory animals (Assortiment-Agro; Russia; veterinary certificate form 3 250 № 3828680, declaration of conformity No. POCC RU.ПН88.Д07428, valid until May 27, 2021) which was put *ad libitum* into the feeding recess of the steel grid cage lid. Animals were fed with water purified in accordance with the requirements of GOST 51232-98. Water in standard drinking bowls with steel nose caps was given *ad libitum*. For bedding the Rehofix corn cob granules (JRS; Germany) were used.

Two series of experiments were conducted.

In the 1<sup>st</sup> series the VRF\_11 pharmacokinetics was studied. VRF\_11 was injected intravenously in the tail vein as the 200 mg/ml solution using the  $0.4 \times 8$  mm needle (27G), in accordance with the rules of aseptic and antiseptic (at a dose of 250 mg/kg).

Concentration of the substance in the blood plasma and brain tissue was determined at different time points. Blood sampling from the tail vein in a volume of 100–150 µl was performed after 15, 30, 60, 120, 240 min, 8, 12, 24 and 48 hours using the EDTA tubes. To study the VRF\_11 accumulation in the brain, rats were euthanized in a CO<sub>2</sub> box, after which the heart muscle was dissected, cannulas were inserted, and the carcass was washed with 1 liter of cold NaCl solution (0.9%). The brain was removed and the cerebral cortex was set apart. The fragment extracted was frozen and stored at –80 °C. Plasma was also frozen and stored at –30 °C.

In accordance with the recommendations on the study of pharmacokinetics [8] groups of animals were formed, 6 rats each (Table 1).

VRF\_11 concentrations in the rats’ plasma and brain tissue samples were determined by high-performance liquid chromatography (HPLC). The SPD-20A absorbance detector (Shimadzu; Japan) was used to determine the VRF\_11 concentration in the 10 µg/ml – 1 mg/ml range. The LC/MS 8030/8040 ultra fast triple quadrupole gas chromatograph mass spectrometer (Shimadzu; Japan) was used to determine the concentration of the substance in the 10 ng/ml – 10 µg/ml range. Calibration curves for the VRF\_11 20–1000 µg/ml and 10 ng/ml – 50 µg/ml concentration ranges were plotted using the VRF\_11 stock solutions and plasma of intact animals.

### Determining the concentration of VRF\_11 in the 10 µg/ml – 1 mg/ml range

To determine the drug concentration in the animals’ blood plasma, the following sample preparation routine was used. Acetonitrile in the amount of 300 µl containing 0.5% formic acid was added to 100 µl of blood plasma. After stirring and centrifuging (CM-50 centrifuge; ELMI; Latvia), 12,499 rpm for 3 min, supernatant was sampled and evaporated at the room temperature for 2 hours using the SpeedVac Savant SPD 1010 vacuum concentrator (Thermo Scientific; USA). The residue obtained was redissolved in 200 µl of the mobile phase. To prepare the mobile phase, 1.36 g of potassium dihydroorthophosphate (KH<sub>2</sub>PO<sub>4</sub>) was dissolved in 850 ml of deionized water. The 1.625 ml of diethylamine and 150 ml of acetonitrile were added to the resulting solution. Chromatographic conditions: isocratic elution mode; NUCLEODUR C<sub>18</sub> ec 250/4.6 HPLC column (Macherey-Nagel; Germany), particle size 5 µm; column temperature 40 °C ± 0.1; eluent flow rate 0.8 ml/min; injection volume 10 µl; wavelength 220 nm.

### Determining the concentration of VRF\_11 in the 10 ng/ml – 10 µg/ml range

To determine the drug concentration in the animals’ blood plasma, the following sample preparation routine was used. Acetonitrile in the amount of 300 µl containing 0.5% formic

**Table 1.** VRF\_11 pharmacokinetics study design (single intravenous administration)

Group №	Plasma sampling	Cerebral cortex
1	15 min; 240 min	240 min
2	60 min; 24 h	24 h
3	30 min; 8 h	8 h
4	48 h	
5	120 min; 12 h	
6		30 min
7		120 min

acid was added to 100 µl of blood plasma. After stirring and centrifuging (centrifugation conditions are similar to those described above), supernatant was evaporated using the vacuum concentrator (conditions described above) and redissolved in the 200 µl of eluent. Chromatographic conditions: Discovery® C18 HPLC Column (Supelco/Sigma-Aldrich; USA), particle size 5 µm, L × I.D. 15 cm × 4.6 mm; column temperature 40 °C ± 0.1; eluent flow rate 0.8 ml/min; injection volume 10 µl. Electrospray ionization (ESI) technique was used for analysis: desolvation line (DL) temperature 250 °C, heat block temperature 400 °C, nebulizer gas flow 2 l/min, drying gas flow 15 l/min, capillary voltage 4.5 kV, gas pressure for CID 60 kPa.

To determine the concentration of VRF\_11 in brain tissue, 1.5 ml of acetonitrile containing 0.5% formic acid was added to 70-100 mg of animal brain, then, the brain was homogenized in a glass handheld homogenizer for 3 minutes. The resulting suspension was centrifuged twice (centrifugation conditions are similar to those described above). Supernatant was evaporated using the vacuum concentrator (conditions described above). A mixture of deionized water with acetonitrile (100:5) in the amount of 300 µl was added to the residue, then, the resulting mixture was stirred actively for 5 minutes. Centrifugation was carried out (conditions described above), and supernatant was analyzed. The mobile phase contained the mixture of 700 ml of deionized water, 3.5 ml of formic acid and 300 ml of acetonitrile. Chromatographic conditions: isocratic elution mode; Discovery® C18 HPLC Column (Supelco/Sigma-Aldrich; USA), particle size 5 µm, 150/4,6; column temperature 40 °C ± 0.1; eluent flow rate 0.8 ml/min; injection volume 10 µl. Electrospray ionization (ESI) technique was used: desolvation line (DL) temperature 250 °C, heat block temperature 400 °C, nebulizer gas flow 2 l/min, drying gas flow 15 l/min, capillary voltage 4.5 kV, gas pressure for CID 60 kPa. Processing and analysis of the results was performed using the LabSolution ver. 5.80 (Shimadzu; Japan) and Borgia 1.03 (Nauka Plus; Russia) software, as well as Microsoft Excel (Microsoft; USA) and Statistica 12 (Statsoft; USA) applications.

In a second series of experiments, cerebral infarction was modeled in rats to investigate the effect of VRF\_11 administered at doses of 250 and 125 mg/kg on the neurological symptoms and behavior.

Experimental cerebral infarction was modeled by endovascular transient occlusion of the middle cerebral artery by the modified Koizumi method [9,10] followed by reperfusion.

The duration of middle cerebral artery occlusion was 90 minutes.

The following groups of animals were formed, 8 rats each:

1. Control group. Animals were injected with saline 24 hours after reperfusion, once a day (5 days).

2. Treatment group. VRF\_11 at a dose of 125 mg/kg was injected intravenously 24 hours after reperfusion, once a day (5 days).

3. Treatment group. VRF\_11 at a dose of 250 mg/kg was injected intravenously 24 hours after reperfusion, once a day (5 days).

Laboratory animals magnetic resonance imaging (MRI) follow-up was performed using the ClinScan system (Bruker BioSpin; Germany) with 7 T magnetic field. To evaluate the cerebral infarction volume, the MRI scanning was performed on the 1<sup>st</sup>, 7<sup>th</sup>, 14<sup>th</sup>, 28<sup>th</sup> day after occlusion. The MRI protocol consisted of obtaining the T2-weighted images with the respiratory synchronization (TurboSpinEcho, Turbo Factor = 10, TR/TE = 5230/46 ms, voxel size 0.117\*0.13\*0.7 mm) in axial projection, starting from the 1<sup>st</sup> day after cerebral infarction modeling. The cerebral infarction volume follow-up was performed using the ImageJ software (Wayne Rasband; USA) analyzing the T2-weighted images. At the first stage, the area on each slice was measured, after which the total infarction volume was calculated by the formula  $V = (S_1 + \dots + S_n) \cdot (h + d)$ , where  $S_1$  was the 1<sup>st</sup> slice area,  $S_n$  was the area of slice  $n$  (mm<sup>2</sup>),  $h$  was the slice thickness (mm), and  $d$  was the interslice gap (mm) [11].

Behavioral changes in rats were evaluated within 4 weeks after stroke modeling. The overall neurological functioning was assessed using the mNSS scale [12]. Motor deficit was evaluated using the following functional tests: the hole board test for rats (OpenScience; Russia) and the open field test (OpenScience; Russia). The hole board test was performed on the 10<sup>th</sup> and 24<sup>th</sup> day after stroke [13]. The open field test was performed on the 16<sup>th</sup> day. During the test the explorative and locomotor behavior was also assessed using the same parameters. In addition, the total path and speed of movement were calculated [14].

Statistical processing of the results was performed using the Statistica 12.0 software (Statsoft; USA). Mann-Whitney U-test, Student t-test for independent samples, as well as the descriptive methods with the definition of the arithmetic mean, standard deviation, standard error of the mean were used. The differences were considered significant at  $p < 0.05$ .

**Table 2.** VRF\_11 blood level in laboratory animals after single intravenous administration at a dose of 250 mg/kg ( $n = 6$ , µg/ml)

Time point/№	1	2	3	4	5	6	M	SD
15 min	666.38	780.89	559.36	297.84	282.59	488.92	512.67	198.69
30 min	567.99	787.9	418.5	202.09	500.19	700.3	529.49	208.71
60 min	533.68	185.1	335.35	285.98	415.33	602.91	393.06	156.43
120 min	60.59	10.43	42.91	50.26	18.39	32.52	35.84	19.14

**Note:** M — mean value for the time point; SD — standard deviation.

**Table 3.** VRF\_11 blood level in laboratory animals after intravenous administration at a dose of 250 mg/kg ( $n = 6$ , ng/ml)

Time point/№	1	2	3	4	5	6	M	SD
4 h	295.99	809.40	659.03	190.36	727.0	567.02	541.47	246.66
8 h	85.87	58.99	41.3	65.97	48.58	51.54	58.71	15.79
12 h	2883.98	1718.41	3074.25	1045.94	2120.61	1955.05	2133.05	753.03
24 h	147.47	126.16	114.34	93.21	105.18	97.93	114.05	20.18
48 h	73.37	62.76	56.88	46.37	52.32	48.72	56.74	10.04

**Note:** M — mean value for the time point; SD — standard deviation.

## RESULTS

**VRF\_11 pharmacokinetics study (intravenous administration at a dose of 250 mg/kg)**

Tables 2 and 3 contain the laboratory animals' VRF\_11 blood concentration levels detected after the single intravenous administration. All the values fit the calibration curve.

The results of the experimental animals VRF\_11 blood level measurement are presented in Fig. 1.

The data presented in Fig. 1, may be approximated satisfactorily by the single compartment model (without absorption), which is described by the following equation:

$$C = A \times \exp(-at),$$

where  $C$  is the studied drug level in the laboratory animals' blood,  $t$  is the time after the drug administration,  $A$ ,  $a$  are the constants of a process describing a pharmacokinetic equation, which are associated with the constants describing the distribution of the studied drug in the body.

As a result of the pharmacokinetic data approximation using the Borgia 1.03 application, the following equation was obtained:

$$C = 580.143 \times \exp(-0.00833 \times t)$$

Table 4 demonstrates the indicators of the main pharmacokinetic parameters:  $C_{\max}$ ,  $T_{\max}$ ,  $AUC_{(0 \rightarrow \infty)}$ ,  $T_{1/2}$ ,  $Cl$ ,  $V_d$ .

**Accumulation of VRF\_11 in the cerebral cortex**

Table 5 demonstrates the concentrations of VRF\_11 in the cerebral cortex homogenate extracts after the single intravenous administration of the drug at a dose of 250 mg/kg. All the values fit the calibration curve.

Thus, VRF\_11 penetrates the BBB, reaching the maximum concentration 30 minutes after administration. The drug is still detected in the rat cerebral cortex 24 hours after injection.

**Monitoring the model of acute cerebral ischemia, dynamics of the infarction volume over time**

The 3 groups of animals were studied, 8 rats each. One day after the modeling of cerebral infarction by the middle cerebral

artery endovascular transient occlusion, the animals underwent MRI to control the volume of the lesion. Assessment of the ischemic lesion volume demonstrated that the modeling was performed correctly. Two rats with small size foci were excluded from the study (Table 5). In treatment group rats, after the MRI confirmation the studied drug was injected in the tail vein at doses of 125 and 250 mg/kg. The control animals were injected with the same volume of saline by the same method.

MRI follow-up results on the 1<sup>st</sup>, 7<sup>th</sup>, 14<sup>th</sup> and 28<sup>th</sup> day after reperfusion demonstrated that the studied substance at doses of 125 and 250 mg/kg had no effect on the average focus volume (compared to control group, which did not receive VRF\_11) (Table 6). The infarction focus volume significantly decreased in all groups of animals by the end of the 1<sup>st</sup> month in relation to the 1<sup>st</sup> day after ischemia.

**Neurological deficit assessment**

Neurological deficit assessment using the mNSS scale was carried out on the 1<sup>st</sup>, 3<sup>rd</sup> and 5<sup>th</sup> day after reperfusion. On the 1<sup>st</sup> day the test was performed prior to the drug administration. According to the mNSS score, there were no significant differences between animals receiving VRF\_11 at doses of 250 and 125 mg/kg and control animals (Table 6). As can be seen from the data presented (Table 7), when comparing neurological deficit scores on the 1<sup>st</sup> and 5<sup>th</sup> day, animals from the VRF\_11 group showed statistically significant differences, whereas in control animals there were no such differences. It should be noted that there was a greater neurological deficit on the 1<sup>st</sup> day after reperfusion in the group receiving VRF\_11 at a dose of 250 mg/kg compared to other groups, while an MRI scanning did not reveal differences in the ischemic foci volume in animals.

**Behavioral response study**

Behavioral study using the open field test, which was carried out on the 16<sup>th</sup> day after reperfusion, revealed significant differences in standing still and grooming duration, as well as in number of visits to the central zone in animals receiving VRF\_11 at doses of 125 and 250 mg/kg compared to control group (Table 8).

In the hole board test 10 days after the ischemia modeling, significant differences were revealed between the control group and the group of animals injected intravenously with VRF\_11

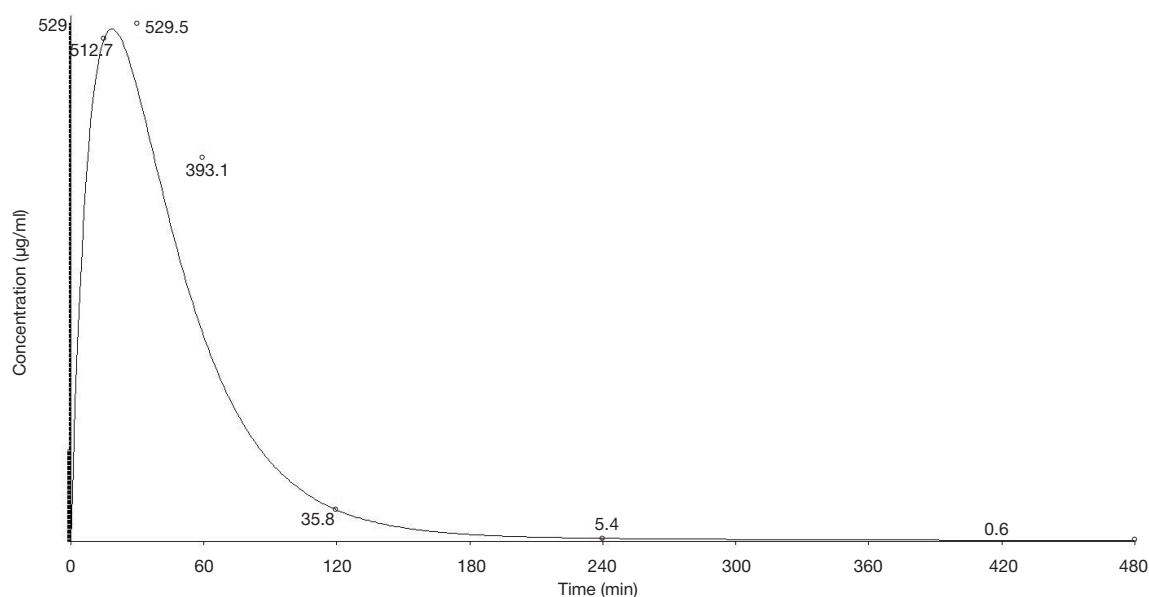


Fig. 1. VRF\_11 kinetics in blood plasma after the single intravenous administration at a dose of 250 mg/kg



**Table 4.** Main pharmacokinetic parameters of VRF\_11 (intravenous administration at a dose of 250 mg/kg)

Parameter	VRF_11
$C_{max}^*$ , $\mu\text{g/ml}$	529
$T_{max}^*$ , h	0.5
$T_{1/2res}^*$ , min	83.2
$AUC_{(0 \rightarrow \infty)}^*$ , min $\times$ ng/ml	69645.1
Cl, ml/min	0.004
$V_d$ , ml	0.862

(125 mg/kg and 250 mg/kg) (Fig. 2). There were differences in horizontal activity (sector crossing  $12.1 \pm 6.8$ ,  $22.5 \pm 10.5$  ( $p < 0.05$ ) and  $20.2 \pm 14.7$  ( $p < 0.07$ )) and vertical lactivity (number of stances  $2 \pm 1.6$ ,  $7.5 \pm 4.0$  ( $p < 0.05$ ) and  $7 \pm 12.1$  ( $p < 0.07$ )), standing still duration ( $46.6 \pm 34.4$ ,  $1.0 \pm 1.3$  ( $p < 0.01$ ) and  $24.1 \pm 21.9$  ( $p < 0.05$ )) (control group, animals receiving VRF\_11 at a dose of 125 mg/kg, and animals receiving VRF\_11 at a dose of 250 mg/kg, respectively). On the 24th day after reperfusion in the hole board test, the experimental animals demonstrated more active explorative behavior compared to control group. Thus, significant различия ( $p < 0.05$ ) differences were revealed in sector crossing (in animals receiving saline the value was  $18 \pm 7.3$ , in the group receiving VRF\_11 at a dose of 125 mg/kg it was  $31 \pm 16.5$  ( $p < 0.03$ ), and in the group receiving VRF\_11 at a dose of 250 mg/kg it was  $26.3 \pm 12.5$  ( $p < 0.05$ )) and in the number of holes ( $5 \pm 3$ ,  $10.5 \pm 2.9$  ( $p < 0.01$ ) and  $8.6 \pm 2.9$  ( $p < 0.05$ ) respectively). The standing still duration significantly decreased only under the influence of VRF\_11 at a dose of 125 mg/kg ( $22.9 \pm 22.8$  and  $0.6 \pm 2.3$  ( $p < 0.01$ )).

## DISCUSSION

Despite the widespread use of effective drugs for endovascular therapy, clinical outcomes after acute ischemic stroke still remain unsatisfactory [15]. Most patients retain motor impairment, their cognitive abilities decrease, and in many patients the psychoemotional sphere is impaired. As a result of neurological complications caused by stroke, neuroprotection and post-stroke rehabilitation has recently become an increasingly urgent problem [16].

The Department of Chemistry of Pirogov Russian National Research Medical University has an extensive experience of working with nootropic drugs [17, 18]. In this study, we used a promising substance, a derivative of 4-phenylpyrrolidinone-2, VRF\_11, which, according to computer simulation, has neuroprotective properties.

The VRF\_11 pharmacokinetics study results (Table 4) allow us to state that the drug penetrates the BBB and remains in the cerebral cortex during the day.

According to its pharmacokinetic parameters, VRF\_11 is slightly different from the known nootropic drugs, such as piracetam and phenotropil. Thus,  $T_{1/2}$  of piracetam administered intravenously is 4–5 hours [19], and  $T_{1/2}$  of phenotropil is 2.77 hours [20]. The molecular weight of piracetam is 142 g/mol, and the molecular weight of phenotropil is 218 g/mol. A tendency to a decrease in half-life with an increase in molecular weight can be observed. Thus, in VRF\_11 with molecular weight 252 g/mol the  $T_{1/2}$  value is 1.26 hours.

VRF\_11 remains in the brain tissue during the day. That is why we have chosen the dosage regimen once a day to avoid the effect of accumulation in the target organ. In the literature there is no clear opinion about the dosage regimen on metabotropic drugs (and on nootropic drugs in particular). Thus, according to official instructions, piracetam is taken up to 3 times a day, and phenotropil once per day. That is why the selection of the dosage regimen during the new compounds studies is one of the most difficult and time-consuming tasks. We have chosen the following algorithm: molecular weight conversion using the closest analogue (phenotropil). The required dose of phenotropil is 100 mg/kg. After recalculation

**Table 5.** VRF\_11 level (ng/g of tissue) in the cerebral cortex homogenate extracts after the single intravenous administration of the drug at a dose of 250 mg/kg

Time, h \ №	1	2	3	4	5	M	SD
0.5	1813.89	1167.11	2129.94	1566.63	2058.27	1747.17	392.69
2	354.12	396.38	363.63	407.07	380.50	380.34	22.01
4	260.34	233.58	289.16	218.68	250.97	250.54	26.88
8	144.54	158.01	171.49	126.96	140.43	148.29	17.05
24	20.63	23.0	18.34	17.37	18.84	19.64	2.22

**Note:** M — mean value for the time point; SD — standard deviation.

**Table 6.** Ischemia focus volume, mm<sup>3</sup> (M  $\pm$  m; n = 8)

Day of scanning	Control (saline)		VRF_11, 125 mg/kg		VRF_11, 250 mg/kg	
	M	SD	M	SD	M	SD
1	131.14	24.60	133.25	33.16	133.66	23.72
7	111.79	24.04	107.53	33.38	115.91	20.75
14	100.43	20.63	93.64*	29.82	106.86	21.87
28	83.04*	15.63	81.6*	26.97	91.16*	20.67

**Note:** M — mean value for the time point; SD — standard deviation; \* —  $p < 0.05$  (comparison of mean values within the same group in relation to the 1<sup>st</sup> day).

**Table 7.** Neurological deficit assessment using the mNSS scale ( $M \pm m$ ;  $n = 8$ )

	Control		VRF_11 125 mg/kg		VRF_11 250 mg/kg	
	Mean	SD	Mean	SD	Mean	SD
1 <sup>st</sup> day	5.43	3.55	6.8	3.6	9.1	2.75
3 <sup>rd</sup> day	4.43	2.63	3.8	2.48	7.1	2.39
5 <sup>th</sup> day	3.71	2.81	2.4*	1.52	6.5*	2.14

Note: \* —  $p < 0.05$  (comparison of mean values within the same group in relation to the 1<sup>st</sup> day).

**Table 8.** Activity indicators in the open field test on the 16th day after reperfusion ( $M \pm m$ ;  $n = 8$ )

	Control		VRF_11 125 mg/kg		VRF_11 250 mg/kg	
	Mean	SD	Mean	SD	Mean	SD
Sector crossing	35.83	9.133	40.87	12.04	42.33*	14.95
Center	0.16	0.4	1.13*	1.13	1.33*	1.75
Standing still, duration	36.83	33.73	9.37*	6.948	21.67	23.09
Grooming, duration	29.167	22.75	10.62*	13.23	17.33	14.08

Note: \* —  $p < 0.05$  (comparison of mean values in relation to the control group).

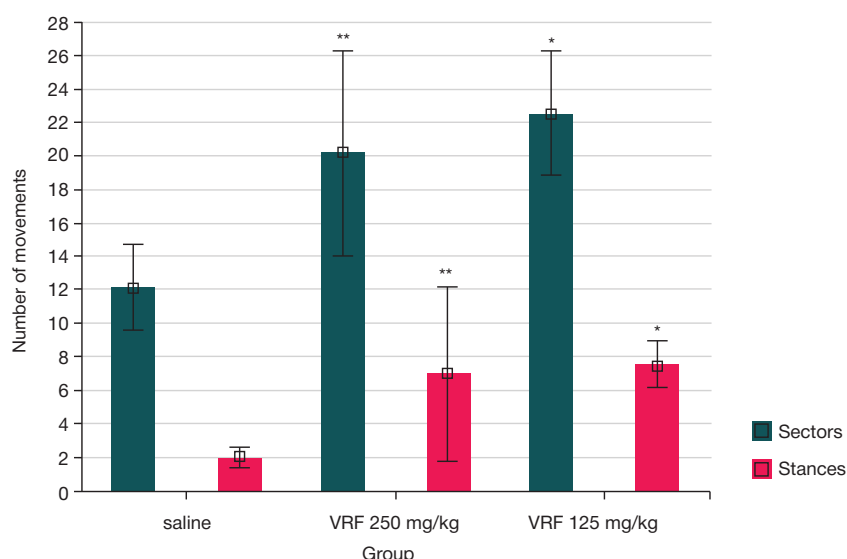


**Fig. 2.** \* —  $p < 0.05$  (comparison of mean values in relation to the control group); \*\* —  $p < 0.07$  (there is a tendency to significant differences when comparing average values in relation to the control group). Animal behavior during the hole board test on the 10<sup>th</sup> day after ischemia modeling

taking into account the molecular weight, the dose of the studied substance was 125 mg/kg. In order to reveal the possible dose dependent effects, a dose 2 times higher than the calculated was used in the study (250 mg/kg).

The dose of 125 mg/kg was more effective for correction of ischemic lesion than the dose of 250 mg/kg, as evidenced by a greater neurological deficit decrease, as well as the explorative behavior increase during the hole board test and the open field test. According to literary sources, the effect of piracetam, on the contrary, is achieved only at high concentrations [21]. Our observations suggest the feasibility of studying a larger range of doses, since different doses of the drug can not only affect its effectiveness, but also lead to opposite pharmacological effects [20].

According to MRI scanning results, VRF\_11 does not affect the volume of the lesion focus, but significantly reduces neurological symptoms in rats. This observation limits the assessment of the test compound as a neuroprotector, but

refers to the possibility of its use among other rehabilitation drugs. The observation is interesting in terms of studying the possible mechanisms of VRF\_11 effect. Certainly, it will be the base of our future studies aimed to find a specific target for the drug.

## CONCLUSIONS

Calculation of the new 4-phenylpyrrolidone-2 derivative (laboratory number VRF\_11) main pharmacokinetic parameters allowed us to come to the following conclusions: 1. VRF\_11 passes through the blood-brain barrier (BBB) and accumulates in the brain tissue. 2. Maximum concentration of VRF\_11 in the studied time range is achieved 0.5 h after the substance administration. 3. After 24 hours, VRF\_11 in the cerebral cortex is on the verge of detection. 4. VRF\_11 at a dose of 125 mg/kg significantly corrects the neurological functions impairment resulting from modeling of focal ischemia in rats.

## References

- Samorodskaja IV, Zajratjan OV, Perhov VI, Andreev EM, Vajsman DSh. Dinamika pokazatelej smertnosti naselenija ot ostrogo narushenija mozgovogo krovoobrashhenija v Rossii i SShA za 15-letnij period. *Arhiv patologii*. 2018; 80 (2): 30–7. <https://doi.org/10.17116/patol201880230-37>
- The top 10 causes of death. World Health Organization 2018. Available at: <https://www.who.int/news-room/fact-sheets/detail/the-top-10-causes-of-death>
- Gupta S, Sharma U, Jagannathan NR, Gupta YK. Neuroprotective effect of lercanidipine in middle cerebral artery occlusion model of stroke in rats. *Exp Neurol*. 2017; (1): 25–37. DOI:10.1016/j.expneurol.2016.10.014.
- Cramer SC. Drugs to enhance motor recovery after stroke. *Stroke*. 2015; 46(10): 2998–3005 DOI:10.1161/STROKEAHA.115.007433.
- Shakova FM, Kalinina TI, Gulyaev MV, Romanova GA. Neyroprotektivnyy i antiamnesticheskiy efekty kombinirovannoy terapii pri ishemicheskom povrezhdenii prefrontal'noy kory v eksperimente. *Patologicheskaya fiziologiya i eksperimental'naya terapiya*. 2018; 62 (2): 39–45. DOI:10.25557/0031-2991.2018.02.39-45.
- Negrebeckiy VV, Kramarova EP, Shipov AG, Baukov Jul, Shmigol TA, Kiseleva NM. Proizvodnoe 4-fenilpirrolidinona-2, sodержashhaya ego kompozitsiya s nootropnoj aktivnost'ju, sposob ih polucheniya i sposob lecheniya ili profilaktiki narushenij nervnoj sistemy. *Patentobladatel': GBOU VPO RNIMU im. N.I. Pirogova Minzdrava Rossii*. Patent RF № 2611623. 28.02.2017.
- Filimonov DA, Druzhilovskiy DS, Lagunin AA, Glorizova TA, Rudik AV, Dmitriev AV, et al. Computer-aided prediction of biological activity spectra for chemical compounds: opportunities and limitation. *Biomed Chem Res Methods*. 2018; 1 (1): 4–8. DOI:10.18097/BMCRM00004.
- Rukovodstvo po provedeniju doklinicheskikh issledovanij lekarstvennykh sredstv. Chast'1. M.: Grif i K, 2012; 944 p.
- Koizumi J. Experimental studies of ischemic brain edema. 1. A new experimental model of cerebral embolism in rats in which recirculation can be introduced in the ischemic area. *Jpn J Stroke*. 1986; (8): 1–8.
- Veinberg G, Vorona M, Zvejniece L, Viskersts R, Vavers E, Liepinsh E, et al. Synthesis and biological evaluation of 2-(5-methyl-4-phenyl-2-oxopyrrolidin-1-yl)-acetamide stereoisomers as novel positive allosteric modulators of sigma-1 receptor. *Bioorganic Med Chem*. 2013; 21 (10):2764–71. DOI:10.1016/j.bmc.2013.03.016.
- Gubskiy IL, Namestnikova DD, Cherkashova EA, Chekhonin VP, Baklaushev VP, Gubsky LV, et al. MRI Guiding of the middle cerebral artery occlusion in rats aimed to improve stroke modeling. *Transl Stroke Res*. 2018; 9 (4): 417–25.
- Lu M, Chen J, Lu D, Yi L, Mahmood A, Chopp M. Global test statistics for treatment effect of stroke and traumatic brain injury in rats with administration of bone marrow stromal cells. *J Neurosci Methods* [Internet]. 2003; 128 (1–2): 183–90.
- Buresh Ya, Bureshova O, Khyuston D P. Metodiki i osnovnye eksperimenty po izucheniyu mozga i povedeniya. *Vysshaya shkola*. 1991; 32 (1):119–22.
- Sestakova N, Puzserova A, Kluknavsky M, Bernatova I. Determination of motor activity and anxiety-related behaviour in rodents: Methodological aspects and role of nitric oxide. *Interdisciplinary Toxicology*. 2013; 6 (3):126–35. DOI:10.2478/intox-2013-0020.
- Goyal M, Menon BK, Van Zwam WH, Dippel DWJ, Mitchell PJ, Demchuk AM, et al. Endovascular thrombectomy after large-vessel ischaemic stroke: A meta-analysis of individual patient data from five randomised trials. *Lancet*. 2016; 387 (10029): 1723–31. DOI:10.1016/S0140-6736(16)00163-X.
- Szelenberger R, Kostka J, Saluk-Bijak J, Miller E. Pharmacological interventions and rehabilitation approach for enhancing brain self-repair and stroke recovery. *Curr Neuropharmacol* [Internet]. 2020; 18(1): 51–64. DOI:10.2174/1570159X17666190726104139.
- Shipov AG, Kramarova EP, Negrebitskiy VV, Pogozhikh SA, Akhapkina VI, Baukov Yul. Metody sinteza, molekulyarnaya i kristallicheskaya struktura fenotropila. *Vestnik RGMU*. 2006; (1): 56–61.
- Golubitskiy GV, Ivanov VM. Analiz siropa Nootsetam metodom gradientnoy vysokoeffektivnoy zhidkostnoy khromatografii. *Vestnik Moskovskogo universiteta. Khimiya*. 2009; 50 (3): 180–4.
- Instrukcija po primeneniju lekarstvennogo preparata dl medicinskogo primeneniya Piracetam. Ministerstvo zdravoohraneniya RF. Available at: [https://backgrls.pharmportal.ru/storage/instructions/%D0%A0\\_N000577\\_01/Instrimg\\_0000061664/%D0%A0\\_N000577\\_01\[2014\]\\_0.pdf](https://backgrls.pharmportal.ru/storage/instructions/%D0%A0_N000577_01/Instrimg_0000061664/%D0%A0_N000577_01[2014]_0.pdf)
- Antonova MI, Prokopov AA, Akhapkina VI, Berlyand AS. Eksperimental'naya farmakokinetika fenotropila u kryss. *Khimiko-farmatsevticheskiy zhurnal*. 2003; 37 (11): 6–8.
- Vostrikov VV. Place of piracetam in the modern practice of medicine. *Rev Clin Pharmacol Drug Ther*. 2017; 15 (1):14–25. DOI:10.17816/rcf15114-25.

## Литература

- Самородская И. В., Зайратьянц О. В., Перхов В. И., Андреев Е. М., Вайсман Д. Ш. Динамика показателей смертности населения от острого нарушения мозгового кровообращения в России и США за 15-летний период. *Архив патологии*. 2018; (2): 30–7.
- The top 10 causes of death. World Health Organization 2018. Available at: <https://www.who.int/news-room/fact-sheets/detail/the-top-10-causes-of-death>
- Gupta S, Sharma U, Jagannathan NR, Gupta YK. Neuroprotective effect of lercanidipine in middle cerebral artery occlusion model of stroke in rats. *Exp Neurol*. 2017; (1): 25–37. DOI:10.1016/j.expneurol.2016.10.014.
- Cramer SC. Drugs to enhance motor recovery after stroke. *Stroke*. 2015; 46(10): 2998–3005 DOI:10.1161/STROKEAHA.115.007433.
- Шакова Ф. М., Калинина Т. И., Гуляев М. В., Романова Г. А. Нейропротективный и антиамнестический эффекты комбинированной терапии при ишемическом повреждении префронтальной коры в эксперименте. *Патологическая физиология и экспериментальная терапия*. 2018; 62 (2): 39–45. DOI:10.25557/0031-2991.2018.02.39-45.
- Негребецкий В. В., Крамарова Е. П., Шипов А. Г., Бауков Ю. И., Шмиголь Т. А., Киселева Н. М. Производное 4-фенилпириролидинона-2, содержащая его композиция с ноотропной активностью, способ их получения и способ лечения или профилактики нарушений нервной системы. Патентообладатель: ГБОУ ВПО РНИМУ им. Н. И. Пирогова Минздрава России. Патент РФ № 2611623. 28.02.2017.
- Filimonov DA, Druzhilovskiy DS, Lagunin AA, Glorizova TA, Rudik AV, Dmitriev AV, et al. Computer-aided prediction of biological activity spectra for chemical compounds: opportunities and limitation. *Biomed Chem Res Methods*. 2018; 1 (1): 4–8. DOI:10.18097/BMCRM00004.
- Руководство по проведению доклинических исследований лекарственных средств. Часть 1. М.: Гриф и К, 2012; 944 с.
- Koizumi J. Experimental studies of ischemic brain edema. 1. A new experimental model of cerebral embolism in rats in which recirculation can be introduced in the ischemic area. *Jpn J Stroke*. 1986; (8): 1–8.
- Veinberg G, Vorona M, Zvejniece L, Viskersts R, Vavers E, Liepinsh E, et al. Synthesis and biological evaluation of 2-(5-methyl-4-phenyl-2-oxopyrrolidin-1-yl)-acetamide stereoisomers as novel positive allosteric modulators of sigma-1 receptor. *Bioorganic Med Chem*. 2013; 21 (10): 2764–71. DOI:10.1016/j.bmc.2013.03.016.
- Gubskiy IL, Namestnikova DD, Cherkashova EA, Chekhonin VP, Baklaushev VP, Gubsky LV, et al. MRI Guiding of the Middle Cerebral Artery Occlusion in Rats Aimed to Improve Stroke Modeling. *Transl Stroke Res*. 2018; 9 (4): 417–25.
- Lu M, Chen J, Lu D, Yi L, Mahmood A, Chopp M. Global test statistics for treatment effect of stroke and traumatic brain injury in

- rats with administration of bone marrow stromal cells. *J Neurosci Methods* [Internet]. 2003; 128 (1–2):183–90.
13. Буреш Я., Бурешова О., Хьюстон Д. П. Методики и основные эксперименты по изучению мозга и поведения. Высшая школа. 1991. 32 (1):119–22.
  14. Sestakova N, Puzserova A, Kluknavsky M, Bernatova I. Determination of motor activity and anxiety-related behaviour in rodents: Methodological aspects and role of nitric oxide. *Interdisciplinary Toxicology*. 2013; 6 (3): 126–35. DOI:10.2478/intox-2013-0020.
  15. Goyal M, Menon BK, Van Zwam WH, Dippel DWJ, Mitchell PJ, Demchuk AM, et al. Endovascular thrombectomy after large-vessel ischaemic stroke: A meta-analysis of individual patient data from five randomised trials. *Lancet*. 2016; 387 (10029): 1723–31. DOI:10.1016/S0140-6736(16)00163-X.
  16. Szelenberger R, Kostka J, Saluk-Bijak J, Miller E. Pharmacological Interventions and Rehabilitation Approach for Enhancing Brain Self-repair and Stroke Recovery. *Curr Neuropharmacol* [Internet]. 2020; 18 (1): 51–64. DOI:10.2174/1570159X17666190726104139.
  17. Шипов А. Г., Крамарова Е. П., Негребцкий В. В., Положих С. А., Ахалкина В. И., Бауков Ю. И. Методы синтеза, молекулярная и кристаллическая структура фенотропила. *Вестник РГМУ*. 2006; (1): 56–61.
  18. Голубицкий Г. В., Иванов В. М. Анализ сиропа Нооцетам методом градиентной высокоэффективной жидкостной хроматографии. *Вестник Московского университета. Химия*. 2009; 50 (3): 180–84.
  19. Инструкция по применению лекарственного препарата для медицинского применения Пирацетам. Министерство здравоохранения РФ. Доступно по ссылке: [https://backgrls.pharmportal.ru/storage/instructions/%D0%A0\\_N000577\\_01/Instrlmg\\_0000061664/%D0%A0\\_N000577\\_01\[2014\]\\_0.pdf](https://backgrls.pharmportal.ru/storage/instructions/%D0%A0_N000577_01/Instrlmg_0000061664/%D0%A0_N000577_01[2014]_0.pdf)
  20. Антонова М. И., Прокопов А. А., Ахалкина В. И, Берлянд А. С. Экспериментальная фармакокинетика фенотропила у крыс. *Химико-фармацевтический журнал*. 2003; 37 (11): 6–8.
  21. Vostrikov VV. Place of piracetam in the modern practice of medicine. *Rev Clin Pharmacol Drug Ther*. 2017;15 (1): 14–25. DOI:10.17816/rcf15114-25.

## CASE REPORT: MORPHOLOGICAL ASPECTS OF BUERGER'S DISEASE

Tsimbalist NS<sup>1</sup>✉, Suftin BA<sup>2</sup>, Kriuchkova AV<sup>1</sup>, Chupyatova EA<sup>1</sup>, Babichenko II<sup>1</sup><sup>1</sup> Peoples' Friendship University of Russia, Moscow, Russia<sup>2</sup> Central Military Clinical Hospital of the National Guard Troops of the Russian Federation, Balashikha, Russia

Buerger's disease is a rather rare pathology characterized by nonatherogenic vascular lesion associated with the inflammation in the intima of the vessel and the thrombus formation. Most often the pathological process affects small and medium caliber arteries. Vascular occlusion can lead to tissue ischemia and the trophic ulcers, and cause the extremity amputation. The disorder pathogenesis has not been fully explored. Literature data indicate that the disease development may be associated with autoimmune processes. The paper presents the results of immunohistochemical study of the material obtained after amputation of the lower extremity in a patient diagnosed with Buerger's disease. The patient had a 15-year tobacco smoking experience. In the inflammatory cell infiltrates around the affected vessels, lymphocytes with CD4, CD8 antigens and IgG immunoglobulin deposits were found, which could be considered as the evidence of the autoimmune mechanisms' involvement. Immunohistochemical reactions with markers of NK cells CD56 and the central component of the C3d complement system were negative. The results of the study suggest that the key role is played by helper and suppressor T lymphocytes, as well as by humoral antibodies of the IgG class.

**Keywords:** Buerger's disease, immunohistochemistry, CD4, CD8, IgG**Author contribution:** Babichenko II, Suftin BA — study concept and design; Suftin BA, Chupyatova EA — data acquisition and processing; Tsimbalist NS, Kriuchkova AV, Babichenko II — manuscript writing; Babichenko II — manuscript editing.**Compliance with ethical standards:** the patient signed the informed consent to the study and publishing of the results.✉ **Correspondence should be addressed:** Natalia S. Tsimbalist  
Kuskovskaya, 1–77, Moscow, 111398; n\_zimb@list.ru**Received:** 09.12.2019 **Accepted:** 15.01.2020 **Published online:** 23.01.2020**DOI:** 10.24075/brsmu.2020.004

## МОРФОЛОГИЧЕСКАЯ ХАРАКТЕРИСТИКА КЛИНИЧЕСКОГО СЛУЧАЯ БОЛЕЗНИ БЮРГЕРА

Н. С. Цимбалист<sup>1</sup>✉, Б. А. Суфтин<sup>2</sup>, А. В. Крючкова<sup>1</sup>, Е. А. Чупятова<sup>1</sup>, И. И. Бабиченко<sup>1</sup><sup>1</sup> Российский университет дружбы народов, Москва, Россия<sup>2</sup> Главный военный клинический госпиталь войск национальной гвардии Российской Федерации, Балашиха, Россия

Болезнь Бюргера — это достаточно редкая патология, для которой характерно неатерогенное поражение сосудов с формированием в интима сосуда воспалительного процесса и образованием тромба. Наиболее часто в патологический процесс вовлечены артерии мелкого и среднего калибра. Окклюзия сосудов может привести к ишемии тканей, появлению трофических язв и стать причиной ампутации конечности. На сегодняшний день патогенез заболевания остается до конца неизученным. Литературные данные указывают на то, что развитие патологии может быть связано с аутоиммунными процессами. В статье представлены результаты иммуногистохимического исследования материала, полученного после ампутации нижней конечности у пациента с клиническим диагнозом болезнь Бюргера, имевшего 15-летний стаж курения. В воспалительных клеточных инфильтратах вокруг пораженных сосудов были обнаружены лимфоциты с антигенами CD4, CD8 и депозиты иммуноглобулинов IgG, которые могли служить подтверждением участия аутоиммунных механизмов в развитии заболевания. Иммуногистохимические реакции с маркерами NK-клеток CD56 и главного компонента системы комплемента C3d оказались отрицательными. Полученные результаты позволяют предположить, что основная роль в цепи патогенеза болезни Бюргера принадлежит Т-лимфоцитам-хелперам и супрессорам, а также гуморальным антителам класса IgG.

**Ключевые слова:** болезнь Бюргера, иммуногистохимия, CD4, CD8, IgG**Вклад авторов:** И. И. Бабиченко, Б. А. Суфтин — концепция и дизайн исследования; Б. А. Суфтин, Е. А. Чупятова — сбор и обработка материала; Н. С. Цимбалист, А. В. Крючкова, И. И. Бабиченко — написание текста статьи; И. И. Бабиченко — редактирование.**Соблюдение этических стандартов:** пациент подписал добровольное информированное согласие на исследование и публикацию материала.✉ **Для корреспонденции:** Наталья Сергеевна Цимбалист  
ул. Кусковская, д. 1, кв. 77, г. Москва, 111398; n\_zimb@list.ru**Статья получена:** 09.12.2019 **Статья принята к печати:** 15.01.2020 **Опубликована онлайн:** 23.01.2020**DOI:** 10.24075/vrgmu.2020.004

Buerger's disease is a rare pathology that is most common in Eastern Europe and Asia. [1]. Thromboangiitis obliterans (TAO) was initially described by Felix von Winiwarter in 1879, a more detailed description of the disorder was presented in 1908 by Leo Buerger [2–5]. Thromboangiitis obliterans (Buerger's disease) is a progressive, nonatherosclerotic disease that most often affects small and medium arteries [2]. Blood vessels of various localization may be involved, most often the disease affects the arteries of the limbs, usually the femoral and radial arteries. In rare cases, the coronary, carotid and visceral arteries are affected [6].

According to literary sources, the incidence of the disease in patients with circulatory disorders ranges from 0.5–5% in

Europe, and in Japan this indicator can reach 16% [6]. The disorder is more frequently found in male smokers [2, 3, 7]. The typical age of onset is 40–45 [4, 8]. The disease pathogenesis may be associated with endothelial dysfunction [9]. Due to the damaging agents' impact, vascular permeability is impaired, inflammation and thrombosis occur [10]. According to a number of authors, the immune homeostasis failure can lead to the development of the disease.

In patients with Buerger's disease, the released by immune cells inflammatory cytokines level is increased, and the inflammatory reaction exacerbates the severity of the disease [9, 10]. In TAO patients, the HLA, A28, Ax, B53 and Bx antigens were detected [11]. The TNF $\alpha$ , IL1 $\beta$ , IL4, IL17 and IL23



blood plasma level increase was also noted. Elevated levels of IL17 and IL23 indicate the autoimmune processes' development caused by an unknown antigen (possibly a nicotine component) [10].

The clinical manifestations of Buerger's disease include claudication, ulcerations on the toes and ischemic rest pain appear over time [2, 4, 6]. A sensation of coldness and a reduced touch sensitivity of the skin of the feet are noted in the affected extremities [5, 12]. For the diagnosis confirmation, it is necessary to eliminate such conditions as thrombophilia, diabetes, embolism and autoimmune disorders [2, 4].

The cornerstone of the TAO treatment is absolute smoking avoidance [2, 4, 13]. In patients who stop smoking the remission occurs, which reduces the risk of amputation [2]. The patients are also treated with adjuvant medications, such as iloprost, vasodilators including the prostaglandin analogues, calcium channel antagonists, anticoagulants and antiplatelet drugs including Aspirin [5, 10, 13]. If the patient does not stop smoking tobacco, the disease would progress, which leads to the extremities' amputation [14].

The paper presents the case of an immunohistochemical study of the affected vessels in patient with Buerger's disease (thromboangiitis obliterans) aimed to clarify the inflammatory infiltrate cellular composition and to identify the IgG deposits.

### Clinical case report

Buerger's disease was diagnosed in 36-year old male with 15-year tobacco smoking experience. The observation period was 6 months. In May 2017, the patient suddenly felt pain in his left foot. He received symptomatic treatment that had no effect. In early June 2017, intensification of pain in the left foot, cold feet, as well as darkening of the toes were noted. The patient was hospitalized, he underwent the left foot Lisfranc amputation because of the left lower leg subacute thrombosis and acute III-degree ischemia. The residual limb (stump) wound did not heal, there were pains in the left foot and lower leg. Swelling of both legs was noted, and flexion contracture of the left knee joint developed. The patient slept in his sitting position. Doppler ultrasonography of the lower extremities' arteries revealed the occlusion of the left anterior tibial artery. Stenosis of the left superficial femoral artery was more than 60%. The dry gangrene of the left lower extremity developed, which led to the amputation at the hip level in August 2017. The clinical diagnosis was TAO with the left anterior tibial artery occlusion, stage IV chronic arterial insufficiency, dry necrosis of the residual limb of the end surface of the left foot soft tissues.

The material was taken from the Central Military Clinical Hospital of the National Guard Troops of the Russian Federation archive. Tissue blocks with tissue fragments taken from the foot and the lower leg were selected for investigation. The sample were subjected to standard processing (tissue sectioning, paraffin blocks preparation, slices' preparation, haematoxylin and eosin staining). The slices were examined using the AxioPlan 2 Imaging microscope (Karl Zeiss; Germany), the pictures were taken using the AxioCam ERc5s camera (Karl Zeiss; Germany).

To study the inflammatory infiltrate cellular composition and detect IgG deposits, an immunohistochemical study was performed using the Quanto protocol. The UltraVision Quanto system (Thermo Fisher Scientific; USA) reagents were used including the horseradish peroxidase (HRP) polymer conjugate. The study was carried out using the Autostainer 360 unit (Thermo Fisher Scientific; UK). The following sera were used

as antibodies: mouse monoclonal antibody against CD8 (Cell Marque; USA), rabbit monoclonal antibody against CD4 (Cell Marque; USA), rabbit polyclonal antibody against IgG (Cell Marque; USA), rabbit monoclonal antibody against CD56 (Epitomics; USA), rabbit monoclonal antibody against C3d (Clone SP7, Thermo Fisher Scientific; UK). The exposure time of antibody on each slice was 20 minutes.

A macroscopic examination of the left lower extremity resected at the level of the middle and lower third of the thigh revealed the foot absence along the metatarsal-tarsal joints (after the Lisfranc amputation) with the unhealed wound and the blue-gray surrounding tissues. The obstructing thrombi of arteries and veins at the level of the popliteal artery were also found. The lower leg muscles were red-yellow and pale. The muscles at the resection level were reddish.

The tissue samples contained the vessels from the left hip, lower leg and foot. Samples were taken in the immediate vicinity of the lesions of gangrene. During a histological examination, necrosis was detected in the foot and lower leg. Mixed thrombi of arteries and veins of the foot and lower leg were revealed, sometimes with recanalization and organization, partial obliteration of the lumen was also noted. Fig. 1 shows a cross section of the foot artery, there are intra-parietal and perivascular fibrosis, necrosis of the vessel wall. Microphotography (Fig. 2) demonstrates the cross section of the lower leg artery with the organized thrombus and recanalization. No thrombotic masses were found in the femoral vessels, however, a partial obliteration of their lumen was noted. There were no atherosclerotic plaques. Mixed thrombi, necrosis of the vessel wall and partial obliteration of the lumen were revealed in the different caliber vessels. In the large vessels, a considerable amount of vasa vasorum was detected, as well as lymphocytes in the wall, due to which the patient was diagnosed with TAO.

The material was subjected to immunohistochemical study. Further microscopy showed that in the vessels of small and medium caliber, mainly in arterioles, positive cytoplasmic reactions took place when using the antibody against the receptor of the T-lymphocytes CD4 subpopulations' marker (mainly in the wall of the lower leg artery (Fig. 3)) and the T-lymphocytes CD8 subpopulations' marker (in the wall of the vessel (arteriole) of the foot (Fig. 4)). IgG deposits were observed on the surface of vascular endothelium and in the vessel walls (Fig. 5). A negative reaction was detected for the antibodies against the CD56 receptor, NK cells markers, as well as against the central component of the C3d complement system.

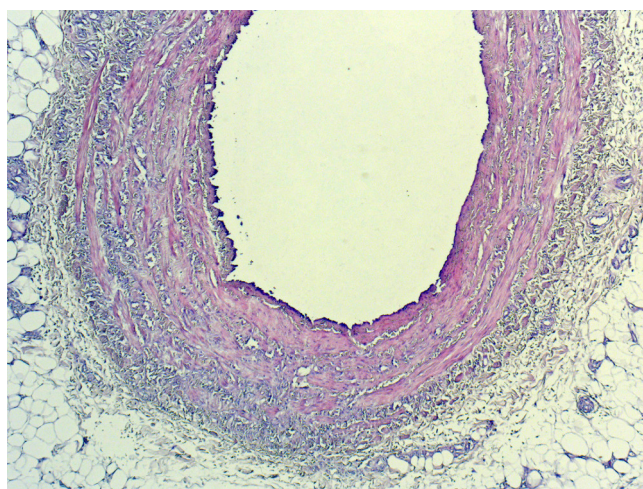


**Fig. 1.** Foot artery cross section. Intra-parietal and perivascular fibrosis. Microphotograph. Hematoxylin and eosin stain (x50)



### Clinical case discussion

In patients with Buerger's disease, the pathological process begins in distally located vessels, progressing to proximally located vessels [2]. The main pathological changes are the formation of thrombi, intra-parietal and perivascular fibrosis of blood vessels [5]. Three phases of the disease are distinguished: acute, subacute and chronic [2, 3]. In the acute phase, the onset of inflammation is noted, associated with neutrophil infiltration and thrombotic vascular occlusion. The vessel walls are relatively intact. In the subacute phase, a thrombus organization occurs with continuing platelet adherence. In the chronic phase, in the absence of inflammatory mediators, blood vessel fibrosis is observed with its blockage by an organized thrombus. Later recanalization may occur [2]. In case of severe pathological changes and ulcers, amputation of the extremity is performed [5, 10]. For treatment the endovascular intervention is used, operations are performed that involve shunting, resection of the posterior tibial veins [13].

In the studied clinical case, the patient's extremity was amputated because of the left leg gangrene. A histological examination of the vessels revealed mixed thrombi, organization phenomena and partial obliteration of the lumen.

When diagnosed, Buerger's disease must be distinguished from other diseases associated with vascular lesion. Thus, in patients with TAO, the vascular lesion is characterized by inflammatory cell infiltration of all three layers of the artery wall. In patients with atherosclerosis, only intima is involved in the pathological process [2]. Migratory thrombophlebitis allows to distinguish Buerger's disease from other types of angiitis. The main histological signs of the disease are the intimal hyperplasia such as capillary angiomatosis, vessels clogged with thrombotic masses, lack of calcification of the vessel middle coat and panflebitis of the veins [13].

The results of our study confirm that the main pathological changes in patients with Buerger's disease are arterial thrombosis with inflammatory infiltration in all three layers of the wall with intimal hyperplasia in the absence of atherosclerosis signs. According to a number of authors [3], the onset and maintenance of the inflammatory response depends on the endothelium integrity. Endothelial dysfunction leads to the endothelium-dependent vasorelaxation impairment. In our study, IgG deposits were found on the surface of the endothelium and in the vessel wall.

An increase in the level of proinflammatory cytokines IL1 $\beta$ , TNF $\alpha$  and IL6 in the Buerger's disease patients' plasma was demonstrated by [10], as well as the increase of the level of Th1 cytokines (IFN $\gamma$  and IL12). For Th2 cytokines, the increase in IL4, IL5 and IL13, together with the decrease in IL10 was noted, as well as an increase in cytokine profiles Th17 (IL17 and IL23), indicating the involvement of autoimmune mechanisms. Some authors [2] suggested that patients Buerger's disease could have specific cellular immunity against arterial antigens, specific humoral anti-arterial antibodies, immune complexes.

The paper [15] demonstrates the results of tissue samples obtained from the artery dorsalis pedis immunohistochemical study aimed to detect the new antigens which could be responsible for local inflammatory reactions and structural changes in patients with TAO. Antigens such as CD34, CD44 and CD90 have been identified. Researchers suggest that the receptor/ligand pair CD90/CD11c plays an important role in attracting mononuclear cells to the site of damage.

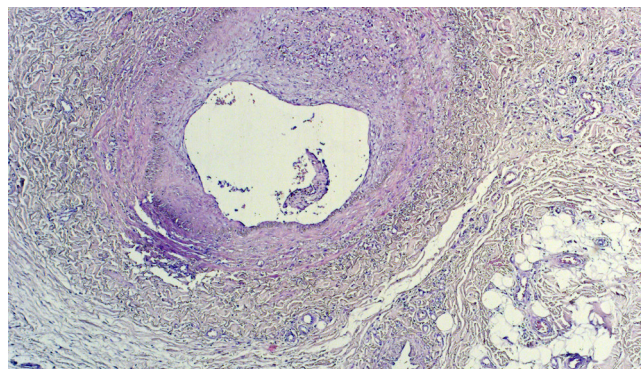


**Fig. 2.** Lower leg artery cross section. Organized thrombus with recanalization. Microphotograph. Hematoxylin and eosin stain (x50)

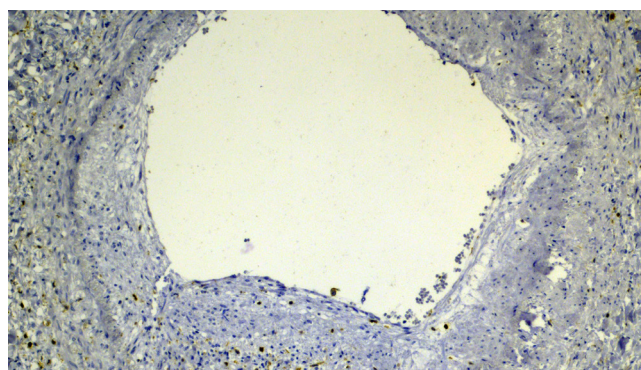


**Fig. 3.** Lower leg artery. Immunohistochemical reaction with antibodies against CD4 protein: cytoplasmic marker localization. Microphotograph. DAB and hematoxylin stain (x100)

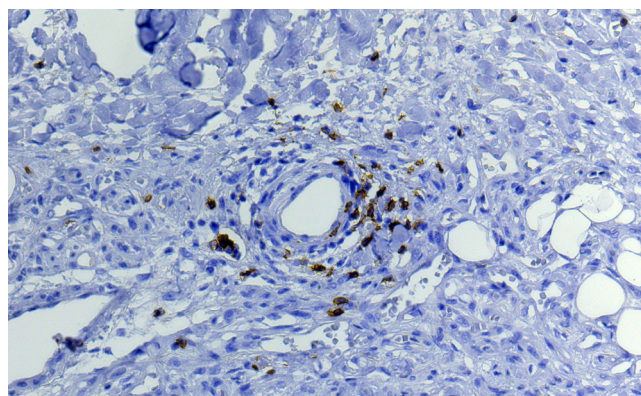


**Fig. 4.** Foot arteriole. Immunohistochemical reaction with antibodies against CD8 protein: cytoplasmic marker localization. Microphotograph. DAB and hematoxylin stain (x200)

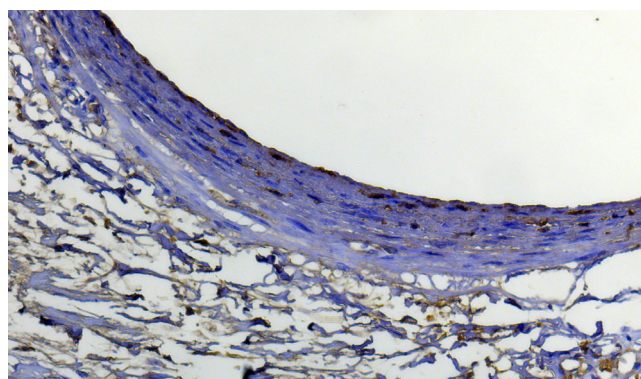


**Fig. 5.** Foot artery. Immunohistochemical reaction with antibodies against IgG protein: endothelial marker localization. Microphotograph. DAB and hematoxylin stain (x200)

In our study the tissue samples were taken from the amputated extremity (foot, leg and hip) of the patient with diagnosed Buerger's disease, having a 15-year tobacco smoking experience. The cells were identified containing markers which could indicate the involvement of the immunity in the pathogenesis of the disease (CD4, CD8, IgG deposits).

## References

- Shionoya S, Leu HJ, Lie JT. Buerger's disease (thromboangiitis obliterans). In: Stehbens WE, Lie JT, eds. Vascular pathology. London: Chapman & Hall Medical, 1995; p. 657–78.
- Qaja E, Fortune MA. Buerger Disease (Thromboangiitis Obliterans). StatPearls [Internet]. 2019 Nov [cited 2019 Nov 11]; [about 3 p.]. Available from: <https://www.statpearls.com/sp/rn/18685/>.
- Rivera-Chavarría IJ, Brenes-Gutiérrez JD. Thromboangiitis obliterans (Buerger's disease). Ann Med Surg (Lond). 2016; (7): 79–82. PubMed PMID: 27144003.
- Seebald J, Gritters L. Thromboangiitis obliterans (Buerger disease). Radiol Case Rep. 2015; 10 (3): 9–11. PubMed PMID: 26649109.
- Li Q-L, He D-H, Huang Y-H, Niu M. Thromboangiitis obliterans in two brothers. Experimental and Therapeutic Medicine. 2013; 6 (2): 317–20. PubMed PMID: 24137181.
- Nobre CA, Vieira WP, da Rocha FE, de Carvalho JF, Rodrigues CE. Clinical, arteriographic and histopathologic analysis of 13 patients with thromboangiitis obliterans and coronary involvement. Isr Med Assoc J. 2014; 16 (7): 449–53. PubMed PMID: 25167694.
- Shilkina NP, Lileeva MA, Drjazhenkova IV, Kaufman EV, Prokopenko AV. Obliterirujushij trombangiit i ateroskleroz sosudov nizhnih konechnostej: kliniko-morfologicheskaja harakteristika. Klinicheskaja gerontologija. 2006; 12 (2): 15–18.
- Elfarra M, Rădulescu D, Peride I, Niculae A, Ciocâlteu A, Checheriță IA, et al. Thromboangiitis obliterans — case report. Chirurgia (Bucur). 2015; 110 (2): 183–7. PubMed PMID: 26011844.
- Igari K, Kudo T, Toyofuku T, Inoue Y. Endothelial dysfunction in

## CONCLUSION

The results of the study suggest that autoimmune mechanisms are involved in the development of the disease, with the key role played by helper and suppressor T lymphocytes, as well as humoral immunity due to IgG.

- patients with Buerger disease. Vasc Health Risk Manag. 2017; (13): 317–23. PubMed PMID: 28860792.
- Dellalibera-Joviliano R, Joviliano EE, Silva JS, Evora PR. Activation of cytokines corroborate with development of inflammation and autoimmunity in thromboangiitis obliterans patients. Clin Exp Immunol. 2012; 170 (1): 28–35. PubMed PMID: 22943198.
- Schmitt J, Schmidt C, Alan C, Haller C, Perrier P. Population genetics, immunologic evaluation and Buerger's disease. Projection through a personal study comprising 127 cases of juvenile arteriopathy. Bull Acad Natl Med. 1993; 177 (7): 1153–64. PubMed PMID: 8149255.
- Wan J, Yang Y, Ma ZH, Sun Y, Liu YQ, Li GJ, et al. Autologous peripheral blood stem cell transplantation to treat thromboangiitis obliterans: preliminary results. Eur Rev Med Pharmacol Sci. 2016; 20 (3): 509–13. PubMed PMID: 26914127.
- Zerbino DD, Zimba EA, Bagrij NN. Obliterirujushij trombangiit (bolezni' Bjurgera): sovremennoe sostojanie problemy. Angiologija i sosudistaja hirurgija. 2016; 22 (4): 185–92.
- Sinclair NR, Laub DR. Thromboangiitis Obliterans (Buerger's Disease). Eplasty [Internet]. 2015 [cited 2015 Apr 10]; [about 6 p.]. Available from: [http://www.eplasty.com/interesting-cases/3591-thromboangiitis-obliterans-\(buerger's-disease\)](http://www.eplasty.com/interesting-cases/3591-thromboangiitis-obliterans-(buerger's-disease))
- Guzel E, Topal E, Yildirim A, Atilla P, Akkus M, Dagdeviren A. Targeting novel antigens in the arterial wall in thromboangiitis obliterans. Folia Histochem Cytobiol. 2010; 48 (1): 134–41. PubMed PMID: 20529829.

## Литература

- Shionoya S, Leu HJ, Lie JT. Buerger's disease (thromboangiitis obliterans). In: Stehbens WE, Lie JT, eds. Vascular pathology. London: Chapman & Hall Medical, 1995; p. 657–78.
- Qaja E, Fortune MA. Buerger Disease (Thromboangiitis Obliterans). StatPearls [Internet]. 2019 Nov [cited 2019 Nov 11]; [about 3 p.]. Available from: <https://www.statpearls.com/sp/rn/18685/>.
- Rivera-Chavarría IJ, Brenes-Gutiérrez JD. Thromboangiitis obliterans (Buerger's disease). Ann Med Surg (Lond). 2016; (7): 79–82. PubMed PMID: 27144003.
- Seebald J, Gritters L. Thromboangiitis obliterans (Buerger disease). Radiol Case Rep. 2015; 10 (3): 9–11. PubMed PMID: 26649109.
- Li Q-L, He D-H, Huang Y-H, Niu M. Thromboangiitis obliterans in two brothers. Experimental and Therapeutic Medicine. 2013; 6 (2): 317–20. PubMed PMID: 24137181.
- Nobre CA, Vieira WP, da Rocha FE, de Carvalho JF, Rodrigues CE. Clinical, arteriographic and histopathologic analysis of 13 patients with thromboangiitis obliterans and coronary involvement. Isr Med Assoc J. 2014; 16 (7): 449–53. PubMed PMID: 25167694.
- Шилкина Н. П., Лилеева М. А., Дряженкова И. В., Кауфман Е. В., Прокопенко А. В. Облитерирующий тромбангиит и атеросклероз сосудов нижних конечностей: клинико-морфологическая характеристика. Клиническая геронтология. 2006; 12 (2): 15–18.
- Elfarra M, Rădulescu D, Peride I, Niculae A, Ciocâlteu A, Checheriță IA, et al. Thromboangiitis obliterans — case report. Chirurgia (Bucur). 2015; 110 (2): 183–7. PubMed PMID: 26011844.
- Igari K, Kudo T, Toyofuku T, Inoue Y. Endothelial dysfunction in

- patients with Buerger disease. Vasc Health Risk Manag. 2017; (13): 317–23. PubMed PMID: 28860792.
- Dellalibera-Joviliano R, Joviliano EE, Silva JS, Evora PR. Activation of cytokines corroborate with development of inflammation and autoimmunity in thromboangiitis obliterans patients. Clin Exp Immunol. 2012; 170 (1): 28–35. PubMed PMID: 22943198.
- Schmitt J, Schmidt C, Alan C, Haller C, Perrier P. Population genetics, immunologic evaluation and Buerger's disease. Projection through a personal study comprising 127 cases of juvenile arteriopathy. Bull Acad Natl Med. 1993; 177 (7): 1153–64. PubMed PMID: 8149255.
- Wan J, Yang Y, Ma ZH, Sun Y, Liu YQ, Li GJ, et al. Autologous peripheral blood stem cell transplantation to treat thromboangiitis obliterans: preliminary results. Eur Rev Med Pharmacol Sci. 2016; 20 (3): 509–13. PubMed PMID: 26914127.
- Зербино Д. Д., Зимба Е. А., Багрич Н. Н. Облитерирующий тромбангиит (болезнь Бюргера): современное состояние проблемы. Ангиология и сосудистая хирургия. 2016; 22 (4): 185–92.
- Sinclair NR, Laub DR. Thromboangiitis Obliterans (Buerger's Disease). Eplasty [Internet]. 2015 [cited 2015 Apr 10]; [about 6 p.]. Available from: [http://www.eplasty.com/interesting-cases/3591-thromboangiitis-obliterans-\(buerger's-disease\)](http://www.eplasty.com/interesting-cases/3591-thromboangiitis-obliterans-(buerger's-disease))
- Guzel E, Topal E, Yildirim A, Atilla P, Akkus M, Dagdeviren A. Targeting novel antigens in the arterial wall in thromboangiitis obliterans. Folia Histochem Cytobiol. 2010; 48 (1): 134–41. PubMed PMID: 20529829.



## THE EFFECT OF ACUTE SOMATIC PAIN ON THE KILLING ACTIVITY OF NEUTROPHILS IN NEWBORN RATS

Alekseev VV<sup>1</sup>✉, Kade AKh<sup>2</sup>

<sup>1</sup> Rostov State Medical University, Rostov-on-Don, Russia

<sup>2</sup> Kuban State Medical University, Krasnodar, Russia

The immune system is subject to all sorts of influences. Pain is one of them, accompanying an organism's existence. It is essential to be aware of and account for age-related characteristics of the innate immunity in order to adequately assess their dynamics in ontogenesis. The literature is scarce on the changes to the killing activity of neutrophils occurring in newborns in response to acute pain. The aim of this study was to detect potential changes to the phagocytic activity of neutrophils in response to an algogenic stimulus in newborn rats. The experiments were carried out in 3-5-day-old rats. Two groups were formed: the control group and the main group, in which acute pain was modelled. Blood samples were collected 2, 30–60 and 120–180 minutes after exposure to the algogenic stimulus. The microbicidal activity of neutrophils was measured using a spectrophotometric modification of the spontaneous/stimulated nitroblue tetrazolium (NBT) reduction test. The results were compared using the Mann-Whitney U test. In the first hour following pain modeling, the stimulated NBT reduction test demonstrated an increase in the measured parameters from 71.5 to 87.4 a.u. ( $p < 0.001$ ); the spontaneous NBT reduction test showed an increase from 50.7 to 58.6 a.u. ( $p < 0.01$ ) 30 to 60 min after exposure. The most pronounced change of the microbicidal activity coefficient was observed 2 min after pain modeling, increasing from 1.40 to 1.72 a.u. ( $p < 0.001$ ). By the end of the experiment, the measured parameters approximated their initial values. During the analysis, we accounted for the fact that the neutrophil response to the algogenic stimulus was unfolding in the setting of microbial colonization occurring in newborns.

**Keywords:** pain, NBT test, newborns, neutrophils, neutrophil microbicidal activity

**Acknowledgements:** the authors thank Ovsyannikov VG, Head of the Department of Pathologic Physiology (Rostov State Medical University) and Boychenko AE, Professor at the Department of Pathologic Physiology, for their valuable advice and feedback; Aboyan IA, Chief Physician of the Clinical Diagnostic Center Health, for granting access to the laboratory equipment of the Center.

**Author contribution:** Alekseev VV conducted the experiment, analyzed and interpreted the obtained results, wrote the manuscript; Kade AKh conceived and designed the study, revised the manuscript for intellectual content and made final corrections.

**Compliance with ethical standards:** the study was approved by the Ethics Committee of Rostov State Medical University (Protocol № 20/17 dated November 23, 2017).

✉ **Correspondence should be addressed:** Vladimir V. Alekseev  
per. Nakhichevskiy, 29, Rostov-on-Don, 344022; alexeev911@gmail.com

**Received:** 17.12.2019 **Accepted:** 07.01.2020 **Published online:** 20.01.2020

**DOI:** 10.24075/brsmu.2020.002

## ВЛИЯНИЕ ОСТРОЙ СОМАТИЧЕСКОЙ БОЛИ НА КИЛЛИНГОВУЮ АКТИВНОСТЬ НЕЙТРОФИЛОВ НОВОРОЖДЕННЫХ КРЫС

В. В. Алексеев<sup>1</sup>✉, А. Х. Каде<sup>2</sup>

<sup>1</sup> Ростовский государственный медицинский университет, Ростов-на-Дону, Россия

<sup>2</sup> Кубанский государственный медицинский университет, Краснодар, Россия

Иммунная система претерпевает влияния различной природы. Один из факторов, сопровождающих жизнедеятельность организма, — боль. Знать и учитывать возрастные особенности факторов врожденного иммунитета необходимо для адекватной оценки изменения их параметров в онтогенезе. В литературных источниках недостаточно данных об особенностях изменения киллинговой активности нейтрофилов в ответ на острую боль у новорожденных. Целью работы было выявить изменения фагоцитарной активности нейтрофилов в ответ на краткосрочный аллогенный стимул у новорожденных крыс. Эксперимент проводили на 3–5-дневных крысках. Были сформированы две группы: контрольная и экспериментальная с моделированием острого аллогенного воздействия. После моделирования осуществляли забор материала через 2, 30–60, 120–180 мин. Для оценки микроbicидной активности нейтрофилов использовали спонтанный и стимулированный методы автоматизированного учета теста с нитросиним тетразолием (НСТ-теста). Сравнение данных проводили на основе *U*-критерия Манна-Уитни. Наблюдали повышение значений спонтанного НСТ-теста с 50,7 до 58,6 у. ед. через 30–60 мин ( $p < 0,01$ ), а также стимулированного НСТ-теста с 71,5 до 87,4 у. ед. ( $p < 0,001$ ) в течение первого часа эксперимента. Максимально выраженное изменение коэффициента микроbicидности наблюдали через 2 мин с 1,40 до 1,72 у. ед. ( $p < 0,001$ ). К концу эксперимента показатели приближались к исходным значениям. При анализе результатов учитывали, что новорожденные крыска испытывают влияние со стороны микробной колонизации, на фоне которой разворачивается реакция нейтрофилов на аллогенное раздражение.

**Ключевые слова:** боль, НСТ-тест, новорожденные, нейтрофилы, микроbicидность нейтрофилов

**Благодарности:** В. Г. Овсянникову, заведующему кафедрой патологической физиологии РостГМУ и А. Е. Бойченко, профессору кафедры патологической физиологии за ценные идеи и критические замечания. И. А. Абоюну, главному врачу КДЦ «Здоровье» за предоставленную возможность использовать оборудование лаборатории.

**Вклад авторов:** В. В. Алексеев — проведение экспериментальной и аналитической части исследования, анализ и интерпретация данных, написание рукописи; А. Х. Каде — разработка концепции и дизайна, проверка интеллектуального содержания, окончательное редактирование.

**Соблюдение этических стандартов:** исследование одобрено этическим комитетом РостГМУ (протокол № 20/17 от 23 ноября 2017 г.).

✉ **Для корреспонденции:** Алексеев Владимир Вячеславович  
пер. Нахичеванский, д. 29, г. Ростов-на-Дону, 344022; alexeev911@gmail.com

**Статья получена:** 17.12.2019 **Статья принята к печати:** 07.01.2020 **Опубликована онлайн:** 20.01.2020

**DOI:** 10.24075/vrgmu.2020.002



There is a large body of evidence that immune responses can be elicited by stimuli other than antigens, including stress [1, 2], infrared light [3], LED light [4], magnetic fields [5], narcotic drugs [6], overtraining [7], etc. On this list, pain should not be an exception.

Alexeeva NS has convincingly demonstrated that neutrophils are involved in the acute algogenic process in adult rats. The reaction she observed was very pronounced but short-lived, which enabled her to define a functional mobilization syndrome in neutrophils primed for effective phagocytosis in case if exposure to a pain-evoking stimulus will escalate into tissue damage, infection, etc. [8].

There are grounds to believe that exposure of newborn rats to an algogenic stimulus will induce a complex of immune reactions, including changes to the phagocytic activity of neutrophils. Among all innate immunity factors, neutrophils have been shown to be the most sensitive to changes occurring in the intrauterine environment and after birth [9].

We searched the available literature for the effects of acute pain on the killing activity of neutrophils in newborn rats but found no relevant information. So, the aim of this study was to detect possible changes in the phagocytic activity of neutrophils in newborn rats in response to an algogenic stimulus.

## METHODS

The study was carried out in newborn 3-5-day-old albino rats with an average weight of 12 to 14 g. The animals were born and housed in standard facilities under a 12:12 light:dark cycle at a comfortable temperature of about 24 °C. The sex of the animals was not factored into. The experiments were conducted in the summer.

Functional activity of neutrophils was tested in 32 experiments. The animals were divided into two unequal groups: the main group ( $n = 24$ ) and the control group ( $n = 8$ ). In the main group, acute pain was modelled by applying an electric stimulus to the skin at the tail base. The intensity of the stimulus was 3 to 4 points on the Waldman–Vasiliev scale modified by Ovsyannikov [10]. Exposure duration was 2 minutes.

After acute somatic pain modeling, the animals were decapitated. Blood samples were collected into test tubes containing 100 u/ml heparin 2, 30–60, 120–180 min after the

experiment. Blood was diluted 1:2 with Hanks' balanced salts solution (PanEco; Russia). Then, the samples were centrifuged with a Ficoll-Verographin density gradient (1.083 g/ml) for 45 min at 1,500 rpm. Microbicidal activity of neutrophils was measured using a spectrophotometric modification of the test of spontaneous/endotoxin-induced nitroblue tetrazolium (NBT) reduction [11]. The test is based on the ability of almost colorless NBT to be reduced by oxygen radicals to deep blue diformazan.

Fifty  $\mu$ l of 0.5% NBT solution were added to each microplate well containing the cell suspension. For the spontaneous reduction test, 50  $\mu$ l of PBS (pH = 7.0) were added to the even rows of the microplate. For endotoxin-stimulated reduction, 50  $\mu$ l of 0.1% latex solution with particle size of 1.5  $\mu$ m (PanEco; Russia) were added to the odd rows. Then the microplate was incubated in an incubator for 24 min at 37 °C. The microplate was read in a Multiskan Sky spectrophotometer (THERMO FISHER SCIENTIFIC; USA) at 540 nm. Mean optical density was measured in 4 wells (2 for the spontaneous reduction test and 2 for the stimulated reduction test). The results were expressed as arbitrary units (1 a.u. = 1,000 optical density units). Then, the microbicidal activity coefficient (MAC) was calculated by dividing the mean optical density in the stimulated-reduction wells by the mean optical density in the spontaneous-reduction wells.

Statistical analysis was conducted in Microsoft Office Excel 2010 Pro (Microsoft; USA), STATISTICA 10.0 (Statsoft; USA). We tested the normality of quantitative data distribution using the Lilliefors-corrected Kolmogorov–Smirnov and Shapiro–Wilk tests; calculated median values (Me), the upper and lower quantiles ( $Q_{0.25}$ ,  $Q_{0.75}$ ), the minimum (Min) to maximum (Max) value range for the data that did not fit into the normal distribution; compared the data using the Mann–Whitney U test. The critical level of significance ( $p$ ) was assumed to be 0.05. The results are presented in this work as Me [ $Q_{0.25}$ ;  $Q_{0.75}$ ] (Min–Max).

## RESULTS

The spontaneous NBT reduction test produced the following results in the control group of newborn rats: Me<sub>sp NBT</sub> = 50.7 a.u. [ $Q_{0.25}$  = 49.3 a.u.;  $Q_{0.75}$  = 52.7 a.u.], Min = 48.9 a.u. and Max =

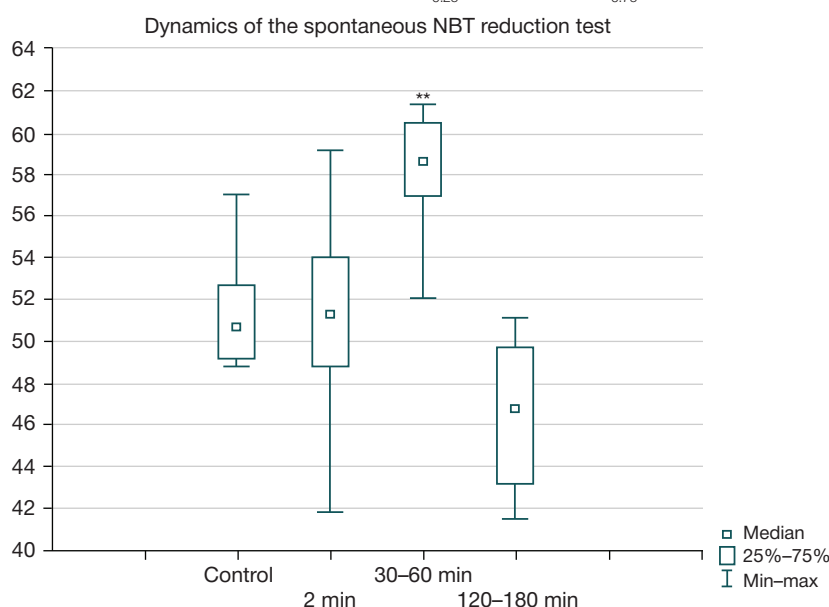


**Fig. 1.** Dynamics of the spontaneous NBT reduction test in newborn rats before and after exposure to the algogenic stimulus. \*\* — differences are significant between the main group and the control animals ( $p \leq 0.05$ )

57.1 a.u. In the main group,  $Me_{sp\ NBT}$  reached 51.4 a.u. [ $Q_{0.25} = 48.8$  a.u.;  $Q_{0.75} = 54.1$  a.u.], Min was 41.9 a.u. and Max was 59.1 a.u. 2 minutes after the algogenic stimulus was applied. In the first hour after exposure,  $Me_{sp\ NBT}$  was 58.6 a.u. [ $Q_{0.25} = 57.0$  a.u.;  $Q_{0.75} = 60.5$  a.u.], Min was 52.1 a.u. and Max was 61.3 a.u. In the third hour of observation,  $Me_{sp\ NBT}$  equaled 46.9 a.u. [ $Q_{0.25} = 43.3$  a.u.;  $Q_{0.75} = 49.8$  a.u.], Min was 41.6 a.u. and Max was 51.1 a.u.

Statistical analysis revealed that algogenic stimulation was activating spontaneous NBT reduction. The differences were significant between the control and the main group and also between the initial response to electrical stimulation and the response recorded 30–60 min after it ( $p < 0.01$ ). Median values yielded by the experiment demonstrate that distribution between the upper and lower quantiles was even; the upper quantile approximated the maximum peak value in the sample. It should be noted that the observed

reaction was short-lasting and quickly depletable. Two hours after pain modeling, the median values of the spontaneous NBT reduction test were lower than in the control group ( $p = 0.05$ ) (Fig. 1).

The stimulated NBT reduction test produced the following results in the control group:  $Me_{st\ NBT} = 71.5$  a.u. [ $Q_{0.25} = 68.0$  a.u.;  $Q_{0.75} = 73.4$  a.u.], Min = 67.2 a.u., Max = 76.5 a.u. These values were higher than in the spontaneous reduction test.

Immediately after algogenic stimulation, all parameters of the stimulated NBT reduction test started to grow, indicating that neutrophils were highly primed to ward off a potential microbial attack. Specifically,  $Me_{st\ NBT}$  was 90.4 a.u. ( $p < 0.001$ ) [ $Q_{0.25} = 87.8$  a.u.;  $Q_{0.75} = 93.0$  a.u.], Min was 84.8 a.u. and Max was 96.3 a.u. Neutrophils retained a high level of microbicidal activity for an hour following exposure to the stimulus:  $Me_{st\ NBT} = 87.4$  a.u. ( $p < 0.001$ ) [ $Q_{0.25} = 78.8$  a.u.;  $Q_{0.75} = 89.9$  a.u.], Min = 77.6 a.u. and Max = 93.0 a.u.

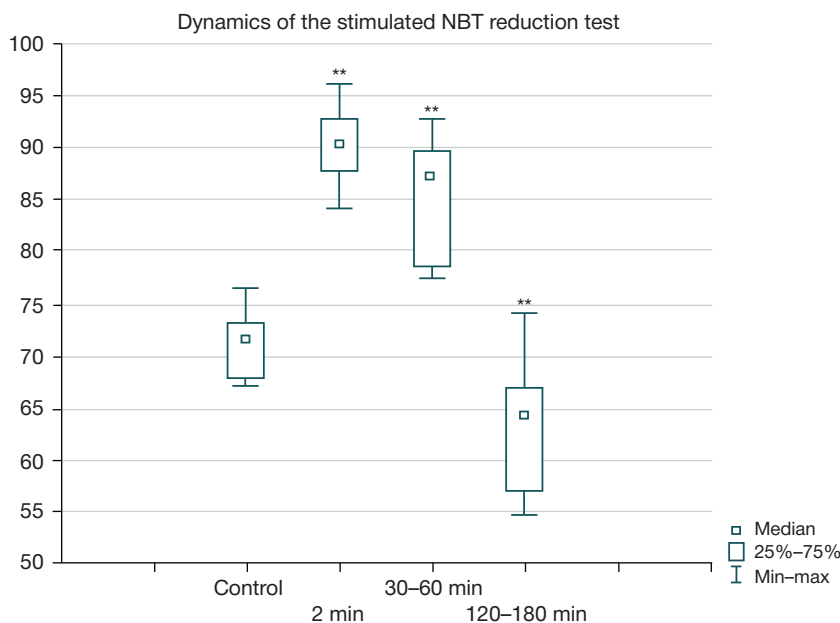


**Fig. 2.** Dynamics of the stimulated NBT reduction test in newborn rats before and after exposure to the algogenic stimulus. \*\* — differences are significant between the main group and the control animals ( $p \leq 0.05$ )

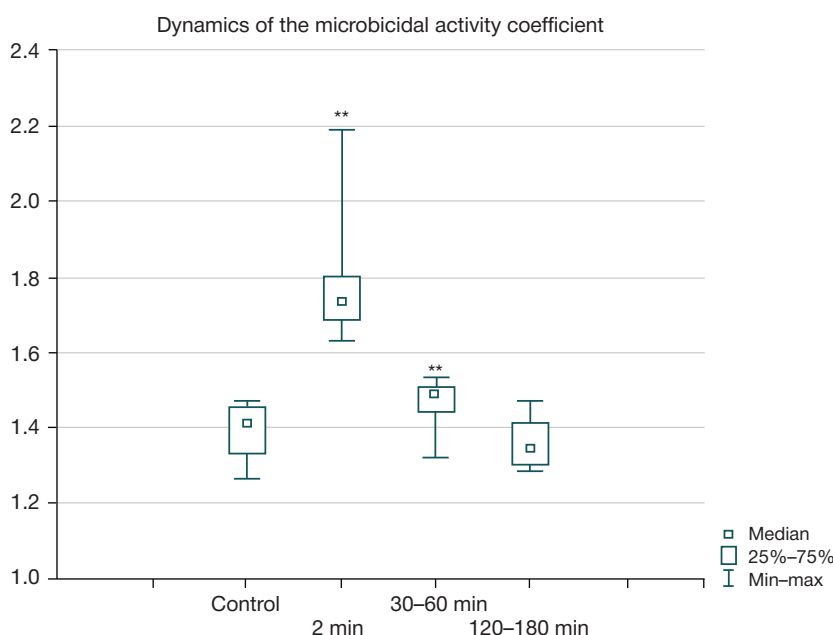


**Fig. 3.** Dynamics of the microbicidal activity coefficient in newborn rats before and after exposure to the algogenic stimulus. \*\* — differences are significant between the main group and the control animals ( $p \leq 0.05$ )

Similar to the spontaneous NBT reduction test, 2 hours after pain modeling microbicidal activity reserves were depleted.  $Me_{st\ NBT}$  declined to 64.5 a.u. ( $p < 0.05$ ) [ $Q_{0.25} = 57.2$  a.u.;  $Q_{0.75} = 66.9$  a.u.], Min decreased to 54.8 a.u. and Max was 74.1 a.u. (Fig. 2).

Knowing that the modified NBT test reflects the metabolic activity of neutrophils, specifically the oxygen-dependent mechanisms underlying their microbicidal effect, we should consider the opinion of its developers about the killing effect of neutrophils being best described by the microbial activity coefficient [12]; the coefficient is calculated by dividing the value of the stimulated NBT reduction test by the value of the spontaneous NBT reduction test.  $Me_{MACcontr} = 1.40$  a.u. [ $Q_{0.25} = 1.33$  a.u.;  $Q_{0.75} = 1.45$  a.u.], Min = 1.26 a.u., Max = 1.47 a.u.

Two minutes after algogenic stimulation, MAC was significantly increased relative to the control value:  $Me_{MAC} = 1.72$  a.u. ( $p < 0.001$ ) [ $Q_{0.25} = 1.68$  a.u.;  $Q_{0.75} = 1.80$  a.u.], Min = 1.63 a.u., Max = 2.19 a.u.

In the first hour after exposure, MAC was declining but was still above the values demonstrated by the control group:  $Me_{MAC} = 1.49$  a.u. [ $Q_{0.25} = 1.44$  a.u.;  $Q_{0.75} = 1.51$  a.u.], Min = 1.32 a.u., Max = 1.53 a.u.

By the end of the experiment, MAC did not differ significantly from the control values:  $Me_{MAC} = 1.34$  a.u. [ $Q_{0.25} = 1.30$  a.u.;  $Q_{0.75} = 1.41$  a.u.], Min = 1.28 a.u., Max = 1.47 a.u. (Fig. 3).

## DISCUSSION

A theoretical framework for understanding the impact of acute somatic pain on the phagocytic activity of neutrophils can only be developed in the context of neuro-immuno-endocrine interactions. Today, there is no doubt that neurogenic, endocrine and immune mechanisms all contribute to maintaining the body's homeostasis. The pathogenesis of pain or at least its initial stage is similar to the unfolding of stress. Stress is not always caused by pain but acute pain is always a stress, which is why stress hormones, specifically catecholamines, are synthesized in response to an algogenic stimulus. The model used in this study was previously exploited to demonstrate that 2 min after applying an algogenic stimulus, adrenalin and noradrenalin levels, whose ratio is age-dependent, increased in peripheral blood [12].

In another study, the electrophysiological analysis revealed that excitation of nociceptors and signal transmission via the ascending pathways led to the activation of brain structures involved in the control of involuntary functions, the hypothalamus in the first place, and synchronized with the activation of neutrophil granulocytes [13].

Apart from neurogenic noradrenalin, the adrenal medulla releases adrenaline and noradrenalin into the bloodstream. These hormones ultimately find their targets and the subsequent events follow a typical stress scenario. Neutrophils are one of such targets; they were shown express both  $\alpha$ - and

$\beta$ -adrenergic receptors [14], which was later confirmed by another study [15]. In our experiments, we observed an increase in the phagocytic activity by the end of the first hour following exposure to the stimulus (in the spontaneous NBT reduction test); in the stimulated NBT reduction test, the phagocytic activity started to increase by minute 2 following pain induction. But by the end of the experiment the phagocytic activity had been restored to the initial level. This can be explained by the activation of beta-adrenoreceptors of neutrophils [16]. Also, it is important to remember that stress is accompanied by elevated production of glucocorticoids that inhibit the functional activity of neutrophils [17].

The obtained MAC values suggest that neutrophils of newborn rats can exert killing activity [11, 18].

We have shown that algogenic stimulation leads to both spontaneous and stimulated NBT reduction, as well as to an increase in the killing activity of neutrophils, which, on the surface, seems to be inconsistent with the conventional concept of functional immaturity of phagocytes in newborns.

One of possible explanations for our findings might lie in the acknowledgement of the early formed capacity of neutrophils to produce a superoxide [19] when their protective potential is reduced [20].

In the neonatal period, the organism of the newborn, including skin, mucosal lining, gastrointestinal and genitourinary tracts and lungs, is actively colonized by microbiota. This process is short-lasting and intense. Although this fact has long entered textbooks, it is still explored in the academic literature from different perspectives [21–23]. But one opinion that is held firm is that an intense antigen load cannot but mobilize the factors of immune defense, still allowing for the fact that the mechanisms of adaptive immunity are immature at the time the child is born. One should agree that innate immunity factors in general and neutrophils in particular (as the most labile cells) play a key role in the first-line defense in the neonatal period. The discovery of the bacterial translocation corroborates this hypothesis [24].

Thus, on the one hand, the innate immunity of newborns is stimulated by microbial colonization and, on the other hand, acts as a background for the unfolding response to a different non-antigen stimulus, which in our case was an algogenic stimulus.

## CONCLUSIONS

1. The killing activity of neutrophils is initiated and enhanced in response to an acute algogenic stimulus. 2. In newborn rats, an antimicrobial response to short-term acute pain demonstrated by neutrophils is short-lived and quickly depletable. 3. The results of this study broaden our knowledge of metabolic activity of neutrophils in response to acute pain in newborns. Our findings can be used in pain research, for adequate assessment of changes occurring in ontogenesis and for prevention of adverse effects pain can have.

## References

1. Garkavi LKh, Ukolova MA, Kvakina EB. Zakonomernost' razvitiya kachestvenno otlichayushchikhsya obshchikh nespetsificheskikh adaptatsionnykh reaktsiy organizma. Nauchnoe otkrytie № 158 ot 3.10.1969. Russian.
2. Shilova YuA, Shilov DYU, Shilov Yul. Vliyaniye stressa na aktivnost' leykotsitov perifericheskoy krovi. Uspekhi sovremennogo estestvoznaniya. 2010; (7): 54–5. Russian.
3. Zhevago NA, Samoilova KA, Obolenskaya KD. The regulatory effect of polychromatic (visible and infrared) light on human humoral immunity. Photochemical & Photobiological Sciences. 2004; 3 (1): 102–8.
4. Ogneva OI, Osikov MV, Gizinger OA, Fedosov AA. Mekhanizm izmeneniya immunnogo statusa pri eksperimental'nom desinkhronoze v usloviyakh svetodionogo osveshcheniya.

- Sovremennyye problemy nauki i obrazovaniya. 2015; (3): 184. Russian.
5. Zyuzya EV, Kalutskiy PV, Ivanov AV. Vliyaniye sochetannogo primeneniya krovezamenitelya perftoran i antibiotika tsefataksim na sostoyaniye immunologicheskikh pokazatey perifericheskoy krovi v usloviyakh modelirovaniya infitsirovannoy rany i vozdeystviya na organizm postoyannogo magnitnogo polya. Vestnik novykh meditsinskikh tekhnologiy. Elektronnoe izdanie. 2013; (1): 80. Russian.
  6. Akperov EK, Tsygan VN, Stepanov AV. Sostoyaniye nespetsificheskoy rezistentnosti u lits, zloupotrebyayushchikh narkoticheskimi veshchestvami. Psikhofarmakologiya i biologicheskaya narkologiya. 2005; 5 (2): 963–5. Russian.
  7. Bazarin KP, Savchenko AA, Kovalev VN, Lazarenko NA, Landenok AV. Neyroseteovoe modelirovaniye vliyaniya faktorov sportivnoy deyatel'nosti na funktsional'nyuyu aktivnost' neytrofilov krovi u kvalifitsirovannykh sportsmenov. Acta Biomedica Scientifica. 2017; 2 (114): 62–8. Russian.
  8. Alekseeva NS. Mekhanizmy izmeneniya fagotsitarnoy aktivnosti leykotsitov pri ostroy vistseral'noy boli [dissertatsiya]. Rostov-na-Donu, 2008. Russian.
  9. Abramova MV. Faktory vrozhdennogo immuniteta u samok kryis i ikh potomstva pri normal'nykh rodakh i bolevooy stimulyatsii [dissertatsiya]. Rostov-na-Donu, 2019. Russian.
  10. Ovsyannikov VG. Ocherki patofiziologii boli. Rostov-na-Donu: Tsvetnaya pechat', 2003; 148 s. Russian.
  11. Kiseleva EP, Polevshchikov AV. Metod avtomatizirovannogo ucheta NST-testa. Klinicheskaya laboratornaya diagnostika. 1994; (4): 27–9. Russian.
  12. Zajnab AM. Vozrastnye osobennosti monoaminergicheskoy reakcii pri ostroy boli [dissertatsiya]. Rostov-na-Donu, 1995. Russian.
  13. Stepanova ES. Vliyaniye pereohlazhdeniya na funktsional'nyuyu aktivnost' leykotsitov [dissertatsiya]. Syktyvkar, 2010. Russian.
  14. Heumann D, Visher TL. Immunomodulation by alpha2-macroglobulin and alpha2-macroglobulin proteinase complexes: the effect on the T lymphocyte response. Eur J Immunol. 1988; (18): 755.
  15. Nicholls AJ, Wen Wen S, Hall P, Hickey MJ, Wong CHY. Activation of the sympathetic nervous system modulates neutrophil function. J Leukoc Biol. 2018; (103): 295–309.
  16. Kachina II, Shilov DYU, Shilov Yul. Vliyaniye agonista beta-adrenoreceptorov geksoiprenalina sul'fata in vitro na fagocitarnuyu aktivnost' neytrofilov perifericheskoy krovi zdorovykh lyudey. Mezhdunarodnyy zhurnal prikladnykh i fundamental'nykh issledovaniy. 2012; (1): 72–3. Russian.
  17. Kolesnikova NV, Nesterova IV, Chudilova GA. Rannie i otdalennyye jeffekty vliyaniya jekzogennogo gidrokortizona na sistemu neytrofil'nykh granulocitov laboratornykh myshej. Gematologiya i transfuziologiya. 1999; 44 (5): 36–40. Russian.
  18. Zinkin VYu, Godkov MA. Sposob kolichestvennoy otsenki kislorodzavisimogo metabolizma neytrofil'nykh granulotsitov cheloveka. Klinicheskaya laboratornaya diagnostika. 2004; (8): 26–9. Russian.
  19. Chirkin AA. Biokhimiya s osnovami gennoy inzhenerii: ucheb. posobie. Vitebsk: UO "VGU im. P. M. Masherova", 2010; 182 s. Russian.
  20. Klimenko NA, Shelest MA. Funktsional'naya aktivnost' neytrofilov perifericheskoy krovi pri khronicheskom bronkhite. Nauchnye vedomosti Belgorodskogo gosudarstvennogo universiteta. Seriya: Meditsina. Farmatsiya. 2013; 11 (154): Vypusk 22: 129–31. Russian.
  21. Zhelnina TP, Brezhneva NI, Osaev NYu. Analiz struktury mikroflory novorozhdennykh. Infektsiya i immunitet. 2016; 6 (3): 26. Russian.
  22. Belyaeva IA, Bombardirova EP, Mitish MD, Potekhina TV, Kharitonova NA. Ontogenez i dizontogenez mikrobioty kishchnoy i detey rannego vozrasta: triggernyy mekhanizm narusheniy detskogo zdorov'ya. Voprosy sovremennoy pediatrii. 2017; 16 (1): 29–38. Russian.
  23. Nikolaeva IV, Tsaregorodtsev AD, Shaykhieva GS. Formirovaniye kishchnoy mikrobioty rebenka i faktory, vliyayushchie na etot protsess. Rossiyskiy vestnik perinatologii i pediatrii. 2018; 63 (3): 13–8. Russian.
  24. Nikitenko NI, Zakharov VV, Borodin AV. Rol' translokatsii bakteriy v patogeneze khirurgicheskoy infektsii. Khirurgiya. 2001; (2): 63–6. Russian.

## Литература

1. Гаркави Л. Х., Уколова М. А., Квакина Е. Б. Закономерность развития качественно отличающихся общих неспецифических адаптационных реакций организма. Научное открытие № 158 от 3.10.1969.
2. Шилова Ю. А., Шилов Д. Ю., Шилов Ю. И. Влияние стресса на активность лейкоцитов периферической крови. Успехи современного естествознания. 2010; (7): 54–55.
3. Zhevago NA, Samoilova KA, Obolenskaya KD. The regulatory effect of polychromatic (visible and infrared) light on human humoral immunity. Photochemical & Photobiological Sciences. 2004; 3 (1): 102–8.
4. Огнева О. И., Осиков М. В., Гизингер О. А., Федосов А. А. Механизм изменения иммунного статуса при экспериментальном десинхронозе в условиях светодиодного освещения. Современные проблемы науки и образования. 2015; (3): 184.
5. Зюзя Е. В., Калущий П. В., Иванов А. В. Влияние сочетанного применения кровезаменителя перфторан и антибиотика цефатаксим на состояние иммунологических показателей периферической крови в условиях моделирования инфицированной раны и воздействия на организм постоянного магнитного поля. Вестник новых медицинских технологий. Электронное издание. 2013; (1): 80.
6. Акперов Э. К., Цыган В. Н., Степанов А. В. Состояние неспецифической резистентности у лиц, злоупотребляющих наркотическими веществами. Психофармакология и биологическая наркология. 2005; 5 (2): 963–5.
7. Базарин К. П., Савченко А. А., Ковалев В. Н., Лазаренко Н. А., Ланденко А. В. Нейросетевое моделирование влияния факторов спортивной деятельности на функциональную активность нейтрофилов крови у квалифицированных спортсменов. Acta Biomedica Scientifica. 2017; 2 (114): 62–8.
8. Алексеева Н. С. Механизмы изменения фагоцитарной активности лейкоцитов при острой висцеральной боли [диссертация]. Ростов-на-Дону, 2008.
9. Абрамова М. В. Факторы врожденного иммунитета у самок крыс и их потомства при нормальных родах и болевой стимуляции [диссертация]. Ростов-на-Дону, 2019.
10. Овсянников В. Г. Очерки патофизиологии боли. Ростов-на-Дону: Цветная печать, 2003; 148 с.
11. Киселева Е. П., Полевщиков А. В. Метод автоматизированного учета НСТ-теста. Клиническая лабораторная диагностика. 1994; (4): 27–9.
12. Зайнаб А. М. Возрастные особенности моноаминергической реакции при острой боли [диссертация]. Ростов-на-Дону: 1995.
13. Степанова Е. С. Влияние переохлаждения на функциональную активность лейкоцитов [диссертация]. Сыктывкар, 2010.
14. Heumann D, Visher TL. Immunomodulation by alpha2-macroglobulin and alpha2-macroglobulin proteinase complexes: the effect on the T lymphocyte response. Eur J Immunol. 1988; (18): 755.
15. Nicholls AJ, Wen Wen S, Hall P, Hickey MJ, Wong CHY. Activation of the sympathetic nervous system modulates neutrophil function. J Leukoc Biol. 2018; (103): 295–309.
16. Качина И. И., Шилов Д. Ю., Шилов Ю. И. Влияние агониста бета-адренорецепторов гексопrenalина сульфата *in vitro* на фагоцитарную активность нейтрофилов периферической крови здоровых людей. Международный журнал прикладных и фундаментальных исследований. 2012; (1): 72–3.
17. Колесникова Н. В., Нестерова И. В., Чудилова Г. А. Ранние и отдаленные эффекты влияния экзогенного гидрокортизона на систему нейтрофильных гранулоцитов лабораторных



- мышей. Гематология и трансфузиология. 1999; 44 (5): 36–40.
18. Зинкин В. Ю., Годков М. А. Способ количественной оценки кислородзависимого метаболизма нейтрофильных гранулоцитов человека. Клиническая лабораторная диагностика. 2004; (8): 26–9.
  19. Чиркин А. А. Биохимия с основами генной инженерии: учеб. пособие. Витебск: УО «ВГУ им. П. М. Машерова», 2010; 182 с.
  20. Клименко Н. А., Шелест М. А. Функциональная активность нейтрофилов периферической крови при хроническом бронхите. Научные ведомости Белгородского государственного университета. Серия: Медицина. Фармация. 2013; 11 (154); Выпуск 22: 129–131.
  21. Желнина Т. П., Брежнева Н. И., Осяев Н. Ю. Анализ структуры микрофлоры новорожденных. Инфекция и иммунитет. 2016; 6 (3): 26.
  22. Беляева И. А., Бомбардинова Е. П., Митиш М. Д., Потехина Т. В., Харитонов Н. А. Онтогенез и дизонтогенез микробиоты кишечника у детей раннего возраста: триггерный механизм нарушений детского здоровья. Вопросы современной педиатрии. 2017; 16 (1): 29–38.
  23. Николаева И. В., Царегородцев А. Д., Шайхиева Г. С. Формирование кишечной микробиоты ребенка и факторы, влияющие на этот процесс. Российский вестник перинатологии и педиатрии. 2018; 63 (3): 13–8.
  24. Никитенко Н. И., Захаров В. В., Бородин А. В. Роль транслокации бактерий в патогенезе хирургической инфекции. Хирургия. 2001; (2): 63–6.

## PROGNOSIS CRITERIA OF THE SEVERE POSTEMBOLIZATION SYNDROME IN PATIENTS WITH UTERINE MYOMA

Nurmukhametova ET ✉, Shlyapnikov ME

REAVIZ Medical University, Samara, Russia

Recently specialists take an interest in organ-preserving methods of uterine fibroids treatment, one of which is uterine artery embolization (UAE). One of the method's negative aspects is the severe postembolization syndrome (PES) development, requiring timely initiation of adequate treatment in order to avoid severe complications that could lead to the organ removal. The study was aimed to search for the prognostic criteria of the severe PES development during the preoperative period. The study included 81 UAE-treated women aged 19–50 with 7–17 week uterine myoma. The patients' anthropometric measurements were used, as well as the skin microcirculation data obtained by laser Doppler flowmetry together with the occlusion test. Based on prognostic criteria, models with AUC (area under ROC curve) > 0.8 were presented. According to the models, the anthropometric predictors of the severe PES were the following: age under 38.5 ( $p < 0.05$ ); BMI lower than 25 kg/m<sup>2</sup> ( $p < 0.05$ ), and microcirculation value (M) prior to UAE below 9.55 PU ( $p = 0.001$ ). Microvascular blood flow during the occlusion test indicate that the higher the oxygen consumption index (I), intravascular resistance (Rc), capillary blood flow reserve capacity in the models, the higher the risk of the severe PES development ( $p < 0.05$ ). Low alpha angle value obtained by the occlusion test ( $p = 0.003$ ) as well as the UVLF value ( $p = 0.004$ ) in the models also indicate the increased risk of severe PES. Multidimensional prognostic modelling admits to expect the severe PES development prior to UAE, which allows the doctor to prepare the woman for specific management and treatment.

**Keywords:** uterine fibroids, uterine artery embolization, postembolization syndrome, laser Doppler flowmetry, prognostic criteria

**Acknowledgements:** to MV Komarova, PhD, Associate Professor of the Samara University Department of Laser and Biotechnological Systems, for assistance in the statistical processing of the results.

**Author contribution:** Nurmukhametova ET, Shlyapnikov ME — the authors contributed to the study and manuscript writing equally.

**Compliance with ethical standards:** the study was approved by the Ethics Committee of the REAVIZ Medical University (protocol № 2 dated January 14, 2019). All patients submitted the informed consent to participation in the study and data publishing.

✉ **Correspondence should be addressed:** Elmira T. Nurmukhametova  
Chkalova, 100, Samara, 443001; nurelm@yandex.ru

**Received:** 31.12.2019 **Accepted:** 19.01.2020 **Published online:** 29.01.2020

**DOI:** 10.24075/brsmu.2020.006

## ПРОГНОСТИЧЕСКИЕ КРИТЕРИИ РАЗВИТИЯ ТЯЖЕЛОГО ПОСТЭМБОЛИЗАЦИОННОГО СИНДРОМА У ПАЦИЕНТОК С МИОМОЙ МАТКИ

Э. Т. Нурмухаметова ✉, М. Е. Шляпников

Медицинский университет «Реавиз», Самара, Россия

В последние годы проявляется интерес к органосохраняющим методам лечения миомы матки, одним из которых является эмболизация маточных артерий (ЭМА). Среди отрицательных сторон метода — развитие тяжелого постэмболизационного синдрома (ПЭС), требующего своевременного начала адекватного лечения с целью избежания грозных осложнений, способных привести к удалению органа. Целью исследования был поиск прогностических критериев развития тяжелого ПЭС в дооперационном периоде. В исследование вошла 81 женщина с миомой матки 7–17 недель в возрасте 19–50 лет, прошедшая лечение методом ЭМА. В работе использовали антропометрические данные пациенток и показатели кожной микроциркуляции, полученные методом лазерной доплеровской флоуметрии (ЛДФ) с проведением окклюзионной пробы (ОП). На основании прогностических критериев построены модели с AUC (область под графиком ROC кривой) > 0,8. Антропометрические предикторы тяжелого ПЭС в моделях: возраст менее 38,5 лет ( $p < 0,05$ ); ИМТ менее 25 кг/м<sup>2</sup> ( $p < 0,05$ ) и показатель микроциркуляции (M) до ЭМА — менее 9,55 пф. ед. ( $p = 0,001$ ). Показатели микрокровотока в ОП свидетельствуют о том, что чем выше значения индекса потребления кислорода (I), внутрисосудистого сопротивления (Rc), резерва капиллярного кровотока (РКК) в моделях, тем выше риск развития тяжелой формы ПЭС ( $p < 0,05$ ). Низкие показатели угла альфа в ОП ( $p = 0,003$ ) и эндотелиальных колебаний UVLF ( $p = 0,004$ ) в моделях также ведут к повышенному риску развития тяжелого ПЭС. Многомерные прогностические модели позволят диагностировать развитие тяжелого ПЭС до проведения ЭМА и подготовить пациентку к определенному послеоперационному ведению и лечению.

**Ключевые слова:** миома матки, эмболизация маточных артерий, постэмболизационный синдром, лазерная доплеровская флоуметрия, прогностические критерии

**Благодарности:** к. б. н., доценту кафедры лазерных и биотехнических систем Самарского университета М. В. Комаровой за консультативную помощь в статистической обработке результатов исследования.

**Вклад авторов:** Э. Т. Нурмухаметова, М. Е. Шляпников — равнозначен на всех этапах работы и написания статьи.

**Соблюдение этических стандартов:** исследование одобрено этическим комитетом медицинского университета «Реавиз» (протокол № 2 от 14 января 2019 г.). Все пациентки подписали информированное добровольное согласие на участие в исследовании и публикацию данных.

✉ **Для корреспонденции:** Эльмира Тимеровна Нурмухаметова  
ул. Чкалова, д. 100, г. Самара, 443001; nurelm@yandex.ru

**Статья получена:** 31.12.2019 **Статья принята к печати:** 19.01.2020 **Опубликована онлайн:** 29.01.2020

**DOI:** 10.24075/vrgmu.2020.006

Uterine fibroids occupy a leading position in the structure of gynecological diseases, they are diagnosed in 20–50% of women of reproductive age [1], and also in 18–56% of patients with impaired fertility [2]. Uterine fibroids worsen the women of reproductive age quality of life due to uterine bleeding, chronic

anemia, lower abdominal pain, pressure on the neighboring organs and deterioration of their functions in the form of the urinary system and gastrointestinal tract function impairment. The treatment main method is the surgical removal of the uterus, which patients and doctors do not always agree with [1]. Recently the

organ preservation techniques have been accepted [2]. Surgical procedures, such as myomectomy via laparoscopy, laparotomy, by the vaginal route, are performed under general anesthesia. There is a minimally invasive endovascular technique requiring no general anesthesia and incision, the uterine artery embolization (UAE). This endovascular technique is minimally invasive, and does not require general anesthesia, which is attractive for patients and doctors. Due to the uterine fibroid's vessels embolization, the nutrition of the nodule is disrupted, which leads to its acute hypoxia and necrosis, acidosis and the absorption of tissue degradation products into the bloodstream. In response to this, in 96% of patients during their early postoperative period (8–36 hours) the postembolization syndrome (PES) of varying severity develops [3]. The PES severity assessment is performed using the scale presented by YuE Dobrokhova et al. [3]. The mild and moderate PES treatment is limited by the appointment of non-opioid analgesics and non-steroidal anti-inflammatory drugs orally, as well as by hospitalization for 1–3 days. In patients with severe PES, opioid analgesics, antibiotic intravenous infusion therapy, correction of coagulation are used. If necessary, the urinary bladder catheterization and other methods are used. The patients with severe PES are at high risk of the severe complications, such as metrorrhagia, pyometra, sepsis and thrombosis which can lead to the organ removal [4–6]. Thus, the question of timely initiation of corrective therapy in the severe PES patients remains important, which would facilitate a milder progression of the disease, serve as a prophylaxis of complications and create a favorable opinion of this treatment method in the patient. Methods have been proposed to reduce pain in the early postoperative period, as pain is the main symptom. During the UAE procedure, it was proposed to administer 100 mg (2.5 ml) of Actovegin prior to the emboli administration in order to increase the uterus parenchymal blood flow, thereby reducing the PES manifestations [7]. Other authors recommend to calculate the minimum number of embolic agents' portions accurately, to reduce the number of complications associated with an overdose of particles, as well as the cost of the procedure due to the price of emboli [8]. The severity of PES can be reduced by the use of varicose veins therapy in the postoperative period, especially in patients with uterine fibroids, suffering from venous and lymphatic insufficiency of the lower extremities [9]. During our study we analyzed the history of patients admitted to UAE and found that age, BMI and nodule location were statistically significant factors affecting the progression of PES. The latter is a qualitative parameter, therefore anthropometric data (quantitative) were used in the prognostic models. Among the examination methods, we distinguished laser Doppler flowmetry (LDF) which was used in the acute period in patients with uterine myoma prior to UAE for the first time. The available literature sources contain data on the study of skin microcirculation in gynecological patients with chronic diseases, but contain no data on the acute diseases [10]. Since PES is the body's response to the UAE procedure, it is a systemic response. LDF reflects changes in skin microcirculation, which characterize whole body's condition [11]. The severe PES development is associated with the risk of complications and with the pronounced influence on the patients' general well-being, unlike the mild and moderate PES. The study was aimed to determine the severe PES development prognostic criteria using the anthropometric data and skin microcirculation data prior to UAE.

## METHODS

In 2016–2019 at the RZHD-Medicina Clinical Hospital, 81 patients aged 18–50 with 7–17 week symptomatic growing

uterine fibroids were surveyed (nodule size 21–115 mm). The average age of the patients was  $39 \pm 6$ .

Inclusion criteria: progressive uterine myoma; clinical symptoms in the form of menometrorrhagia, lower abdomen "dragging" pain; compression of the neighbouring organs associated with frequent urination and constipation; lack of historical data on the conservative therapy effect; woman's decidedness to save the uterus for various reasons: psychological comfort, possible reproductive planning, high risk of surgery, "fear" of general anesthesia and surgery.

All the women were treated by UAE because of the indications. In the early postoperative period the surveyed patients were divided into 3 groups in accordance with the PES severity: mild PES (group I), 36 (44.44%) patients, moderate PES (group II), 30 (37.04%) patients, pronounced PES (group III), 15 (18.52%) patients. In patients with multiple myomas, the the dominant nodule was evaluated. The single nodule uterine fibroid sized 30–110 mm was revealed in 41 (50.6%) patients, the other 40 patients (49.4%) had multiple myomas with the nodules sized 21–115 mm. There were no significant differences between the groups ( $p = 0.705$ ;  $\chi^2 = 0.7$ ).

Exclusion criteria (due to factors affecting the UAE procedure): pelvic inflammatory disease; history of the gonadotropin-releasing hormone agonist or hormone drugs intake (hormonal contraception or hormone replacement therapy) less than the 3 months before the study; pelvic malignant tumors; grade III adenomyosis; allergic reactions to contrast material; negative Allen test; presence of the arteriovenous fistula for the dialysis; Buerger's disease.

Exclusion criteria (due to the factors affecting the LDF results): cardiovascular diseases and severe atherosclerotic vascular disease; diabetes mellitus; chronic venous insufficiency; Raynaud's disease; obliterating endarteritis; injuries; deformations and infectious lesions of the distal phalanx [11].

For patients with submucous and subserous myomas (FIGO (2011) types 0, 1, 6 and 7) other treatment methods were recommended instead of UAE: myomectomy via resectoscopy, laparoscopy, by the vaginal route. The UAE was performed via femoral artery (according to Seldinger technique) in 63 patients, and via radial artery in 18 patients, using the Embosphere microspheres (Biosphere Medikal; USA) sized 500–1200  $\mu\text{m}$ . UAE method, bottles' number and emboli size were determined by the X-ray surgery specialist after consulting the patient and during the diagnostic and therapeutic arterial interventions.

The patients were examined in accordance with the generally accepted scheme: general medical examination, ultrasound with the color Doppler imaging, consultations of the gynecologist, therapist and X-ray surgery specialist, diagnostic D&C or endometrial aspiration with the histopathological examination. In the early postoperative period, the patients develop a symptom complex called postembolization syndrome (PES), characterized by pain of varying intensity, high body temperature, elevated ESR, leukocytosis, impaired cardiovascular function (tachycardia), impaired gastrointestinal tract function (nausea, vomiting, intestinal paresis), impaired urinary tract function (urinary retention), impaired blood coagulation (hyperfibrinogenemia), bloody discharge.

The microcirculation system condition was evaluated prior to UAE by LDF and the occlusion test, which is the closest to the UAE procedure, using the LAKK-O2 unit (Lazma; Russia). Investigation was performed after acclimatization, lasting for 30 minutes in the room with the 21–24 °C temperature. The patients were not allowed to smoke, eat or drink anything that could affect the microcirculation before the examination. The study was carried out in the same room at the same

time (lunch from 12 to 13 h; study from 15 to 17 h), outside of menstruation. The patient was in her sitting position, the upper limb in moderate flexion was placed on the table, sensor was installed in the eponychium of the right hand 3<sup>rd</sup> finger, while the hand was at heart level. For the occlusion test, the tonometer cuff was fixed on the shoulder of the right hand. The test was carried out as follows: within one minute, the baseline blood flow was recorded, then the recording was stopped. After that, the occlusion was created by quick pumping up the pressure in the cuff to the level of 230–250 mm Hg. The further registration of the blood flow for 3 minutes of the occlusion period was carried out. After a 3-minute occlusion, air was quickly released

from the cuff, during the next 6 minutes the perfusion reaction was recorded while the blood flow restored [11].

The data acquired during the study were processed using the software coming with the equipment used. The following indicators were evaluated: M, arithmetic mean value of microcirculation measured in perfusion units (PU);  $\sigma$ , standard deviation (RMS) of the blood flow oscillations amplitude from the M arithmetic mean value; using the wavelet transform, the following indicators: UVLF, VLF, LF, HF, CF, blood flow oscillations of the frequency bands corresponding to endothelial, neurogenic, myogenic, respiratory, cardiac activities respectively (PU); capillary blood flow reserve capacity;  $\alpha$ ,

**Table. 1.** Dominant myoma size and localization

FIGO myoma classification, 2011	PES severity			Intergroup comparison			Whole table comparison, $p$
	Mild ( $n = 36$ ) Abs. (%)	Moderate ( $n = 30$ ) Abs. (%)	Severe ( $n = 15$ ) Abs. (%)	$p^{1-2}$	$p^{1-3}$	$p^{2-3}$	
Intramural myoma, up to 50% in the uterine cavity (type 2)	16 (44.4%)	8 (26.7%)	6 (40.0%)	0.216	0.985	0.569	0.020
Intramural myoma (type 4)	16 (44.4%)	11 (36.7%)	1 (6.7%)	0.698	0.023	0.074	
Subserous myoma, up to 50% in the abdominal cavity (type 5)	3 (8.3%)	6 (20.0%)	6 (40.0%)	0.310	0.021	0.283	
Isthmic myoma (type 8)	1 (2.8%)	5 (16.7%)	2 (13.3%)	0.127	0.420	0.885	
Number of myomas	1.53 $\pm$ 1.02	2.15 $\pm$ 1.50	2.62 $\pm$ 1.75	0.349	0.010	0.624	0.042
Size of dominant fibroid before UAE, mm	58.32 $\pm$ 17.30	55.60 $\pm$ 22.10	54.76 $\pm$ 17.70	0.963	0.843	0.998	0.791

**Note:** myoma nodules' localization comparison was performed using the Pearson  $\chi^2$  test ( $\chi^2 = 15.1$ ), comparison of the nodules' number and size was performed using ANOVA.

**Table. 2.** Anthropometric data of patients and parameters of microcirculation at rest and during the occlusion test prior to UAE for the groups of patients with PES of different severity

	Mild PES (score below 7)	Moderate PES (score 8–14)	Severe PES (score 15–21)	$p^{1-2}$	$p^{1-3}$	$p^{2-3}$	$p^{ANOVA}$
Age, years*	39.72 $\pm$ 6.47	42.10 $\pm$ 5.70	35.07 $\pm$ 5.74	0.310	0.048	0.002	0.002
BMI, kg/m <sup>2</sup> *	26.24 $\pm$ 3.41	27.86 $\pm$ 6.39	23.34 $\pm$ 3.14	0.515	0.020	0.008	0.013
<i>Microcirculation at rest</i>							
M, PU	22.33 (12.98–24.03)	17.55 (10.38–19.15)	7.90 (5.40–15.60)	0.110	0.002	0.011	0.003
$\sigma$ (SD), PU	1.70 (1.40–3.68)	1.25 (1.10–1.40)	3.35 (1.50–3.98)	< 0.001	0.278	< 0.001	< 0.001
VLF, PU	0.98 (0.57–1.02)	0.58 (0.31–0.74)	0.62 (0.52–0.74)	< 0.001	0.005	0.268	< 0.001
LF, PU	0.54 (0.45–0.81)	0.42 (0.28–0.69)	0.42 (0.38–0.54)	0.037	0.054	0.791	0.053
HF, PU	0.17 (0.14–0.19)	0.16 (0.13–0.22)	0.16 (0.14–0.17)	0.583	0.448	0.837	0.729
CF, PU	0.15 (0.14–0.24)	0.22 (0.13–0.37)	0.17 (0.14–0.26)	0.017	0.279	0.242	0.047
I	9.45 (4.67–12.25)	10.93 (8.96–19.47)	3.88 (2.61–4.88)	0.017	< 0.001	< 0.001	< 0.001
Rc	0.19 (0.10–0.27)	0.38 (0.24–0.47)	0.18 (0.08–0.21)	< 0.001	0.489	< 0.001	< 0.001
<i>Blood flow during the occlusion test</i>							
M, PU	15.00 (6.95–17.03)	12.55 (9.05–21.98)	14.80 (3.60–17.50)	0.567	0.166	0.097	0.220
$\delta$ (SD)	11.40 (7.55–13.63)	10.25 (7.73–12.25)	8.30 (2.60–9.40)	0.463	0.042	0.089	0.097
Capillary blood flow reserve capacity, %	166.21 (139.95–219.05)	136.31 (128.33–174.04)	220.09 (134.40–245.11)	0.008	0.414	0.013	0.008
$\alpha$ -Angle	65.89 (54.19–69.27)	50.22 (48.35–65.73)	41.11 (34.92–48.22)	0.051	< 0.001	< 0.001	< 0.001
UVLF	3.15 (2.63–3.72)	2.76 (2.29–3.74)	1.76 (1.21–2.65)	0.241	< 0.001	0.002	< 0.001
VLF	1.75 (1.46–2.61)	1.75 (1.23–2.41)	1.33 (0.81–1.64)	0.312	0.001	0.006	0.003
LF	0.78 (0.63–1.13)	0.95 (0.46–1.01)	1.00 (0.32–1.09)	0.279	0.282	0.981	0.432
HF	0.23 (0.13–0.32)	0.23 (0.17–0.32)	0.27 (0.12–0.44)	0.588	0.694	0.923	0.843
CF	0.15 (0.13–0.19)	0.16 (0.11–0.24)	0.16 (0.12–0.23)	0.380	0.413	0.904	0.592
I	5.90 (4.33–7.28)	7.77 (4.68–8.42)	4.68 (1.82–9.20)	0.039	0.942	0.253	0.125
Rc	0.04 (0.03–0.04)	0.04 (0.03–0.07)	0.06 (0.05–0.09)	0.124	< 0.001	0.004	< 0.001

**Note:** \* — data are presented as standard deviation M  $\pm$  SD; other data are presented as median and interquartile range.



reactive hyperemia curve angle; I, tissue oxygen consumption index; Rc, intravascular resistance.

Statistical processing of the data acquired was performed using the SPSS 21 software (IBM SPSS; USA). Descriptive statistics for quantitative indicators were presented as mean M and standard deviation  $M \pm SD$ . If the distribution was skewed, the data was presented as median and interquartile range. For comparison of groups, we used one-way analysis of variance (ANOVA) or its nonparametric analogue, the Kruskal-Wallis test, together with the intergroup comparison using the Mann-Whitney-Wilcoxon test and Bonferroni correction. Pearson  $\chi^2$  test was used for the nominal data comparison. To assess the contribution of individual characteristics to the risk of severe PES, one-dimensional and multi-dimensional logistic regression was used. The quality of prognosis was evaluated using ROC analysis. The results were considered significant when  $p < 0.05$ .

## RESULTS

Prior to UAE, in the studied groups, no significant differences were revealed in the patients' history, complaints, examination data, myoma size ( $p_{ANOVA} = 0.607$ ), and the dominant nodule size ( $p_{ANOVA} = 0.897$ ). There were differences in the localization and number of myoma nodules (Table 1).

It was found, that in women with low baseline skin microcirculation value, M (7.90 PU) and high perfusion variability value (3.35 PU), severe PES was revealed after UAE (Table 2). The amplitude and frequency spectrum of blood

flow oscillations at rest had no diagnostic value. During the occlusion test, the endothelial and neurogenic components (active microcirculation mechanisms associated with blood flow) could be the severe PES predictors. In particular, the UVLF oscillations value during the occlusion test (endothelial) in the group III was 1.76 PU, which was significantly lower than the values in the group I (3.15 PU.;  $p_{1-3} < 0.001$ ) and II (2.76 PU;  $p_{2-3} = 0.002$ ); the VLF oscillations value during the occlusion test (neurogenic) in the group of patients with severe PES was lower than in the groups of patients with mild ( $p_{1-3} = 0.001$ ) and moderate ( $p_{2-3} = 0.006$ ) PES.

The statistically significant differences in anthropometric characteristics revealed (age, BMI), as well as skin microcirculation parameters (M at rest,  $\delta$  at rest, capillary blood flow reserve capacity during the occlusion test,  $\alpha$ -angle during the occlusion test, UVLF during the occlusion test, VLF during the occlusion test, Rc during the occlusion test) before the procedure became the basis for the most significant risk factors and predictors identification (see Table 2). Logistic regression was a mathematical tool for evaluation of the studied protective factors influence on PES. Predicting the risk of severe PES compared with mild or moderate PES was carried out without dividing the last two categories. At the first stage, one-dimensional models were constructed for the main blood flow parameters, the predictors were forced into the model (Table 3).

During the study, we identified a number of criteria allowing one to predict the severe PES development in the early postoperative period after UAE. Among the anthropometric

**Table 3.** Assessment of the anthropometric characteristics and microcirculation parameters value for predicting severe PES using the one-dimensional logistic regression model

Predictor	OR (95% CI)	p
<i>Anthropometric characteristics</i>	–	–
Age, years	0,87 (0,79–0,96)	0,005
BMI, kg/m <sup>2</sup>	0,77 (0,63–0,94)	0,010
<i>Microcirculation parameters at rest</i>	–	–
M, PU	0,83 (0,74–0,92)	0,001
$\delta$	1,70 (1,09–2,64)	0,019
VLF	0,38 (0,05–3,20)	0,375
LF	0,23 (0,02–3,16)	0,271
HF (step 0.1)*	0,50 (0,15–1,63)	0,248
CF	0,15 (0,00–20,14)	0,452
I	0,58 (0,42–0,80)	0,001
Rc (step 0.1)*	0,58 (0,35–0,96)	0,033
<i>Microcirculation parameters during the occlusion test</i>	–	–
M, PU	0,94 (0,86–1,03)	0,166
$\delta$	0,82 (0,71–0,96)	0,014
Capillary blood flow reserve capacity, %	1,02 (1,00–1,03)	0,008
$\alpha$ -Angle	0,85 (0,78–0,93)	< 0,001
UVLF	0,23 (0,10–0,53)	0,001
VLF	0,14 (0,04–0,53)	0,004
LF	0,46 (0,07–3,18)	0,430
HF (step 0.1)*	1,41 (0,85–2,32)	0,179
CF	0,87 (0,00–183,07)	0,959
I	1,07 (0,91–1,26)	0,422
Rc** (step 0.01)	1,68 (1,27–2,21)	< 0,001

**Note:** \* — odds ratio is optimized for the predictor's increase by 0.1; \*\* odds ratio is optimized for the predictor's increase by 0.01.

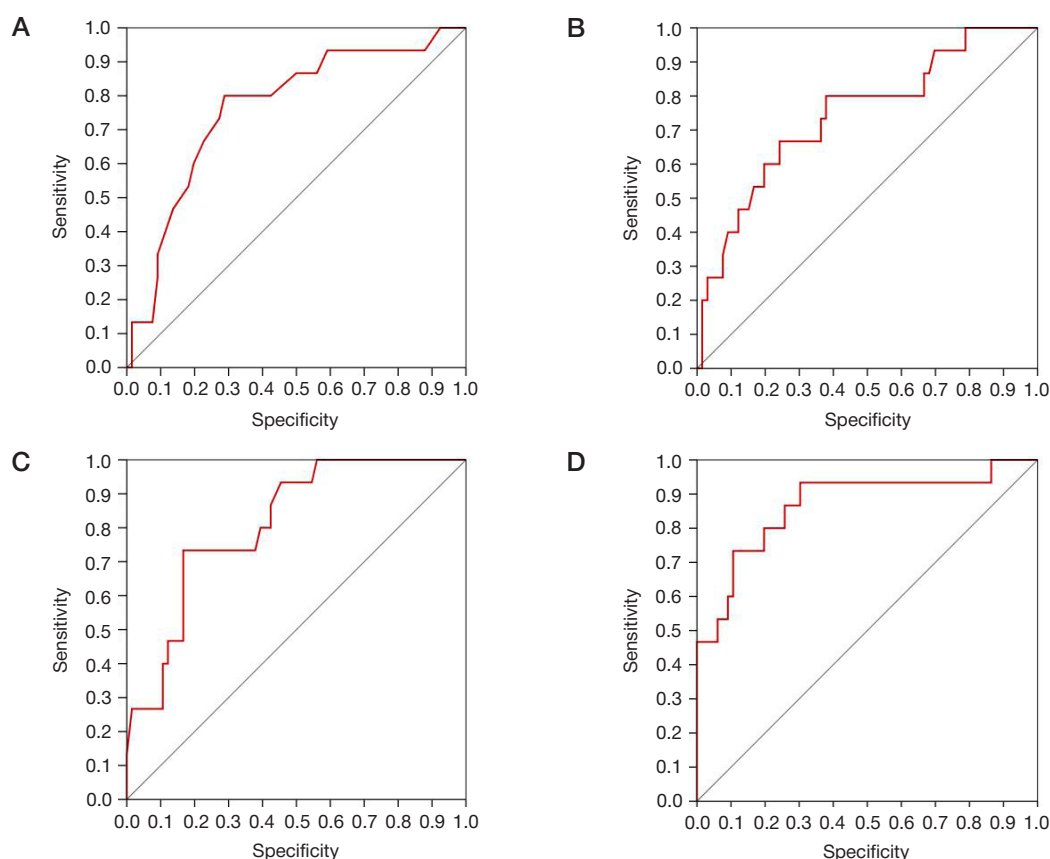


Fig. 1. ROC curves demonstrating the prognostic value of age (A), BMI (B), perfusion rate at rest (C),  $\alpha$  blood flow recovery angle (D)

characteristics, the statistically significant factors affecting PES were the age of the woman and her BMI. In both parameters the odds ratio was less than one: for age OR = 0.87 (0.79–0.96), for BMI OR = 0.77 (0.63–0.94), that's why they could be considered protective factors. According to the models constructed, the greater the age and BMI of the patient, the lower her risk of PES. In order to define which threshold values of the studied traits predicted the development of PES best, as well as to quantify the predictive value of each trait, the ROC curves were used (Fig. 1). The coordinates and the corresponding values of sensitivity and specificity were analyzed. It was found that women aged 38.5 years and younger were at risk of severe PES (sensitivity 80%, specificity 71%). The other risk factor of the severe PES was BMI. According to the data obtained, women with normal body weight and reduced body weight were at risk of severe PES. With the BMI threshold value of 25 kg m<sup>2</sup>, sensitivity of severe PES predicting was 80%, and specificity was 62%. The area under ROC curve for age was  $0.76 \pm 0.068$  ( $p = 0.002$ ), and for BMI it was  $0.74 \pm 0.073$  ( $p = 0.003$ ).

Of the blood flow parameters at rest, the microcirculation value (M) turned out to be highly informational, the area under the ROC curve for M was  $0.81 \pm 0.05$  ( $p < 0.001$ ). The coordinates' analysis of the ROC curve for M demonstrated that 9.55 PU was a reliable threshold value. In women with a perfusion rate at rest prior to planned procedure below 9.55 PU, severe PES development could be expected (sensitivity 73%, specificity 83%). The isolation of individual oscillations of the microvessels using the wavelet analysis at rest without any additional tests was of no predictive value for the diagnosis of severe PES.

The occlusion test, allowing one to simulate the body's response to acute hypoxia, showed a high prognostic potential of the recovery angle  $\alpha$  (area under ROC curve  $0.87 \pm 0.059$ ;

$p < 0.001$ ) (Fig. 1D). Fast recovery after the 3-minute occlusion reduced the risk of severe PES (OR = 0.85 (0.78–0.93);  $p < 0.001$ ). In our opinion, the best threshold value was  $\alpha = 48$  (sensitivity and specificity of the prediction was 80%).

At the next stage the multivariate logistic regression models were plotted using step-by-step selection of potential predictors (Table 4). Since various indicators of blood flow were obtained by the same signal processing, and some of them were derived from the baseline, all of them were interconnected to various extent. Therefore, several models of comparable quality were proposed (Fig. 2).

*Model 1* has been plotted using the anthropometric characteristics. Prediction quality with a threshold probability of 0.25: sensitivity 67%, specificity 88%. Both traits have the OR less than one, therefore, the high values are protective factors; AUC is  $0.81 \pm 0.058$  ( $p < 0.001$ ).

*Model 2* has been plotted using the anthropometric characteristics and the blood flow parameters at rest. As a result of step-by-step selection, only age and M were included in the model. Prediction quality with a threshold probability of 0.35: sensitivity 73%, specificity 89%; AUC is  $0.89 \pm 0.04$  ( $p < 0.001$ ).

*Model 3* has been plotted using the anthropometric characteristics and the occlusion test results ( $\alpha$  angle and capillary blood flow reserve capacity).  $\alpha$  Angle most strongly affects the outcome of traits: its decrease is associated with the increased risk of severe PES. Prediction quality with a threshold probability of 0.25: sensitivity 87%, specificity 91%; AUC is  $0.93 \pm 0.042$  ( $p < 0.001$ ).

*Model 4* is very much like model 3. It has been plotted using the LDF values obtained during the occlusion test according to the wavelet analysis of the original signal. In accordance with the model, endothelial oscillations are the most significant protective factor: their high values decrease

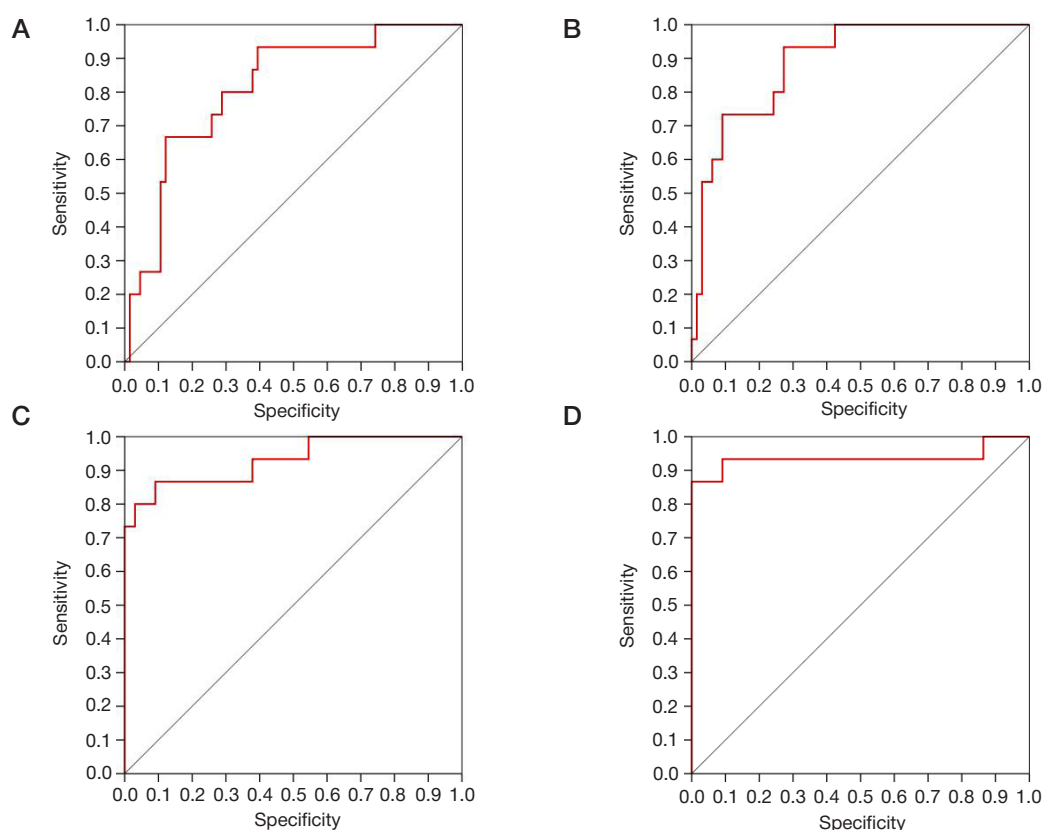


Fig. 2. ROC curves demonstrating the multivariate models prognostic value 1 (A), 2 (B), 3 (C), 4 (D)

the risk of severe PES: OR 0.09 (95% CI: 0.02–0.47). This corresponds the previously revealed effect of the  $\alpha$  angle, which also reflects the intensity of blood flow recovery after the occlusion test. High values of I and Rc increase the risk of severe PES. Prediction quality with a threshold probability of 0.25: sensitivity 87%, specificity 98%; AUC is  $0.94 \pm 0.056$  ( $p < 0.001$ ).

## DISCUSSION

According to the results of other authors, severe PES develops in 10.2% of patients after EMA [3]. Our results suggest that severe PES develops in 18.52% of patients. The difference may be due to the larger number of exclusion criteria associated with LDF, i.e., diseases that impede (distort) the study of

Table 4. Assessment of the anthropometric characteristics and microcirculation parameters for the severe PES prognosis using the multivariate logistic regression models

Variables	Regression coefficient, <i>b</i>	SE <i>b</i>	Wald test	OR (95% CI)	<i>p</i>
<b>Model 1</b>					
BMI, kg/m <sup>2</sup>	–0.19	0.1	3.83	0.83 (0.69–1.00)	0.05
Age, years	–0.11	0.05	4.44	0.89 (0.81–0.99)	0.035
Invariable	7.49	2.68	7.82	–	0.005
<b>Model 2</b>					
M at rest, PM channel	–0.23	0.07	11.04	0.80 (0.70–0.91)	0.001
Age, years	–0.17	0.06	8.17	0.84 (0.75–0.95)	0.004
Invariable	7.71	2.53	9.28	–	0.002
<b>Model 3</b>					
$\alpha$ -Angle during the occlusion test	–0.19	0.06	9.02	0.82 (0.73–0.94)	0.003
Capillary blood flow reserve capacity during the occlusion test, %	0.03	0.01	5.62	1.03 (1.00–1.05)	0.018
Age, years	–0.16	0.08	4.41	0.85 (0.74–0.99)	0.036
Invariable	9.42	3.91	5.81	–	0.016
<b>Model 4</b>					
UVLF during the occlusion test, PU	–2.35	0.81	8.42	0.09 (0.02–0.47)	0.004
I during the occlusion test	0.56	0.21	6.81	1.74 (1.15–2.64)	0.009
Rc during the occlusion test*	62.64	23.22	7.28	1.87 (1.19–2.95)	0.007
Age, years	–0.18	0.08	5.12	0.83 (0.71–0.98)	0.024
Invariable	3.91	3.7	1.12	–	0.290

microvessel blood flow at the nail bed. It is known that the reaction to the same stimulus is more pronounced in youngsters than in older people [12], which, for example, is evidenced by self-assessment using the pain VAS. Perhaps this explains that in the group of patients with severe PES, the average age of women was lower ( $35.07 \pm 5.74$ ), which was considered the risk factor ( $p = 0.005$ ). BMI less than  $25 \text{ kg/m}^2$  was also a risk factor of the severe PES development. According to our results, in overweight individuals, the microcirculation rate is higher, which contributes to milder PES, while all body systems work in an increased regulatory and compensatory mode, and therefore the metabolic load that occurs after UAE is more easily tolerated [12]. According to other data, in 2.8% of patients with myoma size under 12 weeks and in 7.3% of patients with myoma sized over 12 weeks the persistent intestinal paresis with vomiting was observed, which was associated with the reflex action of ischemic areas of the uterus on neighbouring organs, or transient intestinal ischemia as a result of accidental partial embolization of the superior mesenteric artery [3]. In our study, the average size of the dominant nodule was small, and there were no significant differences between the groups (see Table 1) due to the design of the study. Although, the nodules size correlated with the pain severity [13]. We noted that the myoma nodules' localization affected the postoperative period course. The subserous nodules' prevalence in the group of patients with severe PES was a risk factor, since ischemic nodules irritated the intestinal loops, led to nausea, bloating and other manifestations of gastrointestinal tract function impairment after UAE, thereby making PES worse in the early postoperative period (see Table 1). An increase in the amount and duration of bloody discharge (one of the PES symptoms) was caused by uterine fibroids of the submucous and interstitial localization that prevailed in group III [14].

In women with a perfusion rate at rest below 9.55 PU prior to the procedure, the more severe PES was observed. The M value in most of women with severe PES was lower compared with women with milder PES: 53.3% versus 11.1% ( $p = 0.004$ ) and 23.3% ( $p = 0.094$ ). Other researches obtained similar data, the low M value was also considered a risk factor of postoperative complications, in comparison with a group with a high M [15]. This may explain the fact that in patients with reduced M, in order to maintain normal microcirculation function under conditions of changing body metabolism with the development of severe PES, there is an increase in

microcirculation and its regulation (this takes time). It can be assumed that in patients with high M value, the severe PES probability is lower, since microcirculation in the whole body is good and it does not take time to involve regulation mechanisms to maintain homeostasis [12, 16]. Blood flow oscillations, UVLF, VLF, LF, HF, CF (Table 3) at rest, were of no prognostic value. During the occlusion test the endothelial and neurogenic blood flow oscillations changes were detected [17]. Since the occlusion test reflects the intensity of blood flow recovery and the microvessels reserve capabilities, the indicators evaluated have a high prognostic value. After the 3-minute cessation of blood flow during decompression, blood flow in the artery is restored and reactive hyperemia develops (capillary blood flow reserve capacity,  $\alpha$  angle, oxygen consumption index), which leads to the vasodilation causing endothelial production of nitric oxide stimulation through a neurogenic reaction [11, 16]. Slow microvessel blood flow recovery was a severe PES risk factor. Based on the data obtained, multivariate prognosis models were plotted.

## CONCLUSION

In our study, we plotted four severe PES prognosis models. The multivariate models included the severe PES risk factors. Anthropometric characteristics, such as age under 38.5 and BMI lower than  $25 \text{ kg/m}^2$  were included into the models. Among the microcirculation parameters obtained using LDF one need to pay attention to the background microcirculation level. When the M value at rest is under 9.55 PU, there is a high risk of severe PES. Models 1 and 2 plotted using the anthropometric characteristics and the background M level demonstrate AUC limited by 0.8–0.9, which can be considered “very good”. Models 3 and 4 with AUC limited by 0.9–1.0 (“excellent”) use the microcirculation data obtained under the load (occlusion test) prior to UAE, which are of great prognostic value. The higher are the I, R<sub>c</sub> and capillary blood flow reserve capacity values during the occlusion test, the higher is the risk of severe PES. On the contrary, the low value of  $\alpha$  angle during the occlusion test and low value of the UVLF oscillations are associated with the higher risk of severe PES. The doctor can use these prognostic models in his daily practice consulting the patients on the possible PES course and planning the treatment scheme in the earlier period after UAE, thereby facilitating the patient's well-being during the postoperative period.

## References

1. Adamyan LV, Serov VN, Sukhikh GT, Filippov OS, redactory. Klinicheskiye rekomendatsii. Akusherstvo i ginekologiya. Problemy reproduktiv. Spets vyp. 2017; 23 (6). Russian.
2. Shapovalova A. I. Lejomioma matki i reprodukciya. Zhurnal akusherstva i zhenskix boleznej. 2019; 68 (1): 93–101. <https://doi.org/10.17816/JOWD68193-101>. Russian.
3. Dobrohotova YuE, redaktor. Embolizaciya matochnyh arterij. Spb: Eksten Medikal, 2013; 112 s. Russian.
4. Marín-Sánchez P, Sánchez-Ferrer ML. Conservative management of vesical-vaginal fistula after partial uterine and bladder necrosis due to embolization as a treatment for postpartum hemorrhage. Int Urogynecol J. 2015; 26 (5): 773–4. DOI: 10.1007/s00192-014-2617-1.
5. Pillai AK, Kovoor JM, Reis SP, et al. Exposure of a Uterine Fibroid into the Small Bowel through Uterocentric Fistula Presenting with Bowel Obstruction after Uterine Fibroid Embolization: Case Report with Histopathological Correlation. J Vasc Interv Radiol. 2016; 27 (5): 762–4. DOI: 10.1016/j.jvir.2015.11.047.
6. Yu Q, Gabriel G, Hoffman M, Sanampudi S, Jassim T, Raissi D. Uterine-sparing management of pyomyoma after uterine fibroid embolization. Radiol Case Rep. 2019 Jun 12; 14 (8): 1031–5. DOI: 10.1016/j.radcr.2019.05.009.
7. Goryunova TV, Agapov VK, Cvirkun VV, Goloshchapov-Aksenov RS, Skrubert VS, Klimov MM, avtory; Goryunova TV, patentoobladatel'. Sposob lecheniya miomy matki. Patent RF № 2289415, A61K35/14, 20.12.2006. Russian.
8. Pirogova VI, Galanova ZM, Garipov RM, Muhametvaleeva GR, Galimov OV, Buzaev IV, i dr, avtory; Bashkirskij gosudarstvennyj medicinskij universitet, petentoobladatel'. Sposob profilaktiki posleoperacionnyh oslozhnenij embolizacii matochnyh arterij pri miomah matki. Patent RF № 2364335, A61V5/1473, A61K49/12, 20.08.2009. Russian.
9. Yudina TA, Manuhin IB, Tihomirov AL. Optimizaciya postembolizacionnogo perioda u bol'nyh miomoy matki. Akusherstvo i ginekologiya. 2017; (12): 110–4. DOI: <https://dx.doi.org/10.18565/aig.2017.12.110-114>. Russian.
10. Damirov MM, Shaxova OB, Sattarova ZI, Olejnikova ON.



- Sovremennyye podkhody k diagnostike narushenij mikrocirkulyacii v ginekologicheskoy praktike (obzor literatury). Zhurnal im. N.V. Sklifosovskogo «Neotlozhnaya medicinskaya pomoshch'». 2016; (1): 40–4. Russian.
11. Krupatkin AI, Sidorov VV. Lazernaya doplerovskaya floumetriya mikrocirkulyacii krovi: ruk-vo dlya vrachej. M.: Medicine, 2005; 126 s. Russian.
  12. Palcev MA, Paukov VS, redaktory. Patologiya v 2-h tomah: uchebnyk. M.: GEOTAR-Media, 2010; 1024 s. Russian.
  13. Sosin SA, Privorotskiy VV, Zazerskaya IE, Kustarov VN. Prognosticheskie pri-znaki vy'razhennosti boleвого синдрома после эмболизации маточных артерий у женщин с лейомиомой матки. Ginekologiya. 2017; 19 (5): 30–3. DOI: 10.26442/2079-5696\_19.5.30-33. Russian.
  14. Nurmukhametova ET, Shlyapnikov ME. Arkhitektonika miomatoznykh uzlov u zhenshchin. postupivshikh na lecheniye metodom embolizatsii matochnykh arteriy. Vestnik meditsinskogo instituta «Reaviz»: Reabilitatsiya, vrach i zdorovye. 2019; 2 (38): 48–54. Russian.
  15. Musin II, Fatkullina IB, Gazizova GH, Popova EM, Molokanova AR. Primenenie lazernoj dopplerovskoy floumetrii i biologicheskoy obratn oy svyazi s cel'yu profilaktiki erozij setchatogo proteza. Prakticheskaya medicina. 2019; 17 (4): 88–91. DOI: 10.32000/2072-1757-2019-4-88-91. Russian.
  16. Kozlov VI, Azizov GA, Gurova OA, Litvin FB. Lazernaya doplerovskaya floumetriya v ocenke sostoyanii i rasstrojstv mikrocirkulyacii krovi. Metodicheskoe posobie RUDN. Moskva, 2012; 32 s. Russian.
  17. Nurmukhametova ET, Shlyapnikov ME. Diagnosticheskaya znachimost' ocenki sostoyaniya perifericheskogo krvotoka после эмболии маточных артерий. Prakticheskaya medicina. 2018; 16 (8): 106–10. Russian.

## Литература

1. Адамьян Л. В., Серов В. Н., Сухих Г. Т., Филиппов О. С., редакторы. Клинические рекомендации. Акушерство и гинекология. Проблемы репродукции. Спец. вып. 2017; 23 (6).
2. Шаповалова А. И. Лейомиома матки и репродукция. Журнал акушерства и женских болезней. 2019; 68 (1): 93–101. <https://doi.org/10.17816/JOWD68193-101>.
3. Доброхотова Ю. Э., редактор. Эмболизация маточных артерий. СПб: Экстен Медикал, 2013; 112 с.
4. Marín-Sánchez P, Sánchez-Ferrer ML. Conservative management of vesical-vaginal fistula after partial uterine and bladder necrosis due to embolization as a treatment for postpartum hemorrhage. Int Urogynecol J. 2015; 26 (5): 773–4. DOI: 10.1007/s00192-014-2617-1.
5. Pillai AK, Kovoov JM, Reis SP, et al. Exposure of a Uterine Fibroid into the Small Bowl through Uteroenteric Fistula Presenting with Bowel Obstruction after Uterine Fibroid Embolization: Case Report with Histopathological Correlation. J Vasc Interv Radiol. 2016; 27 (5): 762–4. DOI: 10.1016/j.jvir.2015.11.047.
6. Yu Q, Gabriel G, Hoffman M, Sanampudi S, Jassim T, Raissi D. Uterine-sparing management of pyomyoma after uterine fibroid embolization. Radiol Case Rep. 2019 Jun 12; 14 (8): 1031–5. DOI: 10.1016/j.radcr.2019.05.009
7. Горюнова Т. В., Агапов В. К., Цвиркун В. В., Голощапов-Аксенов Р. С., Скруберт В. С., Климов М. М., авторы; Горюнова Т. В., патентообладатель. Способ лечения миомы матки. Патент РФ №2289415, А61К35/14, 20.12.2006.
8. Пирогова В. И., Галанова З. М., Гарипов Р. М., Мухаметвалеева Г. Р., Галимов О. В., Бузаев И. В., и др., авторы; Башкирский государственный медицинский университет, патентообладатель. Способ профилактики послеоперационных осложнений эмболизации маточных артерий при миоме матки. Патент РФ №2364335, А61В5/1473, А61К49/12, 20.08.2009.
9. Юдина Т. А., Манухин И. Б., Тихомиров А. Л. Оптимизация постэмболизационного периода у больных миомой матки. Акушерство и гинекология. 2017; (12): 110–4. DOI: <https://dx.doi.org/10.18565/aig.2017.12.110-114>.
10. Дамиров М. М., Шахова О. Б., Саттарова З. И., Олейникова О. Н. Современные подходы к диагностике нарушений микроциркуляции в гинекологической практике (обзор литературы). Журнал им. Н. В. Склифосовского «Неотложная медицинская помощь». 2016; (1): 40–4.
11. Крупаткин А. И., Сидоров В. В. Лазерная доплеровская флоуметрия микроциркуляции крови: рук-во для врачей. М.: Медицина, 2005; 126 с.
12. Пальцев М. А., Пауков В. С., редакторы. Патология в 2-х томах: учебник. М.: ГЭОТАР-Медиа, 2010. 1024 с.
13. Сосин С. А., Приворотский В. В., Зазерская И. Е., Кустаров В. Н. Прогностические признаки выраженности болевого синдрома после эмболизации маточных артерий у женщин с лейомиомой матки. Гинекология. 2017; 19 (5): 30–3. DOI: 10.26442/2079-5696\_19.5.30-33.
14. Нурмухаметова Э. Т., Шляпников М. Е. Архитектоника миоматозных узлов у женщин, поступивших на лечение методом эмболизации маточных артерий. Вестник медицинского института «Реавиз»: Реабилитация, врач и здоровье. 2019; 2 (38): 48–54.
15. Мусин И. И., Фаткуллина И. Б., Газизова Г. Х., Попова Е. М., Молоканова А. Р. Применение лазерной доплеровской флоуметрии и биологической обратной связи с целью профилактики эрозий сетчатого протеза. Практическая медицина. 2019; 17 (4): 88–91. DOI: 10.32000/2072-1757-2019-4-88-91.
16. Козлов В. И., Азизов Г. А., Гурова О. А., Литвин Ф. Б. Лазерная доплеровская флоуметрия в оценке состоянии и расстройств микроциркуляции крови. Методическое пособие РУДН. Москва. 2012, 32 с.
17. Нурмухаметова Э. Т., Шляпников М. Е. Диагностическая значимость оценки состояния периферического кровотока после эмболии маточных артерий. Практическая медицина. 2018; 16 (8): 106–10.

## SYNTHESIS OF A NOVEL AMIDE DERIVATIVE OF VALPROIC ACID AND 1,3,4-THIADIAZOLE WITH ANTIPILEPTIC ACTIVITY

Malygin AS<sup>1</sup>✉, Demidova MA<sup>1</sup>, Skachilova SYa<sup>2</sup>, Shilova EV<sup>2</sup>

<sup>1</sup> Tver State Medical University, Tver, Russia

<sup>2</sup> All-Russian Research Center for the Safety of Bioactive Substances, Staraya Kupavna, Moscow region, Russia

Valproates are commonly used to treat various forms of epilepsy. Problems accompanying their clinical application include drug resistance, adverse effects, acute and chronic toxicity. Safer anticonvulsants with improved efficacy can be obtained through the chemical modification of valproic acid structure. Thiadiazole-linked amide derivatives of valproates hold great promise because 1,3,4-thiadiazole can improve the drug's bioavailability and reduce its toxicity. The aim of this work was to synthesize a novel amide derivative of valproic acid and 1,3,4-thiadiazole exerting antiepileptic activity. The chemical structure of the synthesized valproate was studied by IR, proton NMR and <sup>13</sup>C-NMR-spectroscopy, mass spectroscopy and elemental analysis. The purity and individuality of the compound was confirmed by thin-layer and high-performance liquid chromatography. Its antiepileptic activity was assessed in the test with intraperitoneally injected 250 mg/kg isoniazid and subsequent Probit analysis. The synthesized N-(5-ethyl-1,3,4-thiadiazol-2-yl)-2-propyl pentane amide (valprazolamide) had the following characteristics. ESI<sup>+</sup>MS:  $m/z$  256.1 [M + H]<sup>+</sup>; MRM transitions:  $m/z$  256.1 —  $m/z$  81.0 and  $m/z$  130.1. The valproate exerted antiepileptic activity against isoniazid-induced seizures in mice. In the test with isoniazid, ED<sub>50</sub> of intraperitoneally injected VPZ was 126.8 mg/kg (95% CI: 65.5–245.4). Its therapeutic index was 7.3.

**Keywords:** antiepileptic drugs, valproic acid, 1,3,4-thiadiazole

**Author contribution:** Malygin AS — laboratory tests; data analysis; literature analysis; manuscript preparation; Demidova MA — study concept and design; manuscript preparation; Skachilova SYa, Shilova EV — synthesis and analysis of the compound; All authors equally contributed to the discussion of the study results.

**Compliance with ethical standards:** the study was approved by the Ethics Committee of Tver State Medical University (Protocol № 4 dated March 26, 2018). The animals were treated in compliance with the guidelines for laboratory practice in preclinical trials (Order 199n of the Russian Ministry of Healthcare dated April 1, 2016, on the *Good laboratory practice*). All tests were carried out in accordance with the guidelines for preclinical trials of medicinal drugs and in compliance with the European Convention for the Protection of Vertebrate Animals Used for Experimental and other Scientific Purposes (Directive 2010/63/EU).

✉ **Correspondence should be addressed:** Alexandr S. Malygin  
Sovetskaya, 4, Tver, 170100; dr.a.s.m@yandex.ru

**Received:** 17.01.2020 **Accepted:** 03.02.2020 **Published online:** 09.02.2020

**DOI:** 10.24075/brsmu.2020.007

## СИНТЕЗ НОВОГО АМИДНОГО ПРОИЗВОДНОГО ВАЛЬПРОЕВОЙ КИСЛОТЫ И 1,3,4-ТИАДИАЗОЛА С ПРОТИВОЭПИЛЕПТИЧЕСКОЙ АКТИВНОСТЬЮ

А. С. Малигин<sup>1</sup>✉, М. А. Демидова<sup>1</sup>, С. Я. Скачилова<sup>2</sup>, Е. В. Шилова<sup>2</sup>

<sup>1</sup> Тверской государственный медицинский университет, Тверь, Россия

<sup>2</sup> Всесоюзный научный центр по безопасности биологически активных веществ, Старая Купавна, Московская область, Россия

Вальпроаты являются основными препаратами для лечения эпилепсии различных форм. Среди проблем, возникающих при их клиническом использовании, — фармакорезистентность, нежелательные побочные реакции, а также проявления острой и хронической интоксикации. Путем модификации химической структуры вальпроевой кислоты возможно создание более эффективных и безопасных антиконвульсантов. Перспективно получение тиадиазолиламидных производных вальпроатов, так как 1,3,4-тиадиазол может повышать биодоступность и снижать токсичность лекарственных средств. Целью работы был синтез нового амидного производного вальпроевой кислоты и 1,3,4-тиадиазола с противоэпилептической активностью. Химическую структуру синтезированного вальпроата исследовали методами ИК-спектроскопии, <sup>1</sup>H-ЯМР, <sup>13</sup>C-ЯМР-спектроскопии, масс-спектроскопии и элементного анализа. Чистоту и индивидуальность подтверждали методами тонкослойной и высокоэффективной жидкостной хроматографий. Противоэпилептическую активность оценивали в тесте антагонизма с изониазидом (250 мг/кг, интраперитонеально) у мышей методом пробит-анализа. В результате исследования был получен N-(5-этил-1,3,4-тиадиазол-2-ил)-2-пропилпентанамид (вальпразоламид). ESI<sup>+</sup>-масс-спектр N-(5-этил-1,3,4-тиадиазол-2-ил)-2-пропилпентанамид —  $m/z$  256,1 [M + H]<sup>+</sup>, MRM-переходы —  $m/z$  256,1 —  $m/z$  81,0 и  $m/z$  130,1. Синтезированный вальпроат оказывал противоэпилептическое действие при изониазид-индуцированных судорогах у мышей. Значение ED<sub>50</sub> (интраперитонеально, мыши) в тесте антагонизма с изониазидом составило 126,8 мг/кг (95% ДИ: 65,5–245,4). Терапевтический индекс был равен 7,3.

**Ключевые слова:** противоэпилептические средства, вальпроевая кислота, 1,3,4-тиадиазол

**Вклад авторов:** А. С. Малигин — экспериментальное исследование, анализ результатов, обзор публикаций по теме статьи, написание текста; М. А. Демидова — концепция и дизайн исследования, написание и редактирование текста; С. Я. Скачилова, Е. В. Шилова — синтез и анализ соединения; все авторы участвовали в обсуждении результатов.

**Соблюдение этических стандартов:** исследование одобрено этическим комитетом Тверского государственного медицинского университета (протокол № 4 от 26 марта 2018 г.). Подопытных животных содержали согласно правилам лабораторной практики при проведении доклинических исследований в РФ (Приказ МЗ РФ № 199н от 01.04.2016 «Правила надлежащей лабораторной практики»). Все эксперименты осуществляли в соответствии с методическими рекомендациями по проведению доклинических исследований лекарственных средств с соблюдением «Европейской конвенции о защите позвоночных животных, используемых для экспериментов или в иных научных целях» (Directive 2010/63/EU).

✉ **Для корреспонденции:** Александр Сергеевич Малигин  
ул. Советская, д. 4, г. Тверь, 170100; dr.a.s.m@yandex.ru

**Статья получена:** 17.01.2020 **Статья принята к печати:** 03.02.2020 **Опубликована онлайн:** 09.02.2020

**DOI:** 10.24075/vrgmu.2020.007

Over 75 million people worldwide suffer from epilepsy, and this number is continuously growing [1–2]. The key challenge of modern epileptology is drug resistance. Only 14.9% of epilepsy patients go into sustained remission. Seizures recur in 48.1% of patients, at a rate of up to 12 episodes a year [3–4]. Half of epilepsy patients are on multidrug antiseizure regimens. Some of them do not benefit from polytherapy or a regimen switch, which often result in a poor quality of life and an increased risk of adverse effects. Noncompliance is another serious concern: in Russia, 18.05% of epilepsy patients do not take their medications [5]. Optimization of antiepileptic pharmacotherapy is a crucial task facing epileptology.

Valproic (2-propylpentanoic) acid holds a special place in the arsenal of anticonvulsant drugs. It was first synthesized in 1882 by Beverly S. Burton and used as a solvent. Its anticonvulsant properties were discovered by accident in 1963 and have been used in clinical practice ever since [6]. Valproates are antiepileptic agents with a broad action spectrum and first-choice drugs in patients with various forms of epilepsy. Long-term studies have demonstrated the efficacy of valproates against all forms of generalized epilepsy [7–9]. However, these compounds have adverse effects, including acute and chronic toxicity [10–12]. Valproates are highly teratogenic and therefore are not recommended to women of reproductive age [13]. Safer anticonvulsants with improved efficacy can be developed by modifying the chemical structure of valproic acid [14].

The aim of the study was to develop a novel anticonvulsant from a group of thiaziazole-linked amide derivatives of valproic acid.

## METHODS

### Reagents

The following reagents were used: 2-amino-5-ethyl-1,3,4-thiadiazole (Acros Organics; Belgium), 2-propylpentanoic acid (Sigma Aldrich; USA), pyridine (LenReaktiv; Russia), isoniazid (Semashko Moschimfarmpreparaty; Russia), hydrochloric acid (LenReaktiv; Russia), 2-propanol (LenReaktiv; Russia), acetonitrile (LC-MS; Scharlau, Spain), ammonium acetate (Panreac AppliChem ITW reagents; USA), ethanol (Medchimprom; Russia), Milli-Q deionized water.

## Equipment

The following equipment was used: an AB Sciex QTrap 3200 MD triple quadrupole mass spectrometer (Sciex; Singapore), an Agilent 1260 Infinity II high-performance liquid chromatography system (Agilent Technologies; Germany), TLC plates (silica gel 60 F 254) (Merck; Germany), a Bruker Avance-400 spectrometer (Bruker; Germany), an Agilent Cary 630 FTIR spectrometer (Agilent; Germany), an EA 1108 analyzer for elemental analysis (Carlo Erba Instruments; Italy), Acculab ALC-80d4 analytical scales (Acculab; USA), an Eppendorf 5810R centrifuge with a cooled rotor chamber (Eppendorf; Germany), a Millipore DirectQ UV water purification system (Millipore SAS; France), an Elmi V-3 vortex mixer (Elmi; Latvia), an Elmi S-3 shaker (Elmi; Latvia), a Thermo dry-block heater (DNA-Technology; Russia), Eppendorf (Eppendorf; Germany) and Black Thermo (Thermo Fisher Scientific; Russia) automated dispensers.

## Identification methods

The chemical structure of the synthesized valproate (N-(5-ethyl-1,3,4-thiadiazol-2-yl)-2-propyl pentane amide) was studied using IR, proton NMR and <sup>13</sup>C-NMR spectroscopy, mass-spectroscopy and elemental analysis. Purity of the obtained compound was evaluated by thin-layer (TLC) and high-performance liquid chromatography (HPLC).

## Tests of antiepileptic activity

The antiepileptic activity of the synthesized valproate was tested using a valproate antagonist (isoniazid). Generalized tonic-clonic seizures were induced in male outbred SNK mice (19–21 g body weight,  $n = 40$ ) by an intraperitoneal injection of 250 mg/kg isoniazid [15]. The animals were kept in a vivarium of Tver State Medical University at a constant temperature of  $22 \pm 2$  °C under a 12/12 light/dark cycle (lights on from 08:00 to 20:00). The animals had free access to food and water. The mice were randomized into 5 groups: the control group (isoniazid-induced seizures) and experimental groups (intraperitoneal administration of 75, 150, 300 and 450 mg/kg valproate 40 min before the isoniazid injection). Video observation lasted for 3 hours to assess latency to the first seizure, record the onset of

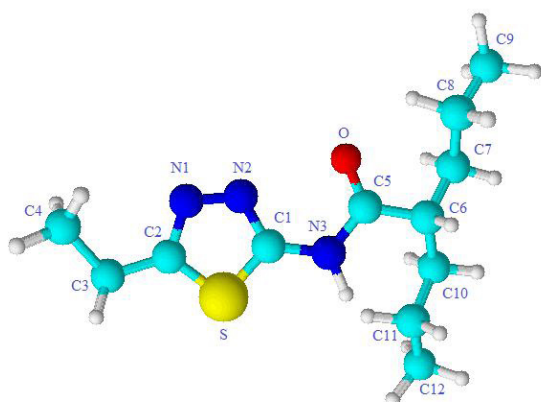


Fig. 1. N-(5-ethyl-1,3,4-thiadiazol-2-yl)-2-propyl pentane amide

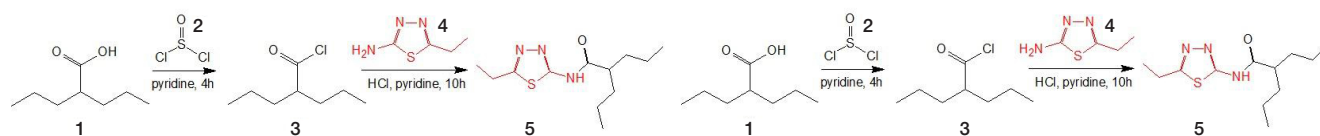
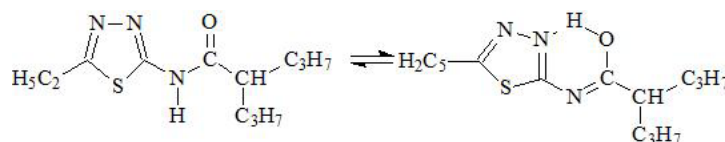


Fig. 2. A schematic representation of N-(5-ethyl-1,3,4-thiadiazol-2-yl)-2-propyl pentane amide synthesis. 1 — 2-propylpentanoic acid; 2 — thionyl chloride; 3 — 2-propylpentanoic acid chloroanhydride; 4 — 2-amino-5-ethyl-1,3,4-thiadiazole; 5 — N-(5-ethyl-1,3,4-thiadiazol-2-yl)-2-propyl pentane amide

clonic and tonic seizures and the outcomes (death or survival). We also calculated  $ED_{50}$  (the median effective dose required to ensure survival of 50% of the animals in the test) and the therapeutic index ( $TI = DL_{50}/ED_{50}$ , i.e. the ratio of the median lethal dose to the median effective dose).

### Statistical analysis

Statistical analysis was carried out in BioStat 2009 (AnalystSoft; USA). The results of the experiment were analyzed using descriptive statistics. The normality of data distribution was tested using the Shapiro-Wilk test. Group means were compared by one-way ANOVA with post-hoc Tukey HSD. Categorical variables were compared using Fisher's exact test. In this work, the data are presented as  $m \pm SEM$ . Finney Probit analysis was applied to calculate  $ED_{50}$ .

## RESULTS

### Synthesis

Fig. 1 shows the synthesized thiadiazole-linked amide derivative of valproic acid, N-(5-ethyl-1,3,4-thiadiazol-2-yl)-2-propyl

pentane amide. Its molecular formula is  $C_{12}H_{21}N_3OS$ . The laboratory name for the compound is valprazolamide (VPZ).

The synthesis of this novel anticonvulsant agent can be broken down in the following stages: halogenation of 2-propylpentanoic acid by thionyl chloride; stoichiometric interaction of the resulting 2-propylpentanoic acid chloroanhydride with 2-amino-5-ethyl-1,3,4-thiadiazole; acidification of the reaction mix by HCl (pH lowered to 1–2) at 5 °C for getting a crystalline precipitate (Fig. 2).

The synthesized compound was purified as described below. Water-soluble impurities were removed by washing the reaction product with cooled water; then, the product was refiltered and recrystallized in 2-propanol after preliminary vacuum-drying at 10 mmHg until its mass was constant (67% yield). Purification quality was assessed with TLC and HPLC.

### Description and identification of N-(5-ethyl-1,3,4-thiadiazol-2-yl)-2-propyl pentane amide

The synthesized pharmaceutical substance is a yellowish-white crystalline powder with a molar mass of 255.14 g/mol and a melting point of 93–94 °C. The powder is barely soluble in water but well soluble in alcohol, acetonitrile and other organic solvents.

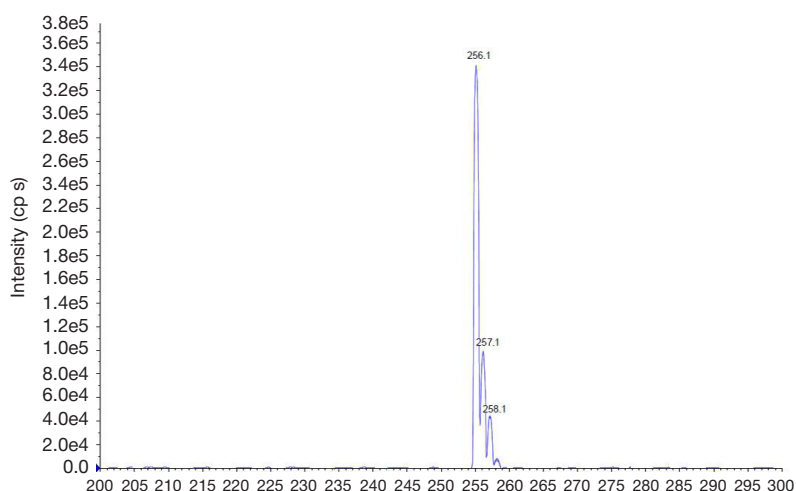


Fig. 3. ESI<sup>+</sup>-mass-spectrum of N-(5-ethyl-1,3,4-thiadiazol-2-yl)-2-propyl pentane amide ( $[M + H]^+$ )

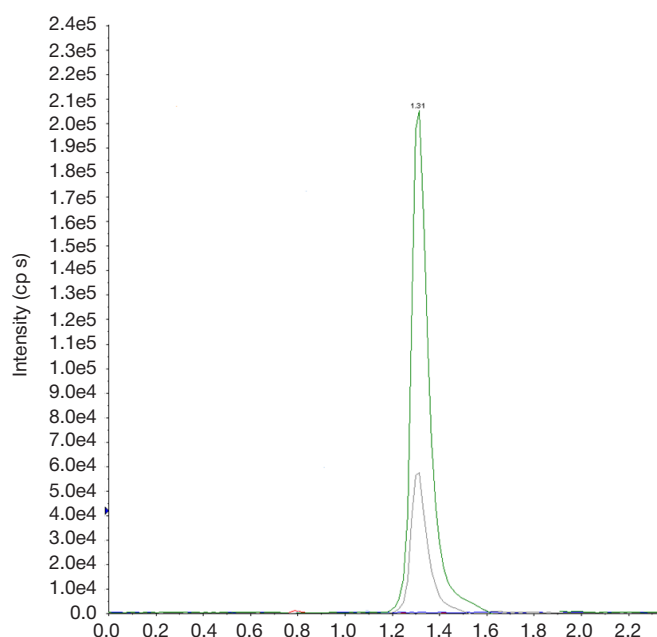


Fig. 4. A chromatogram of N-(5-ethyl-1,3,4-thiadiazol-2-yl)-2-propyl pentane amide



The chemical structure of N-(5-ethyl-1,3,4-thiadiazol-2-yl)-2-propyl pentane amide ( $C_{12}H_{21}N_3OS$ ) was confirmed by elemental analysis and spectroscopy. The predicted content of C in  $C_{12}H_{21}N_3OS$  was 56.44%; H, 8.29%; N, 16.45%; O, 6.26%; S, 12.56%. According to the results of the elemental analysis, the actual content of the elements was as follows: C, 56.39%; H, 8.34%; N, 16.41%; O, 6.26%; S, 12.60%, which was consistent with the chemical structure of the synthesized compound.

Spectroscopy results are shown below. IR spectra (KBr pelleting technique),  $\nu/cm^{-1}$ : 3302, 3030 (NH), 2981, 2959, 2860 (CH), 1545 (NHCO);  $^1H$ -NMR (400 MHz,  $DMSO-d_6$ )  $\delta$  ppm: 0.97 (s, 3H,  $CH_3$ ), 1.33 (s, 2H,  $CH_2$ ), 1.41–1.50 (m, 4H), 2.65 (s, 2H,  $CH_2$ ), 10.63 (s, 1H, NH);  $^{13}C$ -NMR (400 MHz,  $DMSO-d_6$ )  $\delta$  ppm: 13.48, 13.66, 20.06, 24.70, 35.27, 43.22, 155.85, 156.5, 175.00; ESI+MS:  $m/z$  256.1 ( $[M + H]^+$ ); MRM transitions:  $m/z$  256.1  $\rightarrow$   $m/z$  81.1 and  $m/z$  130.1. ESI+ MS for N-(5-ethyl-1,3,4-thiadiazol-2-yl)-2-propyl pentane amide is shown in Fig. 3.

Purity of the synthesized anticonvulsant agent was assessed by HPLC at 50 °C using a Phenomenex synergi 4  $\mu$ m C18 Fusion column (2  $\times$  50 mm). For elution, 90 : 10 methanol : deionized water and 0.1% ammonium acetate were used. Retention time was 1.31 min (Fig. 4).

#### Antiepileptic activity tests in a mouse model of isoniazid-induced seizures

Intraperitoneal administration of 250 mg/kg isoniazid induced generalized tonic-clonic seizures resulting in the death of all control animals. An injection of VPZ given 40 min before isoniazid administration had a dose-dependent effect on the progression of isoniazid-induced seizures in mice ( $p < 0.0001$ ; one-way ANOVA). A 75 mg/kg VPZ dose significantly increased seizure latency (by 1.5-fold) in the experimental groups in comparison with the control animals, but did not prevent seizures or animal death. At 150 and 300 mg/kg, VPZ increased seizure latency and reduced the death rate. In a test with 450 mg/kg VPZ, no seizures were observed for 3 h following isoniazid administration (see Table).

Probit analysis revealed that  $ED_{50}$  of intraperitoneally injected VPZ was 126.8 mg/kg (95% CI: 65.5–245.4) in the test with VPZ antagonist. The therapeutic index was 7.3.

#### DISCUSSION

Candidate anticonvulsant agents must be effective against refractory epilepsy, have fewer side effects and better tolerability, as well as the ability to slow down progression of the disease and modify its course. Additional advantages

include linear pharmacokinetics, simplicity of titration in the clinical setting, ancillary therapeutic effects such as relief of neuropathic pain. Such candidates are usually searched for among novel molecules or developed based on the derivatives of known anticonvulsants.

The possibility of creating new-generation valproates has been shown in the literature [16]. The teratogenicity of their amide analogs is significantly lower than that of valproic acid [17]. Valproic acid amides demonstrate antiepileptic [18], antineuropathic [19–20], antiviral [21–22] and some other properties. A number of 1,3,4-thiadiazole derivatives, including those that contain a valproic acid residue, have been reported to exert anticonvulsant activity [23]. The majority of such derivatives have higher bioavailability and are less toxic than their analogs. This is also true for the valproate synthesized in this study, containing 1,3,4-thiadiazole. Using a mouse model, researchers have demonstrated that  $DL_{50}$  of an intraperitoneally injected 1,3,4-thiadiazole-linked amide derivative of valproic acid is 1.8 times higher than that of valproic acid [24]. The antiepileptic effect of the synthesized valproate has been confirmed in maximal electroshock seizure models and pentylenetetrazole-induced seizure models in mice [25–26]. Considering that VPZ was the most active in a test with a GABAA-receptor antagonist (pentylenetetrazole), we studied the effect of this valproate on the seizures induced by another GABA antagonist isonicotinyldiazide (isoniazid). The proconvulsant effect of isoniazid is linked to the inhibition of GABA synthesis resulting from isoniazid antagonism towards pyridoxal phosphate, a coenzyme of glutamate decarboxylase that catalyzes glutamate conversion into GABA. Antituberculous therapy with isoniazid can cause serious complications in the form of seizures often described as status epilepticus. Isoniazid-induced seizures are poorly controlled by conventional anticonvulsants and cannot always be prevented by pyridoxine intake [27–28]. Valproates are known to inhibit development of isoniazid-induced seizures in a dose-dependent fashion [29]. Our study demonstrates that an injection of N-(5-ethyl-1,3,4-thiadiazol-2-yl)-2-propyl pentane amide before seizure modeling increased latency to the first seizure and reduced the death rate in mice in the isoniazid test. Based on these findings, N-(5-ethyl-1,3,4-thiadiazol-2-yl)-2-propyl pentane amide can be considered a candidate antiepileptic drug with an improved safety profile.

#### CONCLUSIONS

The results of the study confirm that modification of valproic acid with 1,3,4-thiadiazole holds promise for discovering novel anticonvulsant candidate drugs. The advantage of the synthesized N-(5-ethyl-1,3,4-thiadiazol-2-yl)-2-propyl pentane amide is its

**Table.** The effect of N-(5-ethyl-1,3,4-thiadiazol-2-yl)-2-propyl pentane amide (VPZ) on the latency to the first seizure and survival of mice in the test with the VPZ antagonist isoniazid (250 mg/kg injected intraperitoneally)

Test	Dose, mg/kg	LS1, min $m \pm SEM$	Number of surviving mice /total number of mice	Survival, %
NaCl IS + INH	–	31.25 $\pm$ 2.03	0/8	0
VPZ + INH	75	47.75 $\pm$ 2.42*	0/8	0
VPZ + INH	150	72.13 $\pm$ 4.28*	5/8	62.5#
VPZ + INH	300	93.75 $\pm$ 4.77*	7/8	87.5#
VPZ + INH	450	–	8/8	100#

**Note:** \* — statistically significant difference between the experimental group and the control animals (mice with isoniazid-induced seizures treated with NaCl IS before the isoniazid injection) ( $p < 0.05$ ; one-way ANOVA with post-hoc Tukey HSD); # — statistically significant difference between the experimental group and the control ( $p < 0.05$ ; Fisher's exact test). VPZ is valprazolamide (N-(5-ethyl-1,3,4-thiadiazol-2-yl)-2-propyl pentane amide); INH is isoniazid; NaCl IS is the isotonic solution of sodium chloride; LS1 is latency to the first seizure.

ability to prevent development of isoniazid-induced seizures. The compound is not soluble in water, which is a disadvantage, since it hinders manufacturing of its injectable formulations. Further research will be focused on the improvement of the

compound's biological and pharmaceutical properties by loading it onto  $\beta$ -cyclodextrin nanocapsules. Methods of N-(5-ethyl-1,3,4-thiadiazol-2-yl)-2-propyl pentane amide identification can also be applied to test its originality and used in pharmacokinetic studies.

## References

1. Singh A, Trevick S. The epidemiology of global epilepsy. *Neurol Clin.* 2016 Nov; 34 (4): 837–47. PubMed PMID: 27719996.
2. Avakyan GN. Questions modern epileptology. *Epilepsy and paroxysmal conditions.* 2015; 7 (4): 16–21. Russian.
3. Avakyan GN, Belousova ED, Burd SG, Vlasov PN, Ermolenko NA, Kissin MY, et al. Current trends in epileptology: priorities, challenges, tasks and solutions. *Epilepsy and paroxysmal conditions.* 2019; 11 (4): 395–406. Russian.
4. Kalilani L, Sun X, Pelgrims B, Noack-Rink V, Villanueva V. The epidemiology of drug-resistant epilepsy: A systematic review and meta-analysis. *Epilepsia.* 2018; 59 (12): 2179–93. PubMed PMID: 30426482.
5. Avakyan GN, Vlasov PN, Zhidkova IA, Karlov VA, Lebedeva AV, Mikhailovska-Karova EP, et al. Conclusion of the Council of Experts on the use of valproate in patients with epilepsy. *Neurology, neuropsychiatry, psychosomatics. Epilepsy and paroxysmal conditions.* 2015; 7 (1): 69. Russian.
6. Tomson T, Battino D, Perucca E. The remarkable story of valproic acid. *Lancet Neurol.* 2016 Feb; 15 (2): 141. PubMed PMID: 28463122.
7. Voronkova KV, Nikitin AE, Rudakova IG, Vlasov PN, Burd SG, Lebedeva AV, et al. Today's choice of antiepileptic therapy: stages and recommendations. *Epilepsy and paroxysmal conditions.* 2018; 10 (2): 74–81. Russian.
8. Mukhin KYu, Petrukhin AS, Mironov MB. Sodium valproate (Depakine) in achieving remission in patients with idiopathic generalized epilepsy (long-term follow-up). *Neurological journal.* 2004; (4): 34–39. Russian.
9. Perucca E. Pharmacological and therapeutic properties of valproate: a summary after 35 years of clinical experience. *CNS Drugs.* 2012; 16 (10): 695–714.
10. Badalyan OL, Burd SG, Savenkov AA, Avakyan GG, Yutskova EV, Avakyan GN. Comparative evaluation of the efficacy and safety of valproic acid derivatives. *Epilepsy and paroxysmal conditions.* 2014; 6 (2): 39–44. Russian.
11. Schneider NA, Dmitrenko DV. Chronic intoxication with valproic acid in epileptology: diagnosis and treatment. *Neurology, neuropsychiatry, psychosomatics.* 2016; 8 (2): 94–99. Russian.
12. Sztajnkrzyer MD. Valproic acid toxicity: overview and management. *J Toxicol Clin Toxicol.* 2002; 40 (6): 789–801. PubMed PMID:12475192.
13. Tomson T, Battino D, Perucca E. Valproic acid after five decades of use in epilepsy: time to reconsider the indications of a time-honoured drug. *Lancet Neurol.* 2016 Feb; 15 (2): 210–8. PubMed PMID: 26655849.
14. Pessah N, Yagen B, Hen N, Shimshoni JA, Wlodarczyk B, Finnell RH, Bialer M. Design and pharmacological activity of glycinamide and N-methoxy amide derivatives of analogs and constitutional isomers of valproic acid. *Epilepsy Behav.* 2011 Nov; 22 (3): 461–8. PubMed PMID:21959082.
15. Sun XY, Wei CX, Deng XQ, Sun ZG, Quan ZS. Evaluation of the anticonvulsant activity of 6-(4-chlorophenoxy)-tetrazolo[5,1-a] phthalazine in various experimental seizure models in mice. *Pharmacological Reports: PR.* 01 Mar 2010, 62 (2): 273–7. PubMed PMID: 20508282.
16. Trojnar MK, Wierzchowska-Cioch E, Krzyzanowski M, Jargiełło M, Czuczwar SJ. New generation of valproic acid. *Pol J Pharmacol.* 2004 May-Jun; 56 (3): 283–8. PubMed PMID: 15215557.
17. Lin YL, Bialer M, Cabrera RM, Finnell RH, Wlodarczyk BJ. Teratogenicity of valproic acid and its constitutional isomer, amide derivative valnoctamide in mice. *Birth Defects Res.* 2019 Aug 15; 111 (14):1013–23. PubMed PMID: 30325584.
18. Haines KM, Matson LM, Dunn EN1, Ardinger CE, Lee-Stubbs R, Bibi D, McDonough JH, Bialer M. Comparative efficacy of valnoctamide and sec-butylpropylacetamide (SPD) in terminating nerve agent-induced seizures in pediatric rats. *Epilepsia.* 2019 Feb; 60 (2): 315–21. PMID: 30615805.
19. Kaufmann D, Bialer M, Shimshoni JA, Devor M, Yagen B. Synthesis and evaluation of antiallosteric and anticonvulsant activity of novel amide and urea derivatives of valproic acid analogues. *J Med Chem.* 2009 Nov 26; 52 (22): 7236–48. PubMed PMID 19877649.
20. Samur DN, Arslan R, Aydın S, Bektas N. Valnoctamide: The effect on relieving of neuropathic pain and possible mechanisms. *Eur J Pharmacol.* 2018 May 15; (827): 208–14. PubMed PMID: 29522726.
21. Praena B, Bello-Morales R, de Castro F, López-Guerrero JA. Amidic derivatives of valproic acid, valpromide and valnoctamide, inhibit HSV-1 infection in oligodendrocytes. *Antiviral Res.* 2019 Aug; (168): 91–99. PubMed PMID: 31132386.
22. Ornaghi S, Hsieh LS, Bordey A, Vergani P, Paidas MJ, van den Pol AN. Valnoctamide Inhibits Cytomegalovirus Infection in Developing Brain and Attenuates Neurobehavioral Dysfunctions and Brain Abnormalities. *J Neurosci.* 2017 Jul 19; 37 (29): 6877–93. PubMed PMID: 28630251.
23. Jain AK, Sharma S, Vaidya A, Ravichandran V, Agrawal RK. 1,3,4-Thiadiazole and its Derivatives: A Review on Recent Progress in Biological Activities. *Chem Biol Drug Des.* 2013; (81): 557–76. PubMed PMID: 23452185.
24. Malygin AS. Assessment of acute toxicity and neurotoxicity of a new amide derivative of valproic acid and 1,3,4-thiadiazole. *The medicine.* 2019 (3): 37–46. Russian.
25. Malygin AS. Study on the antiepileptic activity of the new amide derivative of valproic acid and 1,3,4-thiadiazole. *Epilepsy and paroxysmal conditions.* 2019; 11 (4): 357–63. Russian.
26. Skachilova SYa, Malygin AS, Popov NS, Demidova MA, avtory; Vladelets patenta: «Vsesoyuznyy nauchnyy tsentr po bezopasnosti biologicheskii aktivnykh veshchestv». N-(5-etil-1,3,4-thiadiazol-2-il)-2-propilpentanamid, obladayushchii protivoepilepticheskoy i obezboivayushchey aktivnostyami. Patent RU № 2 672 887. 13.03. 2018. Russian.
27. Bernasconi R, Klein M, Martin P, Portet C, Maître L, Jones RS, et al. The specific protective effect of diazepam and valproate against isoniazid-induced seizures is not correlated with increased GABA levels. *J Neural Transm.*1985; 63 (2): 169–89. PubMed PMID: 3930661.
28. Asehinde S, Ajayi A, Bakre A, Omorogbe O, Adebesein A, Umukoro S. Effects of Jobelyn® on Isoniazid-Induced Seizures, Biomarkers of Oxidative Stress and Glutamate Decarboxylase Activity in Mice Basic Clin Neurosci. 2018 Nov-Dec; 9 (6): 389–96. PMID: 30719253.
29. Minns AB, Ghafouri N, Clark RF. Isoniazid-induced status epilepticus in a pediatric patient after inadequate pyridoxine therapy. *Pediatr Emerg Care.* 2010 May; 26 (5): 380–1. PubMed PMID: 20453796.

## Литература

1. Singh A, Trevick S. The epidemiology of global epilepsy. *Neurol Clin.* 2016 Nov; 34 (4): 837–47. PubMed PMID: 27719996.
2. Авакян Г. Н. Вопросы современной эпилептологии. Эпилепсия и пароксизмальные состояния. 2015; (4): 16–21.
3. Авакян Г. Н., Белоусова Е. Д., Бурд С. Г., Власов П. Н., Ермоленко Н. А., Киссин М. Я. и др. Проблемы эпилептологии. Ключевые приоритеты, задачи, вызовы и способы их решения. Эпилепсия и пароксизмальные состояния. 2019; 11 (4): 395–406.
4. Kalilani L, Sun X, Pelgrims B, Noack-Rink V, Villanueva V. The epidemiology of drug-resistant epilepsy: A systematic review and meta-analysis. *Epilepsia.* 2018; 59 (12): 2179–93. PubMed PMID: 30426482.
5. Авакян Г. Н., Власов П. Н., Жидкова И. А., Карлов В. А., Лебедева А. В., Михаловская-Карлова Е. П. и др. Заключение Совета экспертов по применению вальпроатов у пациенток с эпилепсией. *Неврология, нейропсихиатрия, психосоматика. Эпилепсия.* 2015; (1): 63–64.
6. Tomson T, Battino D, Perucca E. The remarkable story of valproic acid. *Lancet Neurol.* 2016 Feb; 15 (2): 141. PubMed PMID: 28463122.
7. Воронкова К. В., Никитин А. Э., Рудакова И. Г., Власов П. Н., Бурд С. Г., Лебедева А. В. и др. Современный выбор антиэпилептической терапии: этапы и рекомендации. Эпилепсия и пароксизмальные состояния. 2018; 10 (2): 74–81.
8. Мухин К. Ю., Петрухин А. С., Миронов М. Б. Вальпроат натрия (Депакин) в достижении ремиссии у больных идиопатической генерализованной эпилепсией (долгосрочный катамнез). *Неврологический журнал.* 2004; (4): 34–39.
9. Perucca E. Pharmacological and therapeutic properties of valproate: a summary after 35 years of clinical experience. *CNS Drugs.* 2012; 16 (10): 695–714.
10. Бадалян О. Л., Бурд С. Г., Савенков А. А., Авакян Г. Г., Юцкова Е. В., Авакян Г. Н. Сравнительная оценка эффективности и безопасности производных вальпроевой кислоты: опыт применения. Эпилепсия и пароксизмальные состояния. 2014; 6 (2): 39–44.
11. Шнайдер Н. А., Дмитренко Д. В. Хроническая интоксикация вальпроевой кислотой в эпилептологии: диагностика и лечение. *Неврология, нейропсихиатрия, психосоматика.* 2016; 8 (2): 94–99.
12. Sztajnkrycer MD. Valproic acid toxicity: overview and management. *J Toxicol Clin Toxicol.* 2002; 40 (6): 789–801. PubMed PMID: 12475192.
13. Tomson T, Battino D, Perucca E. Valproic acid after five decades of use in epilepsy: time to reconsider the indications of a time-honoured drug. *Lancet Neurol.* 2016 Feb; 15 (2): 210–8. PubMed PMID: 26655849.
14. Pessah N, Yagen B, Hen N, Shimshoni JA, Wlodarczyk B, Finnell RH, Bialer M. Design and pharmacological activity of glycinamide and N-methoxy amide derivatives of analogs and constitutional isomers of valproic acid. *Epilepsy Behav.* 2011 Nov; 22 (3): 461–8. PubMed PMID: 21959082.
15. Sun XY, Wei CX, Deng XQ, Sun ZG, Quan ZS. Evaluation of the anticonvulsant activity of 6-(4-chlorophenoxy)-tetrazolo[5,1-a] phthalazine in various experimental seizure models in mice. *Pharmacological Reports: PR.* 01 Mar 2010, 62 (2): 273–7. PubMed PMID: 20508282.
16. Trojnar MK, Wierzchowska-Cioch E, Krzyzanowski M, Jargiełło M, Czuczwar SJ. New generation of valproic acid. *Pol J Pharmacol.* 2004 May–Jun; 56 (3): 283–8. PubMed PMID: 15215557.
17. Lin YL, Bialer M, Cabrera RM, Finnell RH, Wlodarczyk BJ. Teratogenicity of valproic acid and its constitutional isomer, amide derivative valnoctamide in mice. *Birth Defects Res.* 2019 Aug 15; 111 (14): 1013–23. PubMed PMID: 30325584.
18. Haines KM, Matson LM, Dunn EN1, Ardinger CE, Lee-Stubbs R, Bibi D, McDonough JH, Bialer M. Comparative efficacy of valnoctamide and sec-butylpropylacetamide (SPD) in terminating nerve agent-induced seizures in pediatric rats. *Epilepsia.* 2019 Feb; 60 (2): 315–21. PMID: 30615805.
19. Kaufmann D, Bialer M, Shimshoni JA, Devor M, Yagen B. Synthesis and evaluation of antiallodynic and anticonvulsant activity of novel amide and urea derivatives of valproic acid analogues. *J Med Chem.* 2009 Nov 26; 52 (22): 7236–48. PubMed PMID 19877649.
20. Samur DN, Arslan R, Aydın S, Bektas N. Valnoctamide: The effect on relieving of neuropathic pain and possible mechanisms. *Eur J Pharmacol.* 2018 May 15; (827): 208–14. PubMed PMID: 29522726.
21. Praena B, Bello-Morales R, de Castro F, López-Guerrero JA. Amidic derivatives of valproic acid, valpromide and valnoctamide, inhibit HSV-1 infection in oligodendrocytes. *Antiviral Res.* 2019 Aug; (168): 91–99. PubMed PMID: 31132386.
22. Ornaghi S, Hsieh LS, Bordey A, Vergani P, Paidas MJ, van den Pol AN. Valnoctamide Inhibits Cytomegalovirus Infection in Developing Brain and Attenuates Neurobehavioral Dysfunctions and Brain Abnormalities. *J Neurosci.* 2017 Jul 19; 37 (29): 6877–93. PubMed PMID: 28630251.
23. Jain AK, Sharma S, Vaidya A, Ravichandran V, Agrawal RK. 1,3,4-Thiadiazole and its Derivatives: A Review on Recent Progress in Biological Activities. *Chem Biol Drug Des.* 2013; (81): 557–76. PubMed PMID: 23452185.
24. Малыгин А. С. Оценка острой токсичности и нейротоксичности нового амидного производного вальпроевой кислоты и 1,3,4-тиадиазола. *Медицина.* 2019; (3): 37–46.
25. Малыгин А. С. Исследование противосудорожной активности нового амидного производного вальпроевой кислоты и 1,3,4-тиадиазола. Эпилепсия и пароксизмальные состояния. 2019; 11 (4): 357–63.
26. Скачилова С. Я., Малыгин А. С., Попов Н. С., Демидова М. А., авторы; Владелец патента: «Всесоюзный научный центр по безопасности биологически активных веществ». N-(5-этил-1,3,4-тиадиазол-2-ил)-2-пропилпентанамид, обладающий противосудорожной и обезболивающей активностями. Патент РФ № 2 672 887. 13.03. 2018.
27. Asehinde S, Ajayi A, Bakre A, Omorogbe O, Adebesin A, Umukoro S. Effects of Jobelyn® on Isoniazid-Induced Seizures, Biomarkers of Oxidative Stress and Glutamate Decarboxylase Activity in Mice. *Basic Clin Neurosci.* 2018 Nov–Dec; 9 (6): 389–96. PMID: 30719253.
28. Minns AB, Ghafouri N, Clark RF. Isoniazid-induced status epilepticus in a pediatric patient after inadequate pyridoxine therapy. *Pediatr Emerg Care.* 2010 May; 26 (5): 380–1. PubMed PMID: 20453796.
29. Bernasconi R, Klein M, Martin P, Portet C, Maître L, Jones RS et al. The specific protective effect of diazepam and valproate against isoniazid-induced seizures is not correlated with increased GABA levels. *J Neural Transm.* 1985; 63 (2): 169–89. PubMed PMID: 3930661.

## EFFICIENCY OF THE GYNECOLOGIC MALIGNANCIES IDENTIFICATION MEASURES AT THE LEVEL OF PRIMARY HEALTH CARE

Bochkova AG<sup>1</sup>✉, Domozhirova AS<sup>2</sup>, Aksenova IA<sup>1,3</sup>

<sup>1</sup> South Ural State Medical University, Chelyabinsk, Russia

<sup>2</sup> Russian Scientific Center of Roentgenoradiology, Moscow, Russia

<sup>3</sup> Clinical Center of Oncology and Nuclear Medicine of Chelyabinsk Region, Chelyabinsk, Russia

In Russia, for more than 10 years, within the framework of national projects, the activities have been carried out aimed at restructuring of the primary and specialized (including high-tech) medical care, as well as strengthening of primary health care directed at early detection of malignant neoplasms. The study was aimed to evaluate the effectiveness of the patient examination rooms for women in improvement of the adjusted cumulative survival of patients with gynecologic malignancies detected actively in 2005–2015 in the Chelyabinsk Region. Using the Population Based Cancer Registry (PBCR) of the Chelyabinsk Region database, the adjusted cumulative survival calculation for patients with cervical cancer (389), uterine corpus cancer (373) and ovarian cancer (161) detected actively in the patient examination rooms of the Chelyabinsk Region (treatment group), as well as for cervical cancer (395), uterine corpus cancer (380) and ovarian cancer (163) detected in patients who sought medical assistance (control group), was performed for the first time. The staging of cervical cancer detected in the examination rooms in 2010–2017 was characterized by the high proportion of I/II stage tumors compared with the rest of patients' population of the Chelyabinsk Region (an average of 50.8 and 46.1% respectively). For uterine corpus cancer the average proportion was 85.5 and 82.0% respectively, and for ovarian cancers it was 42.0 and 37.4% respectively. Analysis of the PBCR of the Chelyabinsk Region for a 10-year period revealed the 5-year adjusted cumulative survival improvement in the actively detected cervical cancer patients compared to the control group (62.3 and 55.8%) respectively ( $p = 0.11$ ). In patients with uterine corpus cancer, it was 82.0% for the main group and 70.4% for the control group ( $p = 0.001$ ). In ovarian cancer patients, no significant differences in the 5-year adjusted cumulative survival were observed (47.5% in the main group, 43.2% in the control group) ( $p = 0.49$ ). Thus, the patient examination rooms are the effective model of the cancer secondary prevention available in the Chelyabinsk Region.

**Keywords:** gynecologic malignancies, early detection, patient examination rooms, secondary prevention of cancer

**Author contribution:** Bochkova AG — research planning, manuscript writing, data acquisition, data analysis and interpretation, literature analysis; Domozhirova AS — research planning, data analysis and interpretation, manuscript editing; Aksenova IA — data acquisition, manuscript writing.

**Compliance with ethical standards:** the study was approved by the Ethics Committee of South Ural State Medical University (protocol № 9 dated November 8, 2018).

✉ **Correspondence should be addressed:** Anna G. Bochkova  
Dovatora, 23, Chelyabinsk, 454091; annabochkova7496@mail.ru

**Received:** 23.12.2019 **Accepted:** 08.01.2020 **Published online:** 22.01.2020

**DOI:** 10.24075/brsmu.2020.003

## ОЦЕНКА ЭФФЕКТИВНОСТИ ПУТЕЙ ВЫЯВЛЕНИЯ ОПУХОЛЕЙ ЖЕНСКИХ ПОЛОВЫХ ОРГАНОВ НА УРОВНЕ ПЕРВИЧНОГО ЗВЕНА ЗДРАВООХРАНЕНИЯ

А. Г. Бочкова<sup>1</sup>✉, А. С. Доможирова<sup>2</sup>, И. А. Аксенова<sup>1,3</sup>

<sup>1</sup> Южно-Уральский государственный медицинский университет, Челябинск, Россия

<sup>2</sup> Российский научный центр рентгенодиагностики, Москва, Россия

<sup>3</sup> Челябинский областной клинический центр онкологии и ядерной медицины, Челябинск, Россия

В России более 10 лет в рамках национальных проектов проводят мероприятия, направленные на преобразование первичной и специализированной, в том числе высокотехнологичной медицинской помощи, усиление роли первичного медико-санитарного звена в целях раннего выявления злокачественных новообразований (ЗНО). Целью исследования было оценить результативность работы женских смотровых кабинетов (СК) в улучшении показателей кумулятивной скорректированной выживаемости (СкВ) больных с ЗНО женских половых органов, выявленных активно с 2005 по 2015 гг. на территории Челябинской области (ЧО). На основе базы данных Популяционного ракового регистра (ПРР) ЧО впервые осуществлены расчеты показателей кумулятивной СкВ больных с ЗНО шейки матки (389), тела матки (373) и яичников (161), выявленных активно в СК ЧО (основная группа), и случаи ЗНО шейки матки (395), тела матки (380) и яичников (163), выявленных в ходе самообращений пациенток (группа контроля). Стадийную структуру активно выявленных случаев ЗНО шейки матки в СК за период 2010–2017 гг. характеризует большой удельный вес I-II стадий по сравнению с остальной популяцией заболевших в ЧО — в среднем 50,8 и 46,1% соответственно, в отношении ЗНО тела матки — 85,5 и 82,0% соответственно, для овариальных раков — в среднем 42,0 и 37,4% соответственно. Анализ базы данных ПРР ЧО за 10-летний период позволил установить увеличение 5-летней кумулятивной СкВ для больных с диагнозом ЗНО шейки матки, выявленных активно в СК по сравнению с контрольной группой — 62,3 и 55,8% соответственно ( $p = 0,11$ ). В отношении ЗНО тела матки — 82,0% в основной группе и 70,4% в группе контроля ( $p = 0,001$ ). У больных с ЗНО яичников достоверных различий в показателях 5-летней кумулятивной СкВ не отмечено — 47,5% в основной и 43,2% в группе контроля ( $p = 0,49$ ). Таким образом, СК — одна из эффективных организационных моделей вторичной профилактики рака на территории ЧО.

**Ключевые слова:** рак женских половых органов, раннее выявление, смотровые кабинеты, вторичная профилактика рака

**Вклад авторов:** А. Г. Бочкова — планирование исследования, подготовка рукописи, сбор данных, анализ и интерпретация данных, анализ литературы; А. С. Доможирова — планирование исследования, анализ и интерпретация данных, редактирование рукописи; И. А. Аксенова — сбор данных, подготовка рукописи.

**Соблюдение этических стандартов:** исследование одобрено этическим комитетом ЮУГМУ Минздрава России (протокол № 9 от 8 ноября 2018 г.).

✉ **Для корреспонденции:** Анна Геннадьевна Бочкова  
ул. Доватора, д. 23, г. Челябинск, 454091; annabochkova7496@mail.ru

**Статья получена:** 23.12.2019 **Статья принята к печати:** 08.01.2020 **Опубликована онлайн:** 22.01.2020

**DOI:** 10.24075/vrgmu.2020.003



Malignant neoplasms are one of the main problems on the agenda of modern medicine, and the leading cause of mortality in developed and developing countries [1, 2]. The economic losses from cancer are due to the significant costs of welfare and social insurance associated with the high cost of treatment, preventive and rehabilitation measures, as well as the long and often persistent disability. Thus, malignant neoplasms can be considered an essential problem of modern society.

The largest part in the structure of oncological morbidity in women in the Russian Federation belongs to the reproductive system malignancies (38.9%), a half of which are gynecologic malignancies.

In 2017 in Russia over 26,000 new cases of uterine corpus cancer (3rd place, 7.8%), over 17,500 cases of cervical cancer (5th place, 5.3%), and over 14,500 cases of ovarian cancer (9th place, 4.3%) were registered [3].

Demographic shift, environmental and reproductive dissonance, general deterioration of women's health along with an increase in the frequency of reproductive system malignancies require targeted and urgent decision-making regarding the prevention, screening and early diagnosis of malignant neoplasms through the interdisciplinary interaction of different specialists.

In Russian Federation, the three-level model of medical care for cancer patients has been put into practice, and primary healthcare is the basic platform on which the preventive measures are implemented. The basis is being formed for developing a motivation for the people to preserve and maintain a good health aimed to reduce mortality and disability due to disease [4].

The reduction of mortality of visually detectable gynecologic malignancies entirely depends on the quality and timeliness of the primary diagnosis [5].

Created in the early 1960s, a powerful network of patient examination rooms proved its high efficiency in the active detection of malignant neoplasms more than once. Thus, the proportion of diagnosed cervical cancer in all registered patients in the 1960s and 1970s reached 40% [6].

The cost-effectiveness of routine check-ups was repeatedly analyzed. The analysis demonstrated that preventive measures, the identification and treatment of patients with precancerous diseases and early forms of cancer require significantly less public spending than the treatment of patients with overt malignancies [7].

The main task of the patient examination room for women is to conduct the routine check-up of all women (over 18), who contacted the medical organizations for the first time during the year for the early detection of visually detectable chronic, pre-tumor and tumor diseases. Externally localized tumors that can be detected during the routine check-up account for 30% of all malignant tumors in people of both sexes and almost 40% in women [8].

It is very important to make the check-ups in the patient examination rooms widespread. Thus, in populations where the screening quality and coverage were high, a significant reduction in the invasive cervical cancer patients was detected [9, 10].

In addition, it is necessary to understand that neither the modern equipment of the patient examination rooms, nor the high qualifications and experience of the conducting the check-up obstetrician would be able to provide high final results if the contingent of women to be examined is not determined, the frequency of check-ups is not established, the flow of visits is not regulated, and a system of additional examination and routing of identified patients is not mastered. Thus, the active position of the primary health care medical organizations heads,

who understand the importance of the routine check-ups in the patient examination rooms and focus on the corresponding area development, becomes relevant.

The study was aimed to evaluate the increased survival rate of patients with gynecologic malignancies in the Chelyabinsk Region through the use of the effective cancer detection in the patient examination rooms.

## METHODS

In our study we used the data on the patients newly diagnosed with the visually detectable gynecologic malignancies registered in the Population Based Cancer Registry (PBCR) of the Chelyabinsk Region database formed in 2005–2017, as well as the reports on the functioning of the patient examination rooms in the Chelyabinsk Region municipalities' health care institutions during the specified period.

The treatment group included 923 patients aged 20 and over, who were diagnosed actively with the malignant neoplasms in the Chelyabinsk Region patient examination rooms in 2005–2015. Moreover, the distribution in accordance with the tumor localization was as follows: cervical cancer was diagnosed in 389 (42.1%) patients, uterine corpus cancer in 373 (40.4%) patients, and ovarian cancer in 161 (17.4%) patients respectively.

The control group included 938 patients aged 22 and over, who sought medical assistance and were diagnosed with the malignant neoplasms during the same period: cervical cancer was diagnosed in 395 (42.1%) patients, while uterine corpus cancer and ovarian cancer in 380 (40.5%) and 163 (17.4%) patients respectively.

The studied group' randomization was performed by the stratometric selection using the totality of the main prognostic signs (age at the time of diagnosis, stage of the disease, tumor morphological structure) in accordance with listed below inclusion and exclusion criteria.

Inclusion criteria: 100% morphologically verified cervical cancer cases, detected actively in the Chelyabinsk Region patient examination rooms (treatment group) or upon the patients' individual appointment requests (control group).

Exclusion criteria: multiple primary malignancy cases, except the cases of combination with the skin basal cell carcinoma; lack of information about the cancer detection circumstances; lack of information about the patient's condition at the end of the year; the status of patients departed to the other regions of the country (according to the PBCR of the Chelyabinsk Region).

In the treatment group with a verified cervical cancer diagnosis, patients with localized tumors prevailed (the total number of patients with the I/II-stage cancer was 199 (51.2%), and in the control group it was 199 (50.4%)) ( $p > 0.05$ ) (Table 1).

The stage distribution of the new uterine corpus cancer cases demonstrated the high proportion of the I/II-stage cancer: 303 (81.2%) patients in the treatment group and 303 (79.7%) patients in the control group ( $p > 0.05$ ). That could be explained by the features of the disease clinical picture, which caused patients to consult doctors early, especially at the premenopausal and menopausal age (Table 2).

Among the ovarian cancer patients, the patients with the III/IV-stage disease prevailed: 96 (59.6%) patients in the treatment group and 96 (58.9%) people in the control group; there were no significant differences ( $p > 0.05$ ) (Table 3).

The treatment group patients with cervical cancer were mainly aged 23–92, the average age was  $51.6 \pm 14.2$ , and the control group patients were aged 20–88, the average age

**Table 1.** Stage distribution in cervical cancer patients (C53) of the treatment and control groups according to the FIGO system (2009)

Groups		Stage of the disease											
		I	IA	IB	II	IIA	IIB	III	IIIA	IIIB	IV	IVA	IV B
Treatment	Abs.	28	22	33	27	8	81	25	2	141	14	4	4
(n-389)	%	7.2	5.7	8.5	6.9	2.1	20.8	6.4	0.5	36.2	3.6	1	1
Control	Abs.	30	23	28	33	4	81	32	4	136	16	4	4
(n-395)	%	7.6	5.8	7.1	8.4	1	20.5	8.1	1	34.4	4.1	1	1

was  $51.4 \pm 14.0$  ( $p = 0.81$ ). It is worth mentioning that it is the women aged 40–59 who are mainly examined in the patient examination rooms, while people aged 39 and younger make up only one fourth of the total number of the patients examined. The poor coverage of young patients with the routine check-ups is reflected in a 1.5-fold increase in the cervical cancer invasive forms detection in the Chelyabinsk Region in this age group over the past 10 years.

The age of the treatment group uterine corpus cancer patients was 31–86 (average age  $62.2 \pm 9.7$ ), and the age of patients in the control group was 35–85 (average age  $61.9 \pm 9.7$ ); there were no significant differences ( $p = 0.72$ ). The highest proportion of the endometrial cancer incidence was observed in women aged 60–69 (130 (34.9%) people in the treatment group and 136 (35.8%) people in the control group).

The age of the treatment group ovarian cancer patients was 20–80 (average age  $57.3 \pm 13.5$ ), and the age of patients in the control group was 20–83 (average age  $57.1 \pm 13.0$  ( $p = 0.90$ )).

The important prognostic factor in the cancer patients' survival rate was the primary tumor morphological type which was verified in all patients of the groups compared. Statistical analysis of both groups of patients with cervical cancer, uterine corpus cancer and ovarian cancer in accordance with the main histological tumor types revealed no significant differences ( $p > 0.05$ ).

Based on the PBCR of the Chelyabinsk Region data, the calculation of adjusted cumulative survival parameters for patients with malignant neoplasms of the cervix, uterus and ovaries was performed for the first time, taking into account the circumstances of the cancer detection. The calculation of survival rates was carried out using the traditional methods of data analysis at the population level. To calculate the survival rate at the population level, the actuarial (dynamic) method was used, taking into account the probable life expectancy and using age-specific mortality tables for each period of the indicator calculation. The reference date was the onset of the disease (date of diagnosis), recommended for survival assessment at the population level. If the indicators of observed survival are calculated taking into account all the causes of death of the cancer patient, for which reason they are indicative, then the indicators of adjusted survival take into account the deaths of cancer patients only of the underlying disease, while those who die from intercurrent diseases are equated to those who was

excluded from the observation; all indicators are expressed in% [11, 12]. The calculation of survival rates and their average errors was carried out using the mathematical part of the PBCR of the Chelyabinsk Region software. The differences were considered significant when  $p < 0.05$

## RESULTS

In 2005–2017 in 27 municipal districts and 16 urban districts of the Chelyabinsk Region, 167 patient examination rooms out of 176 established were actively operating. The total number of patient examination rooms for women was 104. In addition, in municipal districts, the function of the examination rooms was assigned to feldsher-obstetric centers, which operate as the combined patient examination rooms for men and women.

The examination rooms for women are operated by the paramedical staff (feldsher, obstetrician), who has undergone special training in oncology and has the appropriate certificate, or an obstetrician-gynecologist or dermatovenerologist who has undergone advanced training in oncology (the course of at least 72 training hours). According to the requirements, the examination in the patient examination room should target the medical personnel to detect the visually detectable tumors in both male and female patients and not to carry out the selective examination of individual organs and systems.

The importance and effectiveness of this technology for secondary prevention of malignant neoplasms is associated with the following factors:

- medical care accessibility: double shift working, examination during the first visit to the medical institution, no queue and no need to book the voucher for appointment;

- strict adherence to the routing principles for patients with identified pathology and in the case of malignant neoplasm detection, transfer of the patient from hand to hand on the day of contacting a relevant specialist or oncologist with priority of examination;

- mandatory endocervical channel and cervix smears collection and subsequent sample transfer to the cytology laboratory, sample registration, as well as monitoring the number of uninformative smears.

In 2007–2017 over 5 million women (5,136,098) aged over 20 attended the patient examination rooms for examination and cytological screening aimed to detect the precancerous

**Table 2.** Stage distribution in uterine corpus cancer patients (C54) of the treatment and control groups according to the FIGO system (2009)

Groups		Stage of the disease												
		I	I A	I B	II	IIA	IIB	III	IIIA	IIIB	IIIC	IV	IVA	IV B
Treatment	Abs.	99	52	79	14	45	14	24	12	13	4	2	12	3
(n-373)	%	26.5	13.9	21.2	3.8	12.1	3.8	6.4	3.2	3.5	1.1	0.5	3.2	0.8
Control	Abs.	95	60	78	12	47	11	26	18	14	1	2	14	2
(n-380)	%	25	15.8	20.5	3.2	12.4	2.9	6.8	4.7	3.7	0.3	0.5	3.7	0.5

**Table 3.** Stage distribution in ovarian cancer patients (C56) of the treatment and control groups according to the FIGO system (2009)

Groups		Stage of the disease												
		I	IA	IB	IC	II	IIA	IIB	IIC	III	IIIA	IIIB	IIIC	IV
Treatment	Abs.	21	14	1	17	3	2	5	2	26	4	3	31	32
(n-161)	%	13	8.7	0.6	10.6	1.9	1.2	3.1	1.2	16.1	2.5	1.9	19.3	19.9
Control	Abs.	21	16	1	16	4	2	6	1	25	3	3	34	31
(n-163)	%	12.9	9.8	0.6	9.8	2.5	1.2	3.7	0.6	15.3	1.8	1.8	20.9	19

conditions, chronic diseases and malignancies (about 49.5% of women over 20 living in the region). Thus, a certain "reserve" is created out of an average of 50.5% of people who seek medical help much less than once a year, which means they cannot be fully covered by preventive measures, including examinations in the patient examination rooms.

During their work, patient examination rooms proved to be highly effective, which was reflected by the total number of actively detected the visually detectable gynecologic malignancies, but also by the total number of detected chronic and precancerous diseases. Thus, in 2017 the patient examination rooms personnel diagnosed 97,367 of all diseases in women, which was 53.7% more compared to 2007. In the structure of the diseases detected the chronic diseases have the highest proportion: 66,805 (68.61%) cases in 2017, 40,106 (63.3%) cases in 2007; the increase over the 10-year follow-up period was 66.6%. The average detectability of chronic diseases (% of the examined in the examination rooms' patients) was 11.2%. In accordance with their detectability in the patient examination rooms, precancerous diseases were on the 2<sup>nd</sup> place (29,885 (30.7%) patients in 2017, 22,801 (36.0%) patients in 2007; the increase over the specified period was 31.1%, the average detectability for the region was 5.9% of the examined patients number). Malignant neoplasms were on the 3<sup>rd</sup> place in accordance with the detectability in the patient examination rooms. In 2017 677 cancer patients were identified (12.0 per 10,000 surveyed patients), which made up 7.5% of the total number of identified women with cancer in Chelyabinsk Region. Compared to 2007, the increase in the absolute number of identified cancer patients became 1.5 times higher (by 50.8%).

In 2007–2017 the patients examination rooms employees identified 548 uterine corpus cancer patients (8.6% of the total number of endometrioid cancer cases for the region), 567 cervical cancer patients (an average of 12.9% of the number of cervical cancer patients detected in the region) and 254 ovarian cancer patients (6.4% of the total number of ovarian cancer patients in the region). The average proportion of identified I/II-

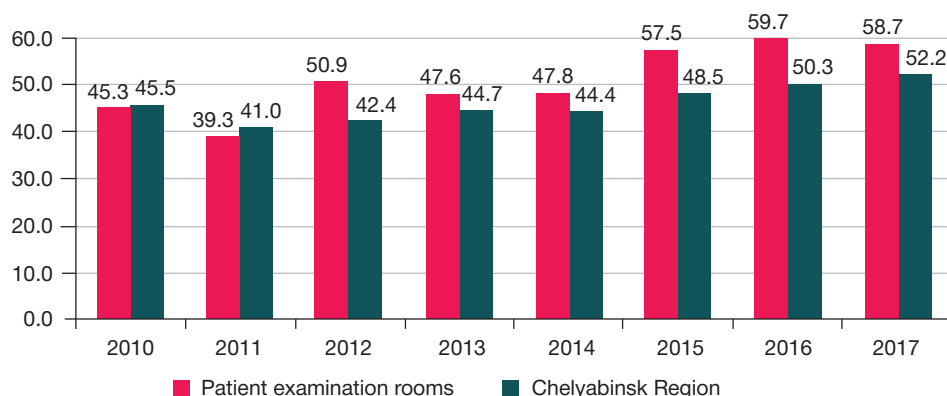
stage uterine corpus cancer patients in 2010–2017 was 85.5%, the proportion of cervical cancer patients was 50.8%, and the proportion of ovarian cancer patients was 42.0%, which was higher than similar indicators for the region (82.0%, 46.1% and 37.4% respectively) (Fig. 1–3).

When evaluating the work of the patient examination rooms, much attention was paid to the indicators of the workload, which were calculated based on the regulated length of the examination room working day (7 hours (shift), examination of four patients per hour, 252 working days per year).

In 2007, at the beginning of the examination rooms' work, the workload reached 51.4%. Starting from 2009, due to the opening of a number of new patient examination rooms, the workload increase was noted up to 77.9% in 2017. We calculated the possible number of identified cancer patients under ideal conditions (100% loading of patient examination rooms). The data obtained allowed us to conclude that with a full load of patient examination rooms for women in the region during 2007–2017 another 3,438 cancer patients would be identified instead of 6,876, i.e., 50.0% higher than the baseline. Of them, the number of I/II-stage cancer patients would be 7,448 instead of 4,986. The method of least squares was used to approximate direct relationship between the number of examined patients and the number of cancer patients identified in the patient examination rooms of the Chelyabinsk Region over the 10-year observation period. The determination coefficient was 0.591, which demonstrated a high correlation of the model with actual data (correlation coefficient  $r = 0.77$ ;  $p = 0.007$ ).

Using cytological screening, in the patient examination rooms from 79.6% women in 2007 to 94.7% women in 2017 were examined, while the coverage with cytological investigations increase towards 100%. In 2007–2017 the total number of collected cytological smears was over 4.5 million (an average of more than 410,000 smears per year).

The most important quality criterion for evaluating the cancer prevention measures effectiveness is the cancer patients' survival rate, which also reflects the adequacy of the detected cancer staging [13].

**Fig. 1.** Dynamics of the I/II stage cervical cancer (C53) proportion in patients identified actively in the patient examination rooms compared with the average rate for Chelyabinsk Region in 2010–2017, %

During the study, it was possible to demonstrate the advantage of the 5-year adjusted cumulative survival in cervical cancer patients identified actively in the patient examination rooms compared with the control group (62.3 versus 55.8%) ( $p = 0.11$ ) (Fig. 4).

In the uterine corpus cancer patients, the significant 5-year survival rate differences were obtained:  $82.0 \pm 2.6$  in the treatment group and  $70.4 \pm 2.6$  in the control group ( $p = 0.001$ ). Figure 5 demonstrates that the survival curves diverge over time.

In the ovarian cancer patients, no significant differences in the 5-year adjusted cumulative survival were detected: 47.5% in the main group and 43.2% in the control group ( $p = 0.49$ ) (Fig. 6). Many authors agree that despite the high sensitivity of most modern diagnostic methods, their specificity is insufficient to differentiate benign and malignant processes in the ovaries, and diagnostic of each and every woman (including those not at high risk) result in minimal impact on mortality [14–16].

## DISCUSSION

The improvement of the cancer early detection system should be started with the most accessible visually detectable cancer, the diagnosis of which does not require expensive diagnostic equipment and in-depth knowledge of oncology in primary health care specialists.

Despite the fact that preventive examinations play a significant role in the malignant neoplasms diagnosis, over the past 10 years in the Russian Federation, the number of patient examination rooms increased by 48% and in 2017 it reached 4989, i.e., an average of patient examination rooms for each of the 85 existing constituent regions of the Russian Federation (for instance, in 2017, in the Chelyabinsk Region

the number of patient examination rooms reached 176), while the number of employees working double shifts was only 20%. Insufficient coverage of the population with the routine check-ups ultimately affects the total low proportion of actively detected cancer patients (25.8% in 2017 in Russian Federation). Despite the visual localization, in 2017, the proportion of cervical cancer patients detected actively in Russia was 42.2%; the proportion of uterine corpus cancer patients (29.1% in 2017) and ovarian cancer patients (18.4% in 2017) attending the check-ups was significantly lower. As a result, in every 2<sup>nd</sup> and 3<sup>rd</sup> patient in Russia, the ovarian and cervical cancer is diagnosed at the III/IV stage (58.5 and 32.4% respectively in 2017), which leads to low survival rates in these groups of patients, despite the number of applied treatment methods [17]. That is why there is now an urgent need for the national preventive programs aimed at the early detection and adequate treatment of preventable cancer types.

Analysis of the PBCR of the Chelyabinsk Region database for the 10-year observation period allowed us to determine, that the 5-year adjusted cumulated survival in patients with cervical cancer identified actively in the patient examination rooms appear to be more advantageous compared with the rest of the patient population (62.3 and 55.8% respectively) ( $p = 0.11$ ). A similar trend is observed in patients with the visually undetectable tumors, such as uterine corpus cancer and ovarian cancer (82.0 versus 70.4% ( $p = 0.001$ ) and 47.5 versus 43.2% respectively ( $p = 0.49$ )).

Such a heterogeneous group of tumors as ovarian cancer for over 30 years has been associated with slight success in long-term treatment outcome with 5-year survival rate not exceeding the 50% threshold (48.4%) [18]. This is mainly due to the lack of reliable screening programs to date

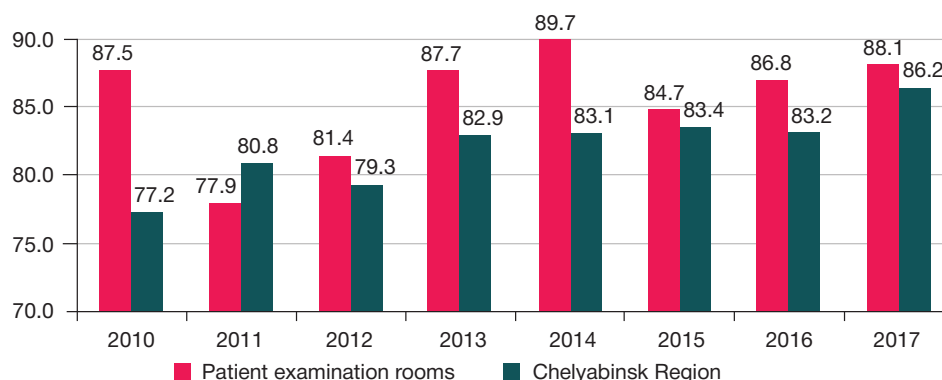


**Fig. 2.** Dynamics of the I/II stage uterine corpus cancer (C54) proportion in patients identified actively in the patient examination rooms compared with the average rate for Chelyabinsk Region in 2010–2017, %

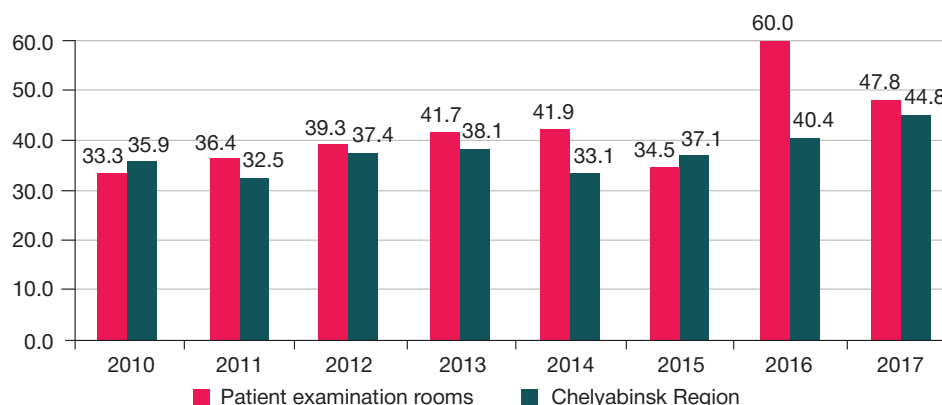


**Fig. 3.** Dynamics of the I/II stage ovarian cancer (C56) proportion in patients identified actively in the patient examination rooms compared with the average rate for Chelyabinsk Region in 2010–2017, %



allowing one to solve the problem of the ovarian cancer early diagnosis.

In general, the effectiveness of the patient examination rooms is due to the following: mass character and threading of the routine check-ups in the examination rooms (examination of at least four patients per hour throughout

the full working day of the clinic on a double shift basis). It is such a load that allows one to sort out the cohort of individuals with clinically non-manifesting pathology types from the total mass of the examined patients for subsequent in-depth examination. Such a task becomes impossible for a narrow specialist due to the fact that, because of the

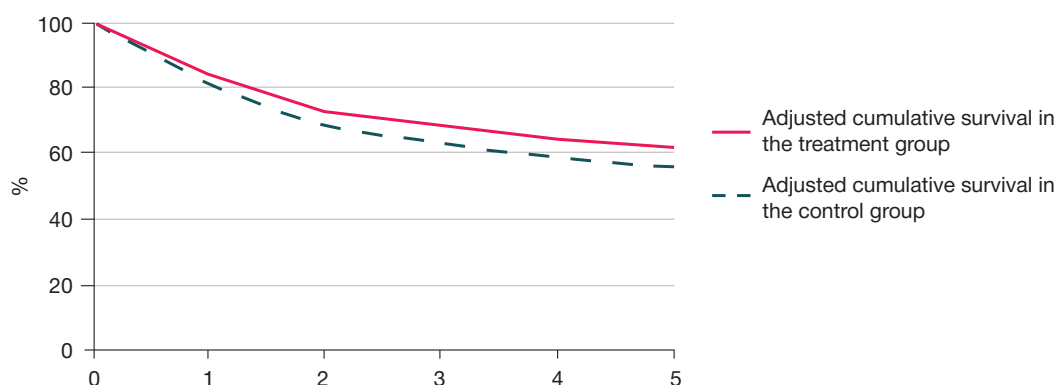


Fig. 4. Adjusted cumulative survival in cervical cancer patients (C53) of the treatment and control groups (PBCR of the Chelyabinsk Region database, 2005–2015), %

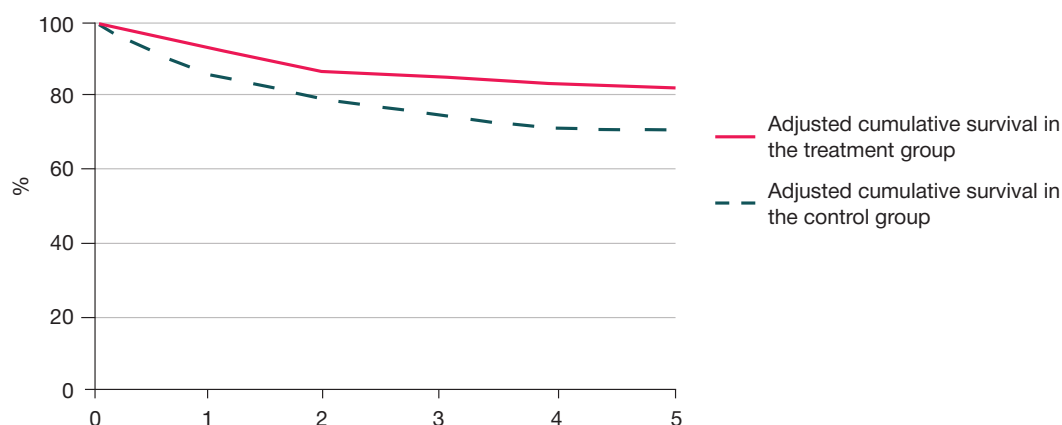


Fig. 5. Adjusted cumulative survival in uterine corpus cancer patients (C54) of the treatment and control groups (PBCR of the Chelyabinsk Region database, 2005–2015), %

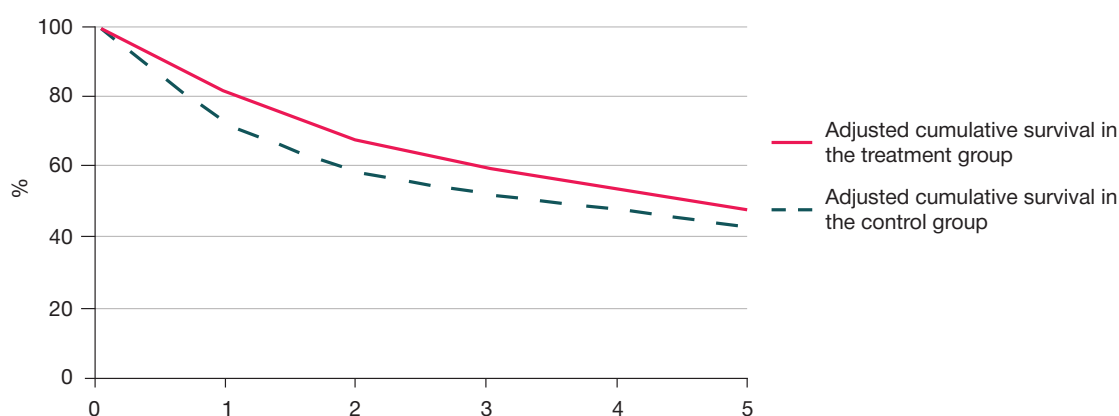


Fig. 6. Adjusted cumulative survival in ovarian cancer patients (C56) of the treatment and control groups (PBCR of the Chelyabinsk Region database, 2005–2015), %

mentality peculiarities, the patients plan a visit to a profile specialist only with a list of specific questions inherent in the particular specialist's qualification. The work is complicated by the need of booking the voucher for appointment, which forces patients to adapt to the schedule and choose the time for the visit. While in the patient examination rooms the patients are offered to get a full examination during their first visit to the health care institution.

According to the check-up results, patients with suspected oncopathology from the very beginning attract close attention of the health care specialists and acquire the right of priority in-depth examination, while the terms of the proposed in-depth examination should fit into a strict time frame, namely 10 days from the date the diagnosis is suspected. Such patients, unlike others, without delay get

into oncological institutions in case of cancer detection, which means they receive all the needed specialized oncological care in a timely manner.

## CONCLUSION

Further development of programs aimed to improve the patient examination rooms' attendance in the Chelyabinsk Region, as well as the introduction of the proposed tactical algorithm in the work of the primary health care unit of the obstetric and gynecological service for the early detection of background, precancerous and malignant neoplasms, in the future will improve cancer early detection rate, and therefore minimize the costs of further treatment and rehabilitation of such patients, and, which is most important, improve the cancer patients survival rate.

## References

1. Sushinskaya TV, Zhordania KI, Payanidi YuG. Analiticheskie aspekty onkologicheskikh zabolevaniy zhenskogo naseleniya Rossii. *Onkoginekologiya*. 2015; (3): 40–3. Russian.
2. Global Cancer Facts & Figures. 3rd edition. Atlanta, Georgia: American Cancer Society. 2015; 61 p.
3. Kaprin AD, Starinskiy VV, Petrova GV, redaktory. Zlokachestvennye novoobrazovaniya v Rossii v 2017 godu (zabolevaemost' i smertnost'). M.: MNIOL im. P.A. Gertsena — filial FGBU «NMICradiologii» Minzdrava Rossii, 2018; 250 s. Russian.
4. Aleksandrova LM, Starinskiy VV, Kaprin AD, Samsonov YuV. Profilaktika onkologicheskikh zabolevaniy kak osnova vzaimodeystviya onkologicheskoy sluzhby s pervichnym zvenom zdravookhraneniya. *Issledovaniya i praktika v meditsine*. 2017; (4): 74–80. Russian.
5. Moshurov IP, Kravets BB, Korotkikh NV. Organizatsionnye rezervy snizheniya smertnosti ot raka sheyki matki. *Onkoginekologiya*. 2014; (4): 28–33. Russian.
6. Krivonos OV, Chissov VI, Starinskiy VV, Aleksandrova LM. Rol'i zadachi smotrovogo kabineta polikliniki kak etapa v organizatsii profilakticheskikh meropriyatiy, napravlennykh na sovershenstvovanie onkologicheskoy pomoshchi naseleniyu: metodicheskie rekomendatsii. M., 2010. Available from: [http://www.oncology.ru/service/organization/exam\\_room.pdf](http://www.oncology.ru/service/organization/exam_room.pdf) (data obrascheniya: 10.11.2019). Russian.
7. Domozhirova AS, Vazhenin AV. Vtorichnaya profilaktika raka v sisteme regional'nogo zdravookhraneniya. M.: Izd-vo RAMN, 2012; 192 s. Russian.
8. Shubin BM, Vinokur ML, Popova AA. Vyyavlenie opukholevykh zabolevaniy v smotrovom kabine. Leningrad: Meditsina, 1980; 208 s. Russian.
9. ACOG Practice Bulletin Number 131: Screening for cervical cancer. *Obstet Gynecol*. 2012; 120 (5): 1222–38.
10. Ronco G, Anttila A. Cervical cancer screening in Europe — changes over the last 9 years. *Eur J Cancer*. 2009; 45 (15): 2629–31. DOI: 10.1016/j.ejca.2009.07.021.
11. Petrova GV, Grecova OP, Kaprin AD, Starinskiy VV. Harakteristika i metody rascheta mediko-statisticheskikh pokazatelej, primenyaemykh v onkologii. M.: FGBU MNIOL im. P.A. Gercena Minzdrava RF, 2014; 40 s.
12. Merabishvili VM. Onkologicheskaya statistika (tradicionnye metody, novye informacionnye tekhnologii): Rukovodstvo dlya vrachej. Izd. 2-e, dop. SPb., 2015; 248 s.
13. Merabishvili VM. Vyzhivaemost' onkologicheskikh bol'nyh. SPb., 2011; 329 s.
14. Urmancheeva AF, Kutusheva GF, Ul'rih EA. Opuholi yaichnika (klinika, diagnostika i lechenie). SPb.: Izd-vo N-L, 2012; 68 s.
15. Jacobs IJ, Menon U, Ryan A, Gentry-Maharaj A, Burnell M, Kalsi JK, et al. Ovarian cancer screening and mortality in the UK Collaborative Trial of Ovarian Cancer Screening (UKCTOCS): a randomised controlled trial. *Lancet*. 2016; 387 (10022): 945–56. PubMed PMID: 26707054.
16. Johnson N. Two large randomised trials show ovarian cancer screening has minimal impact on survival. *BJOG*. 2016; 125 (5): 524–5.
17. Kaprin AD, Starinskiy VV, Petrova GV, redaktory. Sostoyanie onkologicheskoy pomoshchi naseleniyu Rossii v 2017 godu. M.: MNIOL im. P.A. Gercena — filial FGBU «NMICradiologii» Minzdrava Rossii, 2018; 236 s.
18. Howlader N, Noone AM, Krapcho M, Miller D, Brest A, Yu M, et al. SEER Cancer Statistics Review, 1975–2016, National Cancer Institute. Bethesda, MD. Available from: [https://seer.cancer.gov/csr/1975\\_2016/sections.html](https://seer.cancer.gov/csr/1975_2016/sections.html).

## Литература

1. Сушинская Т. В., Жордания К. И., Паяниди Ю. Г. Аналитические аспекты онкологических заболеваний женского населения России. *Онкогинекология*. 2015; (3): 40–3.
2. Global Cancer Facts & Figures. 3rd edition. Atlanta, Georgia: American Cancer Society. 2015; 61 p.
3. Каприн А. Д., Старинский В. В., Петрова Г. В., редакторы. Злокачественные новообразования в России в 2017 году (заболеваемость и смертность). М.: МНИОИ им. П. А. Герцена — филиал ФГБУ «НМИЦ радиологии» Минздрава России, 2018; 250 с.
4. Александрова Л. М., Старинский В. В., Каприн А. Д., Самсонов Ю. В. Профилактика онкологических заболеваний как основа взаимодействия онкологической службы с первичным звеном здравоохранения. *Исследования и практика в медицине*. 2017; (4): 74–80.
5. Мошуров И. П., Кравец Б. Б., Коротких Н. В. Организационные резервы снижения смертности от рака шейки матки. *Онкогинекология*. 2014; (4): 28–33.
6. Кривonos О. В., Чиссов В. И., Старинский В. В., Александрова Л. М. Роль и задачи смотрового кабинета поликлиники как этапа в организации профилактических мероприятий, направленных на совершенствование онкологической помощи населению: методические рекомендации. М., 2010. Доступно по ссылке: [http://www.oncology.ru/service/organization/exam\\_room.pdf](http://www.oncology.ru/service/organization/exam_room.pdf) (дата обращения: 10.11.2019).
7. Доможирова А. С., Важенин А. В. Вторичная профилактика рака в системе регионального здравоохранения. М.: Изд-во РАМН, 2012; 192 с.

8. Шубин Б. М., Винокур М. Л., Попова А. А. Выявление опухолевых заболеваний в смотровом кабинете. Ленинград: Медицина, 1980; 208 с.
9. ACOG Practice Bulletin Number 131: Screening for cervical cancer. *Obstet Gynecol.* 2012; 120 (5): 1222–38.
10. Ronco G, Anttila A. Cervical cancer screening in Europe — changes over the last 9 years. *Eur J Cancer.* 2009; 45 (15): 2629–31. DOI: 10.1016/j.ejca.2009.07.021.
11. Петрова Г. В., Грецова О. П., Каприн А. Д., Старинский В. В. Характеристика и методы расчета медико-статистических показателей, применяемых в онкологии. М.: ФГБУ МНИОИ им. П. А. Герцена Минздрава РФ, 2014; 40 с.
12. Мерабишвили В. М. Онкологическая статистика (традиционные методы, новые информационные технологии): Руководство для врачей. Изд. 2-е, доп. СПб., 2015; 248 с.
13. Мерабишвили В. М. Выживаемость онкологических больных. СПб., 2011; 329 с.
14. Урманчеева А. Ф., Кутушева Г. Ф., Ульрих Е. А. Опухоли яичника (клиника, диагностика и лечение). СПб.: Изд-во Н-Л, 2012; 68 с.
15. Jacobs IJ, Menon U, Ryan A, Gentry-Maharaj A, Burnell M, Kalsi JK, et al. Ovarian cancer screening and mortality in the UK Collaborative Trial of Ovarian Cancer Screening (UKCTOCS): a randomised controlled trial. *Lancet.* 2016; 387 (10022): 945–56. PubMed PMID: 26707054.
16. Johnson N. Two large randomised trials show ovarian cancer screening has minimal impact on survival. *BJOG.* 2016; 125 (5): 524–5.
17. Каприн А. Д., Старинский В. В., Петрова Г. В., редакторы. Состояние онкологической помощи населению России в 2017 году. М.: МНИОИ им. П.А. Герцена — филиал ФГБУ «НМИЦ радиологии» Минздрава России, 2018; 236 с.
18. Howlader N, Noone AM, Krapcho M, Miller D, Brest A, YuM, et al. SEER Cancer Statistics Review, 1975–2016, National Cancer Institute. Bethesda, MD. Available from: [https://seer.cancer.gov/csr/1975\\_2016/sections.html](https://seer.cancer.gov/csr/1975_2016/sections.html).

## INTOLERANCE OF PRESERVATIVE-CONTAINING EYE DROPS IN A GLAUCOMA PATIENT: DIAGNOSTIC AND THERAPEUTIC CHALLENGES

Frolov MA<sup>1</sup>, Kazakova KA<sup>1,2</sup>✉, Dushina GN<sup>1</sup>, Frolov AM<sup>1</sup>, Gonchar PA<sup>1</sup>

<sup>1</sup> Peoples' Friendship University of Russia, Moscow, Russia

<sup>2</sup> Multiprofile Clinic "SM-Clinic", Moscow, Russia

A patient presented to our clinic with stage Ia open-angle glaucoma of the right eye and stage IIa surgically corrected open-angle glaucoma of the left eye. The condition of the ocular surface was interpreted as toxic/allergic conjunctivitis provoked by brimonidine 0.15 %. Brimonidine was substituted with non-selective 0.5%; additionally, topical steroids were prescribed. After steroids were discontinued, some of the symptoms came back, including moderate hyperemia and conjunctival edema, which was interpreted as intolerance to a preservative contained in the eye drops. A decision was made to switch from the  $\beta$ -blocker to its preservative-free formulation; regular IOP monitoring was continued. IOP measured during the next visit was above tolerated, so a preservative-free form of the ocular hypotensive combination drug (an analog of prostaglandin 0.005% with non-selective  $\beta$ -blocker 0.5%) was introduced to the regimen, with further IOP monitoring. Because the initial diagnosis was wrong, damage to the ocular surface had been aggravated by inadequate therapy. Preservative-free hypotensive eye drops are beneficial for the corneal surface and have a positive effect on a patient's adherence to the regimen.

**Keywords:** glaucoma, preservative, brimonidine, preservative-free form, allergic reactions

**Author contribution:** Frolov MA — study planning; data analysis and interpretation; Kazakova KA, Dushina GN, Frolov AM, Gonchar PA — study planning; literature analysis; data acquisition, analysis and interpretation; manuscript preparation.

**Compliance with ethical standards:** the patient gave informed consent to participate in the study and for publication of its results

✉ **Correspondence should be addressed:** Kseniya A. Kazakova  
Miklouho-Maclay, 6, Moscow, 117198; ponomareva\_kseni@mail.ru

**Received:** 26.12.2019 **Accepted:** 09.01.2020 **Published online:** 26.01.2020

**DOI:** 10.24075/brsmu.2020.005

## НЕПЕРЕНОСИМОСТЬ КОНСЕРВАНТОСОДЕРЖАЩИХ ГЛАЗНЫХ КАПЕЛЬ ПРИ ГЛАУКОМЕ: ТРУДНОСТИ ДИАГНОСТИКИ, СЛОЖНОСТИ ЛЕЧЕНИЯ

М. А. Фролов<sup>1</sup>, К. А. Казакова<sup>1,2</sup>✉, Г. Н. Душина<sup>1</sup>, А. М. Фролов<sup>1</sup>, П. А. Гончар<sup>1</sup>

<sup>1</sup> Российский университет дружбы народов, Москва, Россия

<sup>2</sup> Многопрофильный медицинский холдинг «СМ-Клиника», Москва, Россия

В клинику поступил пациент с диагнозом OD о/у глаукома 1a. OS оперированная о/у глаукома IIa. Состояние глазной поверхности расценено как токсико-аллергический конъюнктивит на фоне применения бримонидина 0,15%. Проведена замена бримонидина 0,15% на неселективный  $\beta$ -блокатор 0,5% и назначены стероиды местно. На фоне отмены стероидов было отмечено частичное возобновление симптомов в виде умеренно выраженных гиперемии и отека конъюнктивы, что было расценено уже как непереносимость консерванта. Было решено заменить  $\beta$ -блокатор на бесконсервантную форму под регулярным контролем уровня ВГД, дополнительно рекомендованы слезозаменители, не содержащие консервантов. При следующем визите отмечено повышение ВГД выше толерантного, назначена бесконсервантная форма комбинированного гипотензивного средства (аналог простагландина 0,005% с неселективным  $\beta$ -блокатором 0,5%) под контролем уровня ВГД. Неправильная постановка диагноза в начале лечения усугубила состояние глазной поверхности. Применение препаратов без консерванта благоприятно влияет на поверхность роговицы и повышает комплаентность пациентов.

**Ключевые слова:** глаукома, консервант, бесконсервантная форма препарата, бримонидин, аллергическая реакция

**Вклад авторов:** М. А. Фролов — планирование исследования, анализ и интерпретация данных; К. А. Казакова, Г. Н. Душина, А. М. Фролов, П. А. Гончар — планирование исследования, анализ литературы, сбор, анализ и интерпретация данных, подготовка черновика рукописи.

**Соблюдение этических стандартов:** пациент подписал добровольное информированное согласие на участие в исследовании и публикацию данных.

✉ **Для корреспонденции:** Ксения Александровна Казакова  
ул. Миклухо-Маклая, д. 6, г. Москва, 117198; ponomareva\_kseni@mail.ru

**Статья получена:** 26.12.2019 **Статья принята к печати:** 09.01.2020 **Опубликована онлайн:** 26.01.2020

**DOI:** 10.24075/vrgmu.2020.005

Topical ocular hypotensive therapy is one of the basic therapeutic methods of reducing intraocular pressure (IOP). Daily instillation of hypotensive eye drops is prescribed to 60–80% of patients with glaucoma [1]. Such therapy is often long-lasting or even life-long, and in some cases a combination of several hypotensive drugs is required.

Today, there is an algorithm for prescribing ocular hypotensive drugs. PGF<sub>2</sub> $\alpha$  analogs are often the drugs of first choice since they are the most effective in reducing IOP and have neuroprotective properties. If they fail to work, a switch to prostamides (bimatoprost 0.03%) is recommended. If sufficient IOP reduction cannot be achieved with prostamides, carbonic anhydrase inhibitors can be introduced to the regimen. In the absence of a desired outcome, fixed combination therapy

should be used as a next-line treatment. Here, one-time instillation of bimatoprost and timolol is the most effective [2].

Summing up, ophthalmologists have a vast armamentarium of different classes of ocular hypotensive medications for treating glaucoma; nevertheless, all of these drugs can have adverse effects associated with their active ingredients or preservatives, which most of eye drops have as a component [3].

Recent years have witnessed extensive research, both in Russia and overseas, into the prevalence of ocular surface pathology in patients with primary glaucoma and the effect of preservatives on the ocular surface [4, 5–9]. There is convincing evidence that preservatives cause the loss of goblet cells, as well as mucin deficiency in the tear film, disrupt the structure of the lipid layer, leading to excessive evaporation and



hyperosmolality of the precorneal tear film, produce a cytotoxic effect on conjunctival and corneal epithelial cells, lead to keratinization and inflammatory infiltration in the corneal limbus, provoke elevated cytokines, and maintain inflammatory immune response in the conjunctiva (proinflammatory readiness) [1, 5, 7, 10].

Active ingredients of ocular hypotensive drugs can also have a detrimental effect on the ocular surface. For example, studies have uncovered the mechanisms underlying the development of corneal/conjunctival xerosis in patients receiving instillation of  $\beta$ -blockers, including suppression of tear secretion and the local anesthetic effect on the ocular surface epithelium; the latter means that production of basal tears is understimulated and conjunctival goblet cells fail to produce enough mucin if the ocular surface epithelium is damaged [5].

Importantly, toxic and allergic reactions to ocular hypotensive drugs can be immediate and delayed, complicating the accurate diagnosis and sometimes resulting in inadequate therapy (antibacterial or antiviral drugs, NSAID, etc.), which, in turn, further aggravates ocular surface damage. A study reports that in patients developing allergy to brimonidine (the  $\alpha_2$ -selective adrenergic receptor agonist), the mean duration of therapy before the onset of allergy was 4 to 15 months [11].

The treatment of patients with intolerance to preservatives contained in hypotensive eye drops is accompanied by a number of difficulties:

- intolerance of ocular hypotensive drugs dictates a switch in the regimen, possibly more than once, meaning that the patient incurs additional costs;
- if eye dryness is provoked by the preservatives in the eye drops, preservative-free artificial tears (lubricating eye drops) should be prescribed instead;
- if IOP control cannot be attained by using a one-drug regimen, the patient should be tested for hypersensitivity to the eye drops planned for use [11];
- if the patient develops toxicity, allergy, corneal/conjunctival xerosis or it is impossible to exclude hypotensive preservative-containing eye drops from the regimen, adjunct therapy should be prescribed, including systemic and topical antiallergic agents, steroids (which, in turn, can increase IOP) and regenerants. If these drugs contain preservatives, they can provoke allergy just the same;
- in some cases, polyvalent allergy to ocular hypotensive drugs makes medication therapy impossible, so surgery is recommended.

So far, a few preservative-free ocular hypotensive drugs have been approved for use in the Russian Federation. A positive effect of preservative-free hypotensive agents on the ocular surface in comparison with their preservative-containing counterparts has been demonstrated in multiple studies by both Russian and foreign researchers [1, 4, 12–18]. However, their wide use is hindered by a few obstacles:

- only 7 preservative-free hypotensive eye drops have been approved in the Russian Federation;
- the majority of them contain a  $\beta$ -blocker. The hypotensive effect of  $\beta$ -blockers is known to attenuate over time, necessitating adding more drugs into the regimen. Besides, the application of nonselective  $\beta$ -blockers is limited by their systemic side effects.

### Clinical case

The following clinical case seems interesting. *Patient K.*, 67 years, residing in a remote Russian region, presented with complaints of red, burning, watery eyes; the symptoms had set in half a year before the appointment (see Fig.).

Medical history: Ia open-angle glaucoma of the right eye, IIa surgically treated open-angle glaucoma of the left eye. January 2017, the patient underwent nonpenetrating deep sclerectomy and Ahmed valve implantation into the left eye. Postoperatively, the patient received brimonidine instillation in both eyes. No data were available on preoperative IOP in the left eye. In May 2017, the patient presented to a local ophthalmologist, complaining of pronounced redness of both eyes, and was diagnosed with blepharoconjunctivitis. The patient's conjunctival culture was negative for pathogens, but the patient tested positive for Demodex mites and was prescribed anti-Demodex therapy and subconjunctival injections of gentamicin and dexamethasone, reporting improvement shortly thereafter. However, in the months that followed, the patient had a few episodes of hyperemia. His condition started to deteriorate in early November, 2017. The patient sought medical advice at different clinics in the region of his residence and also outside it. Repeated culture tests were negative; a few mature Demodex mites were detected. A conjunctival smear test revealed elevated white blood cells. The patient was prescribed topical antiseptics, antibiotics, interferon and its inducer, antihistamines, corticosteroids, lubricants for corneal protection, and eye hygiene, with no positive effect.

The patient contacted our clinic in December 2017. On examination: best corrected visual acuity (BCVA) 0.9 OD, 0.8 OS. IOP measured by air-puff tonometry: 18–19 mmHg OD, 20–21 mmHg OS. Eyelids were red and swollen; tear producing organs were intact; excess tear production was observed. The conjunctiva appeared pronouncedly red, with swollen fornices, conjunctival follicles and eyelids; eye discharge was flaky and scanty. Old subepithelial opacities were detected on the retina in both eyes. On palpation, IOP was normal. The condition of the ocular surface was interpreted as toxic/allergic conjunctivitis provoked by brimonidine 0.15%.

### Clinical case discussion

Substituting brimonidine 0.15% with nonselective  $\beta$ -blocker (0.5%) and adding temporary topical steroids to the regimen, with regular IOP monitoring, led to improvement, both subjective and objective. After steroids were discontinued, some of the symptoms came back, including moderate hyperemia and conjunctival edema, which was interpreted as intolerance to a preservative contained in the eye drops. A decision was made to switch from the  $\beta$ -blocker to its preservative-free form; regular



**Fig.** The patient's right eye. Conjunctival and pericorneal hyperemia. Conjunctival follicles and moderate edema of the lower eyelid

IOP monitoring was continued. Additionally, preservative-free artificial tears were recommended. The choice of the marketed form was dictated by the absence of other preservative-free ocular hypotensive drugs in the patient's area of residence.

The patient did not show up for the scheduled checkup examination; we did not hear from him for over 9 months. As he told us later, IOP measurements had been taken at a healthcare facility in the patient's area of residence. The patient contacted us again in October 2018, complaining of deteriorating vision in the left eye. According to the patient and Maklakov tonometer readings in the medical history, IOP in the operated eye had been fluctuating between 15 and 23 mmHg. On examination: Vis OS = 0.2, BCVA = 0.5. The eyelids looked healthy, the eyes were not watery, the conjunctiva also looked normal. Ophthalmoscopy results: pallor of the optic disc, excavation at the margin. Automated static perimetry revealed constriction of the visual field (30°) at the nasal side and multiple absolute central scotomas. IOP: 15 mmHg OD, 24 mmHg OS.

Due to the deteriorating visual acuity and elevated (24 mmHg) IOP in the left eye, the patient was advised to repeat glaucoma surgery at his local healthcare facility. Medication therapy was also prescribed, including a preservative-free formulation of the ocular hypotensive combination drug (an analog of prostaglandin 0.005% with non-selective  $\beta$ -blocker 0.5%). Further IOP monitoring was recommended. Because the prescribed medication was not available in the patient's area of residence, he had to order it from another town.

The recommended glaucoma surgery was not performed. The patient presented to our clinic again in January 2019. The visual field defect was not progressing; the condition of the optic disc was stable. IOP: 16 mmHg OD, 19 mmHg OS. The patients complained of occasional hyperemia, accompanying the intake of artificial tears, which could have been an adverse reaction to the instillation of the prescribed prostaglandin analog. IOP measured at the patient's local healthcare facility was not stable, increasing to 22–24 mmHg in the left eye.

We strongly advised the patient to undergo repeat glaucoma surgery because he had intolerance to preservative-containing ocular hypotensive drugs, the drugs did not ensure a stable hypotensive effect, and he lived in a remote region, which complicated proper treatment monitoring.

## CONCLUSIONS

Misinterpretation of the etiology of conjunctivitis/blepharoconjunctivitis results in polypragmasy. Adding more drugs to the regimen may aggravate damage to the ocular surface and entails costs. In the absence of preservative-free ocular hypotensive eye drops, preservative-containing formulations used for treating glaucoma can trigger its progression. Insufficient reduction of intraocular pressure does not allow a patient to discontinue preservative-containing drugs, which negatively affects the quality of a patient's life and their adherence to the regimen and can lead to repeat surgery.

## References

1. Astahov SYu, Tkachenko NV. Taflotan — pervyj analog prostaglandina-F2 $\alpha$  bez konservantov: preimushchestva v lechenii bol'nyh pervichnoj otkrytougol'noj glaukomoj. *Oftal'mologicheskie vedomosti*. 2016; 9 (2): 59–68.
2. Egorov AE, Glazko NG, Movsisyan AB. Gipotenzivnaya i nejroprotektivnaya terapiya glaukomy: realii i perspektivy. *Russkij medicinskij zhurnal. Klinicheskaya oftal'mologiya*. 2019; 19 (3): 128–36.
3. Yani EV, Seliverstova KE. Toksiko-allergicheskij kon'yunktivit u pacientov s pervichnoj glaukomoj na fone medikamentoznogo gipotenzivnogo lecheniya. *Farmateka*. 2016; 20 (333): 12–14.
4. Elichev VP, Ambarcumyan KG, Fedorov A.A. Kliniko-morfologicheskie dokazatel'stva vliyaniya konservantov na poverhnost' glaza pri pervichnoj otkrytougol'noj glaukome. *Nacional'nyj zhurnal glaukoma*. 2014; 13 (4): 13–22.
5. Brzhetskij VV, Radhuan M. Glaukoma i sindrom "suhogo glaza". *Oftal'mologicheskie vedomosti*. 2014; 7 (2): 37–49.
6. Safonova TN, Fedorov AA, Zabegajlo AO, Egorova GB, Mitichkina TS. Lechenie sindroma "suhogo glaza" pri pervichnoj glaukome. *Nacional'nyj zhurnal glaukoma*. 2015; 14 (4): 36–43.
7. Elichev VP, Ambarcumyan KG. Osobennosti gipotenzivnoj terapii bol'nyh glaukomoj preparatami, ne sodержashchimi konservantov. *Prakticheskaya medicina*. 2012; 4 (59): 194–6.
8. Erb C, Gast U, Schremmer D. German register for glaucoma patients with dry eye. I. Basic outcome with respect to dry eye. *Graefes Arch Clin Exp Ophthalmol*. 2008; 246 (11): 1593–601.
9. Leung EW, Medeiros FA, Weinreb RN. Prevalence of ocular surface disease in glaucoma patients. *J Glaucoma*. 2008; 17 (5): 350–5.
10. Astahov Syu, Graboveckij VR, Nefedova DM, Tkachenko NV. Preimushchestva i nedostatki gipotenzivnyh kapel' bez konservanta. *Oftal'mologicheskie vedomosti*. 2011; 4 (20): 95–97.
11. Shtejner I, Branchevskij S. Problemy differencial'noj diagnostiki otsrochennoj allergicheskoy reakcii u pacientov, poluchajushih mestnoe gipotenzivnoe lechenie glaukomy. *Vrach*. 2016; (12): 62–4.
12. Alekseev IB, Koroleva IA. Beskonservantnye gipotenzivnye preparaty: preimushchestva terapii. *Russkij medicinskij zhurnal. Klinicheskaya oftal'mologiya*. 2019; 19 (3): 137–42.
13. Antonov AA, Kozlova IV, Mitichkina TS, Vedmedenko II. Beskonservantnaya terapiya glaukomy u pacientov, perenesshih keratorefrakcionnye operacii. *Russkij medicinskij zhurnal. Klinicheskaya oftal'mologiya*. 2019; 19 (3): 165–70.
14. Loskutov IA, Korneeva AV. Beskonservantnaya forma fiksirovannoj kombinacii bimatoprost i timolola v povyshenii komplensa i effektivnosti lecheniya pacientov s pervichnoj otkrytougol'noj glaukomoj. *Rossijskij oftal'mologicheskij zhurnal*. 2018; 11 (2): 95–101.
15. Onishchenko AL, Dimaksyan MV, Kolbasko AV, ZHilina NM. Lechenie pervichnoj otkrytougol'noj glaukomy  $\beta$ -ksololom bez konservanta: ocenka gipotenzivnogo efekta i glaznoj poverhnosti. *Vestnik oftal'mologii*. 2015; 131 (20): 76–80.
16. Egorov EA. Novye formy selektivnyh  $\beta$ -blokatorov v lechenii glaukomy. *Klinicheskaya oftal'mologiya*. 2014; 14 (3): 131–5.
17. Bourne R, Kaamiranta K, Lorenz K, Traverso CE, Vuorinen J, Ropo A. Changes in ocular signs and symptoms in patients switching from bimatoprost-timolol to tafluprost-timolol eye drops: an open-label phase IV study. *BMJ Open*. 2019; 9 (4).
18. Pillunat LE, Eschstruth P, Hässemeyer S, Thelen U, Foja C, Leaback R, et al. Preservative-free bimatoprost 0.03% in patients with primary open-angle glaucoma or ocular hypertension in clinical practice. *Clin Ophthalmol*. 2016; 12 (10): 1759–65.

## Литература

1. Астахов С. Ю., Ткаченко Н. В. Тафлотан — первый аналог простагландина-F2 $\alpha$  без консервантов: преимущества в лечении больных первичной открытоугольной глаукомой. Офтальмологические ведомости. 2016; 9 (2): 59–68.
2. Егоров А. Е., Глазко Н. Г., Мовсисян А. Б. Гипотензивная и нейрпротективная терапия глаукомы: реалии и перспективы. Русский медицинский журнал. Клиническая офтальмология. 2019; 19 (3): 128–36.
3. Яни Е. В., Селиверстова К. Е. Токсико-аллергический конъюнктивит у пациентов с первичной глаукомой на фоне медикаментозного гипотензивного лечения. Фарматека. 2016; 20 (333): 12–14.
4. Еричев В. П., Амбарцумян К. Г., Федоров А. А. Клинико-морфологические доказательства влияния консервантов на поверхность глаза при первичной открытоугольной глаукоме. Национальный журнал глаукома. 2014; 13 (4): 13–22.
5. Бржеский В. В., Радхуан М. Глаукома и синдром «сухого глаза». Офтальмологические ведомости. 2014; 7 (2): 37–49.
6. Сафонова Т. Н., Федоров А. А., Забегайло А. О., Егорова Г. Б., Митичкина Т. С. Лечение синдрома «сухого глаза» при первичной глаукоме. Национальный журнал глаукома. 2015; 14 (4): 36–43.
7. Еричев В. П., Амбарцумян К. Г. Особенности гипотензивной терапии больных глаукомой препаратами, не содержащими консервантов. Практическая медицина. 2012; 4 (59): 194–6.
8. Erb C, Gast U, Schremmer D. German register for glaucoma patients with dry eye. I. Basic outcome with respect to dry eye. Graefe's Arch Clin Exp Ophthalmol. 2008; 246 (11): 1593–601.
9. Leung EW, Medeiros FA, Weinreb RN. Prevalence of ocular surface disease in glaucoma patients. J Glaucoma. 2008; 17 (5): 350–5.
10. Астахов С. Ю., Грабовецкий В. Р., Нефедова Д. М., Ткаченко Н. В. Преимущества и недостатки гипотензивных капель без консерванта. Офтальмологические ведомости. 2011; 4 (20): 95–7.
11. Штейнер И., Бранчевский С. Проблемы дифференциальной диагностики отсроченной аллергической реакции у пациентов, получающих местное гипотензивное лечение глаукомы. Врач. 2016; (12): 62–4.
12. Алексеев И. Б., Королева И. А. Бесконсервантные гипотензивные препараты: преимущества терапии. Русский медицинский журнал. Клиническая офтальмология. 2019; 19 (3): 137–42.
13. Антонов А. А., Козлова И. В., Митичкина Т. С., Ведмеденко И. И. Бесконсервантная терапия глаукомы у пациентов, перенесших кераторефракционные операции. Русский медицинский журнал. Клиническая офтальмология. 2019; 19 (3): 165–70.
14. Лоскутов И. А., Корнеева А. В. Бесконсервантная форма фиксированной комбинации биматопроста и тимолола в повышении комплаенса и эффективности лечения пациентов с первичной открытоугольной глаукомой. Российский офтальмологический журнал. 2018; 11 (2): 95–101.
15. Онищенко А. Л., Димаксян М. В., Колбаско А. В., Жилина Н. М. Лечение первичной открытоугольной глаукомы  $\beta$ -ксоллом без консерванта: оценка гипотензивного эффекта и глазной поверхности. Вестник офтальмологии. 2015; 131 (20): 76–80.
16. Егоров Е. А. Новые формы селективных  $\beta$ -блокаторов в лечении глаукомы. Клиническая офтальмология. 2014; 14 (3): 131–5.
17. Bourne R, Kaarniranta K, Lorenz K, Traverso CE, Vuorinen J, Ropo A. Changes in ocular signs and symptoms in patients switching from bimatoprost-timolol to tafluprost-timolol eye drops: an open-label phase IV study. BMJ Open. 2019; 9 (4).
18. Pillunat LE, Eschstruth P, Hässemeyer S, Thelen U, Foja C, Leaback R, et al. Preservative-free bimatoprost 0.03% in patients with primary open-angle glaucoma or ocular hypertension in clinical practice. Clin Ophthalmol. 2016; 12 (10): 1759–65.